ANALYTICA CHIMICA ACTA

International monthly devoted to all branches of analytical chemistry
Revue mensuelle internationale consacrée à tous les domaines de la chimie analytique
Internationale Monatsschrift für alle Gebiete der analytischen Chemie

ELSEVIER SCIENTIFIC PUBLISHING COMPANY

AMSTERDAM

Anal. Chim. Acta, Vol. 79, 1–350, October 1975

Published monthly

Complete in one issue

ANALYTICA CHIMICA ACTA

Publication Schedule for 1975

Vol. 74, No. 1	January 1975	
Vol. 74, No. 2	February 1975	**(completing Vol. 74)**
Vol. 75. No. 1	March 1975	
Vol. 75, No. 2	April 1975	**(completing Vol. 75)**
Vol. 76, No. 1	May 1975	
Vol. 76, No. 2	June 1975	**(completing Vol. 76)**
Vol. 77	July 1975	**(complete in one issue)**
Vol. 78, No. 1	August 1975	
Vol. 78, No. 2	September 1975	**(completing Vol. 78)**
Vol. 79	October 1975	**(complete in one issue)**
Vol. 80, No. 1	November 1975	
Vol. 80, No. 2	December 1975	**(completing Vol. 80)**

Subscription price for 1975 (covering Vols. 74–79): Dfl. 570.00 plus Dfl. 54.00 postage. US$ 265.53 inclusive of postage. Subscribers in the U.S.A. and Canada receive their copies by airmail. Additional charges for airmail to other countries are available on request. For advertising rates apply to the publishers.

Subscriptions should be sent to:
Elsevier Scientific Publishing Company, P.O. Box 211, Amsterdam, The Netherlands.

GENERAL INFORMATION

Languages

Papers will be published in English, French or German.

Detailed information

Authors should consult Vol. 73, p. 435 for detailed instructions. Reprints of this information are obtainable from Dr. Macdonald or from: Elsevier Editorial Series Ltd., Mayfield House, 256 Banbury Road, Oxford (Great Britain).

Submission of papers

Papers should be sent to:

Prof. Philip W. West,
Coates Chemical Laboratories,
College of Chemistry and Physics,
Louisiana State University,
Baton Rouge 3,
La. 70803 (U.S.A.)

or to:

Dr. A.M.G. MacDonald,
Department of Chemistry,
The University,
P.O. Box 363
Birmingham B15 2TT (Great Britain)

Reprints

Fifty reprints will be supplied free of charge. Additional reprints (minimum 100) can be ordered at quoted prices. They must be ordered on order forms which are sent together with the proofs.

DOSAGE DE L'EAU

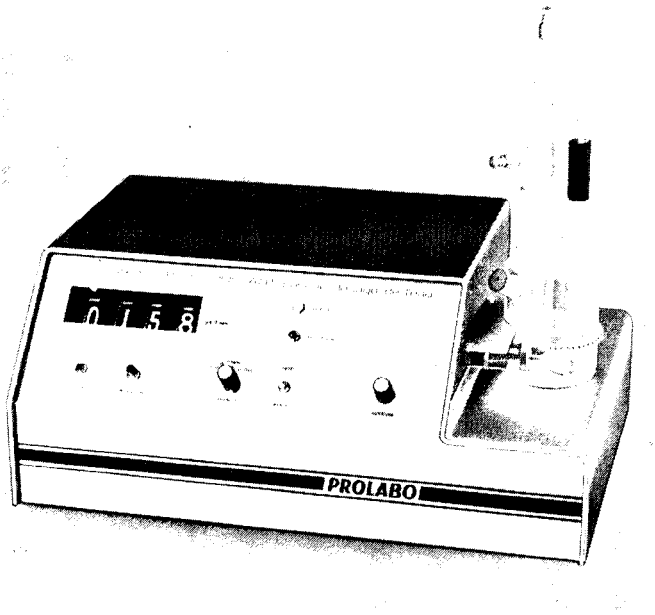

06 756.02

Automate BIZOT et CONSTANT
Dosage par lecture directe de 40 à 10000 microgrammes d'eau

Appareil à fonctionnement **automatique** donnant par **lecture directe** la quantité d'eau contenue dans un échantillon liquide. Son domaine d'emploi s'étend normalement de 5 microgrammes d'eau à 2 000 microgrammes (2 mg); il peut doser à la limite jusqu'à 10 000 microgrammes (10 mg). Le seuil de détection est de 1 microgramme.

Le mode d'emploi est schématiquement le suivant: l'appareil étant en ordre de marche, l'échantillon est injecté dans la cellule de dosage à l'aide d'une seringue. Le dosage s'effectue automatiquement en quelques minutes; lorsqu'il est terminé, un voyant vert s'allume. Le résultat est affiché numériquement sur un cadran à 4 chiffres donnant une lecture en microgrammes d'eau de 0 à 9 999 ou bien en dixièmes de microgrammes de 0 à 9 999 (999,9 microgrammes), selon la sensibilité préalablement choisie. L'appareil est prêt pour injecter l'échantillon suivant: il suffit d'appuyer sur un bouton pour remettre le compteur à zéro.

Ce titrimètre automatique met en œuvre un système de dosage coulométrique dérivé de la méthode de Bizot dont le domaine a été étendu, moyennant l'emploi d'un nouveau réactif, d'une cellule nouvelle et d'un ensemble électronique approprié.

L'appareil est construit d'un seul tenant; la partie de droite contient un agitateur magnétique et reçoit la cellule de dosage.

06 756.02 **Automate Bizot et Constant pour le dosage de l'eau** par lecture directe jusqu'à 10 000 µg (10 mg). Coffret de 43 x 29 x 18 cm pesant 11 kg. Alimentation électrique sur le secteur 220 V 50 Hz. Appareil complet avec cellule de dosage et électrodes, mais sans réactifs. Notice spéciale sur demande.

PROLABO

12, Rue Pelée - 75-PARIS XIe
Téléphone 355.44.88
TELEX: PROLABO PARIS 680566
B.P. 200 75526 PARIS CEDEX 11

CHROMATOGRAPHY OF ENVIRONMENTAL HAZARDS

by **LAWRENCE FISHBEIN,** Chief, Analytical Division, National Center for Toxicological Research, Jefferson, Arkansas, U.S.A.

To cope with the uparalleled need to determine the parameters of environmental abuse, this four-volume work is designed to provide the analytical chemist with a practical text as well as a literature source of selected descriptive chromatographic procedures. Additional priority is given to those methods that may be utilized in a general sense, beyond the analysis of a specific toxicant **per se.** Toxicants such as pesticides, drugs, food and feed additives, and industrial chemicals are considered within the broader framework of their methods of preparation, areas of utility, biochemistry, metabolism and toxicity, and are thus of importance to additional investigation into other areas such as toxicology, pharmacology, biology, genetics and environmental medicine and health.

Volume 1: Carcinogens, Mutagens and Teratogens

1972. 507 pages. US $ 56.25/Dfl. 135.00. ISBN 0-444-40948-3

This volume centers on toxicants of carcinogenic, mutagenic and teratogenic environmental significance with particular focus on those which are pesticides, food and feed additives, drugs and alkylating agents of industrial utility.

Volume 2: Metals, Gaseous and Industrial Pollutants

1973. 649 pages. US $ 62.50/Dfl. 150.00. ISBN 0-444-41059-7

The primary object of this book is to present a survey of the main features of selected chromatographic procedures involved in the detection, separation and determination of the principal metal, gaseous and industrial chemical hazards encountered in the environment. The use of chromatography in environmental studies has many advantages - choice of a given chromatographic method to suit a particular problem; the speed at which separations and detection can be made; the very high sensitivity of instruments which allow the detection of very small amounts of samples. All of these ensure that chromatography has a principal role to play in determining environmental pollutants.

Volume 3: Pesticides

1975. about 840 pages. US $ 108.50/Dfl. 260.00. ISBN 0-444-41185-5

The unique feature of this book is the blending of relevant information regarding the synthesis, areas of utility, degradation and metabolic fate of pesticide toxicants, thus presenting as thorough and cohesive a picture as possible of the specific environmental hazard.

Volume 4: Drugs

1976. In preparation

ELSEVIER SCIENTIFIC PUBLISHING COMPANY

P.O. Box 211, Amsterdam, The Netherlands

Distributed in the U.S.A. and Canada by:
AMERICAN ELSEVIER PUBLISHING COMPANY, INC.,
52 Vanderbilt Ave., New York, N.Y. 10017

16781

ANALYTICA CHIMICA ACTA
Vol. 79 (1975)

ANALYTICA CHIMICA ACTA

International monthly devoted to all branches of analytical chemistry
Revue mensuelle internationale consacrée à tous les domaines de la chimie analytique
Internationale Monatsschrift für alle Gebiete der analytischen Chemie

ELSEVIER SCIENTIFIC PUBLISHING COMPANY

AMSTERDAM

Anal. Chim. Acta, Vol. 79

PRINTED IN THE NETHERLANDS

Analytica Chimica Acta, 79 (1975) 1—7

DETERMINATION OF TOTAL INORGANIC NITROGEN BY MEANS OF THE AIR-GAP ELECTRODE

E.H. HANSEN, J. RŮŽIČKA and N.R. LARSEN
Chemistry Department A, The Technical University of Denmark, Building 207, DK-2800 Lyngby (Denmark)
(Received 10th April 1975)

The determination of the total inorganic nitrogen content is of great analytical importance in pollution and process control, and in food, clinical and agricultural analyses. Provided that the total nitrogen is present as inorganic nitrate, nitrite or as ammoniacal nitrogen, the content may be determined by conventional procedures, which have been greatly simplified by the advent of ammonia gas-sensing electrodes. As the gas electrode measurement is rapid, the time required for analysis is substantially reduced compared to the conventional methods involving distillation. If organic nitrogen-containing compounds are present, the conventional methods are not applicable. In order to preserve all the advantages of ammonia gas-sensing electrodes, the reduction procedure used must be capable of reducing inorganic nitrogen-containing compounds selectively to ammonia.

Although the use of ammonia gas sensors is very attractive, practical difficulties — such as poor mechanical properties of the membrane and possible clogging of the membrane pores — often limits the utility of these highly selective sensors. These shortcomings and limitations are eliminated in the recently introduced air-gap electrode which has been used successfully in various determinations, such as of ammonium ions in waste water [1] and in serum [2]; of urea [3] (via enzymatic degradation) and of hydrogencarbonate [2] in full blood, plasma and serum; of sulphur dioxide in wine [4]; and of the total inorganic and the total organic carbon contents in waters [5]. The air-gap electrode is based on the same principle as other gas sensors, except that it has no gas-permeable membrane. The membrane is replaced by an air gap which separates the surface of the indicator electrode from the sample solution, the entire system being contained in a gas-tight measuring chamber. The electrode is covered by a very thin film of electrolyte, the pH of which is being measured. The greatest advantage of this design is that the electrode never comes into direct physical contact with the sample solution, which can therefore contain components that normally affect the function of all other gas electrodes. Simplicity of design, ease of renewal of electrolyte, and fast response are further advantages gained by replacing the gas-permeable membrane with the air gap.

Originally initiated as a project for determining nitrate and nitrite in inorganic extracts, the investigation described here was extended to the development of a simple, rapid and reliable procedure for the determination of the total inorganic nitrogen content by means of the air-gap electrode. For this purpose, a procedure was required by which all inorganic nitrogen compounds could be reduced reproducibly to ammonia without interference from organic nitrogen compounds present. On the basis of a literature survey, several reduction procedures for nitrate and nitrite solutions (to which organic nitrogen-containing compounds were added) in acidic and alkaline media were investigated in order to establish the optimal operational parameters. Although reduction in acidic medium is inherently preferable, none of the reductants tested (Al powder and Sn(II) or Cr(II) solutions) proved satisfactory. Besides the practical difficulties of håndling chromium(II) solutions, all three reduction procedures were characterized by slow reaction rates; when aluminium powder was used — as has been recommended for the determination of nitrate [6] — it was found that the yield was only 50—60 % for pure nitrate solutions.

In alkaline medium, Ti(III), Fe(II), Al powder and Devarda alloy were examined. While titanium(III) is very effective, aqueous solutions of the reagent are stable only for short periods of time, because of atmospheric oxidation, unless they are very acidic, *e.g.*, *ca.* 6 *M* in sulphuric acid, which makes them inconvenient for practical application. It is noteworthy, however, that the formation of a heterogenous system in the alkaline medium in no way affects the monitoring procedure with the air-gap electrode. The reduction with iron(II), in the presence of copper(II) as catalyst, and the reduction with aluminium powder are rather slow and result in much less than 100 % yield. When Devarda alloy is used, however, very fast and reproducible results can be obtained; the procedure is very convenient, except that precautions must be taken in order to prevent splashing of base onto the electrode surface as a result of the rather vigorous hydrogen evolution. This can be most effectively done by inserting a deflector unit in the measuring chamber. The nitrate/nitrite is reduced within a few minutes; and by taking advantage of the high solubility of ammonia in aqueous solutions, it was established that the reduction and the actual measurement of the ammonia can be performed in two separate operations so that the analysis can be done in a very short time. Furthermore, it was demonstrated that organic nitrogen-containing compounds do not interfere.

The procedure described below permits the determination of the total inorganic nitrogen content by selective reduction to ammonia and subsequent measurement by means of the air-gap electrode.

EXPERIMENTAL

Equipment

The apparatus and the air-gap electrode have been described previously [3]. The macrochamber (23-mm internal diameter) was used throughout. Polyethylene vials (volume *ca.* 8 ml), fitting closely into the chamber cavity, were used to hold the samples so that both reduction and measurement could be done in the same container. In order to prevent splashing of base onto the surface of the electrode, the vials used were provided with a deflector arrangement: each vial was divided by a horizontal cut into two segments — a lower part 14 mm high upon which was placed the 16-mm upper part into the bottom of which the deflector arrangement was incorporated. The deflector consisted of two polyethylene plates, separated *ca.* 3 mm from each other; the lower plate had a central circular hole of 10-mm diameter, and the upper plate had annular cut outs so as to leave a concentric disc of 12-mm diameter.

Reagents

The electrolyte solution was 0.10 *M* ammonium chloride plus 1.0 *M* sodium nitrate to which was added 0.01 % (w/w) wetting agent. The electrolyte was applied to the electrode as outlined previously [3], *i.e.*, the layer was renewed after each measurement. Standard solutions in the range 10^{-4}—10^{-2} *M* ammonium, nitrate and nitrite were prepared by dissolving ammonium chloride, sodium nitrate or sodium nitrite, respectively, in distilled water. The base used was 10 *M* sodium hydroxide. The Devarda alloy (50 % Cu, 45 % Al and 5 % Zn), was of p.a. quality (Riedel-De Haën). All other reagents and chemicals were of p.a. quality.

All pipetting was done by means of MLA Precision Pipettes (Medical Laboratory Automation Inc.), which have a precision of ±1 %.

Measuring procedure

The calibration of the electrode and the actual sample analysis were done in an identical manner: 30—35 mg of Devarda alloy was added to the lower portion of the polyethylene vial containing a magnetic stirring bar; then 100 µl of the 10 *M* base was added by means of a precision pipette followed by 100 µl of standard (or sample). The upper part of the vial comprising the deflector unit was then inserted into the chamber which was subsequently closed by a cylindrical Perspex block (50 × 80 mm). The magnetic stirrer was started and the reduction was allowed to take place for 3.5 min. After this sequence, the stirrer was stopped and the Perspex block was swiftly replaced by the body of the air-gap electrode whereupon the magnetic stirrer was engaged again. The signal was followed on the recorder and when equilibrium

was reached (within 2—3 min), the pH_e was read on the digital pH meter within 0.001 pH_e unit.

All measurements were made at 23 ± 0.5 °C.

Computations

All calibration curves were calculated by means of linear regression analysis on the linear part of the plots on a WANG 700B Programmable Electronic Calculator provided with a WANG 702 Plotting Output Writer.

RESULTS AND DISCUSSION

Calibration and precision data

The reduction method with Devarda alloy was first tested on series of standard solutions (10^{-2}—10^{-4} *M*) containing nitrate or nitrite only, and then on standards to which were added organic nitrogen-containing compounds; in both cases two measurements were recorded for each concentration ($1.0 \cdot 10^{-4}$; $5 \cdot 10^{-4}$; $1.0 \cdot 10^{-3}$; $5.0 \cdot 10^{-3}$; and $1.0 \cdot 10^{-2}$ *M*) and each of these data points was then plotted as $\log[NO_3^-]$ or $\log[NO_2^-]$ against the obtained pH_e values, with linear regression analysis, to give the calibration curves. However, the calibration plots for this electrolyte concentration proved to be linear down to *ca.* $2 \cdot 10^{-4}$ *M* only — a value which is in good agreement with the expected value from a double logarithmic diagram [7] — hence the electrode response for the lowest standard concentration was omitted in the regression analysis. Within the range $5 \cdot 10^{-4}$—10^{-2} *M* nitrate, $\log[NO_3^-]$ as a function of pH_e yielded a straight-line relationship with a slope of 1.095, the standard error being 0.014 pH_e (corresponding to *ca.* 3 %). The regression coefficient was 0.9994. The corresponding data for the nitrite calibration curve were: slope 1.090, standard error 0.015, and regression coefficient 0.9996. Subsequently, a series of 6 mixtures within the concentration range $1 \cdot 10^{-3}$—$1.1 \cdot 10^{-2}$ *M* containing various ratios of nitrate and nitrite were prepared, the ratio between the two constituents varying from 10:1 to 1:10. The rectilinear calibration curve had a slope of 1.085, the standard error being 0.015 and the regression coefficient 0.9990. As all these plots, including a calibration curve based on ammonium chloride standards, were very nearly congruent, it can be concluded that the nitrate and/or nitrite content of samples containing these constituents can be determined reproducibly and with 100 % yield, by this method. Generally, the standard error varied from 0.007 to 0.016 pH_e, *i.e.*, *ca.* 1.7—3 %, including the 1 % deviation inherent in the pipetting procedure. While a reduction time of 3.5 min more than sufficed for the lower concentrations of analyte, concentrations of *ca.* 10^{-2} *M* generally required the whole 3.5 min for total reduction.

To check the method further, standard solutions of nitrate were spiked with known amounts of nitrate and then measured again. To 10.0 ml of

$1.0 \cdot 10^{-3}$ *M* nitrate standards, 100 and 150 µl of $1.0 \cdot 10^{-1}$ *M* nitrate, were added; these solutions were found to contain $2.00 \cdot 10^{-3}$ *M* and $2.48 \cdot 10^{-3}$ *M*, respectively, compared to the calculated values of $1.98 \cdot 10^{-3}$ *M* and $2.46 \cdot 10^{-3}$ *M*.

Effect of l-amino acids and urea

Attention was then turned to the possible effects of organic nitrogen-containing compounds. As the method was originally intended for measurements of inorganic nitrogen in foodstuffs, four of the commonest l-amino acids — l-alanine, l-leucine, l-phenylalanine and l-arginine, — were first examined, both individually in aqueous solutions of the acids and also when added in various quantities to solutions of nitrate and/or nitrite. When subjected to the ordinary 3.5-min reduction procedure, all of the l-amino acids, even in 10^{-2} *M* concentrations, yielded signals corresponding to less than 10^{-4} *M* nitrogen; even when the reduction time was extended to 30 min, no significant signal was observed. Although the amino acids reacted to slightly different degrees, with leucine ostensibly interfering the least, the signal never exceeded that corresponding to $\leqslant 1 \cdot 10^{-4}$ *M* nitrogen. The l-amino acids were then added to nitrate and/or nitrite standards ($1.0 \cdot 10^{-3}$ *M*) in amounts of $5 \cdot 10^{-4}$ *M*, $1 \cdot 10^{-3}$ *M* and $5 \cdot 10^{-3}$ *M*, and the solutions were then measured, along with the unspiked standards, in the usual way. The interference never exceeded the experimental error (*i.e.*, less than *ca.* 3 %).

A series of similar experiments was then done with urea added to $1.0 \cdot 10^{-3}$ *M* nitrate standards in concentrations of $5 \cdot 10^{-4}$—$5 \cdot 10^{-3}$ *M*. Again no significant interference was observed, which implies that this method may prove useful for analysis of urea-containing fertilizers. The inorganic nitrogen content could be determined simply by the present method, while the urea could be assayed rapidly after selective enzymatic degradation to ammonia [3]; total nitrogen could then be ascertained, if necessary, by the Kjeldahl method.

Analysis of waters

Three water samples — river water, untreated waste water, and biologically treated waste water from a local purification plant — were analyzed for total inorganic nitrogen as described above, and additionally for ammoniacal nitrogen, which was done as previously described [3] with a 10^{-2} *M* ammonium chloride electrolyte solution. The water samples were supplied by the Department of Sanitary Engineering of this University where analyses for ammonia, nitrate, nitrite and, after a Kjeldahl digestion, for the total nitrogen content were run on an AutoAnalyzer. The results are summarized in Table I. While the total inorganic nitrogen content in the river water sample was below the detection limit of the electrode, excellent agreement was observed between the results obtained on the AutoAnalyzer and those achieved with the air-gap electrode. Furthermore, it is evident that the organic nitrogen present in the waste-water samples does not interfere in the reduction procedure under the conditions used.

TABLE I

Determination of the ammoniacal and total inorganic nitrogen content in water samples (All results are given as p.p.m.N.)

Sample	NH_3-N		Total inorg.-N		Total N
	Air-gap electrode	Auto-Analyzer	Air-gap electrode	Auto-Analyzer	Kjeldahl analysis
River water	0.17	0.21	<2	0.84	2.4
Untreated waste water	13.6	13.7	21.9	21.9	24.1
Biologically treated waste water	37.9	38.2	39.3	38.9	49.6

Conclusions

The experimental results confirm that it is indeed possible to find suitable conditions and to develop a simple method for the determination of total inorganic nitrogen so that the response of the air-gap electrode reflects the concentration of analyte in a Nernstian manner. The total time for analysis is only 5—6 min, which is a drastic reduction compared to conventional methods. Moreover, the determination is also highly selective.

The work described here was intended to serve as a demonstration of the capability of the electrode for this type of measurement, and a comprehensive investigation was not made. Thus, although nitrite in many systems is present in much smaller quantities than nitrate (*e.g.*, soil solutions and sewage waters), it would be desirable to determine nitrate and nitrite separately by the electrode procedure. One approach might be by enzymatic analysis as mentioned by Hussein and Guilbault [8], who used a two-enzyme system of nitrate and nitrite reductases for selective determination of nitrate; however, as the authors concede, such systems are difficult to handle and much work still has to be done in order to optimize the system. Another alternative is, of course, to remove nitrite by addition of sulfamic acid as described in the literature and most recently by Mertens *et al.* [9].

The authors wish to express their appreciation to Inge Marie Johansen for her conscientious technical assistance; and to Jørgen P. Jørgensen of the Department of Sanitary Engineering for useful discussions and for his help in providing the water samples. This work was in part supported by the Danish Natural Science Research Council.

SUMMARY

A method for determining the total inorganic nitrogen content of aqueous

solutions is described. The inorganic nitrogen is reduced by Devarda alloy to ammonia which is thus measured by means of the air-gap electrode. On a sample volume of 100 μl, the assay takes only 5—6 min, the standard deviation being less than 3 %. Organic nitrogen-containing compounds do not interfere. The method has been tested on solutions of nitrate and nitrite, with and without organic nitrogen-containing compounds present, and has been applied to samples of river water, untreated waste water and biologically treated waste water.

REFERENCES

1 J. Růžička, E.H. Hansen, P. Bisgaard and E. Reymann, Anal. Chim. Acta, 72 (1974) 215.
2 J. Růžička and E.H. Hansen, Anal. Chim. Acta, 69 (1974) 129.
3 E.H. Hansen and J. Růžička, Anal. Chim. Acta, 72 (1974) 353.
4 E.H. Hansen, H. Bergamin Filho and J. Růžička, Anal. Chim. Acta, 71 (1974) 225.
5 U. Fiedler, E.H. Hansen and J. Růžička, Anal. Chim. Acta, 74 (1975) 423.
6 Ammonia Electrode Instruction Manual, Orion Research Inc., Massachusetts, U.S.A.
7 E.H. Hansen and N.R. Larsen, Anal. Chim. Acta, in press. No. 6913.
8 W.R. Hussein and G.G. Guilbautl, Anal. Chim. Acta, 76 (1975) 183.
9 J. Mertens, P. Van den Winkel and D.L. Massart, Anal. Chem., 47 (1975) 522.

Analytica Chimica Acta, 79 (1975) 9—15

ENZYME ANALYSIS BY MEANS OF THE AIR-GAP ELECTRODE — DETERMINATION OF UREASE AND ARGINASE BY MONITORING OF THE INITIAL REACTION RATE

N.R. LARSEN, E.H. HANSEN and G.G. GUILBAULT
Chemistry Department A, The Technical University of Denmark, Building 207, DK-2800 Lyngby (Denmark)
(Received 28th April 1975)

One or more of the products generated in enzyme reactions are frequently species which either themselves are, or through a coupled reaction may yield, protolytic gases, the measurement of which may serve as the basis for determining either substrates or enzymes. The recent advent of potentiometric gas-sensing electrodes has greatly facilitated this type of analysis, since such sensors characteristically possess good selectivity and fast response. Despite these attractive properties, however, practical difficulties — such as possible clogging of the pores of the electrode membrane — can often limit the usefulness of these sensors in samples such as biological fluids. These limitations are eliminated in the recently introduced air-gap electrode which has been used successfully in a variety of analytical determinations, such as of ammonium ions in waste water [1] and in serum [2]; of urea [3—5] (via enzymatic degradation) and of hydrogencarbonate [2] in full blood, plasma and serum; of sulphur dioxide in wine [6]; of the total inorganic and organic carbon contents in waters [7]; and of the total inorganic nitrogen contents in aqueous systems [8]. The air-gap electrode is based on the same principle as other gas sensors, except that it does not have any gas-permeable membrane. The membrane is replaced by an air gap which separates the surface of the indicator electrode from the sample solution, thus effectively preventing problems associated with the presence of surfactants, organic substances or particulate matter in the sample solution.

Whereas earlier applications of the air-gap electrode have involved equilibrium measurements in thermodynamically stable systems, the aim of this paper is to demonstrate how the air-gap electrode can be used for kinetic procedures. The species chosen to illustrate this application are the enzymes urease and arginase, since the assay of their activity requires a kinetic rather than an equilibrium method.

The schemes for the enzyme-catalyzed reactions studied are illustrated in eqns. (1) and (2). In both cases the enzyme activity is determined by following the rate of formation of ammoniacal nitrogen with the air-gap electrode:

$$\text{Urea} \xrightarrow{\text{Urease}} CO_2 + 2\,NH_3 \qquad (1)$$

$$\text{L-Arginine} \xrightarrow{\text{Arginase}} \text{Urea} + \text{L-Ornithine} \xrightarrow{\text{Urease}} CO_2 + 2\,NH_3 \qquad (2)$$

The arginine—arginase system (eqn. 2), in which excess of urease is added in order to ensure complete and prompt conversion of all the urea formed to ammoniacal nitrogen, illustrates the feasibility of using a suitable coupled reaction for an indirect reaction rate determination; this is analogous to the coupled reaction techniques frequently used in spectrophotometric assays.

The reaction rates are determined by monitoring the first few percent of the enzyme reaction; the initial slope of the rate curve then is proportional to the enzyme concentration. For analytical applications this method is undoubtedly the fastest and most direct one [9].

EXPERIMENTAL

Apparatus

The apparatus and the air-gap electrode assembly were in principle identical to those described previously [3], where the microchamber was used. In order to maintain strict temperature constancy, the electrode assembly was thermostated by placing the Perspex tube, containing the combination electrode, in a hollow Perspex block, through which water at constant temperature was passed. The water was then in turn passed through a brass block furnished with a coaxial hole (diameter 23.0 mm, depth 12.5 mm) and fitted with a soft O-ring serving as a gasket. Polyethylene vials fitting closely into the chamber cavity were used to hold the samples and the magnetic stirring bar. This arrangement permitted the temperature of the system to be maintained within ±0.1 °C.

The electrolyte solution was $1.0 \cdot 10^{-2}$ *M* ammonium chloride plus 1.0 *M* sodium nitrate to which was added 0.01 % (w/w) wetting agent. The electrolyte was applied to the electrode as outlined previously [3], *i.e.*, the layer was renewed after each measurement.

In order to monitor the reaction rates directly, a home-made antilog converter was inserted between the pH meter (Radiometer, PHM 51) and the recorder (Radiometer, REC 51/REA 112) so that the recorder registered the concentration of ammoniacal nitrogen directly as a function of time. Only the dynamic measuring range of the electrode was used, *i.e.*, the concentration range within which there is linearity between the logarithm of the concentration of ammoniacal nitrogen and the electrode potential. The concentration scale registered on the recorder was calibrated with ammonium chloride standard solutions adjusted to the same ionic strength and pH as used in the actual enzyme rate determinations.

All pipetting was done with MLA precision pipettes (Medical Laboratory Automation Inc.), having a precision of ±1 %.

Enzymes

Urease (E.C. No 3.5.1.5, from jack beans, Worthington Biochemical Corp.). The enzyme activity, determined by the standard procedure of Gorin *et al.* [10], was found to be 43 units mg^{-1}; one unit corresponds to the formation of 1 μmole of ammoniacal nitrogen per min under the conditions of the standard assay (0.25 *M* urea; 2.5 mg of serum albumin per 10 ml; 0.385 *M* KH_2PO_4/Na_2HPO_4, pH 7.0; and 25.0 °C).

Arginase (L-arginine urea hydrolase, E.C. No 3.5.3.1 from bovine liver, Sigma Chemical Co.). The enzyme activity, determined by the standard procedure [11], was found to be 18 units mg^{-1}, where one unit corresponds to the formation of 1 μmole of urea per min. Solutions of arginase were prepared by preincubating for 4 h at 37 °C in 0.05 *M* manganese(II)—maleate buffer of pH 7.0, with 1 ml of buffer per mg of enzyme; the manganese buffer was prepared from $MnSO_4$ and maleic acid, the pH being adjusted to 7.0 with sodium hydroxide. The conditions of the standard assay procedure were: 0.285 *M* L-arginine, pH 9.5 (HCl), and 37.0 °C.

Chemicals and reagents

All the chemicals used were of p.a. quality. Redistilled water was used in preparing all solutions.

Solutions of the substrate and enzyme were prepared in 0.5 *M* TRIS (tris-(hydroxymethyl)aminomethane). The total buffer concentration was 0.5 *M*, so that changes in pH and ionic strength resulting from the enzymatic reactions could be neglected. The pH was adjusted with hydrochloric acid to 8.20 and 8.70 for the urease and arginase determinations, respectively.

While the solutions of urease in 0.5 *M* TRIS were used as prepared, the arginase was first incubated in the manganese(II)—maleate buffer (see above) and then diluted with 0.5 *M* TRIS to the appropriate volume. Subsequent measurements were carried out within about 4 h.

The stock solutions of urea and arginine were $4.0 \cdot 10^{-2}$ *M* in 0.5 *M* TRIS.

Procedure

The volume of the reaction mixtures was 400 μl in all cases.

For the urease determinations, 200 μl of urease solution of varying activity was added to 200 μl of urea stock solution, *i.e.*, the urea concentration in the mixture was $2 \cdot 10^{-2}$ *M*. The pH was 8.20 (0.5 *M* TRIS), and the temperature was 22.0 ± 0.1 °C.

In the arginase determinations, which were done at 24.0 ± 0.1 °C, 100 μl of arginase of varying activity was added to 200 μl of L-arginine stock solution

and 100 μl of urease solution, thus yielding a mixture of $2 \cdot 10^{-2}$ *M* in L-arginine. The pH was 8.70. The urease activity used (8 units in the final mixture) was found to be sufficient; no changes in the measured reaction rate were observed at the highest arginase activity even when the urease activity was reduced to half its initial value.

RESULTS AND DISCUSSION

Three typical rate curves are shown in Fig.1 for the urea—urease system. The concentration of the ammoniacal nitrogen formed, *i.e.*, $[NH_3] + [NH_4^+]$, *versus* time was directly recorded. The concentrations were established by calibration with standard solutions of ammonium chloride in 0.5 *M* TRIS of the same pH as used in the rate measurements. The lower portions of the curves are dashed, since the lower limit of the dynamic measuring range of the electrode was found to be *ca.* $3 \cdot 10^{-4}$ *M*, which agrees with the value predicted from the graphical method described by Hansen and Larsen [12], for the following parameters: $[NH_4^+]_e = 10^{-2}$ *M*; $pk_a = 9.3$ and log $p' = -1.1$ (partial conversion pH = 8.20). Because of the lack of proportionality between electrode response and concentration below $3 \cdot 10^{-4}$ *M*, the non-linear parts of the rate curves at the start of the reactions cannot be interpreted directly as a lag phase. The curves on Fig.1 comprise only 4 % of the conversion of the initial urea concentration, since $1.6 \cdot 10^{-3}$ *M* ammoniacal nitrogen corresponds to the conversion of $8 \cdot 10^{-4}$ *M* urea (eqn. 1), the initial concentration being $2 \cdot 10^{-2}$ *M*.

The slopes of the linear section of the rate curves, *i.e.*, between *ca.* $5 \cdot 10^{-4}$ and $1.6 \cdot 10^{-3}$ *M* in Fig.1, are representative of the reaction rates and hence

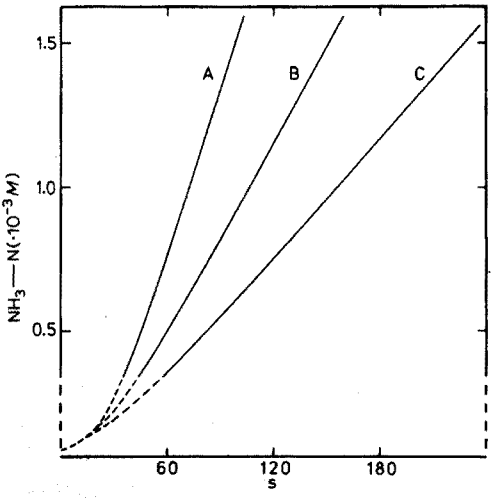

Fig.1. Typical rate curves for the urea—urease reaction. A, B and C correspond to $1.82 \cdot 10^{-2}$, $1.09 \cdot 10^{-2}$, and $7.28 \cdot 10^{-3}$ mg of urease, respectively.

of the urease activities. For the arginine—arginase system entirely analogous rate curves were obtained, *i.e.*, with linearity between $5 \cdot 10^{-4}$ and $1.6 \cdot 10^{-3}$ *M*.

A condition for the determination of the reaction rates (and thus the enzyme activities) in this simple approach is, of course, that the response time of the electrode does not influence the rate curves. In order to check this, some rate curves were calculated for the urea—urease system by removing samples of the reaction mixtures at fixed time intervals and destroying the enzyme by addition of an equal volume of 2.5 *M* sodium hydroxide; the concentration of ammoniacal nitrogen was then measured with the air-gap electrode [1]. The rate curves calculated on this basis were in excellent agreement with those recorded directly (Fig.1); for the two calculated rate curves the slopes in the range $5 \cdot 10^{-4}$—$1.6 \cdot 10^{-3}$ *M* ammoniacal nitrogen were $2.0 \cdot 10^{-4}$ and $5.5 \cdot 10^{-4}$ *M* min^{-1}, while the slopes of the corresponding curves obtained experimentally were (as an average of two runs) $1.96 \cdot 10^{-4}$ and $5.48 \cdot 10^{-4}$ *M* min^{-1}, respectively. It can therefore be concluded that the response time of the electrode does not influence the recorded signals when rates of this order of magnitude are monitored.

In Fig.2 are shown the results for the urease and the arginase determinations. The reaction rates, measured by the slopes of the rate curves (Fig.1), are plotted against the quantity of enzyme in the reaction chamber (liquid volume 400 μl); each point on the figure represents the mean value of two identical experiments. For five identical experiments with $1.09 \cdot 10^{-2}$ mg of urease, the relative standard deviation was 2.8 %.

According to the Michaelis—Menten equation for enzyme catalysis, straight-line relationships such as those in Fig.2 are to be expected. The arginase plot has a linear range of 1.2 decades. The urease plot, however, shows a slight

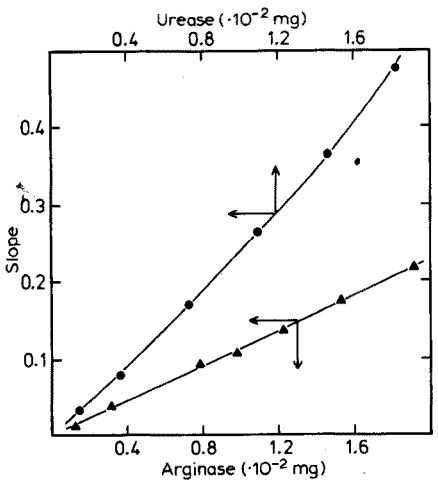

Fig.2. The slope of the rate curves as a function of the amount of enzyme present in the reaction mixtures. (●) Urease, pH 8.20, 22.0 °C. (▲) Arginase, pH 8.70, 24.0 °C. One unit on the ordinate axis corresponds to 1 μmole of ammoniacal nitrogen produced per min.

positive deviation at high enzyme activities, although the curve is still so smooth that it can be readily used as a calibration curve for urease determinations within the interval investigated, that is, 1.1 decade, without difficulties.

The pH value used in the urease determinations, 8.20, is a compromise between the lower limit of sensitivity of the electrode [12] and the optimal pH, 7.0, for the urea—urease reaction [13]. At pH 8.20 under the conditions used, calculation on the basis of Fig.2 shows that the urease activity is about 60 % of the activity found under the conditions of the standard assay, *i.e.*, at pH 7 and 25 °C.

Because the optimal pH (10.2) for the arginine—arginase reaction [14] is too high for the coupled urea—urease indicator reaction, a compromise pH of 8.70 was chosen. Based on Fig.2, the arginase activity calculated (2 moles of ammoniacal nitrogen corresponds to 1 mole of urea) for these experimental conditions is 32 % of the activity found at pH 9.5 and 37 °C, the conditions of the standard assay of arginase.

The results presented in Figs.1 and 2 show that the air-gap electrode is well suited for kinetic methods of analysis, here represented by analysis for enzymes producing ammoniacal nitrogen. With a glass electrode as the indicator electrode, the air-gap electrode can, of course, be used only when one of the products or reactants in the enzymatic reaction, or any coupled reaction, is a protolytic gas; and for kinetic measurements the operational pH range is restricted to the intervals within which the electrode exhibits a Nernstian response to that gas. A simple method for predetermining suitable pH ranges has recently been described [12].

However, this restriction is compensated by the advantage of not being forced to place the sensor in the reaction mixture itself. For example, Guilbault *et al.* [15] and Katz [16] have used ammonium-selective electrodes for urease analyses, but the strong interferences to which the ammonium ion electrodes are subject, particularly from sodium and potassium ions, seriously limit the applicability of these sensors, especially in biological fluids. In order to overcome the sodium and potassium interferences, Guilbault and Hrabankova [17] pretreated the samples by ion exchange, which is not only time-consuming but involves considerable dilution resulting in poorer limits of detection. Thus the high selectivity of gas electrodes in general combined with the air-gap principle, should prove to be a valuable extension of existing potentiometric methods for enzyme and enzymatic analysis. This was initially demonstrated for enzymatic analysis by Hansen and Růžička [3], and by Guilbault and Tarp [4], for urea analyses, and is further proven in this paper.

The enzyme analyses discussed here can be extended to kinetic substrate analysis, since kinetic analysis based on only the initial rate has advantages over equilibrium methods in many instances [9]. Kinetic substrate analysis with the air-gap electrode is currently being investigated in this laboratory. Initial experiments are centered around ammoniacal nitrogen-producing substrates, such as urea and L-amino acids with urease, L-amino acid oxidase and arginase, but will be further extended (for substrate as well as for enzyme

analysis) to substrates which liberate carbon dioxide, since the air-gap electrode as described by Fiedler *et al.* [7] is an excellent carbon dioxide electrode.

The authors wish to express their appreciation to the Danish Natural Science Research Council for partial financial support of this study and for a Guest Professorship for one of us (G.G.G.).

SUMMARY

The air-gap electrode has been used in kinetic chemical analysis, illustrated by the assay of the activities of the enzymes urease and arginase. The determinations are based on monitoring the initial reaction rates of the selective release of ammoniacal nitrogen, which in the arginine—arginase system was ensured by adding excess of urease. The reaction rates measured are in the range $2.5 \cdot 10^{-5}$—$1.5 \cdot 10^{-3}$ M min^{-1}; the relative standard deviation is *ca.* 2.8 %.

REFERENCES

1 J. Růžička, E.H. Hansen, P. Bisgaard and E. Reymann, Anal. Chim. Acta, 72 (1974) 215.
2 J. Růžička and E.H. Hansen, Anal. Chim. Acta, 69 (1974) 129.
3 E.H. Hansen and J. Růžička, Anal. Chim. Acta, 72 (1974) 353.
4 G.G. Guilbault and M. Tarp, Anal. Chim. Acta, 73 (1974) 355.
5 G.G. Guilbault and V. Stokbro, Anal. Chim. Acta, 76 (1975) 237.
6 E.H. Hansen, H. Bergamin Filho and J. Růžička, Anal. Chim. Acta, 71 (1974) 225.
7 U. Fiedler, E.H. Hansen and J. Růžička, Anal. Chim. Acta, 74 (1975) 423.
8 E.H. Hansen, J. Růžička and N.R. Larsen, Anal. Chim. Acta, 79 (1975) 1.
9 H.B. Mark and G.A. Rechnitz in P.J. Elving and I.M. Kolthoff (Ed.), Chemical Analysis, Vol. 24, Interscience-Wiley, New York, 1968.
10 G. Gorin, E. Fuchs, L.G. Butler, S.L. Chopra and R.T. Hersh, Biochemistry, 1 (1962) 911.
11 Worthington Enzyme Manual, Worthington Biochemical Corp., New Jersey, U.S.A., 1972.
12 E.H. Hansen and N.R. Larsen, Anal. Chim. Acta, 78 (1975) 457.
13 S.F. Howell and J.B. Sumner, J. Biol. Chem., 104 (1934) 619.
14 O.A. Roholt Jr. and D.M. Greenberg, Arch. Biochem. Biophys., 62 (1956) 454.
15 G.G. Guilbault, R.K. Smith and J.G. Montalvo, Jr., Anal. Chem., 41 (1969) 600.
16 S.A. Katz, Anal. Chem., 36 (1964) 2500.
17 G.G. Guilbault and E. Hrabankova, Anal. Chim. Acta, 52 (1970) 287.

Analytica Chimica Acta, 79 (1975) 17—26

A UREA-SENSING MEMBRANE ELECTRODE FOR WHOLE BLOOD MEASUREMENTS

D.S. PAPASTATHOPOULOS* and G.A. RECHNITZ
Department of Chemistry, State University of New York, Buffalo, New York 14214 (U.S.A.)
(Received 10th April 1975)

Recently, an automated system for serum urea determinations based on membrane electrodes was described [1], and other workers have published reports [2—4] on urea-sensing enzyme electrodes for use with serum and urine samples as part of the general development of enzyme electrodes [2—9]. A modified electrode system which is suitable for the analysis of whole blood as well as serum has also been reported [10]. While routine analyses in clinical laboratories are generally carried out on serum samples, the current trend toward "stat" and bedside measurements requires sensors which can function in whole blood with a minimum of sample handling and treatment.

This paper describes a sensor designed to function as a urea electrode in such whole blood and serum samples. The requirements of such a device involve good precision and accuracy of the response in the physiological concentration range, a fairly rapid response time, a lifetime of days or weeks in hard use, as well as simple and reliable preparation. It will be seen that these criteria have been largely met in the proposed electrode system which represents an attractive analytical tool for whole blood samples. The electrode employs a small volume of urease enzyme solution in Tris—EDTA buffer to form a thin layer between an outer dialysis membrane and the gas-permeable membrane of a commercial ammonia electrode. The resulting electrode shows good stability and reproducibility with a lifetime of at least three weeks.

EXPERIMENTAL

Apparatus

The urea enzyme electrode was assembled on an Orion ammonia gas-sensing electrode, Model 95-10. Potential measurements were recorded with a Beckman pH/mV recorder, Model 1055. All measurements in standard urea solutions were carried out in a 100-ml thermostated cell at 25 ± 0.5 °C. For the serum and whole blood measurements a 10-ml thermostated cell was used. For routine analysis in whole blood samples, a 10-ml beaker and a Corning Model 12 pH meter were used.

*On leave from the University of Athens, Greece.

A Beckman grating spectrophotometer Model DB-G was used for the spectrophotometric determination of urea in whole blood.

The mathematical treatment of the experimental data and the construction of calibration curves was done with a Hewlett-Packard Model 9100A calculator and plotter.

Reagents

Analytical-grade reagents were used to prepare all buffers and standard urea solutions. All solutions were prepared with distilled deionized water and stored under refrigeration. A 0.1 M Tris buffer and a 0.1 M Tris—10^{-3} M EDTA buffer were made from tris(hydroxymethyl)aminomethane and adjusted to pH 7.0 with hydrochloric acid [11]; for the Tris—EDTA buffer, an appropriate amount of EDTA—disodium salt was dissolved in the Tris solution before the pH adjustment.

The enzyme urease was obtained from Sigma Chemical Co., (type III, Powder Urease Jack Bean, 3700 units/g). The serum standards used were: serum calibration references "Calibrate" (General Diagnostics Div., Warner-Lambert Co.), and normal and abnormal clinical chemistry control serum (Metrix Clinical and Diagnostics Div., Armour Pharmaceutical Co.). The serum standards were reconstituted and stored under refrigeration according to the manufacturer's directions.

Expired date human blood from the Red Cross Blood Bank was used for the preliminary experiments. Fresh human blood samples were provided by the Blood Research Group of State University of New York at Buffalo. Also, ten human whole blood samples from different patients were obtained from Saint Mary's Hospital, Rochester, New York. Sodium citrate was used as the anticoagulant and the samples were stored [12,13] at +4 °C.

Electrode preparation

A 0.2-ml urease (110 units) solution was prepared in 0.1 M Tris—10^{-3} M EDTA buffer containing 150 mg of enzyme per ml. The enzyme solution was stored under refrigeration and could be used for at least two months without significant change of the activity.

Circular dialysis cellophane membranes, of the same size (diameter 1.27 cm) as the ammonia-permeable membranes, were made from dialyzing cellophane membrane sheets (Technicon, type C, part No. 105-1058, pore size 40—60 Å, and thickness 0.127 mm). A specially constructed cutting tool, similar to a paper punch, was used, but a sharpened cork borer works equally well if the thin membrane is held between two sheets of paper.

The gas-permeable membrane is installed with the "dimpled" side down on the spacer. A 10-μl portion of urease solution (5.5 units) is pipetted with an Eppendorf pipet on the "patterned" side of the membrane, and dispersed uniformly on the surface of the membrane by a sterilized glass rod. A cello-

phane membrane, carried by plastic tweezers, is fitted carefully on the enzyme-wetted membrane to avoid the trapping of air bubbles. Thus, a "sandwich" of two membranes with a very thin layer (ca. 80 μm) of enzyme solution is formed. The spacer containing the membranes is installed in the bottom cap of the electrode with the cellophane membrane down, towards the sample solution. The rest of the electrode is assembled according to the manufacturer's instructions [14]. A schematic diagram of the lower part of the assembled urea—enzyme electrode is shown in Fig.1.

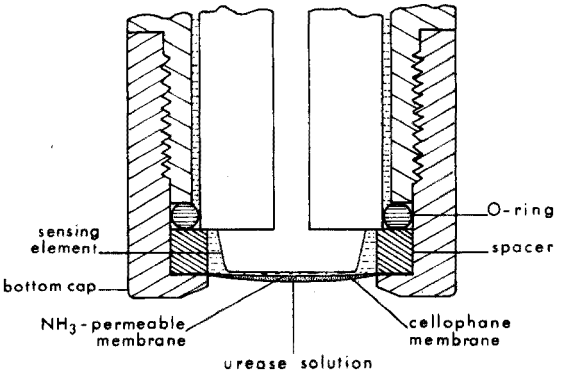

Fig.1. Schematic diagram of the urea-enzyme electrode.

The electrode must be preconditioned by soaking in 0.1 M Tris buffer for 1—2 h before use. Between measurements and overnight the electrode is also stored in the Tris buffer solution.

Procedure for potentiometric measurements in standard urea solutions

Potentiometric measurements for the construction of the calibration curves are done by pipetting aliquots of 1 M urea solution into a thermostated cell containing 100.0 ml of 0.1 M Tris buffer. The solution is magnetically stirred and the steady-state potential recorded.

Procedure for the determination of urea in serum

Reconstituted serum (1.0 ml) is pipetted into a small thermostated cell and 3.0 ml of 0.1 M Tris buffer is added. The solution is mixed with a small glass-coated stirring bar and the electrode immersed. The potential is recorded under stirring, until a steady-rate reading is established. The urea concentration is determined from a calibration curve constructed with separate samples from serum calibration reference solutions "Calibrate".

A standard addition method [15,16] was used in a parallel manner for the determination of urea in serum samples. The procedure was the same as above, except that 5 μl of 0.5 M urea solution was added and the new steady-state potential recorded. The urea concentration of the sample was calculated

from the standard addition expression, with the observed change in the electrode potential, ΔE, between the two measurements and the electrode slope, S. The electrode slope was obtained from a calibration curve. Between the measurements from sample to sample the electrode was rinsed well with distilled deionized water and wiped carefully with absorbent tissue.

Procedure for the determination of urea in whole blood

The standard addition method is used. The blood samples are measured without any pretreatment by mixing 1.0 ml of whole blood and 3.0 ml of 0.1 M Tris buffer in the thermostated cell. The above procedure for serum is used, with a 5-μl portion of standard 0.5 M urea solution for the standard addition.

For the spectrophotometric comparison determination of urea in whole blood, the direct nesslerization method of urease-treated samples was used, as described by Henry and Chiamori [17,18].

RESULTS AND DISCUSSION

A typical calibration curve for the urea enzyme electrode in 0.1 M Tris buffer at pH 7.0, is shown in Fig.2. The electrode develops a linear response for more than two decades of urea concentration, e.g. $5 \cdot 10^{-4}$—$7 \cdot 10^{-2}$ M (3—420 mg urea/100 ml). The slope of the linear portion of the curve is 90.7 mV per concentration decade, with a correlation coefficient of 0.9998.

The reproducibility of the potential measurements in standard urea solutions was periodically checked over a period of one week. The results shown in Table 1 refer to four separate sets of measurements made on the 1st, 2nd, 5th and 10th day after electrode preparation. After the 10th day a small

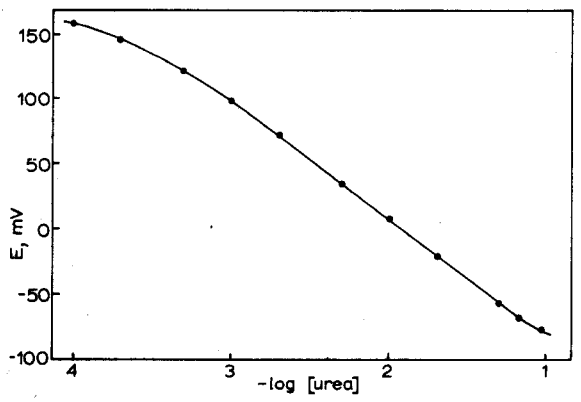

Fig.2. Calibration curve of the urea-enzyme electrode in 0.1 M Tris buffer (pH 7.0) with standard urea solutions.

TABLE 1

Reproducibility of the electrode potential in standard urea solutions

Urea		Electrode potential (mV)[a]
Concentration (M)	mg/100 ml	
$1.0 \cdot 10^{-4}$	0.6	156.2 ± 1.3
$5.0 \cdot 10^{-4}$	3.0	116.4 ± 1.0
$1.0 \cdot 10^{-3}$	6.0	94.8 ± 1.5
$4.97 \cdot 10^{-3}$	29.8	33.0 ± 1.4
$9.90 \cdot 10^{-3}$	59.4	−5.6 ± 1.4
$4.76 \cdot 10^{-2}$	285.6	−59.2 ± 1.2

[a]Average of four sets of measurements made on the 1st, 2nd, 5th, and 10th day after electrode preparation.

shift in the absolute millivolt values was observed, but the electrode slope remained constant for a period of twenty days. The electrode provides a satisfactory reproducible potential even at the lower concentrations. Thus, the non-linear portion of the calibration curve can be used, without significant error, for the determination of urea concentrations lower than $5 \cdot 10^{-4}$ M.

The response time of the electrode is of the order of 5 min when the electrode is shifted from a 10^{-3} M urea solution to a $5 \cdot 10^{-3}$ M solution, or from a 10^{-2} M urea solution to a $5 \cdot 10^{-2}$ M solution. Typical response curves are shown in Fig.3. The response time is longer when the electrode is used in whole blood or serum. In this case, the electrode requires 6—8 min to reach the steady-state potential. Urea electrodes prepared with enzyme solutions containing 25—75 mg enzyme/ml show smaller slope values and generally slower response time.

The electrode behaves in almost the same manner in both aqueous and serum solutions (Fig.4); the calibration curves were obtained from standard urea solutions (curve A) and serum calibration reference solutions (curve B) in 0.1 M Tris buffer. The electrode shows linear response in serum solutions containing 6.0—200.0 mg urea/100 ml, or 2.8—93.4 mg blood urea nitrogen/100 ml, (urea, mg/100 ml = 2.145 × urea nitrogen, mg/100 ml). The normal values for blood urea nitrogen vary [18] from 5 to 25 mg/100 ml and the electrode overlaps this range. There is a shift of the serum calibration curve by about 10 mV, but the slope of the curve is the same as for standard urea solutions, 90 ± 1.5 mV, per concentration decade. The electrode slope remains stable for a period of three weeks; this was checked with serum calibration reference solutions. The stability of the electrode was checked with the same serum reference "Calibrate" (10 mg urea nitrogen/100 ml) for 21 days after electrode preparation; the measurements were made by the standard addition method on freshly prepared samples and the electrode slope was checked with standard urea solutions. Over the 3-week period, the average value found was 10.1 ± 0.3 mg urea nitrogen/100 ml. The same electrode was used during

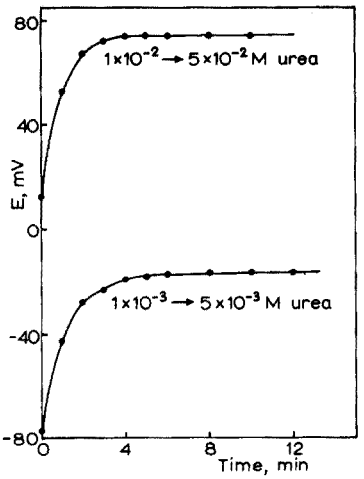

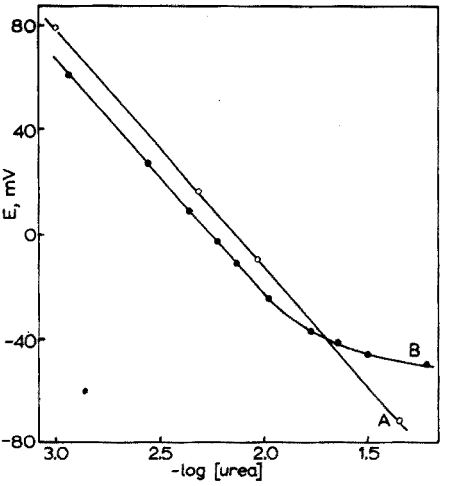

Fig.3. Dynamic response curves of the urea-enzyme electrode.

Fig.4. Comparison of calibration curves for urea in aqueous (curve A) and serum (curve B) samples.

the same period of time to carry out over 150 analyses in serum, whole blood and urea samples.

Analysis of serum and whole blood samples

For the determination of urea in serum samples two different procedures were used, i.e. a calibration curve method and a standard addition method. For the construction of the calibration curve (Fig.5), "Calibrate" serum calibration reference solutions were used; separately prepared Calibrate and Metrix control serum samples were used as unknowns. Typical results from

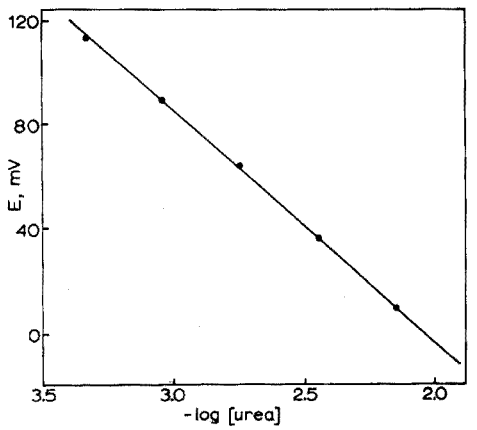

Fig.5. Typical calibration curve for the determination of urea in serum.

both methods are given in Table 2. Both methods gave about the same reproducibility of 3 %. The standard addition method is simpler, faster and cheaper than the calibration curve method because the electrode yields the same slope in both serum and standard urea solutions. Therefore, the slope can be checked periodically with standard urea solutions instead of the expensive serum calibration reference solutions.

TABLE 2

Determination of urea in serum

Taken[a]	Found[b]		Error (%)
Urea-N (mg/100 ml)	Urea-N (mg/100 ml)	Urea (mg/100 ml)	
Calibration curve method			
5.0	5.6 ± 0.0	12.0	−12.0
10.0	10.1 ± 0.1	21.6	+1.0
20.0	19.8 ± 0.4	42.4	−0.5
40.0	40.3 ± 0.4	86.2	+0.8
79.0	80.7 ± 0.5	171.3	+2.2
12.0	11.4 ± 0.0	24.4	−5.0
49.0	47.6 ± 0.3	101.8	−2.8
		Ave. error	3.47 %
Standard addition method			
5.0	5.1	10.9	+2.0
10.0	10.2	21.8	+2.0
20.0	19.0	40.7	−5.0[c]
40.0	41.6	89.0	−3.8
		Ave. error	3.20 %

[a] "Calibrate" serum calibration reference solutions.
[b] Average of four measurements.
[c] The relative standard deviation (n = 5) for 20 mg of urea nitrogen was 3.20 %.

The standard addition method was also used for the determination of urea in whole human blood. For the development of the procedure, expired date human blood from the Red Cross Blood Bank was used. The procedure was checked with fresh blood samples obtained by a venipuncture technique from human adults and analyzed without any pretreatment within 72 h [19]. Concurrently, the samples were also analyzed spectrophotometrically [17,18].

Results obtained with the urea enzyme electrode are compared with the spectrophotometric results in Table 3. The differences between the results of the two methods are not important for clinical situations because urea values in blood, serum or plasma are usually reported without significant figures after the decimal point [18—20].

For a preliminary evaluation of the electrode under simulated routine analysis conditions, ten whole blood samples from hospitalized human pa-

TABLE 3

Comparison of the results of urea determinations in whole blood

Donor	Spectrophotometry		Enzyme electrode		Difference (%)
	Urea-N (mg/100 ml)	Urea (mg/100 ml)	Urea-N[a] (mg/100 ml)	Urea (mg/100 ml)	
D.P.	9.8	20.0	10.3 ± 0.2	22.0	9.1
A.P.	7.7	16.5	8.4 ± 0.3	17.9	7.8
M.S.	13.6	29.5	13.8 ± 0.3	29.5	1.3
R.W.	11.9	24.5	11.8 ± 1.1	25.2	2.8
				Average	5.25

[a] Average of four measurements.

tients were analyzed within 24 h, by the standard addition method. All the measurements were carried out in a 10-ml beaker at room temperature and the millivolt readings were obtained from a Corning pH meter. The electrode slope was determined from standard urea solutions. The same samples had been analyzed at the hospital by the urease-glutamic dehydrogenase method in a DuPont Automatic Clinical Analyzer (ACA) [21]; comparative results are shown in Table 4. The results are also shown in a correlation plot (Fig.6) which indicates good agreement between the two methods. A paired "Student's t" test showed no statistically significant difference (t = 0.691: critical t = 2.262 for 95 % confidence limits). It should be noted the samples included blood from a uremic patient (No. 8). The uremic sample showed acceptable agreement for the two analysis methods and a standard deviation of 0.8 mg/100 ml for four measurements.

TABLE 4

Comparison of the results of urea determinations in whole blood by spectrophotometric analysis and the electrode standard addition method

Patient no.	Urea nitrogen (mg/100 ml)		Difference (%)
	Spectro. method (ACA)	Enzyme[a] electrode	
1	12.2	12.3	0.8
2	18.6	18.0	3.2
3	16.6	17.5	5.4
4	19.0	17.7	6.8
5	10.2	10.2	0.0
6	22.0	21.4	2.7
7	13.2	13.9	5.3
8	29.8	28.6	4.0
9	11.6	12.5	7.7
10	18.0	18.1	0.5
		Average	3.64

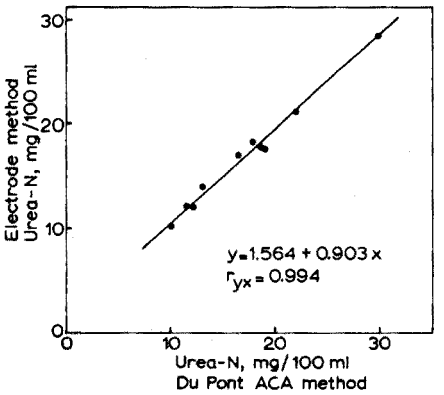

Fig. 6. Comparison of the electrode method for the blood urea determination with the DuPont (ACA) Automatic Clinical Analyzer method (Correl. Coef. 0.994, slope 0.903, intercept 1.56 mg/100 ml).

It can be seen that the electrode method gives excellent results in aqueous, serum, and whole blood samples. The electrode system can be routinely assembled within minutes and has a useful lifetime of at least three weeks in regular use. This good stability and durability can be attributed, in part, to the addition of the EDTA to the enzyme solution layer; the EDTA acts as a stabilizer by complexing trace metals which inhibit urease enzyme activity [22]. The use of the thin dialysis membrane as the outer membrane facilitates diffusion of the substrate into the enzyme solution layer but screens out bulk constituents present in body fluids. Finally, the use of the ammonia-sensing gas electrode largely eliminates interferences from molecular and ionic constituents present in body fluids [1]. The combination of these features yields an electrode system whose overall characteristics are appropriate for clinical whole blood samples with a minimum of sample pretreatment or instrumental cost.

We gratefully acknowledge support of a grant from the National Institutes of Health. Special thanks are due to June Nogle for assistance with the hospital samples.

SUMMARY

The construction and properties of a new urea-sensing membrane electrode capable of making direct urea measurements in whole blood are described. The electrode has a layered structure in which a small quantity of EDTA-stabilized urease enzyme solution is held between an external dialysis membrane and the gas-permeable membrane of a conventional ammonia selective electrode. It is shown that the electrode functions reliably in whole blood samples, used with minimal pretreatment, as well as in serum or aqueous solutions. The range, dynamic response, lifetime, precision, and accuracy of the electrode system are appropriate for clinical measurements in whole blood or serum, and promise to simplify such analyses with an attendant reduction in costs.

REFERENCES

1 R.A. Llenado and G.A. Rechnitz, Anal. Chem., 46 (1974) 1109.
2 G.G. Guilbault and E. Hrabankova, Anal. Chim. Acta, 52 (1970) 267.
3 G.G. Guilbault, G. Nagy and S.S. Kuan, Anal. Chim. Acta, 67 (1973) 195.
4 G.G. Guilbault and M. Tarp, Anal. Chim. Acta, 73 (1974) 355.
5 G.G. Guilbault and J.G. Montalvo, J. Amer. Chem. Soc., 92 (1970) 2533.
6 J.G. Montalvo, Jr., Anal. Biochem., 38 (1970) 357.
7 G.G. Guilbault and F.R. Shu, Anal. Chem., 43 (1972) 2161.
8 G.G. Guilbault and G. Nagy, Anal. Chem., 45 (1973) 417.
9 T. Anfalt, A. Graneli and D. Jagner, Anal. Lett., 6 (1973) 969.
10 E.H. Hansen and J. Růžička, Anal. Chim. Acta, 72 (1974) 353.
11 J.A. Dean (Ed.), Lange's Handbook of Chemistry, McGraw-Hill, New York, 11th edn., 1973.
12 A. Lamela, Introduction to Medical Laboratory Methods, Medical Dept., Harper and Row, New York, 1971.
13 R.P. MacFate, Introduction to the Clinical Laboratory, Year Book Medical Publishers, Chicago, 3rd edn., 1972.
14 Instruction Manual for the Ammonia Electrode, Orion Research Inc., Cambridge, Mass., 1972.
15 R.A. Durst (Ed.), Ion-Selective Electrodes, N.B.S. Spec. Publ. 314, 1969.
16 Newsletter, I(2) 10, 1969, and II(2) 7, 1970 Orion Research, Inc.
17 R.J. Henry and N. Chiamori, Amer. J. Clin.Pathol., 29, (1958) 277.
18 R.J. Henry, Clinical Chemistry: Principles and Technics, Hoeber Medical Div., Harper and Row, New York, 1968.
19 J.S. Annino, Clinical Chemistry: Principles and Procedures, Little, Brown and Co., Boston, 3rd edn., 1964.
20 CRC Handbook of Clinical Laboratory Data, CRC Co., Cleveland, 2nd edn., 1968.
21 C.E. Speicher, M.E. Fetrat, M.L. Fiske and J.B. Henry, Amer. J. Clin.Pathol., 57 (1972) 643.
22 Worthington Enzyme Manual, Worthington Biochemical Corp. Freehold, N.J., 1972.

Analytica Chimica Acta, 79 (1975) 27—34

SOLID-STATE ION-SELECTIVE ELECTRODES AS END-POINT DETECTORS IN COMPLEXIMETRIC TITRATIONS

PART II. BACK-TITRATIONS IN ACIDIC MEDIA

J.M. VAN DER MEER, G. DEN BOEF and W.E. VAN DER LINDEN

Laboratory for Analytical Chemistry, University of Amsterdam, Nieuwe Achtergracht 166, Amsterdam (The Netherlands)

(Received 28th April 1975)

In a previous paper [1] complexiметric titrations of mixtures of metal ions with end-point indication by means of a copper(II)-selective electrode have been discussed. In the present paper, mathematical expressions previously derived for complexiметric back-titrations at a mercury electrode [2] are used to obtain theoretical titration curves in the case of indication with a copper(II)-selective electrode. The theory is shown to be in excellent agreement with the experimental titration curves.

Back-titrations are to be preferred for the determination of metal ions which react slowly with the ligand or for metal ions which interfere with the electrode, like iron(III).

An electronic device which converts the measured potential directly to the metal ion concentration, was used to obtain linear titration curves.

THEORETICAL TITRATION CURVES

For the back-titration of a metal ion N, to which the ligand L is added in excess, with a metal ion M, the relationship between the titration parameter f and the metal ion concentration [M] cannot be easily expressed explicitly [2]. The f—[M] curve may be obtained from the relationships between f and [L] and between [M], f and [L]. If the volume does not change during the titration, the relation between f and [L] is given by:

$$f = \left(1 + \frac{1}{[L]K_{ML}}\right)\left(1 - \frac{[L]}{C_L} - \frac{C_N}{C_L}\frac{[L]K_{NL}}{1 + [L]K_{NL}}\right) \quad (1)$$

and

$$[M] = fC_L/(1 + [L]K_{ML}) \quad (2)$$

where

C_M, C_N and C_L are the concentrations of M, N and L in any form; $C = C_M + C_N$; [M], [N] are the concentrations of the metal ions M and N in any form, the

chelates ML and NL excepted; f (= C_M/C_L) is the titration parameter, if M is the titrant; and K_{ML} and K_{NL} are the conditional stability constants of the complexes ML and NL.

When another metal ion P is present either as a second element to be determined or as an indicator ion, a term for P similar to that of N appears in eqn.(1).

In further calculations, a relationship between [N] and [L] is also needed

$$[N] = C_N/(1 + [L]K_{NL}) \quad (3)$$

In order to obtain a theoretical titration curve, f vs. E, the same equation is used as in the previous paper [1]:

$$E = E' + S \log \{[Cu] + K'_{Cu,N}[N] + D_{Cu}\} \quad (4)$$

EXPERIMENTAL

Reagents

All solutions were prepared from analytical-grade chemicals and redistilled water. Metal ions were added as sulphates or nitrates.

Apparatus

Details about the construction of the electrode and its calibration have been given previously [1]. All measurements were made with a digital Philips pH meter PW 9408, in its mV-mode. The reference electrode was a Beckman saturated calomel electrode (no.39400) with a quartz junction.

An electronic device [3] was used to convert the potential from the mV-meter to a linear signal. This instrument offers the possibility of introducing values for E' and S obtained from calibration.

Procedure for potentiometric titrations

The solution (10 ml) containing the metal ion N and an excess of ligand, and buffered at pH 4.75 with $5 \cdot 10^{-2}$ M acetate buffer, was placed in the titration vessel; 5 or 10-μl increments of the copper(II) titrant were added at 2-min intervals from a Metrohm microburette E 457. The concentration of the titrant was such that between 100 and 200 μl were needed to reach the equivalence point.

RESULTS

The theoretical titration curves were calculated by means of eqns.(1—4). The theoretical and experimental titration curves did not fit when the selectivity coefficients determined for the direct titrations were used in the back-titrations. A decrease in the selectivity coefficients by a factor of 10 resulted

in a good fit. Hence the selectivity of the electrode appeared to be better in back-titrations than in direct titrations.

The limit of detection of the electrode as a function of the ligand concentration proved to be the same for Trien and EDTA. This suggests that the conditional stability constant has no influence on the value of the limit of detection. The solubility of the electrode material apparently is not the only factor which determines the limit of detection.

f—E Curves

Some typical examples of back-titrations are presented together with the theoretically expected curves. The theoretical and experimental curves for the titration of EDTA and Trien with copper(II) are presented in Figs.1 and 2 for

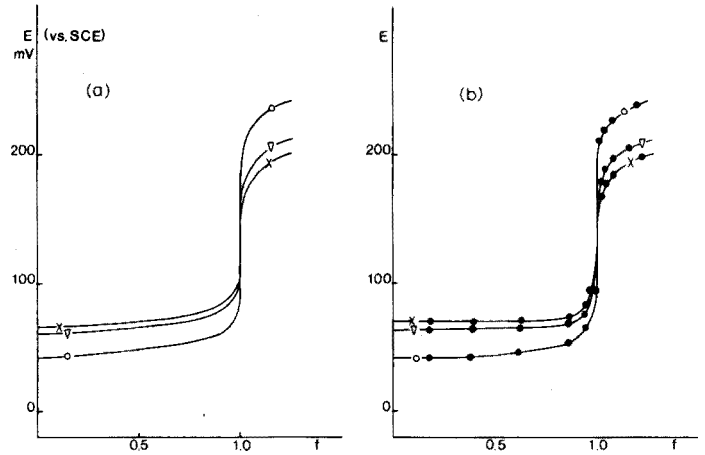

Fig.1. Titration curves for EDTA with copper(II). (-○-) 10^{-3} M, (-▽-) 10^{-4} M, (-x-) $5 \cdot 10^{-5}$ M. (a) Theoretical. (b) Experimental.

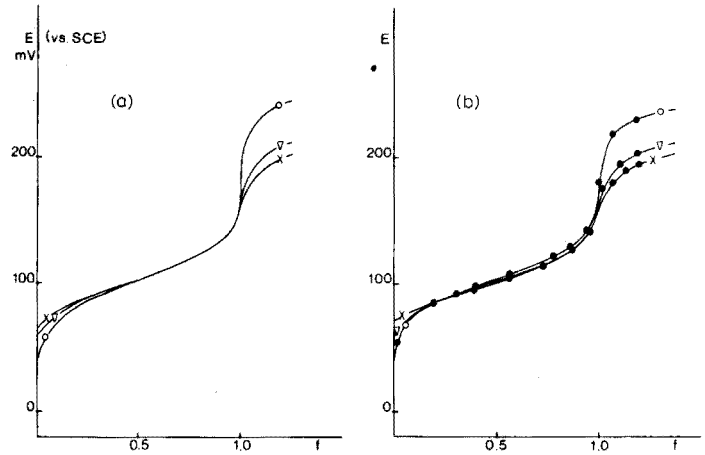

Fig.2. Titration curves for Trien with copper(II). (-○-) 10^{-3} M, (-▽-) 10^{-4} M, (-x-) $5 \cdot 10^{-5}$ M. (a) Theoretical. (b) Experimental.

different concentrations of the ligands. There is a good agreement between theory and experiment. If there were no influence from the limit of detection of the copper(II) electrode, the titration curves would coincide before the equivalence point and would be determined only by the conditional stability constant of the complex involved. This is indeed the case for Trien (Fig. 2(a)) apart from the beginning of the curve where the limit of detection of the electrode affects the titration curve. As would be expected, the limit of detection has a much more pronounced effect in the case of EDTA (Fig.1(a)) as the stability constant of the copper(II)—EDTA complex is much larger than that for the copper(II)—Trien complex.

From Figs.1 and 2 it can be concluded that EDTA is a much more suitable ligand for these back-titrations than Trien.

Figure 3 gives the theoretical and experimental titration curves for the back-titrations of $5 \cdot 10^{-4}$ M solutions of some metal ions with copper(II), the analytical concentration of EDTA being 10^{-3} M. There is a good agreement between the theoretical and experimental curves. Iron(III), nickel(II), zinc(II) and cadmium(II) can be determined, although for the latter two elements the accuracy and precision are less satisfactory. The stability constant of the complex of manganese(II) with EDTA is too small for the determination of this metal ion.

The theoretical curves for back-titrations of zinc(II) at different concentrations in an excess of EDTA with copper(II) and the corresponding experimental curves are shown in Fig.4. Here again is a good agreement between theory and experiment. The potential jump at the equivalence point is too small to allow the determination of $5 \cdot 10^{-5}$ M zinc(II).

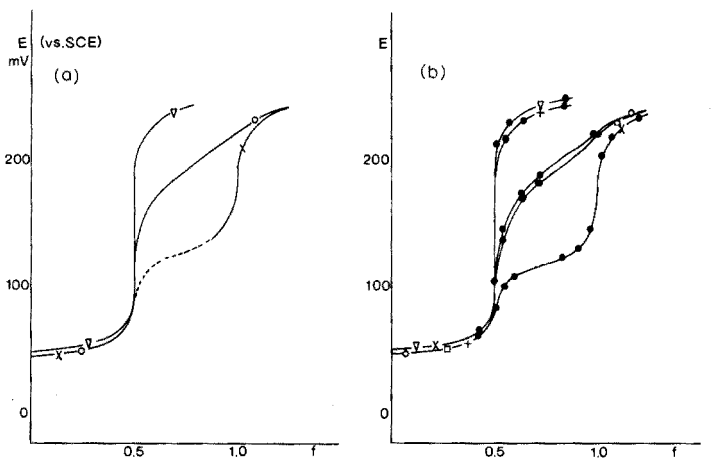

Fig.3. (a) Theoretical curves for the back-titration of $5 \cdot 10^{-4}$ M iron(III) (-▽-), zinc(II) (-○-) and manganese(II) (-x-) with copper(II). (b) Experimental curves for the back-titration of $5 \cdot 10^{-4}$ M iron(III) (-▽-), nickel(II) (-+-), zinc(II) (-○-), cadmium(II) (-□-) and manganese(II) (-x-). $C_{EDTA} = 10^{-3}$ M.

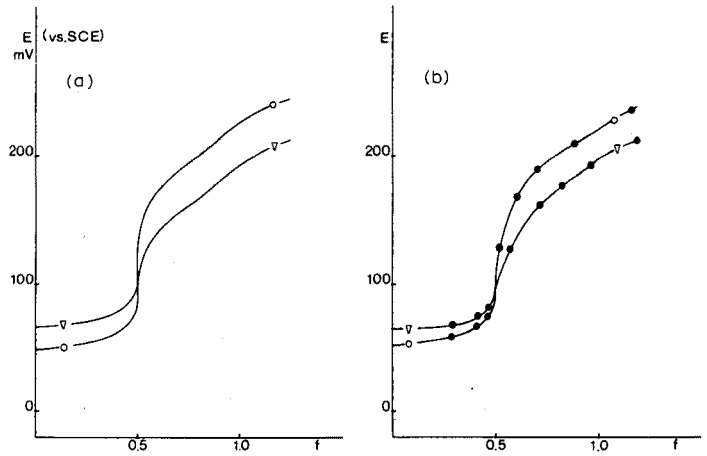

Fig.4. Titration curves for the back-titration of different concentrations of zinc(II) with copper(II). (–○–) $5 \cdot 10^{-4}$ M, (–▽–) $5 \cdot 10^{-5}$ M; $C_{EDTA} = 2C_{Zn}$. (a) Theoretical. (b) Experimental.

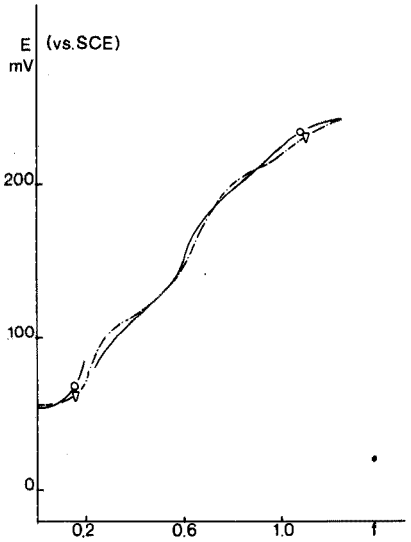

Fig.5. Theoretical (–○–) and experimental (–▽–) titration curves for the back-titration of a mixture of $4 \cdot 10^{-4}$ M manganese(II) and $4 \cdot 10^{-4}$ M zinc(II) with copper(II); $C_{EDTA} = 10^{-3}$ M.

Figure 5 shows the back-titration of a mixture of $4 \cdot 10^{-4}$ M manganese(II) and $4 \cdot 10^{-4}$ M zinc(II) in 10^{-3} M EDTA with copper(II); both theoretical and experimental curves are drawn. As the titration proceeds the relative importance of the limit of detection, D_{Cu}, decreases. The theoretical curve before $f = 0.2$ is the curve of the D_{Cu} value as a function of the free EDTA concentration, whereas the line after $f = 0.2$ does not take into account the limit of detection. From the experimental curve it can be seen, however, that D_{Cu} still slightly affects the curve for $f > 0.2$.

f—[M] Curves

As the *f—E* curves do not always produce satisfactory end-points, an attempt was made to obtain better end-points from linearized titration curves. According to eqn.(4):

$$10^{(E - E')/S} = [\mathrm{Cu}] + K'_{\mathrm{Cu,N}}[\mathrm{N}] + D_{\mathrm{Cu}} \qquad (5)$$

where N is a divalent ion. The electronic device produced a signal equal to $10^{(E - E')/S}$

In all the titrations mentioned so far, the metal to be determined was complexed by EDTA added in excess, so that the first equivalence point appeared when the excess of the ligand had been titrated. Further addition of the titrant resulted in a sharp increase in the copper(II) activity. The extent to which the activity increases depends on the conditional stability constants of both CuL and NL.

Theoretical and experimental linearized curves for the back-titration of zinc(II) are given in Fig.6. It is obvious that linearized curves still produce satisfactory end-points for $5 \cdot 10^{-5}$ M zinc(II). Even for the back-titration of a mixture of zinc(II) and manganese(II), each of the equivalence points can be obtained by linear indication (Fig.7).

In order to test the applicability of these back-titrations for routine analysis, the accuracy and precision for the back-titration of zinc(II) were determined

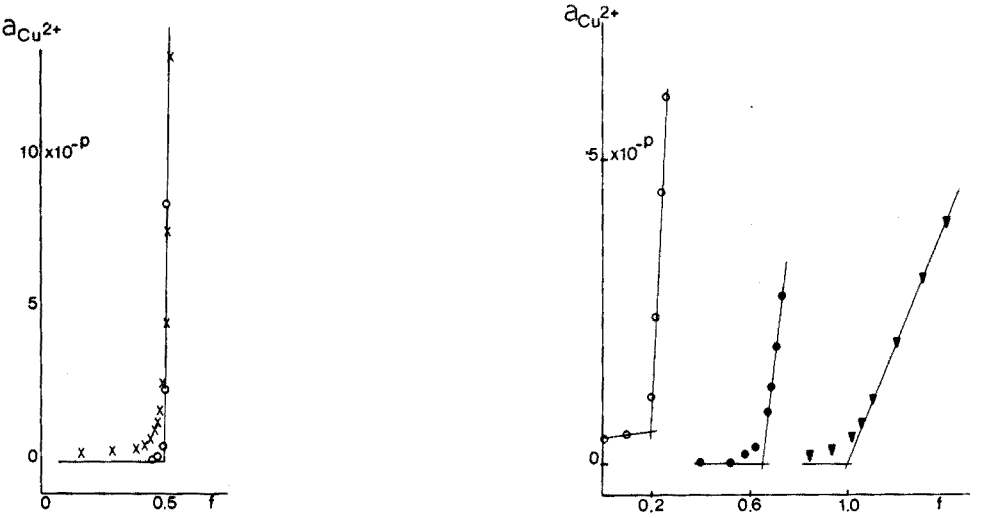

Fig.6. Theoretical and experimental linear titration curves for the back-titration of different concentrations of zinc(II). (-○-) $5 \cdot 10^{-4}$ M, (-x-) $5 \cdot 10^{-5}$ M, (—) Theoretical. $p_{\circ} = 8; p_{x} = 9$.

Fig.7. Experimental plots of the copper(II) activity vs. the titration parameter for the back-titration of a mixture of $4 \cdot 10^{-4}$ M manganese(II) and $4 \cdot 10^{-4}$ M zinc(II). The appropriate values of the scale on which the activity is plotted are: $p_{\circ} = 9$, $p_{\bullet} = 6$; $p_{\blacktriangledown} = 4$.

and compared with the titration of the ligands. Figure 8 shows the linearized titration curves for 10^{-4} M EDTA and Trien. The end-points are easily established and are almost independent of the scale on which the value of the activity is plotted. Table 1 gives the results of the titration of 10^{-3} M, 10^{-4} M and $5 \cdot 10^{-5}$ M solutions of EDTA and Trien respectively. Accuracy and precision proved to be satisfactory even for Trien which, however, cannot be used for the determination of zinc(II) because of the low value of the conditional stability constant of the zinc(II)—Trien complex. The linearized curves for the back-titration of zinc(II) can be seen in Fig.6. The results are summarized in Table 2. The accuracy and precision of the titration of $5 \cdot 10^{-4}$ M and $5 \cdot 10^{-5}$ M zinc(II) are adequate, but for 10^{-5} M zinc(II), large systematic errors occur. The scale on which the value of the activity is plotted strongly affects the accuracy of the titrations as is shown in Fig.9, where the same linearized curve for the back-titration of $5 \cdot 10^{-5}$ M zinc(II) is presented for three different scales. Correct end-points in the back-titration of zinc(II) can be obtained when the use of points of the titration curve far from the equivalence point is avoided. As discussed by Whitfield et al. [4], the end-point should be estimated from points within 10 % of the equivalence point.

In conclusion, it can be stated that a solid-state copper(II)-sensitive CuS/Ag_2S precipitate-based electrode (Selectrode) appears to be very well suited to complexiметric back-titrations of metal ions when copper(II) is used as the back-titrant and EDTA as the ligand. Potentiometric titration curves as well as linearized curves produce quite well defined end-points even for concentrations as low as 10^{-5} M.

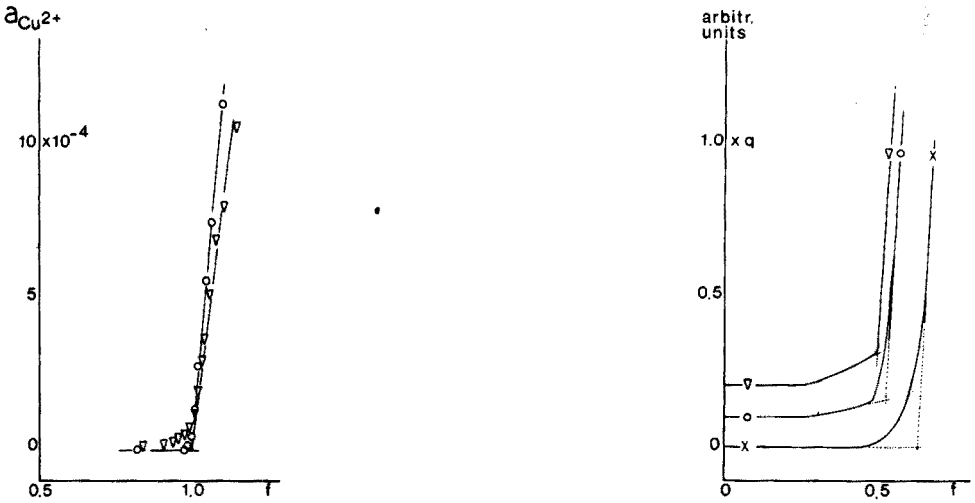

Fig.8. Experimental linear curve for the titration of 10^{-4} M EDTA (–○–) or Trien (–▽–) with copper(II).

Fig.9. Experimental linear curve for the back-titration of $5 \cdot 10^{-5}$ M zinc(II) for different values of the scale on which the activity is plotted. $q_{\nabla} = 5$, $q_{\circ} = 10$, $q_{x} = 100$.

TABLE 1

Titrations of EDTA and Trien with copper(II)

Ligand taken μmole/10 ml	Ligand found μmole/10 ml	Error (%)	s [a] (%)
EDTA			
9.950	9.950	0	0
0.995	1.012	+ 1.7	0.6
0.498	0.525	+ 5.4	1.0
Trien			
9.100	9.100	0	0.06
0.910	0.937	+ 2.6	0.6
0.455	0.487	+ 6.9	1.4

[a] For 3 determinations.

TABLE 2

Back-titration of zinc(II) in an excess of EDTA with copper(II)

Zinc(II) taken (μmole/10 ml)	Zn(II) found (μmole/10 ml)	Error (%)	s [a] (%)
4.775	4.784	+ 0.2	0.16
0.478	0.495	+ 3.3	0.5
0.0955	0.1075	+ 12.5	1.8

[a] For 6 determinations.

The authors are indebted to Miss M. Klaver and Mr. A. Moerkerken for experimental help.

SUMMARY

The determination of several metal ions in the concentration range 10^{-2}—10^{-5} M by means of complexiметric back-titrations with a copper(II)-selective indicator electrode is described. The ligand, in most cases EDTA, is added in excess, which is then back-titrated with copper(II). There is good agreement between the theoretical and experimental titration curves.

REFERENCES

1 J.M. van der Meer, G. den Boef and W.E. van der Linden, Anal. Chim. Acta, 76 (1975) 261.
2 U. Hannema and G. den Boef, Anal. Chim. Acta, 49 (1970) 35.
3 J.M. van der Meer and J.C. Smit, Chem. Instrum., in press.
4 M. Whitfield, J.V. Leyendekkers and J.D. Kerr, Anal. Chim. Acta, 45 (1969) 399.

Analytica Chimica Acta, 79 (1975) 35—45

AUTOMATED POLAROGRAPHIC ANALYSIS

PART I. DESIGN OF FLOW-THROUGH CELLS AND DEAERATION UNIT

WALTER LUND and LISE-NETTE OPHEIM

Department of Chemistry, University of Oslo, Blindern, Oslo 3 (Norway)

(Received 24th March 1975)

Automated analysis of discrete samples by the AutoAnalyzer principle (Technicon) has been widely applied in all types of chemical analysis. Usually the systems employ optical detection of the species of interest; the application of polarographic detection in automated analysis of this type has received relatively little attention. Lento [1] has studied the polarographic behaviour of cadmium, lead and zinc in an automated system of the AutoAnalyzer type, whereas Fleet *et al.* [2,3] have reported the determination of calcium and magnesium with a similar system. Recently, Silvestri *et al.* [4—6] and Cullen *et al.* [7] have described automated systems for the polarographic analysis of pharmaceutical products.

For automated polarographic analysis of discrete samples, the cell design is of great importance for proper functioning of the whole system; a cell with a small hold-up volume is essential for successful analyses of small sample volumes. In the present paper, the advantages and disadvantages of various types of polarographic flow-through cells are discussed.

In polarographic analysis dissolved oxygen must usually be removed from the sample solution before the measurement. In manual analysis this is usually done by bubbling nitrogen through the solution for 10—15 min. When a polarographic flow-through cell is used as detector in automated analysis, the problem of removing oxygen may be dealt with in different ways. For a system of the AutoAnalyzer type, the first thing to be considered is the use of an inert gas instead of air for segmenting the flow streams. Lento [1] claims that the solutions are saturated with the inert gas in this way, so that dissolved oxygen is removed, provided that the segmented stream is passed through a time-delay coil before entering the detector. Silvestri *et al.* [4—6] mixed their sample solutions with a large excess of deaerated supporting electrolyte, to minimize the effect of dissolved oxygen. Recently, Cullen *et al.* [7] reported effective deaeration by allowing the gas-segmented stream to pass a 14-turn mixing coil. None of these procedures removes dissolved oxygen completely, although the concentration of oxygen in the sample solutions is markedly diminished, as an equilibrium is attained between the

nitrogen and oxygen present inside the flow system. The introduction of a mixing coil into the flow system usually results in an increase in the response time of the system, owing to mixing of consecutive solutions.

In the present paper a new method of deaerating sample solutions in automated analysis is described; the deaeration is done before the sample solutions enter the flow system.

Automated polarographic systems seem to be particularly useful for pharmaceutical analysis. For the present investigation chlordiazepoxide in sulphuric acid was chosen as the model system. The polarographic determination of this compound has been reported previously [8]; in 0.01 *M* sulphuric acid chlordiazepoxide exhibits two polarographic waves, with half-wave potentials at −0.30 V and −0.65 V *vs.* Ag/AgCl, respectively. In all the experiments described here, a constant potential of −0.49 V was applied to the working electrode, and the resulting current was recorded as a function of time. The samples which were analyzed were either *ca.* 100 p.p.m. chlordiazepoxide in 0.01 *M* sulphuric acid, or solutions containing only the supporting electrolyte, *i.e.* 0.01 *M* sulphuric acid.

EXPERIMENTAL

Apparatus

The general outline of the automated system is shown in Fig.1. In principle it is based on the AutoAnalyzer system (Technicon), with a gas-segmented flow stream, which is moved by a peristaltic pump from the sampler to the detector unit. The sampler consisted of a sampler tray with 40 cups (2-dram vials), an electronic timer and a deaeration unit, all of which were built in this laboratory. However, commercially available instrumentation may be easily adapted to the present system. The movement of the peristaltic pumps (Ismatec, Mini-Micro 2; 20 r.p.m.) was controlled by the timer unit, which allowed the pumps to be stopped during the sample shifts. The halt period, which was adjustable, was usually set to 2 s.

The detector unit consisted of a flow-through cell, made of perspex, into which was fitted a dropping mercury electrode (DME) with a Radiometer B 400 capillary and a counter electrode. The counter electrode was either a platinum wire, a platinum gauze or a mercury pool (see below). The reference electrode, a Metrohm EA 427 Ag/AgCl saturated KCl electrode, was placed outside the cell, in the mercury waste bottle. The potential of the DME was controlled by a potentiostat, which was built in this laboratory. The current was recorded with a Radiometer Servograph REC 51. Pump tubing, debubbler and other equipment were purchased from either Technicon or Elkay. Unless otherwise stated, argon gas was used for deaeration of the sample solutions, and also for segmenting the flowing sample stream between the pump and the detector cell.

The flow-through cells and the deaeration unit needed are discussed in detail below.

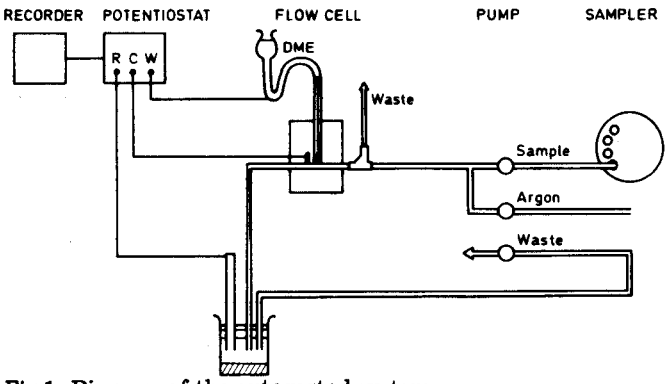

Fig.1. Diagram of the automated system.

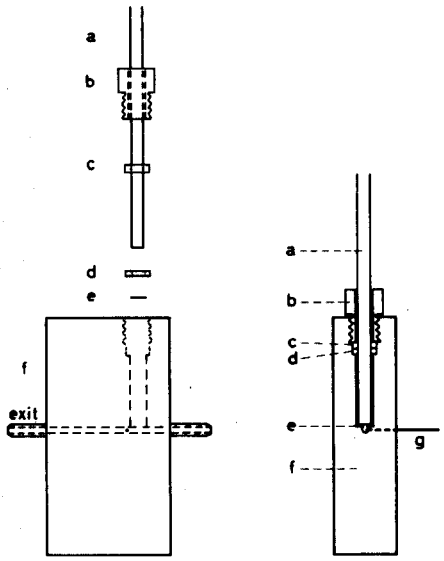

Fig. 2. Polarographic flow-through cell. (a) DME capillary; (b) screw; (c) metal ring, which is sealed to the capillary; (d) rubber o-ring; (e) thin rubber ring; (f) perspex cell; (g) platinum counter electrode. A cut through the cell is shown to the right. The cell is here turned 90°, relative to the left figure.

FLOW-THROUGH CELLS

Various designs of cell were studied; all the cells were made of perspex. The fitting of the DME capillary is illustrated in Fig.2. A metal ring (c) is sealed to the capillary (a) and a tight fitting is obtained by means of the screw (b) and a rubber o-ring (d). The diameter of the central hole through the cell is 2 mm. In Fig.2 the counter electrode is a platinum wire, which is sealed into the perspex near the DME. A slightly different approach is illustrated in

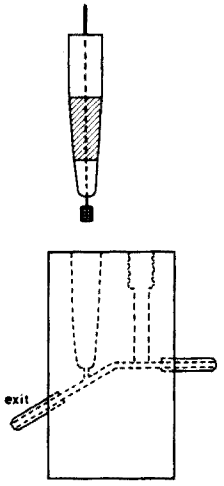

Fig. 3. Cell with a platinum gauze counter electrode.

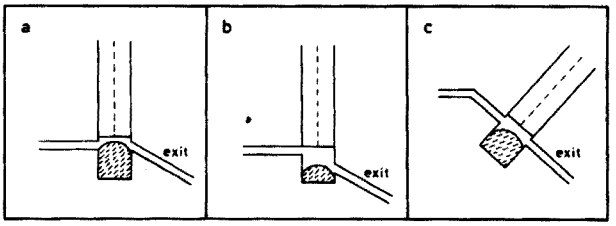

Fig. 4. Schematic drawing of the cells based on a mercury pool counter electrode.

Fig. 3, where a platinum gauze is used as counter electrode. Three cells, all based on a mercury pool counter electrode, are shown in Fig. 4. The functioning of the various cells is discussed below.

Fitting of the DME capillary

Surprisingly little information is available in the literature about the fitting of the DME capillary into the flow cell, although it is of great practical importance. The approach adopted by Lento [1], *i.e.* permanent sealing of all fittings into the cell with an epoxy resin, seems highly unsatisfactory, because it should be easy to remove the capillary from the cell for cleaning and exchange. It would also be advantageous to use ordinary capillaries directly; for this reason the procedure described by Blaedel and Strohl [9], who ground the capillary with mercury flowing through it, also seemed unattractive. Obviously there are many ways of solving these problems. The approach chosen here is illustrated in Fig. 2, and was used for all the cells shown in Figs. 2—4. A tight fitting of the DME capillary to the cell was obtained by means of a metal ring, which was sealed to the capillary, a rubber o-ring and a screw. With this arrangement the capillary can be removed easily from the cell, and replaced in exactly the same position. Correct positioning of metal ring (c) is important, to avoid high pressure on the capillary tip, as this would result in a somewhat irregular drop-time.

Problems associated with the mercury pool counter electrode

The first cells were made according to the design of Lento [1], with a mercury pool counter electrode. As a three-electrode system was used here, the reference electrode was placed outside the cell. In Lento's case the mercury pool served as the reference electrode; according to Lento, "The convex shape of the mercury meniscus formed by the pool prevented excess build-up of mercury in the cell, since the mercury droplets falling from the electrode did not coalesce with the mercury pool. Rather, owing to the sharp incline of the exit side of the cell, these droplets passed in a steady stream to waste". However, the stated behaviour of this type of cell (Fig. 4(a)) was not confirmed; the mercury drops accumulated at the mercury pool, instead of passing to waste, resulting ultimately in short circuiting of the working and counter electrodes. Hence, a cell with a slightly different design was made. With this cell (Fig. 4(b)), the mercury indeed passed through the exit tube without blocking the cell, but this happened only at irregular intervals, and so much mercury then left the pool at once that it caused irregularities in the flow rate. A cell similar to the one shown in Fig. 4(b) has recently been used by Cullen *et al.* [7].

A third version of the Lento cell was then made. The functioning of this cell (Fig. 4(c)) was better than that of the two earlier cells, but the marked tilting of the capillary gave rise to somewhat irregular drop times.

An additional disadvantage of all these cells based on a mercury pool counter electrode is that they have a relatively large hold-up volume. The various difficulties associated with the above cells can be ascribed to the mercury pool. Therefore, this design was abandoned, and the use of a platinum counter electrode was investigated. For the cells shown in Figs. 2 and 3 a platinum wire and a platinum gauze electrode, respectively, were used. Both these cells gave satisfactory results; the cell shown in Fig. 2 was easier to make, and was therefore preferred.

Electrode configuration

As can be seen from Fig. 1, the reference electrode was placed outside the cell, in the mercury waste bottle; this made the construction of the cell very simple. It was found that the *iR* drop between the reference and working electrodes was negligible.

As shown above, the position and size of the counter electrode may affect the performance of the cell. Preferably the counter electrode should be placed after the DME (in relation to the flow) so that the oxidation products are not detected by the working electrode, and it should be close to the working electrode, to minimize the *iR* drop between these electrodes. The area of the counter electrode did not appear to be critical, as the two cells (Figs. 2 and 3) functioned equally well. However, the large counter electrode was not so easily positioned close to the working electrode.

Position of debubbler

In an automated system of the AutoAnalyzer type the liquid flow is segmented by means of gas bubbles, to prevent cross-contamination of samples. These gas bubbles must be removed by a debubbler before the solution enters the detector. In order to obtain low response times for the system, the debubbler must be placed close to the working electrode. Fleet *et al.* [2,3] have described a cell in which a hole near the DME served as a debubbler. However, this arrangement was found not to provide effective and reliable removal of the gas bubbles.

DEAERATION UNIT

The deaeration unit is shown in Fig. 5. Dissolved oxygen is removed from three sample solutions (c) simultaneously, by bubbling argon gas through three thin outlets (b), while the sampling probe (a) dips into the left of these cups and aspirates the sample. At the end of the pre-set sampling time the sampling/deaeration head rises vertically, and the sampler tray rotates one notch, presenting the next sample cup for aspiration. With this arrangement, a given sample is deaerated for a time equal to twice the sampling time, before aspiration starts. The thin outlet tubes which are used allow very effective bubbling of the argon gas; this results in very effective deaeration of the small sample volumes (*ca.* 5 ml). Thus the simultaneous deaeration of only two sample solutions frequently provides satisfactory removal of oxygen, if the sampling time is not too short. The sampling probe and gas outlets (stainless steel syringe nozzles) are equipped with tips of polyethylene tubing. The position of the deaeration head can be adjusted relative to the sampler tray, by means of suitable adjustment screws.

The deaeration system described above may be easily adapted to commercial samplers, as explained later in this paper.

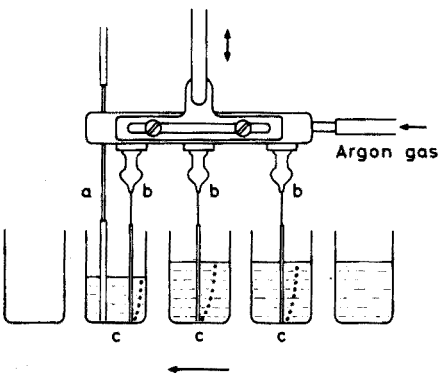

Fig. 5. Deaeration unit with sampling probe. (a) sampling probe; (b) gas outlets; (c) vials (2 drams) with sample solutions. The sampler tray moves from right to left as indicated.

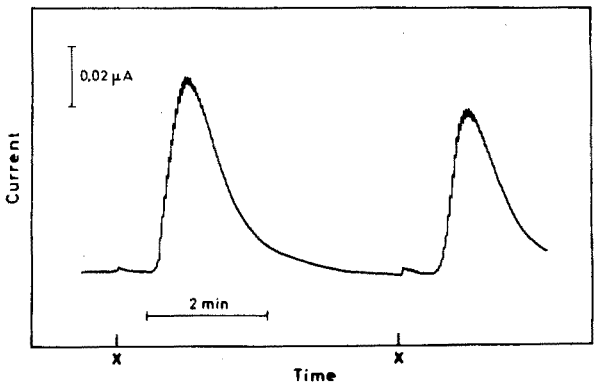

Fig. 6. Effect of dissolved oxygen on the current—time curve for separate samples of the supporting electrolyte, with only one gas outlet for deaeration. The potential is −0.49 V *vs.* Ag/AgCl. The sample shifts are indicated by *X*.

Effect of deaeration time

The effectiveness of the deaeration can be seen from Fig. 6, where a current—time curve for separate samples of the supporting electrolyte is shown; only one gas outlet, placed beside the sampling probe, was used in this case. When the aspiration starts (indicated by X), the sample solution is saturated with air, and as this solution reaches the detector, there is a marked increase in current, owing to the polarographic reduction of oxygen at −0.49 V. However, continuous bubbling of argon through the solution gradually removes oxygen, so that the current decreases and reaches a constant value after *ca.* 3 min, indicating that the oxygen has been removed. Thus, provided that the sampling time is kept above 3 min, deaeration may be carried out with a single gas outlet, positioned beside the sampling probe. However, the use of more than one gas outlet is recommended, as the sample solutions can then be completely deaerated before the aspiration starts. Alternatively, pump stoppage during sample shifts may be used for this purpose.

Effect of pump stop during sample shifts

When the sampling probe shifts from one sample cup to the next, air is normally drawn into the system. This air segment prevents consecutive sample solutions from being mixed, and is thus usually considered to be an advantage of the AutoAnalyzer system. However, when a polarographic detector is used, the introduction of air into the system causes an increase in the background current, owing to the polarographic reduction of oxygen. This is illustrated in Fig. 7, curve b, where a current—time curve for separate samples of the supporting electrolyte is shown. A high fluctuating background current is obtained in this case, although the sample solutions are fully deaerated before the aspiration starts, in contrast to the experiments described in the preceding

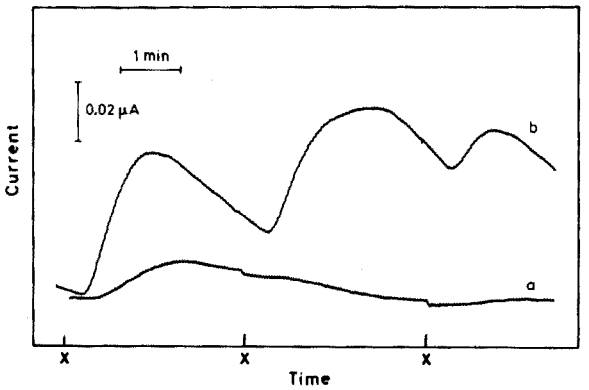

Fig. 7. Effect of oxygen, aspirated during the sample shifts, on the current—time curve for separate samples of the deaerated supporting electrolyte. (a) no pump stop; (b) pump stop during sample shifts. The sample shifts are indicated by *X*. The potential is −0.49 V *vs.* Ag/AgCl.

section. The aspiration of air into the system during the sample shift, which lasts *ca.* 1 s, may be prevented by halting the movement of the peristaltic pump during the transfer of the sampling probe. The resulting current—time curve (Fig. 7, curve a) indicates that a much lower background current is then obtained.

To make a more quantitative study of the effect of pump stop during sample shifts, series of solutions containing *ca.* 100 p.p.m. chlordiazepoxide were analyzed, both with and without pump stop during sample shifts; a wash solution was used between each sample. The pump stop procedure invariably gave the lower standard deviation. Typically, the relative standard deviations with and without pump stop were 1.2 % and 2.4 %, respectively, when a sampling time as well as a wash time of 2 min was used. Thus, as far as the precision of the method is concerned, the mixing of consecutive solutions, which will necessarily occur in the absence of an air segment between different samples, seems to be of minor importance compared to the effect of dissolved oxygen.

When a commercial sampler unit with a wash reservoir is employed, the technique with pump stop during sample shifts may be used with particular advantage. Apart from preventing the introduction of air into the system during the sample shifts, a complete deaeration of the sample solutions may be ensured before aspiration of the sample, with only a single gas outlet placed beside the sampling probe. This is done simply by extending the pump stop period so that aspiration of a new sample is not started until deaeration is complete. Finally, the pump stop technique facilitates the use of an "expanded-scale" procedure, which may be useful for improving the precision of the analytical method used [10].

Choice of inert gas

As indicated in Fig. 5, the sample cups used were open at the top. Hence, air could diffuse into the cups during deaeration. Experiments were carried out, with series of chlordiazepoxide solutions, to see if this effect would be minimized by deaerating with an inert gas denser than air. Three types of inert gas were studied: highly purified nitrogen, spectroscopically pure argon, and technical welding argon. The same gas was always used both for deaeration and for segmenting the flow streams. It was found that argon invariably gave better precision than nitrogen; there was no significant difference between the two types of argon gas. As welding argon is inexpensive, this gas therefore seems to be the gas of choice for most purposes. Details of these experiments will be given in a subsequent paper, in which the effect of other experimental parameters on the precision of automated polarographic analysis will be discussed [10].

DISCUSSION

The flow-through cells described above were easily made from perspex blocks. The design (Fig. 2) proved to be both simple and reliable, and facilitated easy cleaning and exchange of the DME capillary. The best counter electrode was found to be a platinum wire, which was positioned close to the DME, at the downstream side. A mercury pool counter electrode should be avoided, as it frequently causes irregular flow rates, and even short-circuiting of the cell. The position of the reference electrode seemed not to be critical; this electrode was therefore placed in the mercury waste bottle, and this rendered the construction of the flow-through cell particularly simple.

Very effective deaeration of the sample solution was obtained by using the deaeration unit shown in Fig. 5. When all three gas outlets were used, the sample solutions were fully deaerated before aspiration started. If a commercial sampler is to be employed, deaeration can be done by placing a single gas outlet beside the sampling probe. In this case the peristaltic pump should be stopped for a given time before the aspiration of a new sample starts, to allow for the complete deaeration of this solution. The pump should always be halted during transfer of the sampling probe, to prevent aspiration of air into the system during sample shifts. Argon was found to be preferable to nitrogen for deaeration, probably because of its higher density, which prevented more effectively the diffusion of air into the open sample cups.

Automated polarographic systems seem to be particularly useful for pharmaceutical analysis. Frequently, only one of the components in a pharmaceutical product is electroactive, so that the automated analysis may be carried out at a constant potential. A typical current—time curve obtained with the automated system described here, is shown in Fig. 8. The curve represents the analysis of solutions containing 96, 98 and 100 p.p.m. chlordiazepoxide, respectively, at a constant potential of −0.49 V; a wash solution

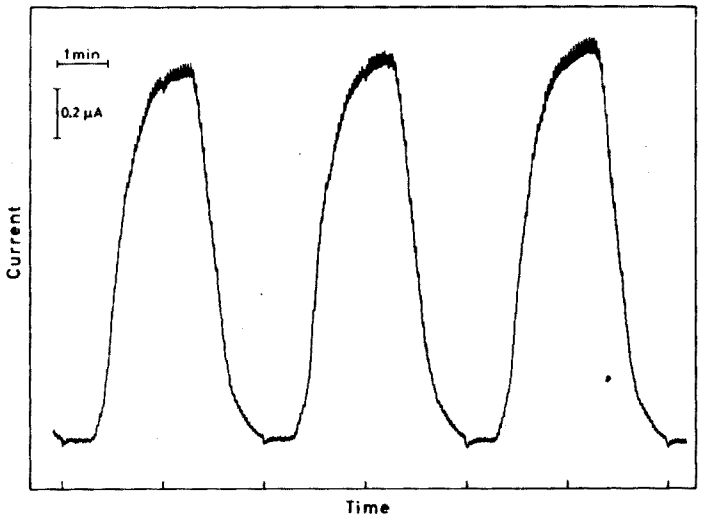

Fig. 8. Current—time curve for the analysis of solutions containing 96, 98 and 100 p.p.m. chlordiazepoxide in 0.01 *M* sulphuric acid. Sampling time 2 min, wash time 2 min, potential −0.49 V *vs.* Ag/AgCl. The sample shifts are indicated on the time axis.

containing the supporting electrolyte (0.01 *M* sulphuric acid) was used between each sample. The sampling time and the wash time were 2 min. As can be seen from Fig. 8, a somewhat longer sampling time would be needed in order to obtain a steady-state current for each sample. However, this is not necessary, as the concentrations of the samples are usually calculated relative to standard solutions which are analyzed under exactly the same experimental conditions.

A series of 25 solutions of chlordiazepoxide was analyzed, giving a relative standard deviation of 2.4 %; when the peristaltic pump was halted during the sample shifts, the analysis of the same series of solutions gave a standard deviation of 1.2 %. It was also found that the precision could be improved significantly by using an expanded scale procedure, which will be discussed in a later paper.

Tablets were also analyzed with the automated system described here: tablets containing 10 mg of chlordiazepoxide were dissolved in 10 ml of 0.1 *M* sulphuric acid, and the solutions were diluted to 100 ml with water and analyzed directly without filtration of the insoluble material. The response time and precision obtained were quite similar to the results obtained for the pure chlordiazepoxide solutions. Other substances, *e.g.* diazepam, were also determined successfully. Details of these analyses will be published in the near future.

We would like to thank our instrument workshop for constructing the sampler/deaeration unit and the flow-through cells. We are also grateful to siv.ing. Sverre Grimnes for designing the timer unit and the potentiostat, and to Dr. Tor Waaler and Professor Einar Jacobsen for their interest in this work.

SUMMARY

The design of polarographic flow-through cells for automated analysis of discrete samples is discussed. A simple way of fitting the DME capillary into the cell is described, and the problems associated with the use of a mercury pool counter electrode are discussed. A platinum wire or gauze counter electrode downstream from the DME is more satisfactory. The reference electrode may be placed outside the flow cell, *e.g.* in the mercury waste bottle. A new method for the deaeration of sample solutions is also described; argon is bubbled through the solutions in the sample cups just before aspiration. The effect of various experimental parameters on the deaeration is described. Pump stoppage during sample shifts is advantageous. The adaptation of the deaeration method to commercial samplers is explained. The application of the proposed automated system for the determination of chlordiazepoxide is discussed.

REFERENCES

1 H.G. Lento, Automation in Analytical Chemistry, Technicon Symposia, 1966, Vol I, Mediad, White Plains, New York, 1967, p. 598.
2 B. Fleet, S. Win and T.S. West, Automation in Analytical Chemistry, Technicon Symposia, 1967, Vol II, Mediad, White Plains, New York, 1968, p. 355.
3 M.D. Booth, B. Fleet, Soe Win and T.S. West, Anal. Chim. Acta, 48 (1969) 329.
4 S. Silvestri, Pharm. Acta Helv., 47 (1972) 209.
5 A. Cinci and S. Silvestri, Farmaco, Ed. Prat., 27 (1972) 28.
6 P. Bargagna, A. Cinci and S. Silvestri, Farmaco, Ed. Prat., 27 (1972) 89.
7 L.F. Cullen, M.P. Brindle and G.J. Papariello, J. Pharm. Sci., 62 (1973) 1708.
8 E. Jacobsen and T.V. Jacobsen, Anal. Chim. Acta, 55 (1971) 293.
9 W.J. Blaedel and J.H. Strohl, Anal. Chem., 36 (1964) 445.
10 W. Lund and L.N. Opheim, in preparation.

Analytica Chimica Acta, 79 (1975) 47—58

DOSAGE DES THIOLS PAR POLAROGRAPHIE A IMPULSIONS

FRANCIS PETER et ROBERT ROSSET

Laboratoire de Chimie Analytique, Ecole Supérieure de Physique et de Chimie de Paris, 10, rue Vauquelin, 75231 Paris Cedex 05 (France)

(Reçu le 2 mai 1975)

Dans un précédent mémoire [1] nous avons montré que l'électrode à membrane de sulfure d'argent (électrode dite "spécifique" des ions sulfure) permettait de suivre commodément par potentiométrie à courant nul le dosage des sulfures et des thiols (mercaptans) par précipitation par l'argent(I). Toutefois, la sensibilité de cette méthode n'est pas meilleure que 10^{-4} M, soit 10 p.p.m. pour un thiol de masse moléculaire 100.

La polarographie classique est couramment utilisée dans l'industrie pétrolière pour le dosage des fonctions soufrées dans les essences. Généralement, le tracé polarographique permet de déterminer la présence ou l'absence de sulfure d'hydrogène, de thiols, de soufre élémentaire de disulfure et de polysulfures organiques [2—4], mais la sensibilité de la polarographie classique est limitée, elle aussi, à 10^{-4} M et, d'autre part, la complexité des phénomènes à l'électrode fait que la forme des polarogrammes obtenus se prête mal aux analyses de routine (voir plus loin, Fig.8).

Recherchant une méthode beaucoup plus sensible nous avons pensé appliquer au dosage des thiols la polarographie à impulsions. La sensibilité de cette technique est en effet de 10^{-8} M pour les systèmes réversibles ($n = 2$); d'autre part il existe maintenant des appareils d'un prix à peine supérieur à celui d'un polarographe classique; il en résulte que l'emploi de la polarographie à impulsions se généralise dans le contrôle industriel de routine.

Les réactions électrochimiques

Sur électrode à gouttes de mercure les thiols ne s'oxydent pas en disulfures; il y a oxydation du mercure avec formation de thiolate mercure(I) insoluble [5—7] qui est instable et se dismute en thiolate mercure(II) et mercure [8—10] de sorte que la réaction électrochimique globale est:

(1) en milieu acid tamponné, $pH < pK_A$, K_A étant la constante d'acidité du thiol dans le milieu considéré:

$$Hg\downarrow + RSH - 2\,e^- \rightleftarrows Hg(RS)_2\downarrow + 2\,H^+ \qquad (1)$$

Le potentiel de demi-vague dépend de la concentration du thiol et si le système électrochimique est réversible, il varie comme – 0,029 log | RSH | à 20 °C; il varie de plus comme – 0,058 pH.

(2) en milieu alcalin, pH > pK_A, le système électrochimique est:

$$Hg\downarrow + 2\ RS^- - 2\ e^- \rightleftarrows Hg(RS)_2\downarrow$$

Le potentiel de demi-vague est indépendent du pH.

Compte tenu de l'insolubilité des thiols en solution aqueuse nous avons effectué les tracés polarographiques en milieu méthanol—benzène 3 : 1 en volume tamponné à pH 9,7 par le mélange acide acétique—acétate de sodium 0,1 M (l'origine de l'échelle de pH est définie par pH 1 pour une solution d'acide perchlorique 0,1 M). Dans ce milieu, à ce pH, les thiols sont sous leur forme acide RSH [11].

Polarographie à impulsions

Nous avons opéré selon le mode dérivé. L'appareil utilisé permettait de choisir la polarité des impulsions par rapport au potentiel continu imposé. On obtient alors des pics dont le potentiel E_p est relié au potentiel de demi-vague par:

$$E_p = E_{1/2} \pm \frac{\Delta E}{2}$$

ΔE étant l'amplitude de l'impulsion. Le choix entre le signe + et le signe – dépend de la nature de la vague polarographique et de la polarité de l'impulsion selon le tableau suivant:

	Impulsion négative [a]	Impulsion positive [b]
Vague d'oxydation	+	–
Vague de réduction	–	+

[a] Signifie que l'impulsion diminue, en valeur algébrique, la tension continue appliquée.
[b] Signifie que l'impulsion augmente, en valeur algébrique, la tension continue appliquée.

PARTIE EXPERIMENTALE

On se reportera précédemment [1] pour tout ce qui concerne les produits chimiques et la préparation des solutions.

Le polarographe à impulsions est un appareil Solea-Tacussel type PRG 5 comprenant: (a) Un potentiostat. (b) Un générateur d'impulsions: les impulsions sont imposées juste avant la chute de chaque goutte de mercure; leur amplitude peut être choisie entre 0 et 100 mV, et leur durée est réglable de

18 ms à 98 ms lorsqu'il s'agit d'impulsions d'amplitude constante. Leur polarité peut être inversée. (c) Une base de temps: le temps de goutte réglable de 0,1 à 9,9 s par commande d'un marteau électromagnétique. (d) Un amplificateur de courant: l'échantillonnage du courant s'effectue pendant les huit dernières ms de l'impulsion. La sensibilité est réglable entre 12,5 nA et 25 mA, pleine échelle. (e) Un pilote: permettant de faire varier la vitesse de balayage des potentiels de 0,1 mV s^{-1} à 100 mV s^{-1}, l'étendue de potentiel explorée et le sens de ce balayage. (f) Les circuits d'amortissement réglables et des filtres.

Cet appareil est associé à un enregistreur potentiométrique (Solea-Tacussel, EPL 2) dont la vitesse de déroulement du papier est asservie à la vitesse de balayage des potentiels de l'organe pilote. Le potentiel imposé a été constamment contrôlé au moyen d'un millivoltmètre digital (Solea-Tacussel, ISIS 4000).

Pour le dosage proprement dit des thiols, nous avons choisi une impulsion négative qui donne les pics les plus grands. Son amplitude était de 50 mV. Le temps de goutte à été fixé à 2 s, la durée de l'impulsion à 48 ms et la vitesse de balayage à 1 mV s^{-1}.

L'électrode de référence est une électrode $Hg/HgCl_2$ /KCl saturé en solution dans le méthanol Solea-Tacussel.

La cellule du polarographe doit être parfaitement étanche pour éviter les pertes de thiols par oxydation ou volatilité. Nous avons fait réaliser une cellule en verre monobloc avec une jonction étanche souple entre le capillaire et la cellule (Fig.1).

Dans le cas du sulfure d'hydrogène et de l'éthanethiol qui sont très volatils et très oxydables on maintient pendant le tracé des polarogrammes une pression d'azote constante de 40 mm de mercure. Cette surpression p dans la cellule modifie la pression h de mercure au-dessus du capillaire (hauteur de la colonne de mercure). La surface S de la goutte, proportionnelle à cette hauteur à la puissance 2/3, est alors diminuée. La hauteur H des pics obtenus est, en première approximation, proportionnelle à S et doit donc être corrigée pour pouvoir être comparée à celles obtenues sous pression atmosphérique:

$$H_{\text{corrigée}} = H_{\text{mesurée}} \cdot \left(\frac{h}{h-p}\right)^{2/3}$$

Pour les autres thiols, moins volatils, il suffit, après dégazage par barbotage d'azote, de maintenir un faible courant d'azote au-dessus de la solution.

Le mercure qui s'écoule du capillaire doit être éliminé afin de l'empêcher de stagner au fond de la cellule où il risque d'être oxydé par les traces d'oxygène résiduel en présence de thiol avec formation d'eau oxygénée ou d'eau selon:

$$2\,RSH + Hg\downarrow + O_2 \rightarrow Hg(RS)_2 + H_2O_2$$

$$2\,RSH + Hg\downarrow + \tfrac{1}{2}\,O_2 \rightarrow Hg(RS)_2 + H_2O$$

ce qui est gênant pour deux raisons: il y a consommation de thiol d'où les erreurs par défaut qui peuvent être importantes dans le cas des traces; l'eau oxygénée éventuellement formée n'est pas chassée par le barbotage d'azote et elle

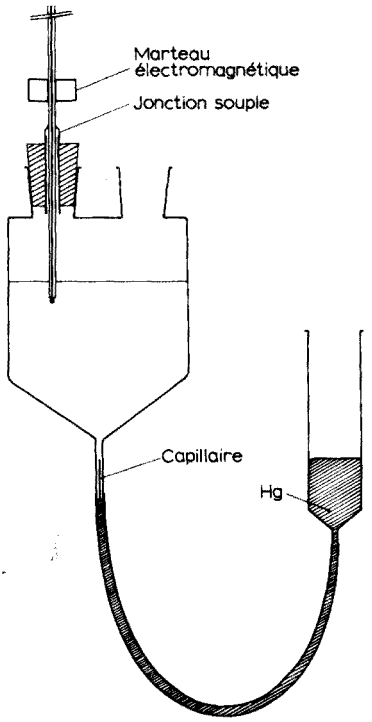

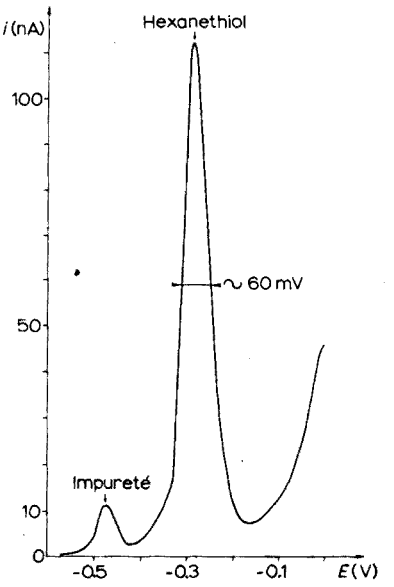

Fig.1. Schéma de la cellule utilisée en polarographie à impulsions.

Fig.2. Polarogramme à impulsions d'une solution d'hexanethiol $4 \cdot 10^{-6}$ M. Sensibilité du polarographe, 1/10.

est réductible en donnant un pic très étalé d'où une ligne de base perturbée. Le mercure est donc éliminé au fur et à mesure par le canal d'un tube capillaire soudé au fond de la cellule.

Moyennant cet ensemble de précautions les pertes en sulfure d'hydrogène sont de l'ordre de 5 % par heure pour une solution $3 \cdot 10^{-6}$ M; elles sont pratiquement nulles pour tous les thiols dont le nombre d'atomes de carbone de la molécule est supérieur ou égal à 2.

RESULTATS EXPERIMENTAUX ET DISCUSSION

Comme la polarographie à impulsions est une méthode d'analyse des traces, nous avons surtout étudié la polarographie des thiols et du sulfure d'hydrogène dans la gamme de concentrations 10^{-7}–10^{-4} M.

Qu'il s'agisse du sulfure d'hydrogène, des thiols aliphatiques linéaires ou ramifiés ou d'un thiol aromatique, le benzènethiol, on obtient par polarographie à impulsions "dérivée" un pic unique, fin et bien défini dès que la concentration dans la solution dépasse 10^{-7} M, soit environ 3 parties par milliard pour le sulfure d'hydrogène.

La Fig.2 représente un pic caractéristique obtenue dans le cas de l'hexanethiol à la concentration $4 \cdot 10^{-6}$ M (soit 0,5 p.p.m. environ) et à 1/10 de la sensibilité maximale du polarographe. (Le solvant, bien que de qualité dite "pour analyse", comporte des impuretés à l'état de traces détectables en polarographie à impulsions. Dans le benzène notamment, on trouve des produits soufrés thioféniques ou même des thiols à des concentrations voisines de 10^{-7} M.)

Potentiels de pic

Les valeurs des potentiels de pic (E_p) pour l'ensemble des composés étudiés sont rassemblées dans le Tableau 1. Les potentiels de pic des thiols en solution 10^{-7} M sont compris entre −0,23 et −0,34 V vs. ECS; pour le sulfure d'hydrogène, E_p est égal à −0,52 V. E_p comme $E_{1/2}$ varie avec la concentration du thiol et nous avons donné dans le Tableau 1 les valeurs de E_p pour une concentration 10^{-3} M; Le potentiel de demi-vague devrait varier, si les systèmes électrochimiques étaient réversibles, de 29 mV par décade de concentration; expérimentalement, cette variation est de 25 à 30 mV pour les thiols et de 12,5 mV environ pour le sulfure d'hydrogène. Exception faite de ce dernier, les variations de E_p correspondent bien aux prévisions.

Par ailleurs, on peut remarquer que les potentiels des pics des thiols aliphatiques linéaires ou ramifiés sont très peu différents; malgré le bon pouvoir de résolution de la polarographie à impulsions (45 mV), il sera impossible de séparer par cette technique les différentes familles de thiols présentes dans un mélange.

TABLEAU 1

Polarographie à impulsions du sulfure d'hydrogène et des thiols. Potentiels de pic pour deux concentrations

Thiol	E_p (V) (10^{-7} M)	E_p (V) (10^{-3} M)	Thiol	E_p (V) (10^{-7} M)	E_p (V) (10^{-3} M)
H_2S	−0,52	−0,58	3-Butanethiol	−0,24	−0,36
Ethanethiol	−0,23	−0,34	Hexanethiol	−0,25	−0,38
n-Propanethiol	−0,23	−0,34	*n*-Dodécanethiol	−0,32	−0,42
Isopropanethiol	−0,24	−0,34	Tert-dodécanethiol	−0,28	−0,39
1-Butanethiol	−0,25	−0,35	Benzènethiol	−0,34	−0,45
2-Butanethiol	−0,24	−0,34			

Variation de la hauteur du pic en fonction de la concentration

Sur la Fig.3, nous avons représenté les hauteurs de pic en fonction de la concentration avec des échelles linéaires, et cela pour différents domaines de variation de cette concentration. La variation de la hauteur du pic est linéaire

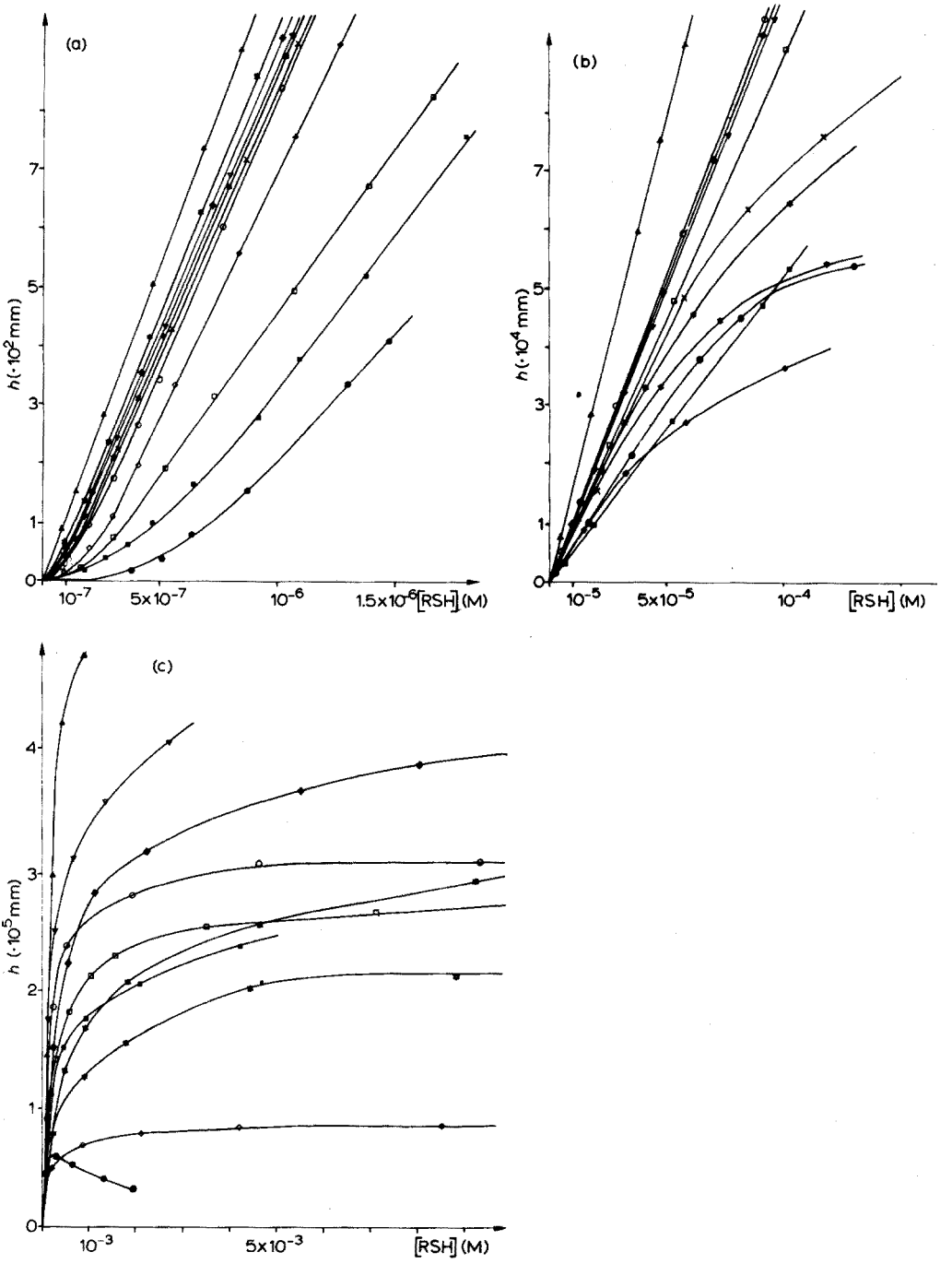

Fig.3. Variation de la hauteur du pic (ramenée à la sensibilité maximale du polarographe) en fonction de la concentration en thiol (a) 10^{-7} —$2 \cdot 10^{-6}$ M; (b) 10^{-5}—$2 \cdot 10^{-4}$ M; (c) 10^{-3}—10^{-2} M.
(▲) H_2S. (☆) 3-Butanediol. (◆) 1-Propanethiol. (▽) Ethanethiol. (★) 2-Butanethiol. (x) Isopropanethiol. (○) 1-Butanethiol. (◇) 3-Dodecanethiol. (□) 1-Hexanethiol. (■) 1-Dodecanethiol. (●) Benzenethiol.

avec la concentration du thiol de 10^{-7} M (ou de 10^{-6} M pour l'hexanethiol, le dodécanethiol et le benzènethiol) jusqu'à 10^{-4} M ou $5 \cdot 10^{-5}$ M.

On constate d'autre part que la pente des droites obtenues qui mesure la sensibilité de la méthode est d'autant plus forte que le thiol est à chaîne plus courte, ou, à longueur de chaîne égale, plus ramifiée. Au-delà de $5 \cdot 10^{-5}$ M, la courbe s'infléchit et la hauteur du pic tend vers une valeur limite, plus rapidement si le thiol est de chaîne plus longue ou plus ramifiée.

La largeur du pic à mi-hauteur est de 60 mV pour des impulsions d'une amplitude de 50 mV. Cela traduit un système rapide dans le cas d'un échange bi-électronique [12].

La proportionnalité entre la hauteur de ce pic et la concentration, aux faibles valeurs de celle-ci, conduit à penser que ce pic correspond à la réaction d'oxydation du mercure en présence de thiol selon:

$$Hg\downarrow + 2\ RSH - 2\ e^- \rightarrow Hg(RS)_2\downarrow + 2\ H^+ \qquad (1)$$

Toutefois, les phénomènes sont un peu plus compliqués que ce qui précède.

Rappelons d'abord que les polarogrammes ont été tracés avec une impulsion "négative", c'est-à-dire une impulsion qui rend le potentiel de l'électrode plus négatif que le potentiel imposé (Fig.4a). Or, le polarographe à impulsions dont nous disposions permettait d'inverser la polarité de l'impulsion par rapport au balayage du potentiel continu. Si on trace les polarogrammes avec une impulsion "positive", c'est-à-dire une impulsion qui rende le potentiel de l'électrode plus positif que le potentiel imposé (Fig.4b), on constate que la hauteur du pic diminue d'environ 50 % et que sa largeur à mi-hauteur est sensiblement doublée. Cela signifie que la réaction de réduction du thiolate mercure(II):

$$Hg(RS)_2\downarrow + 2\ H^+ + 2\ e^- \rightarrow Hg\downarrow + 2\ RSH \qquad (2)$$

est plus rapide que la réaction inverse d'oxydation du mercure en présence de thiol:

$$Hg\downarrow + 2\ RSH - 2\ e^- \rightarrow Hg(RS)_2\downarrow + 2\ H^+ \qquad (3)$$

Nous avons, par ailleurs, tracé les courbes électrocapillaires représentant le temps de goutte en chute libre en fonction du potentiel imposé à l'électrode (Fig.5) en l'absence et en présence de thiols. On constate que, lorsque le poten-

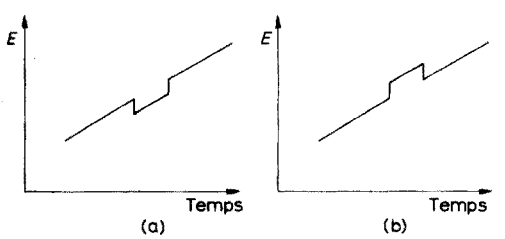

Fig.4. Polarité de l'impulsion par rapport à la tension continue imposée. (a) Impulsion négative. (b) Impulsion positive.

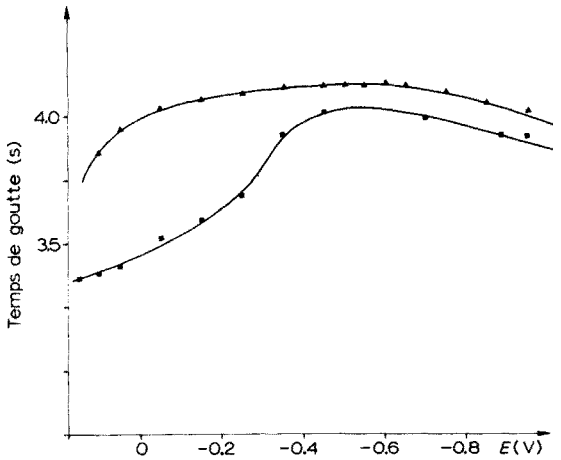

Fig.5. Influence du butanethiol sur la variation du temps de goutte de l'électrode en fonction du potentiel: (▲) solvant seul; (■) 1-butanethiol $2{,}5 \cdot 10^{-3}$ M.

tiel devient supérieur à −0,40 V vs. ECS, le temps de goutte diminue fortement, ce qui indique la formation d'un produit insoluble à l'électrode [13]. De plus, le point d'inflexion de la courbe vers −0,30 V vs. ECS permet de supposer une adsorption à la surface de l'électrode [14].

Enfin, l'enregistrement du courant continu d'électrolyse en fonction du temps a été réalisé pour différents potentiels (Fig.6). Aux potentiels suffisamment négatifs pour que l'oxydation du mercure ne se produise pas, à −0,40 V par exemple, le courant continu d'électrolyse varie de la façon habituelle: il augmente en même temps que la surface de la goutte croit, s'annule lorsque celle-ci se détache et ainsi de suite. Dès que la réaction électrochimique considérée a lieu, par exemple à −0,35 V, la variation du courant continu est profondément différente: le courant croît, passe par un maximum puis décroît

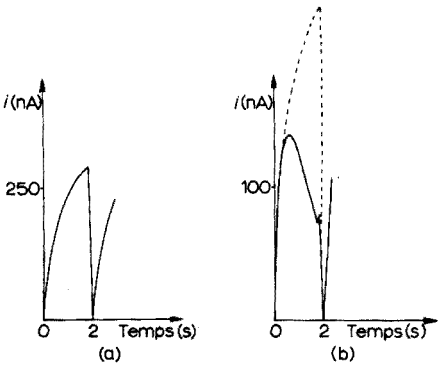

Fig.6. Variation du courant continu d'électrolyse en fonction du temps. Hexanethiol, $1{,}4 \cdot 10^{-3}$ M: (a) $E = -0{,}40$ V; (b) $E = -0{,}35$ V. En tireté sur la figure (b) on a figuré la manière dont le courant augmenterait si l'électrode ne se recouvrait pas d'un composé insoluble et isolant.

avant même la moitié du temps de goutte. La goutte de mercure s'est donc recouverte d'une couche d'un produit insoluble et isolant.

Cet ensemble de phénomènes s'interprète de la manière suivante:

(1) Le mercure s'oxyde en présence de thiol selon eqn.(1)

(2) Le thiolate mercure(II) formé, insoluble, est adsorbé à la surface de la goutte de mercure et recouvre celle-ci (d'où l'accident sur la courbe électrocapillaire). Cette hypothèse d'adsorption du thiolate par le mercure a déjà été formulée pour la cystéine dans l'eau [15] ou pour certains thiols aliphatiques en solution alcoolique [16].

(3) Etant isolant, le thiolate mercure(II) augmente considérablement la résistance de l'électrode de sorte que le courant continu décroît alors que la surface de la goutte continue à croître dès que l'électrode est entièrement recouverte de thiolate mercure(II).

(4) Si l'on impose une impulsion négative, le pic observé correspond à la réduction du thiolate mercure(II) formé au cours du régime stationnaire imposé à l'électrode selon eqn.(2).

Avec une impulsion positive, il s'agit de la réaction inverse. Le fait que le pic obtenu soit beaucoup,plus grand avec des impulsions négatives que positives indique que la réduction du thiolate adsorbé correspond à un système plus rapide que l'oxydation du mercure en présence de thiol.

(5) Le fait qu'il s'agisse d'une réaction électrochimique couplée à une réaction d'adsorption à l'électrode explique que la hauteur du premier pic tende vers une valeur limite lorsque la concentration en thiol augmente, plus rapidement si le thiol est de chaine plus longue ou plus ramifiée. En effet, la surface de la goutte de mercure sera d'autant plus aisément recouverte que le thiolate aura lui-même une surface plus grande, donc correspondra à un thiol à chaîne plus longue ou plus ramifiée.

En conclusion, le pic obtenu en polarographie à impulsions correspond à la réaction d'oxydation du mercure en présence de thiol avec adsorption sur le mercure de l'électrode du thiolate formé. Dans le cas d'une impulsion négative, c'est la réduction du thiolate mercure(II) formé en régime stationnaire qui est observée et le pic obtenu est d'un plus grand intérêt au point de vue analytique (sensibilité et résolution meilleures).

Influence du pH

Peter [11] a montré que le mélange méthanol—benzène 3 : 1 se comportait du point de vue des réactions acide—base comme du méthanol pur et le tampon acide acétique—acétate correspond à un pH voisin de 9,7 pour un produit ionique de 16,4. Nous avons tracé quelques polarogrammes en milieu très basique (soude 0,1 M) et en milieu acide (tampon acide nitrique—nitrate de sodium). Le pic se déplace, comme prévu, vers les potentiels négatifs en milieu basique.

Les valeurs du potentiel de pic en fonction du pH sont représentées Fig.7: la pente de 67 mV/unité de pH est sensiblement conforme aux prévisions

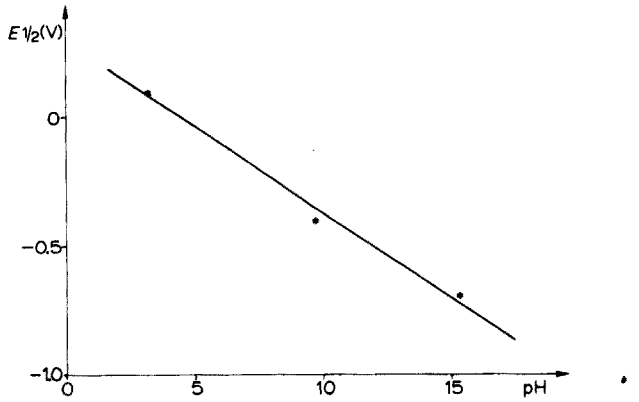

Fig.7. Variation du potentiel de pic en fonction du pH (solution d'hexanethiol $1{,}4 \cdot 10^{-3}$ M).

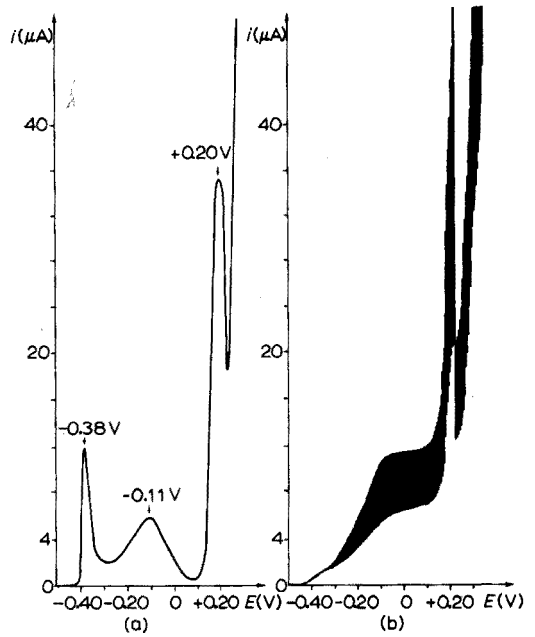

Fig.8. Polarogramme d'une solution d'hexanethiol $1{,}4 \cdot 10^{-3}$ M. (a) Polarographie à impulsions (sensibilité, 1/4000). (b) Polarographie classique.

théoriques (59 mV). L'augmentation de sensibilité de la méthode en milieu acide ne présente qu'un intérêt limité au point de vue pratique, en raison des difficultés expérimentales considérables qu'entraîne la forte volatilité des thiols thiols légers et du sulfure d'hydrogène dans ces milieux.

Quand la concentration en thiol devient supérieure à 10^{-4} M, l'allure générale des polarogrammes se complique notablement: au premier pic, s'en ajoutent deux autres, l'un très étalé vers −0,11 V, l'autre très proche du pic

d'oxydation du mercure dans le solvant vers +0,20 V (Fig.8). Ces phénomènes, qui sont sans intérêt en analyse puisqu'il suffit de diluer la solution pour les faire disparaitre ont été étudiés en détail ailleurs [11]. Disons simplement que le pic vers –0,11 V correspond toujours à l'oxydation du mercure en présence de thiol, mais il n'apparaît qu'une fois la goutte de mercure de l'électrode entièrement recouverte d'une couche de thiolate mercure(II) insoluble et isolant. L'autre pic s'explique par un phénomène de passivation de l'électrode.

CONCLUSION

La polarographie à impulsions des thiols permet d'atteindre une sensibilité de l'ordre de 10^{-7} M, soit de l'ordre de 3 parties par milliard si on la compte en soufre (pour les thiols contenant un atome de soufre par molécule). On gagne ainsi un facteur 1000 par rapport à la polarographie classique et à la potentiométrie sur électrode indicatrice des ions sulfure.

Dans le domaine de concentration où la polarographie à impulsions est intéressante, c'est-à-dire de 10^{-4} à 10^{-7} M, les phénomènes sont simples. On observe un pic unique lié à l'oxydation du mercure en présence de thiol avec adsorption du thiolate formé sur le mercure de l'électrode.

La polarographie à impulsions est donc bien adaptée au dosage des traces de thiols dans les produits pétroliers et ses performances limites vont bien au-delà des exigences actuelles concernant la teneur en soufre des essences et hydrocarbures liquides.

RESUME

Le dosage des thiols a été étudié par polarographie à impulsions. Les phénomènes sont simples et on obtient un pic unique tant que la concentration du thiol est inférieure à 10^{-4} M. La réaction électrochimique est l'oxydation du mercure en présence de thiol avec adsorption du thiolate de mercure formé sur l'électrode. La sensibilité la meilleure est obtenue en utilisant une impulsion qui rend le potentiel de l'électrode plus négatif que le potentiel imposé ce qui correspond à la réduction du thiolate formé en régime stationnaire. La sensibilité de la méthode est d'environ 10^{-7} M soit de 3 parties par milliard si on la compte en soufre. Les valeurs des potentiels de pic sont données pour H_2S, neuf thiols aliphatiques et le benzènethiol. La hauteur du pic est proportionnelle à la concentration jusqu'à $5 \cdot 10^{-5}$ M environ. En revanche les phénomènes sont complexes lorsque la concentration est supérieure à 10^{-4} M et ne permettent pas une utilisation commode de la méthode en analyse.

SUMMARY

The determination of thiols has been studied by pulse polarography. A single peak is obtained if the concentration is less than 10^{-4} M. The electrochemical reaction involves oxidation of mercury in presence of the thiol with adsorption of the mercury thiolate on the electrode. The method is more sensitive with a negative pulse; this corresponds to reduction of the mercury thiolate formed during the drop life. The sensitivity is about 10^{-7} M, i.e. 3 p.p.b. calculated as sulfur. Peak potential values are given for H_2S, nine aliphatic thiols and benzenethiol. Peak height is proportional to concentration up to about $5 \cdot 10^{-5}$ M. The phenomena are more complicated for concentrations higher than 10^{-4} M so that the method is not then analytically useful.

BIBLIOGRAPHIE

1 F. Peter et R. Rosset, Anal. Chim. Acta, 64 (1973) 397.
2 J.H. Karchmer, Anal. Chem., 30 (1958) 80.
3 P. Zuman, Organic Polarographic Analysis, Vol.12, Pergamon, Londres, 1964, p.152—171 et 206—209.
4 H. Wenck, E. Schwabe, F. Schneider et L. Flohe, Z. Anal. Chem., 158 (1972) 267.
5 I.M. Kolthoff et C. Barnum, J. Amer. Chem. Soc., 62 (1940) 3061.
6 G. Sartori et A. Liberti, J. Electrochem. Soc., 97 (1950) 20.
7 W. Stricks, I.K. Frischmann et R.G. Mueller, J. Electrochem. Soc., 109 (1962) 518.
8 R. Cecil et J.R. McPhee, Advan. Protein Chem., 14 (1959) 255.
9 W. Stricks et I.M. Kolthoff, J. Amer. Chem. Soc., 74 (1952) 4646.
10 W. Stricks et I.M. Kolthoff, J. Amer. Chem. Soc., 75 (1953) 5673.
11 F. Peter, Thèse de Doctorat, Paris, 1974 (No. d'Enregistrement au C.N.R.S.: AO 10704).
12 E.P. Parry et R.A. Osteryoung, Anal. Chem., 37 (1965) 1634.
13 R.E. Benesch et R. Benesch, J. Phys. Chem., 56 (1952) 648.
14 S.K. Tiwari et A. Kumar, Electrochim. Acta, 17 (1972) 2085.
15 I.M. Issa, A.A. El Samahy, R.M. Issa et Y.A. Temerik, Electrochim. Acta, 17 (1972) 1615.
16 H. Holzapfel et K. Schöne, Talanta, 15 (1968) 391.

Analytica Chimica Acta, 79 (1975) 59—67

ELECTROCHEMICAL OXIDATION OF α-HYPONITRATE ION AND ITS ANALYTICAL APPLICATIONS

A. CINQUANTINI, G. RASPI and P. ZANELLO
Istituto di Chimica Generale, Università di Siena, 53100-Siena (Italy)
(Received 11th April 1975)

The polarographic behaviour of α-hyponitrate ion, α-$N_2O_3^{2-}$, over a wide pH range was first investigated by Călusaru [1], who reported the existence of an anodic wave between 0.0 and —0.4 V, and a cathodic wave which develops at pH values below 6. In another paper [2], the formation of a cobalt(III)—α-hyponitrate complex was used for analytical purposes, for this complex gives rise to a catalytic polarographic wave, which is well developed in ammonia—ammonium chloride buffers. Unfortunately, this method of polarographic determination of α-hyponitrate ion is rather delicate, because the α-$N_2O_3^{2-}$ ion is sufficiently stable only in strongly alkaline medium, and it is not applicable when hydroxylamine is present in the mixture.

This paper describes a detailed examination of the electrooxidation of α-hyponitrate ion in alkaline media at a dropping mercury electrode and the use of the d.c. and a.c. polarographic waves for quantitative purposes. The polarographic and amperometric methods proposed here are sensitive, accurate and reproducible; the a.c. polarographic peak permits the determination of α-hyponitrate in solutions at pH 11.0, even if a large amount of hydroxylamine [3] is present in the mixture.

EXPERIMENTAL

Apparatus

A Princeton Applied Research (PAR) Electrochemistry System Model 170 was used. A.c. measurements were made with phase-sensitive detection and an applied alternating voltage of 10mV (peak-to-peak). The polarographic cell, Metrohm Model E876-20, was a water-jacketed three-electrode cell mantained at 25 ± 0.1 °C by a Haake FE water thermostat. Saturated silver—silver chloride electrodes, connected to the solution by a saturated potassium chloride bridge with a fritted glass disk, were used as the reference and auxiliary electrodes. A tungsten wire auxiliary electrode was used in a.c. measurements.

The cell for controlled potential electrolysis and coulometric determinations employed a mercury pool working electrode (area, 18 cm^2); both the reference and the auxiliary electrodes were saturated mercury(I) sulphate electrodes,

separated from the test solution by bridges consisting of a solid mixture of silica gel and sodium sulphate (3:2). The hanging mercury drop electrode (HMDE) was a Metrohm Model E 410.

All potential values are referred to the saturated calomel electrode.

Chemicals

Sodium α-hyponitrate was prepared by a modification of Angeli's [4] method:

$$C_4H_9ONO_2 + NH_2OH + 2\ NaOCH_3 \rightarrow \alpha\text{-}Na_2N_2O_3 + C_4H_9OH + 2\ CH_3OH$$

The material was purified by precipitation with methanol from aqueous solution; samples were standardized by potentiometric titration [5] at 1 °C under nitrogen with standard hydrochloric acid solutions and/or by oxidation in alkaline solution at room temperature with an excess of hexacyanoferrate(III), followed by back-titration of the excess with arsenious oxide or vanadyl sulphate solution to a potentiometric end-point [6].

Buffer solutions were prepared from analytical reagent-grade chemicals; the pH values of the supporting electrolytes were checked with a Metrohm E388 potentiometer and a glass electrode, except for the 0.1—1 *M* sodium hydroxide solutions. In this range the pH was calculated from the corresponding hydroxide ion concentration. The ionic strength was kept constant at 1 by adding potassium nitrate, whenever necessary.

Polarographic and voltammetric procedures

Test solutions were prepared by dissolving known amounts (5—15 mg) of solid sodium α-hyponitrate in 40 ml of an appropriate buffer. As the material was observed to react slowly with atmospheric oxygen, the buffer solution was previously deaerated by bubbling pure nitrogen gas for 10 min. Alternatively, a *ca.* 0.01 *M* α-$Na_2N_2O_3$—0.1 *M* NaOH stock solution was prepared, deaerated and standardized by the procedures described above. More dilute solutions were prepared by dilution as they were needed.

Coulometric and macroscale electrolysis procedure

For controlled-potential coulometry, 150 ml of a 1.0 m*M* solution of sodium α-hyponitrate in 0.1 *M* sodium hydroxide was placed in the working electrode compartment of the coulometric cell; the nitrogen flow was continued during the electrolysis. The procedure of macroscale electrolysis was essentially the same, except that the working electrode compartment of the cell was filled with deaerated 0.1—1 *M* sodium hydroxide solution containing about 120 mg of sodium α-hyponitrate. This compartment was sealed with a rubber stopper through which passed a glass tube, connected via a Tygon tubing to a gas buret, in which any nitrogen oxide flushed out of the electrolysis solution was collected.

Identification and determination of electrolysis products

After completion of the macroscale electrolysis, nitrite ion in the solution was detected from the u.v. spectra; then solid NaH_2PO_4 was added to obtain a buffer solution pH $\leqslant$ 8 and nitrite ion was determined voltammetrically with a platinized platinum microelectrode with periodic renewal of the diffusion layer [7,8].

The gaseous product of electrolysis was identified as NO and determined by absorbing it in an alkaline solution of hydrogen peroxide. Analysis showed that the yield of nitrite and nitric oxide was 90 % or better, based on the amount of sodium α-hyponitrate electrolyzed.

RESULTS AND DISCUSSION

D.c. polarography

The anodic wave of α-hyponitrate ion was carefully investigated in alkaline solutions. The half-wave potential appears to be independent of pH ($E_{1/2}$ = −0.325 ± 0.005 V in the pH range of 10.5—14), indicating that neither hydrogen nor hydroxide ions are involved in the electrode reaction in this region. Reproducible data at pH values lower than 10.5 are not obtainable, because the decomposition rate of α-hyponitrate ion becomes large. Between pH 12 and 14 the wave is quite well defined; the slope of the plateau becomes more pronounced as the pH increases, and at the same time the plateau becomes shorter as the mercury discharge encroaches on the wave. From the polarographic curves, the slope, defined by $E_{3/4} - E_{1/4}$, was found to be very close to the Nernstian value of 59 mV. Between pH 10.5 and 12 the wave is distorted and the polarographic slope depends on the pH. The slope was 87 mV at pH 10.5, 90 mV at pH 11.0 and 73 mV at pH 11.7, indicating a certain amount of irreversibility, expecially at lower pH values.

It was also found that, with 2.48 m*M* α-hyponitrate ion in 0.1 *M* sodium hydroxide, the value of $i_d h_{corr}^{-1/2}$ was constant and equal to 1.57 ± 0.04 μA $cm^{-1/2}$ over a twofold range of values of h_{corr}, the height of the column of mercury above the capillary after correction for back-pressure effects. This indicates that the current is diffusion-controlled. In the same supporting electrolyte, the diffusion current is proportional to the concentration of α-hyponitrate ion between 0.08 and 1.3 m*M*. Over this range the mean value of i_d/C was 3.17 ± 0.15 μA $mmole^{-1}$ l for a capillary with the characteristics m = 1.536 mg s^{-1} and t = 5.86 s at the potential of measurement. The temperature coefficient of the mean limiting current is +1.5 % $degree^{-1}$ in 0.1 *M* sodium hydroxide solution, over the temperature range 10—30 °C.

Controlled potential electrolysis and coulometry

Coulometry of α-hyponitrate ion in aqueous solutions of pH 13—14 indi-

cated that one electron per ion was transferred. Analysis for nitric oxide liberated during the oxidation showed that one mole NO per mole of sodium α-hyponitrate electrolyzed was evolved. After large-scale electrolysis at controlled potential, nitrite ion was found to be the only other product in essentially quantitative yield (Table I).

TABLE I

Electrolysis products and coulometric *n*-values for the electrochemical oxidation of sodium α-hyponitrate at a mercury electrode[a]

Supporting electrolyte	α-$Na_2N_2O_3$ electrolyzed (mmole)	NO found (mmole)	NO_2^- found (mmole)	*n*
0.1 *M* NaOH—0.9 *M* KNO_3	0.60	0.58	0.59	0.97
	0.93	0.90	0.95	0.97
1.0 *M* NaOH	0.68	0.65	0.69	0.98
	1.00	0.98	0.98	0.96

[a] The potential was controlled at —0.200 V *vs.* SCE.

All these results suggest that the electrochemical oxidation of α-hyponitrate ion proceeds according to the overall equation:

$$\alpha\text{-}N_2O_3^{2-} \rightarrow NO_2^- + NO + e^-$$

The parallelism between these results and the reaction of α-$N_2O_3^{2-}$ with hexacyanoferrate(III) ion [6,9] suggests once more an analogy between reductions or oxidations at the electrode and reductions or oxidations in the homogeneous phase [10].

A.c. polarography

The d.c. polarographic step is reflected in an a.c. polarographic wave, the peak potential of which (E_p = —0.30 V) is close to the half-wave potential and is independent of pH. The a.c. wave is symmetrical about the peak potential and the width at half-height, $\Delta E_{p/2}$, is about 100 mV, which is close to the theoretical value for a reversible one-electron reaction. The a.c. current [$I(\omega t)$] varies linearly with the α-hyponitrate concentration in the range 0.075—1.01 m*M*.

In order to obtain more detailed information on the mechanism of the electrooxidation of α-hyponitrate ion, the influence of the drop life, *t*, and of the frequency, ω, of the superimposed potential on the peak potential and on the current function were investigated. It was found that E_s is shifted anodically as *t* and ω are increased; $I(\omega t)$ increases at low values of *t* and decreases at low values of ω.

These results suggest that the electrooxidation of α-hyponitrate ion at the mercury electrode proceeds through a reversible or quasi-reversible charge transfer, followed by an irreversible, very fast, chemical reaction.

Voltammetry at the HMDE

In order to confirm the suggested mechanism of electrooxidation of α-hyponitrate ion, cyclic sweep voltammograms were run at the HMDE in aqueous solutions of pH 12—14. At sweep rates of 20 mV s^{-1}, α-hyponitrate ion shows a single anodic peak, the peak potential (E_p) of which is independent of pH (E_p = —0.32 ± 0.02 V). As the potential sweep rate (v) is increased, the peak shifts to more positive potentials. At low values of v, E_p shifts by about 30 mV with a 10-fold increase in the scan rate; as v is increased, lesser magnitudes of this shift are observed, until E_p becomes nearly constant and independent of v. However, cyclic sweep voltammetry gave no indication of any cathodic peak after the anodic peak was scanned, nor was any indication found at high scan rates (*e.g.* 200—500 V s^{-1}).

Hypothesis on the mechanism

The structure of the α-hyponitrate ion has never been unequivocally determined and three structures have been proposed:

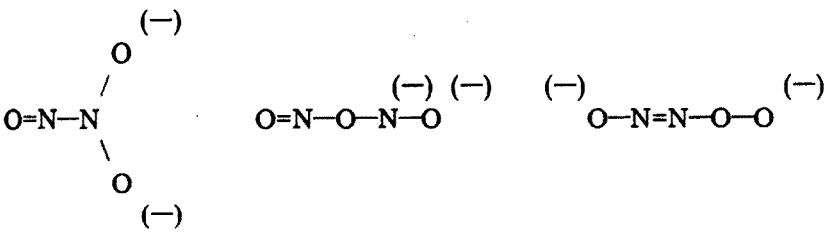

I II III

The u.v. [11] and i.r. [12] spectra, calorimetric measurements [13], the pK values [5] of α-hyponitrate ion and isotopic analysis [14] of the products of an asymmetric decomposition of the α-$N_2O_3^{2-}$ ion asymmetrically labelled with ^{15}N, have suggested structure I as most probable.

The above experimental data demonstrate clearly that α-hyponitrate ion is electrochemically oxidized between pH 10.5 and 14 in a pH-independent, 1-electron process to give nitrogen oxide and nitrite ion as the ultimate products. The pH-independence of the voltammetric peak potential and of the polarographic half-wave potential implies that in this pH range protons are not involved in the rate-determining process. The effect of increasing potential sweep rates in cyclic voltammetry and the variations of the peak potential and the current function in a.c. polarographic studies support the

view that the overall electrode process follows an electron-capture type of mechanism. The only reasonable reaction for the initial 1-electron charge-transfer reaction of α-hyponitrate ion (a) is formation of an anion-radical (b). The following chemical process probably involves a homolytic scission of the nitrogen—nitrogen bond of (b) and an electronic rearrangement, with formation of nitric oxide (c) and nitrite ion (d):

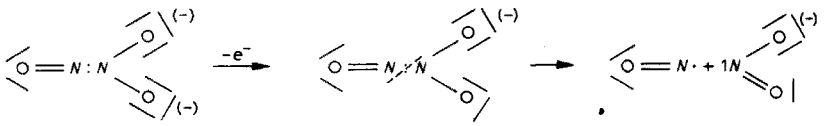

(a) (b) (c) (d)

ANALYTICAL APPLICATIONS

Amperometric titration of α-hyponitrate solutions

The methods [11,15,16] proposed for the determination of the α-hyponitrate ion are generally laborious and time-consuming. In a previous note [6] it was shown that α-hyponitrate can be determined in alkaline solutions by oxidation at room temperature with hexacyanoferrate(III) ion according to the equation:

$$Fe(CN)_6^{3-} + \alpha\text{-}N_2O_3^{2-} \rightarrow Fe(CN)_6^{4-} + NO + NO_2^-$$

Amperometric and biamperometric end-point detection methods were proposed, the changes in current intensity caused by the $Fe(CN)_6^{3-}/Fe(CN)_6^{4-}$ couple being followed with bright platinum electrodes.

As shown above, the DME allows the oxidation of α-hyponitrate ion to be studied in alkali hydroxide solutions. The corresponding wave is well shaped and its limiting current, which is diffusion-controlled, can be used to follow directly the decrease in the α-hyponitrate concentration during its titration with hexacyanoferrate(III). A higher sensitivity can then be attained. In the vicinity of the equivalence point, the reaction is rather slow and it is advisable to proceed slowly; the titration of about 10 mg of sodium α-hyponitrate requires *ca.* 50 min. Hydroxylamine interferes seriously, but nitrate and hyponitrite do not interfere; the accuracy of the method is not affected by large quantities (ten times that of α-hyponitrate) of nitrite ion.

On the basis of the results obtained, the following procedure is suggested.

Procedure. Place 40 ml of 0.5—1.0 *M* sodium hydroxide solution in a polarographic cell thermostatted at 25 °C. Remove oxygen by bubbling prepurified nitrogen and add 4—20 mg of sodium α-hyponitrate. Titrate with 0.05 *M* potassium hexacyanoferrate(III) solution at —0.140 V(SCE), bubbling

nitrogen through the solution after each addition of the reagent. Take care to wait a sufficient time at each measurement point until the current has decayed to a steady value. After correction for dilution, plot the values of the mean limiting diffusion current observed, after stabilization, against the volume of the reagent added. Determine the end-point from the intersection of this point with the zero line which corresponds to the residual current of the supporting electrolyte at −0.140 V; the cathodic current is due to the electroreduction of the excess of titrant.

The results of some titrations of various quantities of sodium α-hyponitrate are summarized in Table II.

TABLE II

Amperometric titration of α-hyponitrate.
(Titration in 1 *M* NaOH with 0.0495 *M* hexacyanoferrate(III) solution. Applied voltage: −0.140 V *vs.* SCE.)

α-$Na_2N_2O_3$ (mg)		No of detns.	Relative error (%)	s	s_r (%)
Taken	Found				
4.80	4.82	8	+0.5	0.04	1.9
6.20	6.14	8	−1.0	0.05	2.5
8.20	8.27	4	+0.9	0.15	2.8
10.20	10.18	4	−0.2	0.07	1.3
12.90	12.96	4	+0.5	0.12	0.5
13.70	13.55	4	−1.1	0.15	2.8
16.70	16.77	2	+0.4	—	—
20.80	20.66	2	−0.7	—	—

Determination of α-hyponitrate in presence of hydroxylamine

As the oxidation potentials of hydroxylamine and α-hyponitrate are close together in 1 *M* sodium hydroxide and the waves overlap, the problem of separating the α-hyponitrate wave in both d.c. and a.c. polarography makes the determination of α-hyponitrate virtually impossible in such a medium. However, the oxidation wave of hydroxylamine shifts toward more positive potentials [3] with decreasing pH by about 85 mV per pH unit; as mentioned above, the oxidation wave of α-hyponitrate is not affected by decreasing pH. At pH 11.0 a suitable compromise between the various requirements can be achieved. At this pH value, a useful separation (*ca.* 170 mV) is possible between the oxidation waves of hydroxylamine and α-hyponitrate, and the latter compound is still sufficiently stable. It is possible to determine the α-hyponitrate

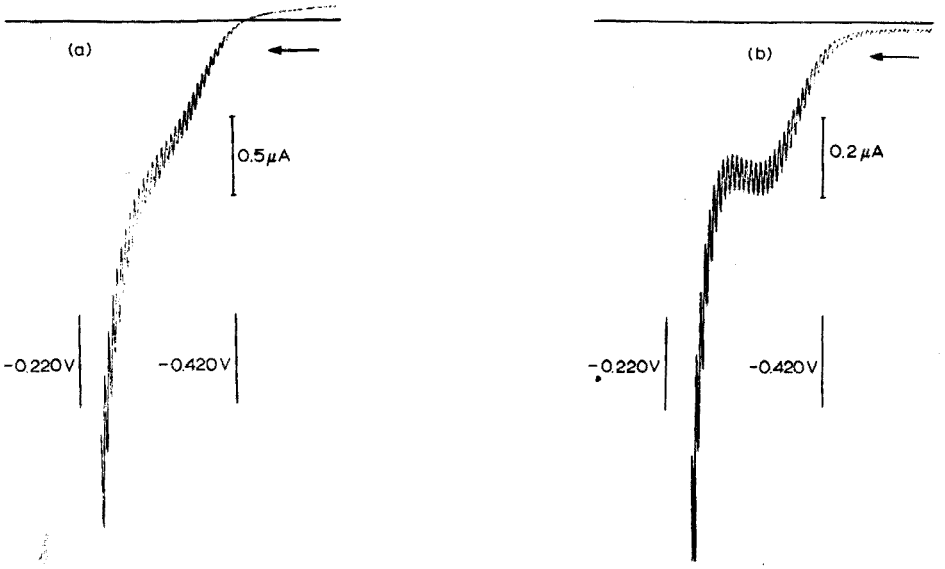

Fig.1. Polarographic curves of $3.6 \cdot 10^{-4}$ *M* α-$N_2O_3^{2-}$ and $1.92 \cdot 10^{-2}$ *M* NH_2OH in buffer solution at pH 11.0 (a) d.c., (b) a.c.

TABLE III

A.c. polarographic determination of α-hyponitrate in solutions buffered at pH 11.0 in presence of various amounts of hydroxylamine[a]

NH_2OH (mg)	α-$Na_2N_2O_3$ (mg)		Error (%)	$\frac{[NH_2OH]}{[\alpha\text{-}N_2O_3^{2-}]}$
	Taken	Found[a]		
1.26	0.50	0.49	−2.0	9.3
4.75	0.88	0.89	+1.1	20.0
9.90	1.00	1.01	+1.0	36.7
25.25	1.75	1.78	+1.7	53.3
30.00	3.50	3.47	−0.9	31.8
12.62	4.35	4.37	+0.5	10.6
33.00	4.85	4.80	−1.1	25.1
66.00	4.85	4.78	−1.5	50.3

[a] Mean of duplicate determinations.

ion by either d.c. or a.c. polarographic techniques, by a standard addition method, when the molar ratio of hydroxylamine to α-hyponitrate is less than 10; for higher values (up to *ca.* 50), only a.c. polarography permits reproducib results (Fig.1).

The results of some a.c. polarographic determinations of various quantities of sodium α-hyponitrate in the presence of hydroxylamine are summarized in Table III.

We are grateful to the Consiglio Nazionale delle Ricerche of Italy for financial support (cont. n. CT74.00731.03).

SUMMARY

α-Hyponitrate ion is electrochemically oxidized at mercury electrodes: the reaction proceeds by an initial 1-electron oxidation to give an anion radical which decomposes to give nitrogen oxide and nitrite as the ultimate products. The d.c. polarographic wave of α-hyponitrate ($E_{1/2}$ = —0.325 V *vs.* SCE) in 0.1 *M* sodium hydroxide can be used for the determination of α-hyponitrate in the range 0.08—1.3 m*M*; a.c. polarography (E_p = —0.30 V *vs.* SCE) is useful in the range 0.075—1.0 m*M*. Amperometric titration with 0.05 *M* hexacyanoferrate(III) is suitable for determinations of 5—20 mg of sodium α-hyponitrate. A.c. polarography at pH 11.0 allows α-hyponitrate to be determined in the presence of 50-fold amounts of hydroxylamine.

REFERENCES

1 A. Cãlusaru, C.R. Acad. Sci., Ser. C, 263 (1966) 232.
2 A. Cãlusaru, J. Electroanal. Chem. Interfacial Electrochem., 12 (1966) 341.
3 G.R. Rao and L. Meites, J. Phys. Chem., 70 (1966) 3620.
4 A. Angeli, in F.B. Ahrens and W. Herz (Eds.), Sammlung Chemischer und Chemisch-Technischer Vorträge, Stuttgart, 1908, Bd. 13, S. 8, Fussnote 2.
5 P.E. Sturrock, J.D. Ray, J. MacDowell and H.R. Hunt Jr., Inorg. Chem., 2 (1963) 649.
6 G. Raspi and A. Cinquantini, Anal. Chim. Acta, 72 (1974) 200.
7 G. Raspi and F. Pergola, Chim. Ind. (Milan), 45 (1963) 1398.
8 R. Guidelli, F. Pergola and G. Raspi, Anal. Chem., 44 (1972) 745.
9 L. Cambi, Gazz. Chim. Ital., 59 (1929) 770.
10 P. Zuman in P. Zuman and I.M. Kolthoff (Eds.), Progress in Polarography, Vol. 1, Interscience, New York, 1962, p.319.
11 C.C. Addison, G.A. Gamlen and R. Thompson, J. Chem. Soc., London, (1952) 338, 346.
12 R.D. Feltham, Inorg. Chem., 3 (1964) 900.
13 H.R. Hunt, Jr., J.R. Cox, Jr. and J.D. Ray, Inorg. Chem., 1 (1962) 938.
14 D.N. Hendrickson and W.L. Jolly, Inorg. Chem., 8 (1969) 693.
15 J. Vaprek-Siška, F. Smirous and V. Pliška, Collect. Czech. Chem. Commun., 24 (1959) 1175.
16 G. Kortum and B. Finkh, Z. Phys. Chem., Abt. B, 48 (1941) 42.

Analytica Chimica Acta, 79 (1975) 69—78

CONTRIBUTION A L'ELECTROCHIMIE DES THIOLS ET DISULFURES

PARTIE III. POLAROGRAPHIE D.C., A.C., ET POLAROGRAPHIE DIFFERENTIELLE A IMPULSIONS DE L'ACIDE THIOBARBITURIQUE ET DU PENTOTHAL SODIQUE

C.A. MAIRESSE-DUCARMOIS, G.J. PATRIARCHE et J.L. VANDENBALCK

Institut de Pharmacie, Université Libre de Bruxelles, Avenue F-D Roosevelt 50, 1050 Bruxelles (Belgique)

(Reçu le 20 decembre 1974)

Poursuivant l'étude consacrée à l'électrochimie des thiols et disulfures [1—3] nous nous sommes intéressés à l'acide thiobarbiturique et à son dérivé le pentothal sodique. Ces deux composés sont d'une importance pharmacologique considérable ayant servi de noyau de base à un grand nombre de produits pharmaceutiques doués d'une activité anesthésiante.

L'intérêt présenté par l'étude de ces substances s'est déjà concrétisé dans la littérature par les importants travaux de Smyth *et al.* [4] qui se sont intéressés plus particulièrement aux équilibres acide—base, à la polarographie d.c. et à l'étude spectrale approfondie d'une série de dérivés substitués de ces deux molécules. Le but du présent travail est d'élucider leur mécanisme de réduction [5—7] en utilisant des méthodes telles que les polarographies conventionnelle (d.c.), alternative (a.c.) et différentielle à impulsions (p.p.)

PARTIE EXPERIMENTALE

L'appareillage utilisé de même que les réactifs sont identiques à ceux décrits antérieurement [1, 2].

POLAROGRAPHIE D.C. ET A.C.

Acide thiobarbiturique

Etude en fonction du pH. L'étude de ce composé est effectuée dans les mêmes milieux que ceux utilisés pour le glutathion [2] et l'échelle des pH explorée se situe entre 1,5 et 11,9 pour une concentration fixe de $5 \cdot 10^{-4}$ *M*. On observe trois vagues anodiques dans la zone de pH 4—9 (voir Tableau I). La première correspond à la liaison carbone—soufre, les deux suivantes étant des vagues d'adsorption. A des pH inférieurs à 4, la vague d'oxydation, située à potentiel relativement positif, n'apparait pas, masquée par l'oxydation du

TABLEAU I

Comportement polarographique A.C. et D.C. de l'acide thiobarbiturique ($5 \cdot 10^{-4}$ *M*) en fonction du pH

pH	*D.c.* $E_{1/2}$ [a]	$E_{3/4} - E_{1/4}$ (*mV*)	*A.c.* E_p [a]	*D.c.* $E_{1/2}$ [a]	$E_{3/4} - E_{1/4}$ (*mV*)	*A.c.* E_p [a]	*D.c.* $E_{1/2}$ [a]	$E_{3/4} - E_{1/4}$ (*mV*)	*A.c.* E_p [a]	*D.c.* $E_{1/2}$ [a]	*A.c.* E_p [a]
1,5				+0,020	10	+0,020	—0,210	5	—0,210	—1,120	—1,165
2,0				+0,007	10	+0,010	—0,255	5	—0,255	—1,165	
3,0				+0,010	10	+0,010	—0,235	8	—0,240		
4,0	+0,040	8	+0,040	—0,010	10	—0,005	—0,330		—0,330		
4,3	+0,040	10	+0,040	—0,010	10	—0,005	—0,350		—0,345		
5,5	+0,025	10	+0,020	—0,047	7	—0,045	—0,480	8	—0,475		
7,8	—0,020	10	—0,015	—0,115	5	—0,120	—0,415		—0,420		
9,0	—0,115	13	—0,110	—0,190	5	—0,175	—0,450	8	—0,450		
10,8	—0,210	20	—0,220	—0,305							
11,9	—0,255	25	—0,260								

[a] V *vs* ECS

mercure; tandis qu'à pH supérieur à 10, c'est la deuxième vague d'adsorption qui disparait.

Ce dérivé, ne comportant aucun substituant sur son noyau, est soumis à des phénomènes d'adsorption particulièrement intenses, semblables à ceux observés pour la thiourée et ses dérivés [7]. La première de ces vagues d'adsorption se développe très nettement entre pH 1,5 et 10,8, avec intensité maximale au pH 4. Ses $E_{1/2}$ se différencient sensiblement de ceux observés pour son homologue le pentothal comme nous pouvons le voir en comparant les Tableaux I et III.

Les valeurs de $E_{3/4} - E_{1/4}$ sont proches de 10 mV dans presque toute l'échelle de pH envisagée; ce n'est qu'à pH 12 que cette valeur atteindra 25 mV pour la vague d'oxydation.

La courbe électrocapillaire à 3 inflexions, réalisée avec une solution $2 \cdot 10^{-4}$ *M* en acide thiobarbiturique, à pH 8, illustre clairement ces phénomènes. (Fig.1).

Malgré les phénomènes d'adsorption observés, l'intensité de la première vague varie linéairement avec la concentration. Elle est proportionnelle à la racine carrée de la hauteur de la colonne de mercure; son coefficient de température, déterminé entre 20°C et 30°C, est de ±3 % par degré, ce qui correspond donc aux critères établis par la diffusion [5].

Etude en fonction de la concentration. A des concentrations supérieures ou égales à $1 \cdot 10^{-3}$ *M*, il y a apparition du dérivé organomercuriel, déjà mis en évidence pour d'autres composés [1, 2]. Cette onde est suivie de la vague d'oxydation de la liaison C=S dans toute la zone des concentrations envisagées.

Deux vagues anodiques se dessinent à des potentiels plus négatifs, la première reste définie jusqu'à concentration $5 \cdot 10^{-5}$ *M*, la deuxième disparaissant déjà à des concentrations inférieures à $5 \cdot 10^{-4}$ *M* (Tableau II).

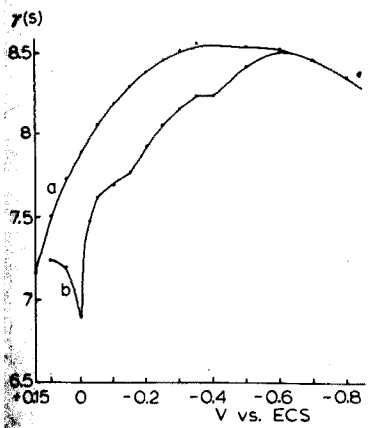

Fig.1. Courbes électrocapillaires. (a) Electrolyte de support seul (tampon pH 8), (b) électrolyte de support additionné d'acide thiobarbiturique ($2 \cdot 10^{-4}$ *M*).

TABLEAU II

Comportement polarographique de l'acide thiobarbiturique en fonction de la concentration (Tampon pH 9,2; Borax 0.05 *M*—KNO_3 0.5 *M*.)

Concentration (*M*)	$E_{1/2}$ [a]	$E_{1/2}$ [a]	$E_{3/4} - E_{1/4}$ (mV)	$E_{1/2}$ [a]	$E_{3/4} - E_{1/4}$ (mV)	$E_{1/2}$ [a]
$5 \cdot 10^{-3}$	-0,007	-0,120	5	-0,180	5	-0,550
$1 \cdot 10^{-3}$	-0,010	-0,120	5	-0,180	7	-0,530
$5 \cdot 10^{-4}$	-0,015	-0,120	5	-0,175	7	-0,515
$1 \cdot 10^{-4}$	—	-0,115	20	-0,205	25	—
$5 \cdot 10^{-5}$	—	-0,115	30	-0,200	—	—

[a] V *vs.* ECS.

Pentothal sodique

Ce composé, dérivé sodique de l'acide thiobarbiturique disubstitué en C_5 par un radical ethyle et un radical méthyl-1-butyle, devrait présenter des analogies avec le composé décrit ci-dessus, ce qui n'est pas le cas, voir Figs.2—5.

Etude en fonction du pH. Cette étude a été effectuée entre pH 3 et 10,9, à l'aide d'une solution $5 \cdot 10^{-4}$ *M* de pentothal. En raison de sa faible solubilité dans l'eau à pH inférieur à 8, nous avons été contraint de modifier la composition de l'électrolyte de base en y incorporant 20 % d'éthanol préalablement redistillé.

De pH 6,6 à 9, trois vagues se dessinent nettement: les deux premières sont anodiques, la troisième est cathodique. En dessous du pH 6,6, ces vagues anodiques, qui se situent à des valeurs de $E_{1/2}$ relativement positives, sont masquées

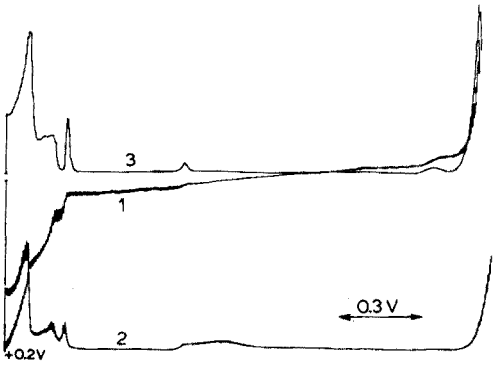

Fig.2. Polarogrammes d.c., a.c. et p.p. d'une solution $5 \cdot 10^{-4}$ *M* en acide thiobarbiturique (pH 5). (1) D.c. sensibilité 2,5 μA; (2) a.c. sensibilité 5 μA; temps de chute de gouttes 0.9 s; (3) p.p. sensibilité 2,5 μA, amplitude surimposée 20 mV, temps de chute de gouttes 2 s, retard 1 s 8; durée de l'impulsion 40 ms; vitesse de déroulement 2 mV s^{-1}.

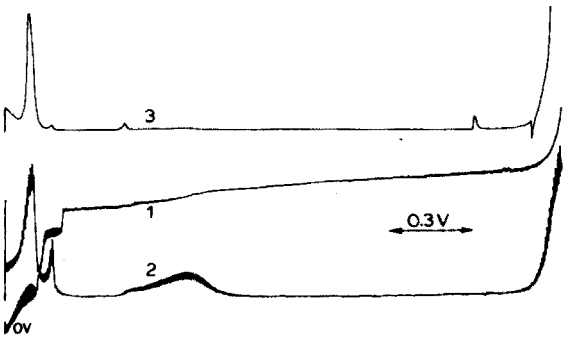

Fig.3. Polarogrammes d.c., a.c. et p.p. d'une solution $5 \cdot 10^{-4}$ *M* en acide thiobarbiturique (pH 9). (1) D.c. sensibilité 2,5 μA; (2) a.c. sensibilité 5 μA; temps de chute de gouttes 0.9 s; (3) p.p. sensibilité 5 μA, amplitude surimposée 20 mV, temps de chute de gouttes 2 s, retard 1 s 8, durée de l'impulsion 40 ms, vitesse de déroulement 2 mV s^{-1}.

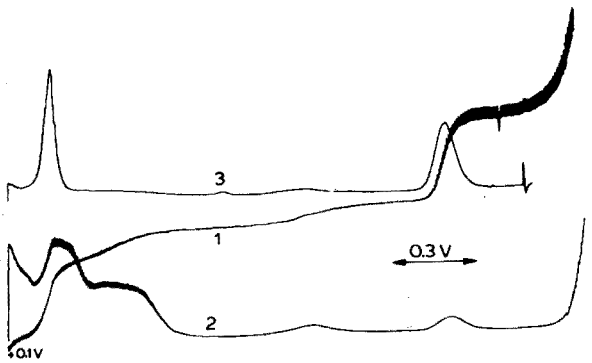

Fig.4. Polarogrammes d.c., a.c. et p.p. d'une solution $5 \cdot 10^{-4}$ *M* en pentothal (pH 8). (1) D.c. sensibilité 2,5 μA; (2) a.c. sensibilité 5 μA; temps de chute de gouttes 0.9 s; (3) p.p. sensibilité 2,5 μA, amplitude surimposée 20 mV, temps de chute de gouttes 2 s, retard 1 s 8, durée de l'impulsion 40 ms, vitesse de déroulement 2 mV s^{-1}.

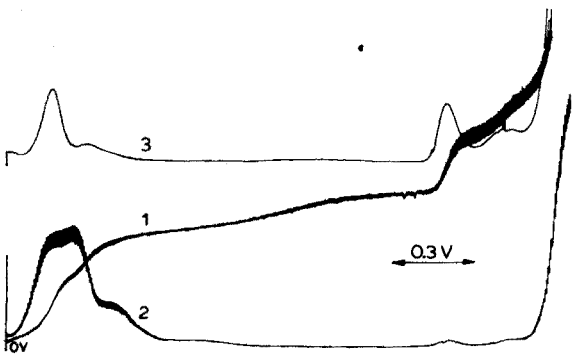

Fig.5. Polarogrammes d.c., a.c. et p.p. d'une solution $5 \cdot 10^{-4}$ *M* en pentothal (pH 10). (1) D.c. sensibilité 2,5 μA; (2) a.c. sensibilité 5 μA; temps de chute de gouttes 0.9 s; (3) p.p. sensibilité 1,25 μA, amplitude surimposée 20 mV, temps de chute de gouttes 1 s, retard 0.8 s, durée de l'impulsion 40 ms, vitesse de déroulement 4 mV s^{-1}.

par l'oxydation du mercure; la vague cathodique ne se développe pas étant entravée par la décharge des protons. Par contre, entre pH 10 et 11, la vague cathodique se dédouble; mais la première portion de la vague diminue en augmentant le pH et finit par disparaitre à pH 12. Les potentiels de demi-palier restent proches de ceux observés pour l'acide thiobarbiturique jusqu'à pH 9. Au delà, ceux-ci sont déplacés vers des potentiels de plus en plus négatifs.

Si l'on examine les valeurs des potentiels de demi-palier de la vague d'oxydation en fonction du pH, le tracé obtenu montre une variation linéaire..On observe deux légères inflexions aux pH 7,5 et 10,6 correspondant aux constantes d'ionisation de la molécule, comme l'ont déjà montré Smyth *et al.* [4]. La vague cathodique est indépendante du pH jusqu'à 8. A partir de cette valeur qui est proche du pK_2 du pentothal, la nouvelle vague formée se déplace vers des potentiels plus positifs au fur et à mesure que le pH croît.

Les mesures effectuées en a.c. peuvent être comparées aux ondes observées en d.c.; cependant, le pic correspondant à la vague d'oxydation se dédouble entre pH 9 et 10 (Tableau III).

Etude en fonction de la concentration. La concentration en pentothal affecte fortement le nombre et la nature des vagues. Des concentrations supérieures à $5 \cdot 10^{-3}$ *M* laissent apparaître trois vagues anodiques et une onde cathodique dont les $E_{1/2}$ sont respectivement de –0,075 V, –0.200 V, –0.330 V et –1,520 V *vs.* ECS. A $1 \cdot 10^{-3}$ *M*, la première vague se dessine sous forme d'un maximum du second ordre et disparait si la concentration diminue.

Pour des valeurs comprises entre $5 \cdot 10^{-4}$ *M* et $1 \cdot 10^{-4}$ *M*, seule la vague d'oxydation apparait nettement, la vague cathodique étant masquée par la décharge

TABLEAU III

Comportement polarographique a.c. et d.c. du pentothal-Na ($5 \cdot 10^{-4}$ *M*) en fonction du pH

		D.c.		A.c.	D.c.		A.c.	D.c.		A.c.
		$E_{1/2}$ [a]	$E_{3/4} - E_{1/4}$ (mV)	E_p [a]	$E_{1/2}$ [a]	$E_{3/4} - E_{1/4}$ (mV)	E_p [a]	$E_{1/2}$ [a]	$E_{3/4} - E_{1/4}$ (mV)	E_p [a]
pH	6,6	+0,030	45	–0,050	–0,230	90	–0,230	–1,485	40	–1,5
apparent	7,6	–0,025	50	–0,060	–0,330	90	–0,330	–1,490	40	–1,5
pH	8,0	–0,055	35	–0,070	–0,310	65	–0,300	–1,490	40	–1,5
exact	9,0	–0,110	40	–0,105 –0,175	–0,400	70	–0,375	–1,535	40	–1,5
	9,9	–0,165	45	–0,165 –0,245	–0,300	60	–0,400	–1,590 épaulement à –1,800	40	–1,6
	10,9	–0,220	40		–0,340	55	–0,305	–1,615 –1,765	40 50	–1,6 –1,7
	11,7	–0,285	40				–0,365	–1,745	50	

[a] V *vs.* ECS.

du support. Si l'on diminue encore la concentration, le courant capacitif l'emporte et entrave le développement de l'onde elle-même (Tableau IV).

Nature des courants. L'origine de la vague, apparaissant au potentiel le plus positif, doit être attribuée à la formation d'un composé d'adsorption entre thiol et mercure.

La deuxième vague qui correspond à l'oxydation de pentothal ($E_{1/2}$ = −0.05 V *vs.* ECS) est régie par la diffusion, l'intensité du courant variant linéairement avec la concentration entre $6 \cdot 10^{-4}$ *M* et $2 \cdot 10^{-4}$ *M*.

Il en est de même pour la vague cathodique située à −1,49 V, dont les intensités varient linéairement avec la racine carrée de la hauteur de mercure.

Par contre, la vague dont le potentiel se situe à −0,310 V *vs.* ECS n'est pas fonction de la hauteur de mercure; on observe la formation d'un intermédiaire pentothal—mercure. La pente de la droite obtenue en portant les valeurs de log $(i_d - i)/i$ *vs.* E est de 29 mV avec mise en jeu de deux électrons (Fig.6).

La vague cathodique serait due ici, d'après Smyth *et al.* [4], à une réduction de la forme monoprotonée à pH inférieur à 10 et de la forme monoprotonée—thiolate aux pH plus élevés, avec mise en jeu de deux électrons.

POLAROGRAPHIE DIFFERENTIELLE A IMPULSIONS

Acide thiobarbiturique

Les divers facteurs modifiant le comportement impulsionnel de l'acide thiobarbiturique ont été envisagés en milieu tampon pH 9 et pour une concentration $5 \cdot 10^{-4}$ *M*. Comme nous l'avons déjà signalé (voir polarographie d.c. et a.c.) l'acide thiobarbiturique est soumis à des phénomènes d'adsorption plus marqués que son dérivé disubstitué: ainsi la largeur du pic à mi-hauteur est toujours nettement plus faible que celle observée pour le pentothal et les intensités de pic sont supérieures pour une concentration identique des deux dérivés.

TABLEAU IV

Comportement polarographique du Pentothal-Na en fonction de la concentration (Tampon pH 9,2: 0.05 *M* Borax—0.5 *M* KNO_3)

Concentration (*M*)	$E_{1/2}(a_1)$ [a] (V *vs.* ECS)	$E_{1/2}(a_2)$ [b] (V *vs.* ECS)	$E_{3/4} - E_{1/4}$ (mV)	$E_{1/2}(a_3)$ [c] (V *vs.* ECS)	$E_{1/2}$ (cath.) (V *vs.* ECS)
$1 \cdot 10^{-2}$	−0,075	−0,230	10	−0,420	−1,525
$5 \cdot 10^{-3}$	−0,075	−0,200	10	−0,335	−1,520
$1 \cdot 10^{-3}$	—	−0,130	25	−0,305	−1,515
$5 \cdot 10^{-4}$	—	−0,130	45	−0,240	−1,515
$1 \cdot 10^{-4}$	—	−0,110	40	−0,190	—
$5 \cdot 10^{-5}$	—	Non mesurable	Non mesurable	−0,180	—

[a] Potentiel de 1/2 vague de la première vague anodique.
[b] Potentiel de 1/2 vague de la deuxième vague anodique.
[c] Potentiel de 1/2 vague de la troisième vague anodique.

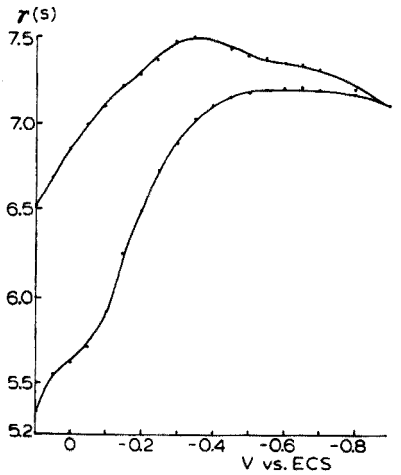

Fig.6. Courbes électrocapillaires. (a) Electrolyte de support seul (tampon pH 8), (b) électrolyte de support, additionné de pentothal ($5 \cdot 10^{-4}$ *M*).

Une faible variation de l'amplitude influence très peu le potentiel de pic de la vague anodique et la largeur du pic à mi-hauteur. La relation liant l'intensité de pic avec l'amplitude est pratiquement linéaire entre les valeurs allant de 10 à 50 mV (*i*p de 0,805 à 7,160 μA); on observe une forte inflexion pour une amplitude supérieure à cette valeur.

Le temps de chute des gouttes n'a qu'une très faible influence sur le potentiel de pic et sur sa largeur à mi-hauteur; il intervient cependant dans la diminution de l'intensité du pic. Si le temps de chute de gouttes passe de 4 s à 1 s (et retard à l'impulsion de 3s 8 à 0s 8), l'intensité de pic ne vaut plus que 65 % de sa valeur initiale (2,16 μA).

Comme dans le cas du pentothal, la vitesse de balayage modifie légèrement le potentiel du pic et sa largeur à mi-hauteur, par contre l'intensité de pic de l'acide thiobarbiturique diminue fortement de 1,960 à 1,421 μA, si le potentiel passe de 1 mV s^{-1} à 4 mV s^{-1}.

La linéarité de l'intensité de pic (E_p = –0.10 V *vs.* ECS) ne se vérifie pas pour les concentrations de $4 \cdot 10^{-4}$ à $8 \cdot 10^{-4}$ *M*. Le graphique présente deux segments de droite, dont le point de rencontre se situe vers $5 \cdot 10^{-4}$ *M*.

Pentothal

On examine les divers facteurs influençant le comportement polarographique impulsionnel du pentothal, à pH 9 et avec une solution $5 \cdot 10^{-4}$ *M*. Dans tous les essais, l'impulsion d'une durée de 40 ms et d'une amplitude de 20 mV est appliquée 0,2 s avant la chute de la goutte. Le temps de chute de gouttes est de 2 s, et la vitesse de balayage 2 mV s^{-1}.

Si l'amplitude croit de 10 à 100 mV, les potentiels de sommet de pics se déplacent vers des valeurs plus positives (E_p = —0,125 à —0,067 V *vs.* ECS et

−1.555 à −1.500 V *vs.* ECS), la largeur du pic à mi-hauteur grandit et se modifie. Les intensités de pic varient linéairement si l'amplitude reste faible; au delà de 50 mV, le tracé obtenu, en portant la valeur de l'amplitude en abscisses et l'intensité de pic en ordonnées, s'incurve particulièrement pour la vague cathodique

Si le temps de chute de gouttes diminue de 4 s à 1 s, les potentials de pic (E_p = —0,125 et —1,555 V *vs.* ECS) se déplacent légèrement vers des valeurs plus positives, la largeur du pic à mihauteur ne diminue que faiblement, et l'intensité de pic correspondant à la vague anodique est la plus fortement affectée: ainsi son intensité n'atteint plus que 30 % de sa valeur initiale (970 nA) si le temps de chute de gouttes passe de 4 s à 1 s, par contre l'intensité du pic dû à la vague cathodique vaut encore 64 % de sa valeur initiale (570 nA).

L'influence de la vitesse de balayage sur les potentiels de pic est très faible; la largeur du pic à mi-hauteur peu modifiée pour le premier pic, l'est un peu plus pour le second, et l'intensité de pic dû à la vague cathodique grandit beaucoup plus (de 390 à 570 nA) si la vitesse de balayage passe de 4 V s^{-1} à 0.5 V s^{-1}.

Les paramètres étant maintenus constants, on constate que la variation d'intensité des pics en fonction de la concentration est linéaire; ce qui permet de doser le pentothal à l'échelle microanalytique avec une bonne précision (Tableau V).

En conclusion, les tracés obtenus par polarographie à impulsions pour l'acide thiobarbiturique sont assez décevants. Ils correspondent à ceux obtenus par polarographie classique.

Ainsi, en milieu acide, le pic dû à la vague anodique est déformé par celui de la vague d'adsorption qui le suit de très près; un deuxième pic d'adsorption se développe à un potentiel plus négatif. Les pics d'adsorption sont beaucoup plus étroits que les pics obtenus pour un tracé normal et sont même parfois inversés, tant cette adsorption est forte sur la goutte de mercure.

Les meilleurs résultats sont observés en milieu alcalin: le pic correspondant à la réaction électrochimique se développe bien et les pics d'adsorption sont minimisés.

TABLEAU V

Etude en fonction de la concentration (Tampon pH 9)

Concentration ($\cdot 10^{-4}$ *M*)	$E_p(a)$ (V *vs.* ECS)	$i_p(a)$ (nA)	$\omega_{1/2}$ (mV)	$E_p(c)$ (V *vs.* ECS)	$i_p(c)$ (nA)	$\omega_{1/2}$ (mV)
8	—0,1254	1025	76	−1,545	735	85
7	−0,125	875	75	−1,550	650	85
6	−0,125	790	75	−1,550	560	85
5	−0,120	580	72,5	−1,545	465	85
4	−0,120	435	70	−1,555	375	85

Par contre, le comportement électrochimique du pentothal est fort différent les phénomènes d'adsorption sont moins accusés: le pic correspondant à la vague anodique en milieu alcalin est bien développé; il s'accompagne d'un épaulement dû à l'adsorption. Aux potentiels beaucoup plus négatifs se dessine un pic dont le sommet correspond au potentiel de 1/2 palier de la vague cathodique.

A pH 10, la vague cathodique se dédouble; deux pics apparaissent sur le tracé impulsionnel.

Nos remerciements vont au Fonds National de la Recherche Scientifique (F.N.R.S.) pour l'aide apportée à l'un d'entre nous (G.J.P).

RESUME

L'étude électrochimique de l'acide thiobarbiturique et du pentothal sodique est réalisée par les polarographies conventionnelle, alternative et différentielle à impulsions. On observe des phénomènes d'adsorption très importants, particulièrement pour l'acide thiobarbiturique, ainsi que des différences dans le tracé polarographique des deux composés.

Le nombre de vagues est fonction, dans les deux cas, du pH et de la concentration.

SUMMARY

D.c., a.c. and differential pulse polarography were used to elucidate the electrochemical behaviour of thiobarbituric acid and sodium pentothal.

Important adsorption phenomena were shown, particularly for thiobarbituric acid. Considerable differences were found in the polarographic curves of the two compounds. The number of waves obtained depends on the concentration and the pH for both compounds.

BIBLIOGRAPHIE

1 C.A. Mairesse-Ducarmois, G.J. Patriarche et J.L. Vandenbalck, Anal. Chim. Acta, 71 (1974) 165.
2 C.A. Mairesse-Ducarmois, G.J. Patriarche et J.L. Vandenbalck, Anal. Chim. Acta, 76 (1975) 299.
3 C.A. Mairesse-Ducarmois, J.L. Vandenbalck et G.J. Patriarche, J. Pharm. Belg., 28 (1973) 300.
4 W.F. Smyth, G. Svehla et P. Zuman, Anal. Chim. Acta, 51 (1970) 463; 52 (1970) 129; J. Electroanal. Chem. Interfacial Electrochem., 30 (1971) 101.
5 P. Zuman, The Elucidation of organic electrode processes, Academic Press, New York, 1963.
6 B.B. Damaskin, O.A. Petrii et V.V. Batrakov, Adsorption of organic compounds on electrodes, Plenum Press, New York, 1971, p.267.
7 M. Baizer, Organic Electrochemistry, M. Dekker, New York, 1973, Ch.16.

Analytica Chimica Acta, 79 (1975) 79—91

FLOW INJECTION ANALYSIS

PART II. ULTRAFAST DETERMINATION OF PHOSPHORUS IN PLANT MATERIAL BY CONTINUOUS FLOW SPECTROPHOTOMETRY

J. RŮŽIČKA and J.W.B. STEWART*

Centro de Energia Nuclear na Agricultura (CENA), C.P. 96, 13400 Piracicaba, S.P. (Brasil)

(Received 7th April 1975)

Flow injection analysis is a new approach to automation of chemical analyses, based on continuous flow measurement. This very simple method utilizes rapid injection of an aqueous sample into a continuously moving carrier stream of a reagent. The injected sample forms a zone which is then transported towards a detector, which continuously records the absorbance, or changes of electrode potential, etc. As the sampling period is very short, usually less than two seconds, a very high sampling rate can be achieved. This in turn allows the use of a quickly moving carrier stream, which in contrast to the AutoAnalyser concept, does not need to be segmented by air. The advantages of this approach were discussed in the first paper of this series [1], where the first results obtained on model systems were reported. The purpose of the present work was to prove the practical usefulness of this new approach for routine analysis, and to investigate the interrelation of such important parameters as sample volume, tube diameter, tube length, peak height and sampling rate, so that guidelines could be established for the best design of the manifold, and so that the limitations of flow injection analysis could be recognized.

The determination of phosphate after acid digestion of plant organic matter, was chosen, as this analysis is one that is frequently required in agricultural and environmental research, and also because the number of samples which have to be analysed annually in the CENA laboratories approaches a figure of 15,000. Furthermore the same method could be used to determine phosphorus in water samples, soil extracts, blood samples, etc. [2—8], all of which are generally determined by automated methods owing to the number of analyses required. Any improvement in this sampling rate would have obvious significance to many commercial and routine laboratories.

---

*UNDP/IAEA Experts in Radiochemistry and Soil Science, respectively, assigned to Project BRA/71/556, on leave from the Chemistry Department A, Technical University of Denmark, Lyngby, Denmark, and from the Department of Soil Science, University of Saskatchewan, Saskatoon, Canada.

The method is based on wet oxidation of the plant organic matter by a mixture of nitric and perchloric acids, and subsequent spectrophotometric measurement of phosphate in an acidified solution of ammonium molybdate containing ascorbic acid [2].

EXPERIMENTAL

Sample injection

Samples were injected manually, by means of disposable 1-ml plastic syringes through a septum located on a plastic tube in which the carrier stream of a reagent was being pumped by a peristaltic pump. The overall arrangement is shown in the flow diagram (Fig. 1). Details of the injection technique and of the construction of the injection port were reported previously [1].

Apparatus

This consisted of a peristaltic pump model 8511, 60 r.p.m. (Polymetron, Hombrechtikon, Switzerland), a spectrophotometer model DB, connected to a recorder model 1005 (both Beckman Inc., Fullerton, California) and a flow-through cuvette (Helma, type 178-QS; light path 10 mm, volume 0.08 ml). The dual-beam mode was used, the carrier stream liquid serving as a blank in a 10-mm stationary cuvette.

The manifold was entirely made of polyethylene and tygon tubing, of the noncollapsible wall-type. A Y-shaped connector was made in a small perspex block, and a mixing coil was made by winding the required length of plastic tube around a larger glass tube with a diameter of *ca.* 5 cm. The connections were made by short pieces of tygon or silicone rubber tubing into which the transmission tubing just fitted tightly. As both the length (Fig. 3) and the inne diameter (Fig. 6) of the tubing have an important effect on the flow pattern, the length of the analytical line between the point of injection and the flow cell should be measured. Moreover, as the inner diameter of the plastic tubes can vary slightly from the manufacturers' specifications it is advisable to chec by measuring, at room temperature, the length of the tube which is filled by exactly 1.00 ml of water. The most suitable tubing for routine analysis was

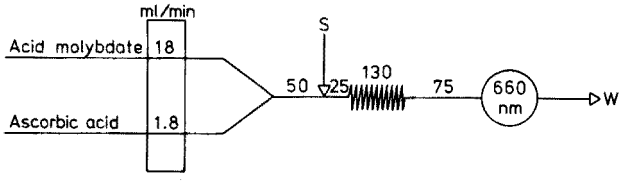

Fig. 1. Flow diagram. Molybdate and ascorbic acid are pumped and jointly form a carrier stream of reagent into which 0.50 ml of the sample (S) is injected. After passage through a mixing coil the absorbance of the molybdenum blue is measured in a flow cuvette at 660 nm and the stream continues to waste (W). The total length of the analytical line is 230 cm, of which the coil constitutes 130 cm. For tube diameter, see text.

found to be polyethylene tubing of 0.95—1.20 mm i.d. (140 cm ml^{-1} of water to 95 cm ml^{-1} of water).

Reagents

All chemicals were A.R. grade, and distilled—deionized water was used for all experiments. The acid molybdate reagent consisted of 0.005 *M* ammonium heptamolybdate in 0.4 *M* nitric acid—5 % ethanol mixture. Unless otherwise stated, the ascorbic acid was an aqueous 5 % solution.

Plant material

Bean samples (*Phaseolus vulgaris* L) were taken from field trials, dried for 48 h at 65 °C, and then ground in a Wiley mill to pass a 0.5-mm sieve.

Decomposition procedure

Either a 1.0 or 0.5 g sample of dried, ground, plant material was placed in a 100-ml Kjeldahl flask, then 10 ml of concentrated nitric acid were added and the flask was heated for 2 h; then 2 ml of perchloric acid (72 %) was added and the mixture was heated for a further 1—2 h. This mixture was cooled and then diluted to 70 ml with water.

Standards

Phosphorus standard solutions were made from potassium dihydrogenphosphate (50 μg P ml^{-1} requires 0.2195 g of KH_2PO_4 per litre).

Computations

All calibration curves were calculated by means of linear regression analysis with a Hewlett-Packard Programmable Electronic Calculator Model 9810A.

RESULTS AND DISCUSSION

The classical molybdenum blue procedure involves the primary reaction of phosphate with molybdenum(VI) to form 12-molybdophosphoric acid and its subsequent reduction to the heteropolyphosphomolybdenum blue. While the first reaction is very fast, and reaches completion within milliseconds [3], the reduction reaction is slower [2] and even in the AutoAnalyser method, which does not require that reaction equilibrium be reached, double mixing coils and even heated delay coils are used to allow sufficient colour development [4—7]. Thus, although the molybdenum blue method is reliable, as it is not affected by the yellow coloration of some plant digests, it is often replaced by the faster, but less sensitive, vanadomolybdophosphate method. The previous results [1], however, indicated that even the molybdenum blue method could be adapted for flow injection analysis, provided that the concentration of reductant was increased. When the manifold shown in Fig. 1 was used with polyethylene tube of 1.15 mm i.d., it was found (Fig. 2) that the sensitivity of the phosphate determination, *i.e.* the speed of the reduction

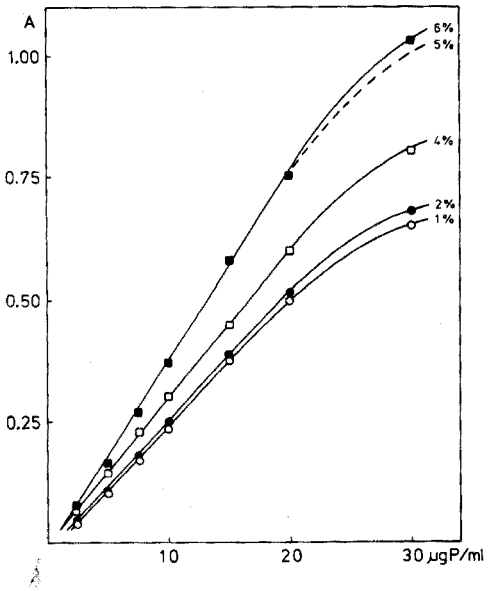

Fig. 2. Influence of the ascorbic acid concentration (1—6 %) on the determination of phosphate as molybdenum blue. Line length 230 cm; i.d. 1.15 mm.

reaction, increased as the concentration of the ascorbic acid solution was increased from 1 % to 6 %. With a 10 % solution of ascorbic acid, precipitation of molybdate occurred in the conduits of the system, hence 5 % ascorbic acid was adopted as a reasonable compromise between economy of reagent and linearity of calibration line.

Effect of line length

The line length is defined as the portion of the tubing, within which the sample and reagent are mixed, the colour develops and the absorbance is measured. This distance between the point of injection and the flow-through cell should be kept as short as possible, yet should still be long enough to allow sufficient time for colour development. By inserting different coil lengths (65 cm, 130 cm, 195 cm, 240 cm and 380 cm) into an otherwise unchanged analytical line and by running 10 $\mu g\ ml^{-1}$ and 20 $\mu g\ ml^{-1}$ phosphate standards, Fig. 3 was obtained, from which it is evident that an optimal line length, which allows maximal sensitivity, can be found for a particular chemical reaction. It is interesting to note that an extremely short line length of 75 cm resulted in a large measurement error. The reason can be seen from Fig. 4, curve a (recorded at a high paper speed); the valley at the top of the peak shows that a central portion of the sample zone has not had sufficient time to mix, and develop the colour, with the reagent present in the carrier stream. As the length of the analytical line increases the peak develops fully (Fig. 4, curves b, c) and then, because of dilution, decreases again. Obviously,

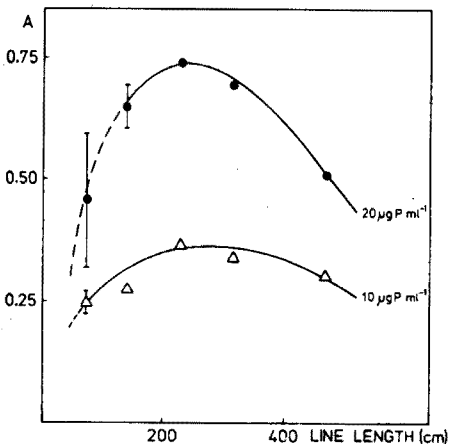

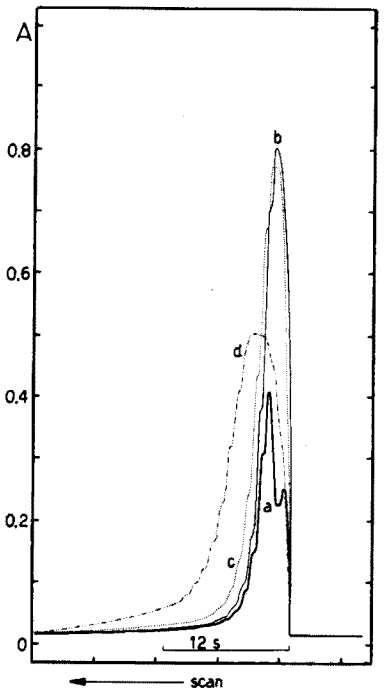

Fig. 3. Influence of the length of the analytical line on the peak height of 10 µg ml^{-1} standards. Tube i.d. 1.15 mm. Optimal line length 250—350 cm. Note the large error of measurement, as indicated by bars, with line lengths below 200 cm (compare Fig. 4).

Fig. 4. Influence of the length of the analytical line on the form of the peak and half-wash time, obtained with a 25 µg P ml^{-1} solution and standard tubing of 1.15 mm i.d. (a) 75 cm ($W_{1/2} \simeq 0.8$ s). (b) 140 cm ($W_{1/2} = 1.1$ s). (c) 205 cm ($W_{1/2} = 1.3$ s). (d) 465 cm ($W_{1/2} = 2.0$ s). Note the valley on top of peak (a) which is caused by insufficient mixing and equilibration of the sample zone.

slow reactions would not be suitable for the flow injection method unless they could be speeded up by heating or catalysis. However, by replacing one coil by another one, the sensitivity of the measurement can be adjusted according to the level of analyte in the samples, so that it remains within the instrument range.

Effect of sample volume

The influence of the sample volume was investigated with line lengths of 230 cm and 415 cm (1.15-mm i.d. tubing). As one would expect, the sensitivity increases with the sample volume until a point is reached where the reagent concentration and degree of mixing are not sufficient to obtain linear calibration curves (Fig. 5, *cf.* Figs. 3 and 4). Decreasing the sample volume decreases the sensitivity and increases the error of the analysis. Thus, by comparing the influence of the line length and of the injected volume, it

became apparent that the optimal sample volume is between 0.4 and 0.6 ml; this offers the best reproducibility and is convenient to inject. Therefore the sensitivity can be more easily and reliably adjusted by changing the line length and tube diameter than by altering the sample volume.

Effect of tube diameter

Tube diameter also has a significant effect on the flow parameters, influencin primarily the half-wash time and thus the maximum achievable sampling rate. To investigate this, the whole line length was made of tubing ranging from 0.80-mm to 1.5-mm i.d.; the total tube length in each experiment was 269 cm. Except for the thinnest tube, where the 25 μg P ml^{-1} standard consistently showed a negative deviation, all calibration curves were strictly linear. When peak heights (absorbances) were plotted *versus* tube volume per ml (Fig. 6), a set of straight lines was obtained with all tubes of internal diameter less than 1.5 mm. Obviously a decrease in the internal diameter of the tubing improves sensitivity and flow parameters, but tubing with internal diameters of 0.80 mm or less were difficult to use, because of the pressure imposed on the system at the moment of injection which could cause leakage at the tube connectors. It should be pointed out, however, that tubing of less than 0.80-mm i.d. could be used with micro samples of less than 0.20 ml provided

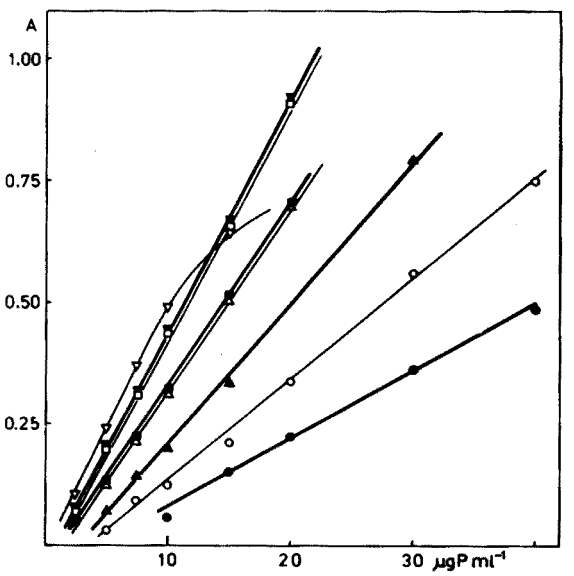

Fig. 5. Relationship between the sample volume and line length, the peak height and linearity of the calibration curve. 1.15-mm i.d. tubing; 5 % ascorbic acid. Short line (230 cm): injected volume (▽) 0.80 ml; (□) 0.60 ml; (△) 0.40 ml; (○) 0.20 ml. Long line (415 cm): injected volume (▼) 0.80 ml; (■) 0.60 ml; (▲) 0.40 ml; (●) 0.20 ml. Note that a large volume injected in a short line results in a loss of linearity (curve (▽)) while injection of a smaller volume in a longer line extends the linear range (compare curves (▲) and (○) with Fig. 2).

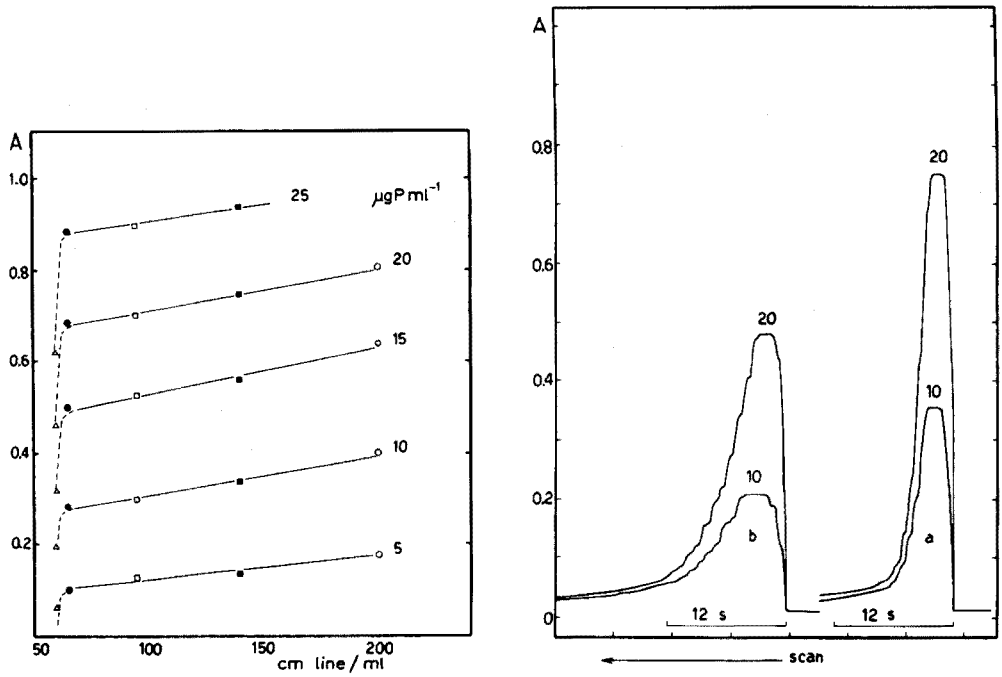

Fig. 6. Relationship between the internal diameter of the tubing and the peak height. Line length, 269 cm (coil 169 cm). Tube diameter is expressed in specific volume (cm ml^{-1}). Tube i.d.: (△) 1.5 mm; (●) 1.4 mm; (□) 1.15 mm; (■) 0.95 mm; (○) 0.80 mm.

Fig. 7. Relationship between the internal diameter of the tubing, peak height and half-wash time. Line length 269 cm; 10 μg P ml^{-1} and 20 μg P ml^{-1} standards. (a) 0.95 mm i.d. (half-wash time, 0.93 s). (b) 1.5 mm i.d. (half-wash time, 3 s). $W_{1/2}$ was obtained by analysis of fall curves.

that special syringes were used to allow precise injection of these small volumes.

Tubing with large internal diameter, however, allows significant sample dilution by the carrier stream, which causes a decrease in sensitivity, an increase in half-wash time and a decrease in the sampling rate. For example, manifolds made of 0.95-mm and 1.5-mm i.d. tubing (Fig. 7 (a) and (b)) had half-wash times of 0.93 s and 3.02 s, respectively, as calculated from the shape of the respective fall curves. For a sample: wash ratio of 1:1.5 and 75 % peaking, maximal sampling rates of 774 analyses per hour (0.95 mm i.d.) and 240 analyses per hour (1.5 mm i.d.) can be theoretically achieved. At these rates, approximately 5 % of the colour of the preceding peak will still be present in the flow cell while the maximum of the next peak is recorded. This computation takes into account the length of the plateau at the top of the peak, but the influence of the residence time on the sampling rate must still be considered.

In practice it is, of course, impossible to reach the highest sampling rate

by manual injection and it is indeed doubtful that rates over 600 samples/h would ever be utilized. Yet, these outstanding flow parameters are very useful; for it can be calculated easily that at a sampling rate of, *e.g.*, 420 analyses per hour in a manifold made of 0.95-mm i.d. tubing with a line length of 269 cm, the carry-over would be less than 1 %. This was checked in an experiment (Fig. 8) where no interaction between 5 μg ml^{-1} and 25 μg ml^{-1} standards was observed at a very high sampling rate of 420 analyses per hour.

Timing of injections

Injection timing is closely related to the residence time of the sample within the analytical line length. Considering the simplest case when only one sample zone is present within the analytical line length at a time, the maximum sampling frequency is determined by the half-wash time and by the line length. Thus, with 0.95-mm i.d. tubing and a line length of 269 cm, the residence time will be *ca.* 6 s, at a pumping rate of 20 ml min^{-1}. If the sample is always injected at the moment when the recorder pen starts to fall, a total sample period of less than 9 s can be achieved (half-wash time $\simeq$ 0.93 s). Thus, at the foot of the next peak only 1.6 % of the colour of the preceding peak will be left in the flow cell. In practice, however, an even higher sampling frequency

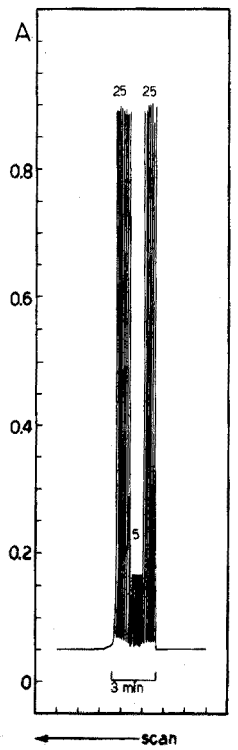

Fig. 8. Flow injection analysis for phosphate (5.0 μg P ml^{-1} and 25 μg P ml^{-1}) at a sampling rate of 420 samples per h. Line length, 269 cm; i.d., 0.95 mm.

can be reached because the injection of 0.5 ml of sample within 2 s increases the flow rate instantaneously to about 35 ml min^{-1}. This slightly decreases the residence time of the sample in the analytical line, further speeds up the washing of the flow cell and thus allows more closely spaced sampling. Consequently, a sampling frequency of 420 samples per hour, corresponding to a time gap of about 8 s, was achieved with this analytical line, with no detectable carry-over between successive samples (Fig. 8).

The above arguments clearly support the choice of shortest analytical line with an i.d. close to 1 mm. Should the line need to be made longer either because of a slow chemical reaction or because several reagents must be added to the carrier stream successively, it would be practical to choose the line length and injection timing so that a sample is never injected at the moment when the maximum of the preceding one is just passing through the flow cell. This can easily be achieved by choosing the line length so that the residence time is a suitable multiple of the half-wash time for that particular system. Thus several evenly spaced sample zones can be present within the sample line at the same time; the spacing of the samples can be maintained by injecting each new sample at the beginning of a fall in the curve.

The speed of injection and the flow rate were not varied in this study. The Polymetron pump accommodated tubes of 1.0, 2.0 and 3.0 mm i.d. which yielded flow rates of 18, 8 and 1.8 ml min^{-1} under the conditions used. Although combinations of these tubes would have given some further choice of flow rates, this type of study was postponed until a peristaltic pump with a continuously variable flow rate becomes available. The influence of the injection speed on the peak height was not studied in detail, because any slow manual injection is subject to a large experimental error. Obviously, the slower the injection, the longer the sample zone, and so the lower the peak and the sensitivity of the measurement. Fortunately, at high injection velocities very good reproducibility can be achieved in manual sampling injection (see below); the particular combination of tube diameter, injection port geometry, needle length and gauge allows the formation of short reproducible sample zones as soon as sample introduction into the carrier stream reaches a certain rate.

Routine analyses

Routine analyses were done with the manifold (Fig. 1) made of 1.15-mm i.d. tubing with a total line length of 320 cm (coil length 200 cm). As the plant digest solutions contained phosphate in the range 8—40 μg P ml^{-1}, 1.15-mm i.d. tubing was chosen in order to keep the absorbance signal within the instrument range. For similar reasons, the line length was long and the wave length was 620 nm. This approach was chosen rather than simple dilution as the same plant digests also had to be analysed for ^{32}P, potassium and calcium. Samples (0.50 ml) were injected manually, so that only one sample was in the line at a time, each being analysed in triplicate. Figure 9 shows a typical recording, with — from left to right — a sequence of P standards, thirty plant digests and the same sequence of P standards. As can be seen from

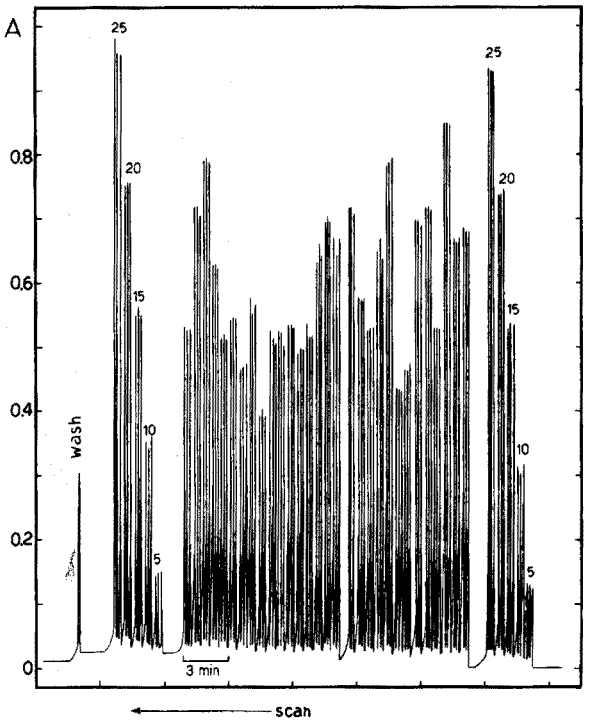

Fig. 9. Routine analyses for phosphorus in plant digests. Line length 320 cm, 1.15 mm i.d. tubing. From right to left: standards of 5.0, 10.0, 15.0, 20.0 and 25.0 μg P ml^{-1}, followed by thirty plant digests and phosphate standards. All samples were analysed in triplicate. Last peak on left is a wash effected by injecting 1 *M* NaOH. Average sampling rate of digested samples was 250 analyses per hour.

the record, the baseline increased slightly during the measurement, because of deposition of molybdenum blue in the flow cell, despite the addition of alcohol to the carrier stream. Therefore, whenever necessary, the system was washed by injecting 0.5 ml of 1 *M* NaOH (the last peak to the left). An average standard deviation of 1.32 % was obtained for this particular series of thirty samples (Table I) which were analysed at an average sampling rate of 250 samples per hour.

In order to keep pace with this rate in routine analyses, two persons were needed for manual injection, one filling and washing the syringes, and the other adjusting the volume and injecting the sample with the same syringe repeatedly three times. As there is no "warm up" or delay period, the baseline can be adjusted immediately and the instrument can be used for short periods at a time as the need arises, with a good economy of reagent consumption and time. Even at the slow sampling rate of 250 analyses per hour, smaller amounts of reagents are used than with the manual method (Table II).

The precision and accuracy, compared to the manual method [8], can be seen from a comparison of the phosphate results obtained on the same 30 samples

TABLE I

Determination of phosphorus in plant digests by flow injection and by a manual method

(Phosphorus expressed as % P in dry plant matter)

Sample No.	Manual method [8] Mean[a]	Flow injection[b]	
		Mean[c]	s_r (%)
1	0.130	0.131	1.07
2	0.130	0.128	0.59
3	0.173	0.160	0.48
4	0.108	0.105	0.26
5	0.157	0.137	0.38
6	0.127	0.134	0.56
7	0.147	0.144	0.64
8	0.094	0.087	1.59
9	0.151	0.149	1.00
10	0.129	0.125	3.19
11	0.102	0.104	0.57
12	0.119	0.112	0.59
13	0.136	0.136	0.69
14	0.127	0.127	2.42
15	0.133	0.134	0.91
16	0.121	0.124	2.73
17	0.089	0.102	2.68
18	0.092	0.097	1.02
19	0.101	0.104	0.58
20	0.100	0.101	2.72
21	0.083	0.100	2.54
22	0.079	0.079	1.81
23	0.106	0.109	2.66
24	0.092	0.092	0.86
25	0.106	0.105	0.56
26	0.101	0.100	1.78
27	0.101	0.119	0.98
28	0.140	0.147	0.51
29	0.131	0.134	2.00
30	0.098	0.102	1.35
Mean value	0.117	0.116	1.32
Difference (μg)	0.2		
(%)	1.0		

[a] Analysed in duplicate.
[b] See also Fig. 9. The regression coefficient for standards in flow injection was 0.99987.
[c] Analysed in triplicate.

TABLE II

Comparison of reagent consumption of manual and flow injection methods

(g of material per analysis)

Method	Reagent			
	Ascorbic acid	Molybdate	Acid[a]	Water
Flow Injection				
225 analyses h^{-1}	0.02	0.03	0.12	5.3
420 analyses h^{-1}	0.01	0.02	0.06	2.8
Manual method [8]	0.02	0.05	0.90	25.0

[a] Manual method, H_2SO_4. Flow injection, HNO_3.

shown in Table I. No statistical difference at the 0.1 % level could be found between the two sets of values. It is interesting to note that the 30 samples in duplicate took two persons 3—4 h manually with pipettes, volumetric flasks, etc., whereas the 30 samples in triplicate were completed in 30 min by the injection procedure.

CONCLUSIONS

Although the flow injection method is still in an early stage of development, it shows great promise, as it allows the routine analyses of phosphate to be made at a sampling rate of 250 samples per hour, with an average standard deviation of 1.32 %. At sampling rates as high as 420 samples per hour, still no carryover was observed, and the flow parameters indicate the possibility of reaching sampling rates in excess of 700 samples per hour for determination of phosphate by the molybdenum blue method. Other advantages compared with manual or even conventional automated continuous flow analysis are equally obvious: the consumption of reagents is minimized, and the cost of equipment is very low, apart from the peristaltic pump. If the analytical requirement is less than a few hundred analyses per day, manual injection is tolerable, but a higher analytical load will, unquestionably, require construction of an automated injector with an appropriate timer. This would allow the inherent capacity of the system to be employed fully.

The great simplicity of construction, low cost and versatility should encourage widespread use of this system. Further, in a similar manner to the AutoAnalyser system, flow injection offers good control of reaction conditions, which allows the analytical use of reactions that do not go to completion or form unstable products. An added advantage is that the flow injection system can be ready instantly for analysis and is therefore useful even when only a few determinations are required.

The optimal flow parameters have now been established on an empirical basis and the usefulness of the system has been demonstrated for one type of analysis; further analytical methods will be adapted for the flow injection method and the possibility of multi-component analysis will be investigated. With regard to the determination of phosphate in lower amounts than in plant material, *e.g.* in water or soil extracts, experiments are under way, based on the addition of antimony to improve the sensitivity.

The authors wish to express their thanks to the Director and staff of CENA for providing facilities and encouragement in this work and to Dr. E.H. Hansen, Chemistry Department A, The Technical University of Denmark, for vital support.

SUMMARY

The effect of sample volume, tube length, tube diameter, peak height and sampling rate on the determination of phosphorus in acidic plant digests was investigated, and optimal conditions for the flow injection method are described. Sampling rates of 420 samples per hour were achieved without incurring problems from carryover of samples, and evidence was obtained that rates as high as 700 samples per hour are possible. The flow injection method was proved to be suitable for routine analyses and has obvious advantages over other automated or manual methods in sampling rate, simplicity of design and cost.

REFERENCES

1 J. Růžička and E.H. Hansen, Anal. Chim. Acta, 78 (1975) 145.
2 J. Murphy and J.P. Riley, Anal. Chim. Acta, 27 (1962) 31.
3 A.C. Javier, S.R. Crouch and H.V. Malmstadt, Anal. Chem., 41 (1969) 239.
4 J.W. Hamm, F.G. Radford and E.H. Halstead, Technicon Symposia, Auto. Anal. Chem., (1970) 65.
5 G.H. Stanley and G.R. Richardson, Technicon Symposia, Auto. Anal. Chem., (1970) 305.
6 L.P. Tyler and A.F. Biles, Technicon Symposia, Auto. Anal. Chem., (1970) 313.
7 Technicon AutoAnalyser II, Industrial method 94-70 W, Technicon, Tarrytown, New York, July 1973.
8 F.S. Wantabe and S.R. Olsen, Soil Sci. Soc., Amer. Proc., 29 (1965) 677.

Analytica Chimica Acta, 79 (1975) 93—99

QUANTITATIVE MEASUREMENTS OF INORGANIC AND ORGANIC ARSENIC BY FLAMELESS ATOMIC ABSORPTION SPECTROMETRY

ARTHUR W. FITCHETT, E. HUNTER DAUGHTREY, JR. and PAUL MUSHAK*

Department of Pathology, University of North Carolina at Chapel Hill, Chapel Hill, North Carolina 27514 (U.S.A.)

(Received 17th February 1975)

The measurement of arsenic, particularly at low levels, still remains troublesome to workers in analytical biochemistry and toxicology. While classical methods have involved spectrophotometric techniques [1], acceptance of atomic absorption spectrometry as a more desirable approach is increasing with the continuing evolution of improved instrumentation.

As with earlier methods, a major step in most atomic absorption spectrometric assays for arsenic is the isolation of arsenic from the sample by chemical reduction to the volatile arsine(s), followed by transfer to a sample cell or solution. This reduction and transfer is not without hazard [2]. Most techniques to date have the additional disadvantage of being total element assays, with no differentiation possible as to the chemical form of the arsenic present. Recent studies involving arsenic in ecosystems, however, suggest that the determination of the chemical type of arsenic may be, at least in some cases, highly desirable. Braman and Foreback [3] have reported studies, dealing with selected human subjects and with environmental samples, which indicate that organoarsenicals such as dimethylarsenic are excreted by man and are contained as such in some forms of marine life. Sewage bacteria, furthermore, have been shown to alkylate arsenic [4—6].

As part of a program concerned with metal pollutant biochemical pathology, we have pursued the development of analytical methods which bypass the necessity of arsine generation and also permit some distinction as to the chemical nature of arsenic present in various samples.

EXPERIMENTAL

Apparatus

A Perkin-Elmer Model 306 atomic absorption spectrometer with the HGA 2100 graphite furnace accessory was employed. Compensation for high background radiation intensity of the furnace was achieved with a deuterium

*To whom correspondence should be addressed.

arc background correction unit. Absorption measurements were made at the 193.7-nm As line, with a Perkin-Elmer arsenic electrodeless discharge lamp as the source.

Glassware

Arsenical(s) were extracted from water or urine in 40-ml and 2-dram glass screw-cap vials. Vessel preparation consisted of a soap and water wash, followed by immersion in analytical-grade (1+1) nitric acid (24 h), finally rinsing copiously with deionized water. The screw caps were prepared for initial use by removing the cap liner and adhesive for immersion in xylene for 1 d to remove any adhering residue. Subsequent routine cleaning involved a soap and water rinse, soaking for 24 h in saturated EDTA solution, and final deionized water rinses. All other glassware was cleaned thoroughly with (1+1) nitric acid and rinsed with deionized water.

Reagents

Arsenic working solutions were prepared by dilution of a 1,000-p.p.m. arsenic stock solution (Fisher Atomic Absorption Standard). The organoarsenical standards were cacodylic acid for dimethylarsenic and diiodomethylarsenic for monomethylarsenic. Analytical-grade reagents were used throughout.

Extraction procedure

Samples of water or urine (5.0 ml) are pipetted into acid-washed 40-ml vials, the necks of which are wrapped with several turns of 0.5-in. teflon tape to prevent leakage on sealing. Add 10 ml of 12 *M*, arsenic-free, hydrochloric acid, seal the vial, agitate for several min (Vortex-Genie shaker) to ensure mixing, and place in a water bath for 1 h,at 60–70 °C. Remove, cool, and add 2.0 ml of low-arsenic potassium iodide solution (1.0 g ml^{-1}). Mix for 15 s, then leave for *ca.* 10 min. Add 5.0 ml of reagent-grade chloroform which has first been equilibrated with 12 *M* hydrochloric acid, seal the vessel, and mix at maximum speed. After separation of the layers by centrifugation at 2000 r.p.m. for 5 min, transfer 4.0 ml of the chloroform layer to a 2-dram acid-washed vial containing 2.0 ml of either deionized water (inorganic arsenic) or dilute (0.005 *M*) sodium dichromate solution (total inorganic + organic arsenic). Care must be exercised not to transfer any of the upper aqueous phase. Reextract the arsenical(s) into the appropriate aqueous medium by shaking for 1 min; then centrifuge. Transfer aliquots (20 μl) of the sample to the graphite furnace by acid-washed disposable plastic tips mounted on an Oxford micropipettor or similar transfer apparatus.

RESULTS AND DISCUSSION

The simple chemical basis of the method described in this report involves the reduction of any inorganic arsenate present to arsenite, and conversion of this species and of any methylated arsenicals to the iodides, both steps occurring in strongly acidic media containing iodide. Removal of arsenic iodide(s) from the medium to an organic phase, *e.g.* chloroform, is then followed by re-extraction into an aqueous medium, such redistribution being achieved with deionized water or the other aqueous conditions described below. The literature includes several successful reports employing a similar approach but varying in the instrumentation and extraction solvents employed [7, 8].

Before optimization of the solution and extraction parameters, it was necessary to determine the best instrumental settings for the flameless atomic absorption spectrometry of arsenic. A commercially available arsenic electrodeless discharge lamp provided highly satisfactory analytical data compared to the conventional arsenic hollow-cathode lamp. Operation of the discharge lamp at 10 W rather than the recommended 8 W, furnished the best compromise between stability, baseline noise and signal intensity. This may be a function of an individual lamp, and may not represent the best condition for all lamps.

The optimal furnace atomization temperature was chosen by measuring the arsenic absorption signal at various atomization temperatures. A plot of absorption signal *versus* atomization temperature is shown in Fig.1; 2500 °C gave the best compromise between signal and background noise.

Figure 2 gives a plot of absorption signal *versus* charring temperature for aqueous inorganic arsenic standards. At 500 °C there is only slight loss of

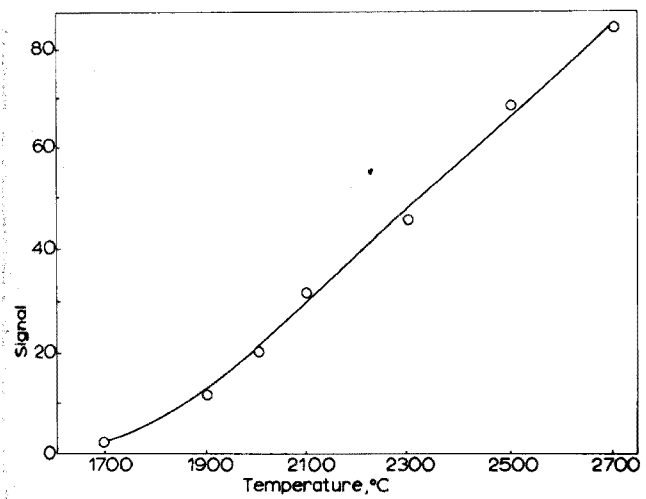

Fig.1. Absorption signal for As as a function of atomization temperature with D_2-arc correction and aqueous As standard (20 µl of 0.1 p.p.m.). Dry, 20 s at 100 °C; char 20 s at 250 °C; atomize 15 s.

signal intensity, relative to 200 °C, but this is more than compensated by using a higher matrix ashing temperature.

In a related study, efforts to determine the minimum charring temperature necessary for the direct analysis of urine showed that 900 °C was necessary for complete removal of sample matter, but this temperature led to loss of arsenic.

Typical recorder traces of background-corrected arsenic signals as a function of medium are shown in Fig.3. The urine blanks furnished arsenic levels within the range cited for normal urine arsenic values [9].

Calibration curves obtained for aqueous arsenic solutions were not linear

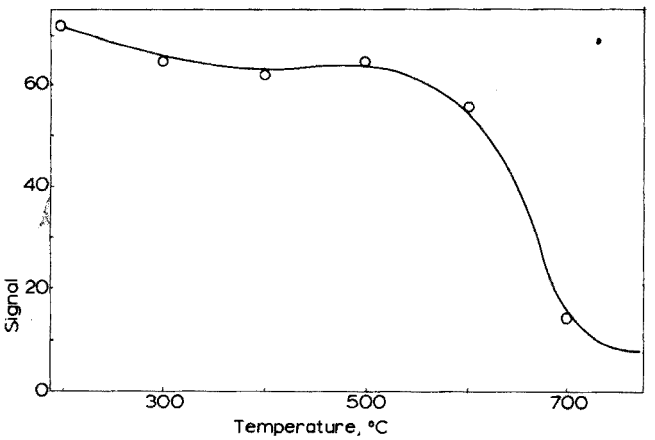

Fig.2. Absorption signal for As as a function of charring temperature with D_2-arc correction and aqueous As standards (20 μl of 0.1 p.p.m.). Dry, 20 s at 100 °C; char 60 s; atomize 15 s at 2500 °C.

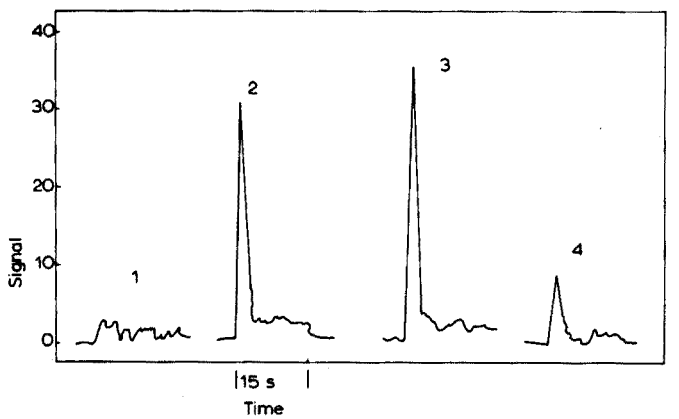

Fig.3. Determination of As in urine. Parameters: dry at 100 °C for 20 s, char at 500 °C for 20 s, atomize at 2500 °C for 15 s. (1) Reagent blank; (2) aqueous As standard, 0.1 p.p.m.; (3) urine extract with added As to give 0.05 p.p.m. added; (4) urine extract without added As.

above 1.0 p.p.m. of the element, partly because measurement of peak height rather than area [10] was used. The use [10] of an electronic integrator, extended the range of linearity.

Removal of arsenic iodide(s) from organic media, *e,g.* chloroform, into an aqueous phase devoid of strong acid and iodide is possible since under these conditions the iodides hydrolyze to water-soluble oxy—arsenic species, as predicted for arsenic triiodide, by the equilibrium:

$$AsI_3 + 3\ H_2O \rightleftharpoons H_3AsO_3 + 3\ HI$$

The optimum amounts of 12 *M* hydrochloric acid and of iodide solution were determined by taking 5 ml of water or urine and varying the relative amounts of reagents. These studies, based on arsenic in urine recovery, showed that an acid volume of 10 ml was required.

In urine, and certain water samples, arsenic appears to be bound partially to biomolecules, particularly as arsenate esters. Therefore heating the sample, after the addition of acid was tried, to assist in rendering the arsenic available for iodination. Sample heating was carried out before the addition of any iodide, inasmuch as appreciable formation of iodine is observed if iodide is added beforehand.

Care must be observed in isolating the chloroform layer after extraction of the aqueous reaction medium, especially of urine, since any carryover of the aqueous medium was observed to yield peaks which interfered with measurement of the arsenic signal.

Table I presents recovery and precision data for the determination of inorganic arsenic in water and urine. With both media arsenic recovery was good with satisfactory precision.

The problem of the possible occurrence of arsenic in various chemical forms necessitated the inclusion in this study of various arsenicals with emphasis on mono- and dimethylarsenic.

When instrumental parameters optimal for assessment of inorganic arsenic and an identical reaction/extraction scheme were used, arsenic present as mono- or dimethylarsenic could not be detected. The form of the arsenical iodides when re-extracted into aqueous media from chloroform was not established, but these species are apparently too volatile under conditions of ashing and drying temperatures to remain in the sample tube. This problem was successfully surmounted by the use of an oxidant in the final aqueous extraction step.

TABLE I

Recovery data for inorganic arsenic added to water or urine

Medium	As added (p.p.m.)	No. of samples	Recovery (%)	s_r
Water	0.05	6	87.0	3.0
Urine	0.25	8	93.1	7.9

Various oxidants at different concentrations were evaluated; best results were obtained with a dilute solution of dichromate (0.005 *M*)

Thus, the tandem use of two final aqueous extraction steps permits the determination of inorganic arsenic only when deionized water is used as the final extractant and the determination of inorganic and methylated arsenic (total arsenic if one assumes that methylated arsenicals are the chief organic arsenic species) if dichromate solution is used. The difference in the levels measured thus furnishes an indirect measure of the organic arsenic content of the samples.

Of interest in this regard is the chemical interaction of dichromate with methyl arsenicals to yield less volatile species. Alkyl arsenicals are remarkably stable to chemical degradation [3] even under drastic conditions; the dichromate seems to oxidize the arsenical rather than cause demethylation to inorganic arsenic. The behavior of arsenic towards dilute solutions of dichromate was not studied with reference to the resulting chemical nature of the arsenic products.

Results of analyses for alkyl arsenicals are presented in Table II and analyses of mixtures of inorganic, mono- and dimethylarsenic are given in Table III. Good recoveries with adequate precision were obtained.

TABLE II

Recovery data for methylated arsenic added to water or urine

Medium	Organoarsenical	Amount As added (p.p.m.)	No. of samples	Recovery (%)	s_1
Water	Methyl [a]	0.10	5	92.7	8
Water	Dimethyl [b]	0.10	6	98.7	3
Urine	Dimethyl	0.10	6	88.4	3

[a] As diiodomethylarsine.
[b] As cacodylic acid.

TABLE III

Recovery of mixed arsenicals [a] in water or urine
(6 samples were analyzed in each case)

Medium	Amount total As (p.p.m.)	Recovery	s_r
Urine	0.05	92.3	5.3
Water	0.05	92.3	5.3
Water [b]	0.05	33.0	1.0 — total
		87.0	3.0 — inorganic

[a] Percent (p.p.m.) in mixture: inorganic, 38.0; dimethyl, 46; methyl, 16.
[b] Dichromate omitted from aqueous extraction step.

Current efforts are directed towards the development of techniques for more detailed differentiation of the organic arsenicals which may be encountered in water and urine samples.

Generous support of this investigation by the National Institutes of Health, Grant No.ES-00481, and partial support by the National Institutes of Health, Training Grant No.GM-92, is gratefully acknowledged.

SUMMARY

Procedures are described for the determination of arsenicals in water and urine by flameless atomic absorption spectrometry; these avoid the isolation and transfer of arsine(s) and permit some differentiation between the inorganic and organic (methyl) arsenic content of a sample. Samples of water or urine are heated with hydrochloric acid, and treated with iodide ion. Arsenic species, as the iodides, are extracted into chloroform and then either re-extracted into deionized water for measurement of inorganic arsenic, or re-extracted into dilute dichromate solution for total arsenic determination; the difference furnishes levels of organic arsenic. Aliquots of the final aqueous extracts are analyzed by graphite-furnace atomic absorption spectrometry, with an arsenic electrodeless discharge lamp. The lower detection limit for water and urine was 10 p.p.b. The recoveries (and s_r values) were: 87.0 % (3.0) and 93.0 % (7.9), for inorganic arsenic in water and urine, respectively; 92.3 % (5.3) for mixtures of inorganic and methylated arsenic (total arsenic) in water and urine; and 98.7 % (3.9) and 88.4 % (3.6) for dimethylarsenic in water and urine, respectively.

REFERENCES

1 I. Sunshine (Ed.), Handbook of Analytical Toxicology. Chemical Rubber Co., Cleveland, 1969, pp.605, 717.
2 J.W. Robinson, R. Garcia, G. Hindman and P. Slevin, Anal. Chim. Acta, 69 (1974) 203.
3 R.S. Braman and C.C. Foreback, Science, 182 (1973) 1247.
4 F. Challenger, Chem. Rev., 36 (1945) 315.
5 B.C. McBride and R.S. Wolfe, Biochemistry, 10 (1971) 4312.
6 D.P. Cox and M. Alexander, Appl. Microbiol., 25 (1973) 408.
7 A.R. Byrne, Anal. Chim. Acta, 59 (1972) 91.
8 K. Tanaka, Jap. Anal., 9 (1960) 700.
9 J.D. Bauer, P.G. Ackerman and G. Toro (Eds.), Clinical Laboratory Methods, C.V. Mosby Co., St. Louis, 1974, p.793.
10 P. Schramel, Anal. Chim. Acta, 72 (1974) 414.

Analytica Chimica Acta, 79 (1975) 101—108

SPECTROFLUORIMETRIC DETERMINATION OF THALLIUM IN SILICATE ROCKS WITH RHODAMINE B IN THE PRESENCE OF ALUMINUM CHLORIDE

MARIAN M. SCHNEPFE

U.S. Geological Survey, Reston, Virginia 22092 (U.S.A.)

(Received 24th February 1975)

Geochemical studies of the thallium content of silicate rocks require accurate and reasonably rapid methods of determination of thallium in the 0.01—1.00 p.p.m. range. Although neutron-activation methods are sufficiently sensitive [1—3], they require expensive instrumentation. Spectrographic methods require preconcentration procedures to attain the required determination limits and to attain representative sampling [4]. Atomic absorption spectrometry has been applied to the determination of thallium; using a flameless atomic absorption method, Sighinolfi [5,6] obtained a detection limit of *ca.* 20 p.p.b. with 0.2 g of sample. Spectrophotometric methods for the determination of thallium with rhodamine B have been of limited use at the submicrogram level [7—13]. Onishi [12], after making comparative studies of the photometric and fluorimetric rhodamine B methods concluded that the fluorimetric determination was no more sensitive than the photometric one. However, Matthews and Riley [13] reported a sensitivity of 0.01 μg of thallium on the basis of three times the standard deviation of the fluorescence intensity of the blank.

In this work, various conditions were investigated to obtain a more sensitive spectrofluorimetric method for the determination of thallium in silicate rocks. The method was applied to the determination of thallium in U.S. Geological Survey standard rocks, G-1 and W-1, after an acid decomposition and a dithizone separation.

EXPERIMENTAL

Reagents

Dithizone (0.1 % w/v). Dissolve 1.00 g of dithizone in 1 l of chloroform. Filter through a coarse sintered glass filter. Protect the solution from unnecessary exposure to light.

Aluminum chloride (50 % w/v). Dissolve by heating 500 g of aluminum chloride hexahydrate in 250 ml of (1+1) hydrochloric acid and dilute to 1 l.

Rhodamine B stock solution (0.2 % w/v). Dissolve 0.200 g of rhodamine B in 100 ml of 1.5 *M* hydrochloric acid. Prepare other rhodamine B solutions by successive dilutions with 1.5 *M* hydrochloric acid.

Thallium(III) stock solution (100 μg Tl ml^{-1}). Dissolve by heating on a steambath 111.7 mg of thallium sesquioxide in 10 ml of (1+1) sulfuric acid. Dilute to 1 l. Prepare standard solutions by successive dilutions with 0.5 % (v/v) sulfuric acid.

Apparatus

The dithizone separations were performed by mixing the phases in a separatory funnel with an air stream as described by Greenland and Campbell [14]. Conventional shaking, however, works equally well.

A Baird Atomic Fluorispec, Model Sf-1, with a xenon arc source and 1-cm quartz cells was used.

Procedure

Accurately weigh 1-g samples and transfer to lidded 50-ml Teflon beakers. Run two blanks with each set of determinations. Add 10 ml of 40 % hydrofluoric acid and 10 ml of 17 *M* nitric acid. Cover the beakers, heat on a steambath for at least 4 h, and evaporate the solution to dryness. Treat the residue with 5 ml of 12 *M* hydrochloric acid and evaporate to dryness to destroy the nitrates. Repeat with 5 ml more of hydrochloric acid. Dissolve the residue in *ca.* 30 ml of solution which contains 1 g of l-ascorbic acid, 4 ml of 50 % (w/v) sodium citrate solution, *ca.* 10 ml of concentrated ammonia liquor, and 10 ml of 50 % (w/v) potassium cyanide solution; the pH of the final solution should be 10.5 ± 0.5. Transfer the solution to a 125-ml separatory funnel (with Teflon stopcocks) and extract four times with 10 ml of the dithizone solution by bubbling air through the mixture for 2 min or by hand shaking for the same time. After draining each organic phase into a second separatory funnel, pass 5 ml of chloroform through the aqueous solution into the second separatory funnel in order to rinse the funnel stem. Discard the aqueous phase. Wash the combined dithizone extract twice with 10 ml of 0.015 *M* ammonia solution by mixing the phases for 2 min. Transfer the organic phase to a third funnel and discard the aqueous phase. Strip thallium from the organic phase by extracting with two 20-ml portions of 0.15 *M* nitric acid. Combine the extracts and rinse with *ca.* 10 ml of chloroform to remove excess of dithizone. Discard the organic phase. Evaporate the aqueous phase to dryness on a steambath. To destroy organic matter add a 0.5-ml portion of (1+1) sulfuric acid and 0.5 ml of 30 % hydrogen peroxide. Cover and heat on a steambath for about 1 h, then uncover and heat for about 1 h. Add 5 ml of 12 *M* hydrochloric acid and evaporate the solution for *ca.* 2 h to remove the hydrochloric acid. Repeat the treatment with hydrochloric acid. To ensure the oxidation of the thallium to the trivalent state, add 1 ml of 1 % (v/v) bromine solution

in constant-boiling hydrobromic acid and heat the solution until it is colorless. Transfer the solution to a 25-ml volumetric flask and make to volume.

Transfer an appropriate aliquot to a 50-ml beaker; add 10 ml of the aluminum chloride solution, and 5 ml of 6 *M* hydrochloric acid and dilute to *ca.* 30 ml. Prepare standard solutions containing 0, 0.05, 0.10, 0.50, and 1.00 μg of thallium(III) and having the prescribed amounts of aluminum chloride and hydrochloric acid in a 30-ml volume. Mix, cover, and allow to stand overnight or a minimum of 8 h. Transfer the beaker content to a dry separatory funnel or a funnel rinsed well with 1.5 *M* hydrochloric acid. Add 1 ml of 0.05 % rhodamine B solution and extract with 10.0 ml of benzene by shaking for 1 min. Drain the organic layer first into a small Pyrex beaker and then into a 15-ml Pyrex centrifuge tube, holding back aqueous droplets. Cover the tube to minimize evaporation and allow to stand for 1—2 h. Then pour the extract into a 1-cm cell and measure the fluorescence intensity at 580 nm with the excitation wavelength set at 560 nm. Make appropriate corrections for the reagent blanks and relate the net fluorescence intensity to a calibration curve. Use solutions of rhodamine B in 1.5 *M* hydrochloric acid as reference standards to maintain the instrument at a given sensitivity.

RESULTS AND DISCUSSION

Sample decomposition

As thallium compounds are relatively volatile at elevated temperatures, dry ashing is avoided. Kuznetsov and Myasoedova [15] noted that losses of thallium occurred during fusion of silicates with sodium carbonate, but that no loss occurred if these samples were decomposed at low temperatures with hydrofluoric acid and either sulfuric or hydrochloric acids. Sill and Peterson [16] observed no significant thallium losses when ores and flue dusts were fused with a mixture of sodium sulfate and sulfuric acid followed by addition of sodium fluoride. However, Fornaseri and Penta [17], using radio-tracer ^{204}Tl, showed that prolonged fuming of thallium solutions with hydrofluoric acid and either sulfuric or perchloric acids caused volatilization of thallium. Because of the volatile nature of thallium at high temperatures, sample decompositions in this study were restricted to steambath temperatures, as in the method of Matthews and Riley [13], who obtained quantitative recoveries of thallium when they decomposed silicate samples with a mixture of hydrofluoric and nitric acids.

Isolation of thallium

Because some elements interfere in the determination of thallium with rhodamine B, a dithizone extraction was used. The only metals reacting with dithizone in a slightly basic medium containing cyanide are bismuth, indium, lead, tin, and thallium. Citrate greatly hinders the indium extraction [18].

None of these reacts with rhodamine B except for indium and thallium. In the final rhodamine procedure, almost 100 μg of indium can be tolerated. Inasmuch as the indium content of most rocks is less than 1 p.p.m., it is unlikely that indium will interfere in the determination of thallium.

The oxidation of dithizone by iron is very pronounced in alkaline solutions. Sill and Peterson [16], as well as Onishi [9], called attention to this problem. They overcame the oxidative attack of iron on the dithizone by the addition of hydroxy ammonium chloride followed by careful heating of the solution to minimize the decomposition of cyanide. Minczewski *et al.* [8] used l-ascorbic acid as a reductant before the dithizone extraction of the thallium. This study confirmed the effectiveness of l-ascorbic acid without the necessity of heating the solution. No oxidation of dithizone was noted in the presence of 100 mg of iron(III) when 1 g of l-ascorbic acid was added before the cyanide.

After stripping of thallium from the dithizone extract, organic matter that would cause fluorescence must be destroyed. Fuming with a mixture of nitric and perchloric acid is generally effective in the elimination of organic matter. However, perchloric acid proved to be a serious interference in the rhodamine B determination of thallium. Even small amounts of residual perchloric acid in the blanks resulted in high fluorescence intensity. Therefore, organic matter was decomposed by a combination of sulfuric acid and hydrogen peroxide after evaporation of the dilute nitric acid back-extract.

The concentration of dilute solutions of thallium tended to decrease as time increased. When dilute solutions of thallium were evaporated in the absence of acid in Pyrex vessels, the thallium values were low. However, if these residues were heated on a steambath with the prescribed hydrochloric acid and aluminum chloride in the covered vessel, the thallium was apparently redissolved.

Effect of hydrochloric acid concentration and aluminum chloride on the extraction of rhodamine B chlorothallate complex with benzene

Initial studies with 0.1 μg of thallium and 0.5 ml of 0.1 % rhodamine B per 30 ml volume in which the hydrochloric acid was varied from 0 to 6 *M* showed the greatest sensitivity for thallium at 1.5 *M*. These results are in good agreement with those of Onishi [9], who reported an extraction coefficient of *ca.* 13 and 93 % recovery of thallium from a 1.6 *M* hydrochloric acid solution with a single benzene extraction. A hydrochloric acid concentration of 1.5 *M* was adopted for this study.

Various chlorides were added to the 1.5 *M* hydrochloric acid solution in an effort to enhance the sensitivity of the fluorimetric determination of thallium. Initial tests with 0.1 μg of thallium and 0.5 ml of 0.1 % rhodamine B were made in which the chloride of sodium, magnesium or aluminum was added. All three salts enhanced the fluorescence of the thallium; the aluminum salt was selected for further work. The amount of the aluminum chloride hexahydrate in a final 30-ml volume of 1.5 *M* hydrochloric acid was varied from 0 to 10 g in increments of 1 g. The highest sensitivity was obtained

when the quantity of the aluminum salt was 5 ± 1 g. Tests in the presence of 5 g of the aluminum salt in which the hydrochloric acid was varied from 1 to 3 *M* showed that maximal sensitivity was obtained with 1.5 *M* hydrochloric acid.

In earlier work in which benzene extraction of rhodamine B chlorothallate was used in the absence of any added salt, the optical cells had a purple cast after the benzene extract had been drained. Relatively little staining of the cells was noted when the aluminum salt was present. Moreover the fluorescence of the blanks decreased in the presence of aluminum chloride, presumably because of the decreased solubility of rhodamine B in benzene.

When Onishi's value [9] of the extraction coefficient was used for the volumes of the aqueous and organic phases employed here, it was calculated that 80 % of the thallium was separated by a single extraction. (Should the separation be 100 % then the net fluorescence intensity should increase by 25 %.) Because it was found that the addition of aluminum chloride resulted in a more than 500 % increase in the fluorescence of the thallium, another mechanism must be acting in addition to "salting-out". The aluminum chloride results in a complex of higher specific fluorescence intensity, perhaps an ion-association complex.

Effect of rhodamine B concentration and time

The concentration of the rhodamine B used in the procedure is not critical: 1 ml of 0.05 % (w/v) in 1.5 *M* hydrochloric acid was as effective or slightly more so with 0.1 μg of thallium than a solution twice as concentrated in producing a higher ratio of the net fluorescence of the thallium complex to the fluorescence of the blank. The 1 ml of 0.05 % rhodamine B adopted in the procedure gives a mole ratio of dye to thallium exceeding 100 for the thallium range required. The use of 1.5 *M* hydrochloric acid to prepare the aqueous rhodamine B solution increases the net fluorescence intensity by reducing the fluorescence intensity of the blanks. For this reason, if the separatory funnels contain water droplets they should be rinsed with 1.5 *M* hydrochloric acid before introduction of sample solution.

The reagent concentrations prescribed here may not indeed be the optima. Thus, in establishing the optimal hydrochloric acid concentration, the rhodamine B concentration seemed less critical and was therefore fixed rather arbitrarily.

The extraction time for separating the rhodamine B chlorothallate complex was varied from 1 to 10 min and found not to be critical; an extraction time of 1 min was selected for the procedure.

The fluorescence intensity of the benzene-extracted rhodamine B chlorothallate complex depends primarily on the reaction time between the thallium(III) and chloride ions and to a lesser extent on the time after the benzene extraction of the complex. The reaction of chlorothallate ion with rhodamine B in 1.5 *M* hydrochloric acid is almost instantaneous.

Maximal fluorescence intensity was attained much more quickly in the presence of aluminum chloride. The net fluorescence intensity of the benzene-extracted thallium complex increased by only 50 % when the reaction time between the thallium(III) and chloride was varied from 5 min to 20 h, when the recommended amount of aluminum chloride was used, whereas in the absence of aluminum chloride, it increased by 300 %. When the reaction time between the thallium(III) and chloride was 5 min, the prescribed amount of aluminum chloride increased the fluorescent intensity by more than a factor of 4. When the reaction was allowed to proceed overnight, the effect of aluminum chloride was less marked.

The rhodamine B chlorothallate complex appears as a colloidal suspension in benzene, and its fluorescence intensity decreases as time increases. It decreases most rapidly during the first hour after the extraction and at about the same rate for all solutions in the range 0—1 μg of thallium. However, the relative percentage decrease is most pronounced at lower concentrations of thallium. For consistent results, fluorescence measurements should be made after at least 1 h and within 4 h of extraction; the same timing should be used for all sample and standard solutions.

Calibration curve, sensitivity and reproducibility

In the prescribed procedure the net fluorescence intensity varies directly with the concentration of thallium in the range 0—5 μg; above 6 μg a negative deviation from Beer's law resulted. A detailed examination of the curve in the range 0—0.1 μg of thallium also showed conformity to Beer's law, provided that the fluorescence was measured between 1 and 4 h after the benzene extraction. Replicate measurements of 0.01—1.00 μg showed a relative standard deviation of 5 %.

To reproduce the fluorescence intensity of the benzene extracts over a period of time, a stable reference standard with excitation and emission spectra similar to those of the extracted thallium complex is necessary. Onishi [12] reported that an aqueous solution of rhodamine B excited with the 365-nm mercury line resulted in an emission maximum at about 575 nm. It was found here that rhodamine B solution in 1.5 *M* hydrochloric acid has excitation and emission spectra almost identical with those of the benzene-extracted rhodamine B chlorothallate complex; the fluorescence intensity is approximately one-tenth that of a solution of the same rhodamine B concentration without hydrochloric acid. A $2 \cdot 10^{-4}$ % (w/v) solution of rhodamine B in 1.5 *M* hydrochloric acid was found suitable for making instrument settings for the 0.1-p.p.m. level of thallium. For other levels, rhodamine B concentrations varying from 10^{-5} % to 10^{-3} % (w/v) in 1.5 *M* hydrochloric acid were found to be convenient.

Comparison of spectrofluorimetric and spectrophotometric sensitivities

Onishi [9,12] compared the photometric and fluorimetric methods and concluded that the photometric was as sensitive as the fluorimetric method. When the method proposed here was used, and the absorbances and the fluorescence intensities of the benzene-extracted blank and of the rhodamine B chlorothallate (nominally 1.0 μg Tl/10 ml of benzene) were measured in 1-cm cells, the absorbances of 1 μg of thallium and blank were respectively 0.041 and 0.013, whereas the ratio of the fluorescence intensities was 100/1. On the basis of the above data, and on the assumption that the net absorbance measured should be least 0.005 and the net fluorescence intensity should be at least double the blank, the proposed spectrofluorimetric method possesses a sensitivity of 0.01 μg, which is about an order of magnitude more sensitive than the spectrophotometric procedure.

Recovery of ^{204}Tl in the benzene extraction of the rhodamine B chlorothallate

The completeness of the extraction was tested, with ^{204}Tl tracer. A solution containing *ca.* 0.3 μg of β-emitting thallium(III) in a 31-ml volume was extracted by the recommended procedure. Aliquots of the two phases were evaporated and their β-activities were compared with appropriate counting standards; 85 % of the thallium was isolated in the benzene phase and 12 % in the aqueous phase.

Test of the procedure

Duplicate determinations of the thallium content in U.S. Geological Survey standard rocks G-1 and W-1 showed 1.09 ± 0.01 and 0.110 ± 0.005 p.p.m. thallium, respectively. These values are in reasonable agreement with values given in Table I.

The author wishes to express her appreciation to Joseph I. Dinnin for assistance in the literature search and to L. Paul Greenland for providing the radiotracer thallium.

SUMMARY

A sensitive spectrofluorimetric procedure with rhodamine B in the presence of aluminum chloride is given for determining submicrogram and microgram quantities of thallium in silicate rocks. Samples are decomposed with a mixture of hydrofluoric and nitric acids and then treated with hydrochloric acid. Thallium is extracted as its dithizonate with chloroform from an alkaline medium containing ascorbate, citrate, and cyanide and then back-extracted with dilute nitric acid. After destruction of the organic matter and treatment with bromine, hydrochloric acid, aluminum chloride, and rhodamine B, the

TABLE I

Determination of thallium in U.S. Geological Survey standard rocks by different laboratories

Thallium (p.p.m.)		Method	Ref.
G-1	W-1		
1.06	0.102	Neutron activation analysis	1
1.08	0.121, 0.116	Neutron activation analysis	2
1.3	0.17	Neutron activation analysis	3
1.3	0.11	Spectrographic	4
—	0.105—0.110	Flameless atomic absorption spectroscopy	5
1.3[a]	0.13[a]		19
1.24[b]	0.110[b]		20
1.09 ± 0.01	0.110 ± 0.005	Spectrofluorimetric	Present method

[a] Values given by Fleischer.
[b] Average value given by Flanagan.

fluorescence intensity of the benzene-extracted rhodamine B chlorothallate is measured. The limit of determination is approximately 0.01 p.p.m. for a 1.0-g sample. The thallium contents of U.S. Geological Survey standard rocks G-1 and W-1 were found to be 1.09 ± 0.01 and 0.110 ± 0.005 p.p.m., respectively.

REFERENCES

1 J.C. Laul, I. Pelly and M.E. Lipschutz, Geochim. Cosmochim. Acta, 34 (1970) 909.
2 G. Marowsky and K.H. Wedepohl, Geochim. Cosmochim. Acta, 35 (1971) 1255.
3 D.F.C. Morris and R.A. Killick, Talanta, 4 (1960) 51.
4 Carlos A.R. de Albuquerque and John R. Muysson, Chem. Geol., 9 (1972) 167.
5 G. Paolo Sighinolfi, At. Absorption Newslett., 12 (1973) 136.
6 G. Paolo Sighinolfi and Adelaide M. Santos, Geochim. Cosmochim. Acta, 38 (1974) 641.
7 C.L. Luke, Anal. Chem., 31 (1959) 1680.
8 J. Minczewski, E. Wieteska and Z. Marczenko, Chem. Anal. (Warsaw), 6 (1961) 515.
9 Hiroshi Onishi, Bull. Chem. Soc. Jap., 30 (1957) 567.
10 R.E. Van Aman and J.H. Kanzelmeyer, Anal. Chem., 33 (1961) 1128.
11 J.F. Woolley, Analyst (London), 83 (1958) 477.
12 Hiroshi Onishi, Bull. Chem. Soc. Jap., 30 (1957) 827.
13 A.D. Matthews and J.P. Riley, Anal. Chim. Acta, 48 (1969) 25.
14 L.P. Greenland and E.Y. Campbell, Anal. Chim. Acta, 67 (1973) 29.
15 V.I. Kuznetsov and G.V. Myasoedova, J. Appl. Chem. USSR, 29 (1956) 2017.
16 Claude W. Sill and Heber E. Peterson, Anal. Chemistry, 21 (1949) 1266.
17 A. Fornaseri and A. Penta, Met. Ital., 55 (1963) 437.
18 I. May and J.I. Hoffman, J. Wash. Acad. Sci., 38 (1948) 329.
19 M. Fleischer, Geochim. Cosmochim. Acta, 33 (1969) 65.
20 F.J. Flanagan, Geochim. Cosmochim. Acta, 37 (1973) 1189.

Analytica Chimica Acta, 79 (1975) 109—124

METHODOLOGY FOR HIGH-FLUX ABSOLUTE MULTIELEMENT NEUTRON ACTIVATION ANALYSIS — ENVIRONMENTAL BASELINES BY ANALYSIS OF TREE RINGS

ENZO RICCI

Oak Ridge National Laboratory, Oak Ridge, Tennessee 37830 (U.S.A.)

(Received 11th March 1975)

Absolute activation analysis was first used by Clark and Overman [1] and Boyd [2] to determine manganese in aluminum, and was later described in detail by Taylor and Havens [3]. However, until recently this method has not been favored because of the strict calibration and control necessary to avoid systematic error, and because of lack of accurate data on cross-sections, resonance integrals and decay schemes.

The comparator method becomes cumbersome when applied to multielement analysis [4], and "triple comparator" [5] and "monostandard" techniques [6] have been reported. The advent of the Ge(Li) detector and the small computer, in addition to new accurate determinations of nuclear data, has finally opened the way for absolute n.a.a.

The absolute method is based on the solution of the activation equation [3] for the number of target atoms, *i.e.*, for the concentration of the trace elements which yield the observed radionuclides. Apart from a knowledge of activation and decay parameters, the method requires careful calibration of detector efficiency and flux determinations. Furthermore, special precautions must be taken when high neutron fluxes are used. The methodology necessary for the development of a reliable absolute instrumental method in this High-Flux Laboratory is described in this paper, since no comprehensive account is available in the literature. The accuracy of the proposed method is demonstrated by multielement analysis of three standard reference materials. Finally, an application to the determination of environmental baselines and chronological contamination levels by analysis of tree-core samples is reported. Methodology, controls and applications are relevant to other n.a.a. facilities and can easily be adapted to them.

EXPERIMENTAL

The High-Flux Laboratory and pneumatic system have already been described [7]. Briefly, rabbits containing the samples are pneumatically transferred to, and bombarded in, the beryllium reflector of the high-flux isotope reactor (h.f.i.r.). The thermal flux is $5 \cdot 10^{14}$ cm^{-2} s^{-1} and the thermal-to-

resonance flux ratio is 35—45. Polyethylene, magnesium and graphite rabbits can be used. Polyethylene rabbits become brittle during bombardments longer than 20 s but are normally used because longer bombardments are seldom necessary at the high activation rates. The magnesium and graphite rabbits are satisfactory in irradiations as long as 72 h. The severity of the h.f.i.r. bombardment conditions often causes samples to darken and become sticky (see below). To avoid material losses, the samples are normally sealed in lidded polyethylene rabbit inserts which are counted directly after bombardment.

Usually a 10-s bombardment allows determinations of Mg, Al, Cl, V and Mn, by means of short-lived nuclides, a subsequent 5-min irradiation then allows determinations of Na, K, Br, As, W by counting 1—2 days later, and Ca, Sc, Cr, Fe, Co, Zn, Se, Rb, Ba by counting after 7—10 days. Counting is done with a Ge(Li) detector of 12 % efficiency and a Nuclear Data 50/50 system; this 4096-channel analyzer is coupled to an 8K PDP-15 computer. The MONSTR overlay system of programs [8] is used to process the γ-ray spectra and compute the final results in p.p.m. by the absolute method. Calculations are based on the well known activation equation for each element:

$$A = \frac{cgaN_0}{W}(\Phi_t\sigma_0 + \Phi_r I_0)(1 - e^{-\ln 2 \cdot t/T}) \qquad (1)$$

which is solved for c, the concentration of the element, of atomic weight W (target nuclide fractional abundance a), in a sample of weight g. Conventional symbols are used to represent thermal and resonance activation parameters; T is the half-life of the radioactive product and t is the time of bombardment.

The flux monitors are two 20-mg aluminum alloy discs containing *ca.* 0.1 % of manganese and gold, respectively; significant resonance activation is induced in gold, while it is small in manganese. MONSTR uses the two monitor count rates in a system of two equations, each of which is analogous to eqn. (1), which are solved for the thermal and the resonance flux.

METHODOLOGY

The method of multielement, instrumental absolute n.a.a. is rapid, efficient and sensitive, provided that all possible sources of systematic error are considered, and that precautions are taken to insure accuracy, precision and reliability. Such aspects are discussed in detail below.

Calibration of detector efficiency

Two independent sets of absolute radioactivity standards (NBS SRM-4216 and IAEA-256) were used to calibrate the Ge(Li) detector for four detector–source distances: 3, 10, 27 and 39 cm. The multi-radionuclide standard NBS SRM-4216 is a weightless point source containing ^{57}Co, ^{60}Co, ^{85}Sr, ^{88}Y, ^{109}Cd, ^{113}Sn, ^{139}Ce and ^{203}Hg, while IAEA-256 is a set of 9 point sources, ^{22}Na, ^{54}Mn, ^{57}Co, ^{60}Co, ^{88}Y, ^{113}Sn, ^{137}Cs and ^{203}Hg, each mounted between two aluminum

discs. Relative standards of ^{56}Co, ^{75}Se, ^{133}Ba and ^{152}Eu were also used to ensure continuity in the efficiency calibration curves. Figure 1 shows the 10-cm geometry curve.

The MONSTR program [8] fits efficiency curves with polynomials. Each curve requires two fits, one before and one after the maximum. In the curve of Fig.1, the maximum occurs at 103.3 keV. By means of the polynomial coefficients so obtained, the values of the four curves could be reproduced with errors smaller than the following: for 3 cm, 5.7 %; 10 cm, 6.9 %; 27 cm, 8.9 %; 39 cm, 3.8 %. The internal consistency of calibration among the four geometries was also checked by determining the absolute activity of two radioactive sources — ^{110m}Ag at 27 and 39 cm, and ^{75}Se at 3, 10 and 27 cm. The standard deviations of independent determinations were 1.6 % for ^{110m}Ag, and 3.5 % for ^{75}Se.

The calibration parameters were checked further by redetermining the absolute activities of some of the original calibrated sources. Results were satisfactory; deviations of the redetermined values from the certified calibration data are given in Table I. The high value for ^{203}Hg at 39 cm is attributed to the low activity of this nuclide (T = 46.61 days) in the NBS standard.

Absolute counting of cylindrical inserts

The standards for efficiency calibration are all point sources, whereas samples are counted while they are enclosed in their rabbit inserts. A correction is thus necessary to account for geometrical differences and sample thickness. To evaluate this correction for organic samples, it was assumed that their

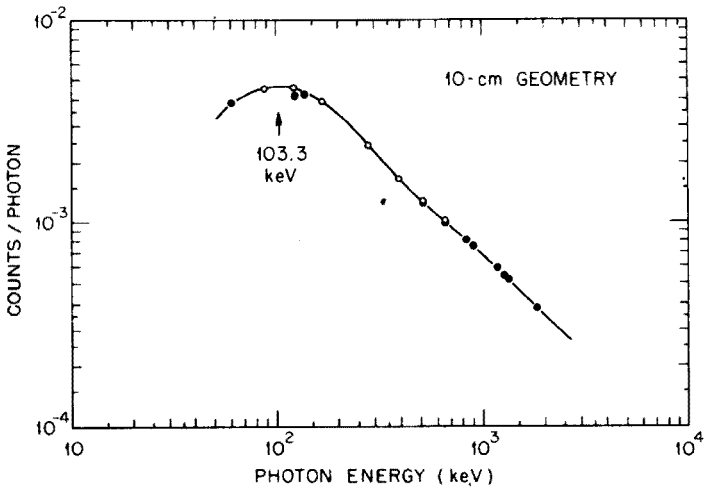

Fig.1. Calibration curve of the efficiency for the Ge(Li) detector. Source detector distance, 10 cm. Sources: (○) NBS SRM-4216; (●) IAEA-256. Curve continuity between distant points was insured with points (not shown) from relative sources of ^{56}Co, ^{75}Se, ^{133}Ba and ^{152}Eu.

TABLE I

Check of calibration of Ge(Li) detector efficiency
(Percent deviations of redetermined absolute activities from original calibrations of NBS and IAEA standards. The calibrated standard was IAEA-256 for the ^{241}Am result, and SRM-4216 for all other results.)

Nuclide	γ-Ray (keV)	Geometry (cm)			
		3 cm	10 cm	27 cm	39 cm
^{241}Am	59.5	−7.0	−5.9	−9.9	−7.2
^{57}Co	122	+5.2	−1.1	−0.52	+0.56
^{139}Ce	166	+8.3	+0.45	−9.0	−4.0
^{203}Hg	279	+1.8	+0.98	−9.5	+18.3
^{113}Sn	392	−1.8	−2.3	−8.9	−1.7
^{85}Sr	514	−4.2	−0.83	+8.3	+6.9
^{137}Cs	662	−3.1	−4.3	−3.7	−5.8
^{60}Co	1173	+1.7	+4.9	+5.7	+6.0
^{60}Co	1333	+3.0	+2.0	+3.1	+2.2
^{88}Y	898	−1.2	+1.2	+0.80	+1.2
^{88}Y	1836	−0.81	+3.5	+4.6	+3.3

photon absorption coefficients were approximately those for water, and that activation was homogeneous throughout the inserts.

Equal aliquots of ^{24}Na, ^{82}Br and ^{75}Se solutions were measured on counting cards (point source) and in water-filled inserts. These sources were then counted — the center of the insert being at the same distance from the detector as the point source — and ratios of point source/insert were obtained for 26 γ-rays from 66.04 to 2754.10 keV. Figure 2 shows these results; as expected the ratios decrease with increasing γ-energy because photon absorption in the insert decreases. Curves for different source-detector distances approximately coincide. The correction factors are important (14—17 %) for low-energy γ-rays, but become negligible (*ca* 5 %, *i.e.*, within the precision of the method) for photon energies above 500 keV.

Flux independence of time and space

The neutron flux is remarkably constant with time for the h.f.i.r. The reactor cycle lasts 22 days, at the end of which the fuel element canister is replaced by a fresh one. Typically, the thermal flux increases by about 4 % during the first day of the cycle and only 3 % more during the following 21 days (0.14 % per day). All bombardments are made within 5—6 h, and the first day is carefully avoided. The resonance flux is slightly less constant, but its significance in activation (eqn.1) in the h.f.i.r. is minimized by the large (35—45) thermal-to-resonance flux ratio.

Flux variation within the volume of the insert, at the bombardment site, is also very small. Activation of six titanium wires [7] placed vertically around

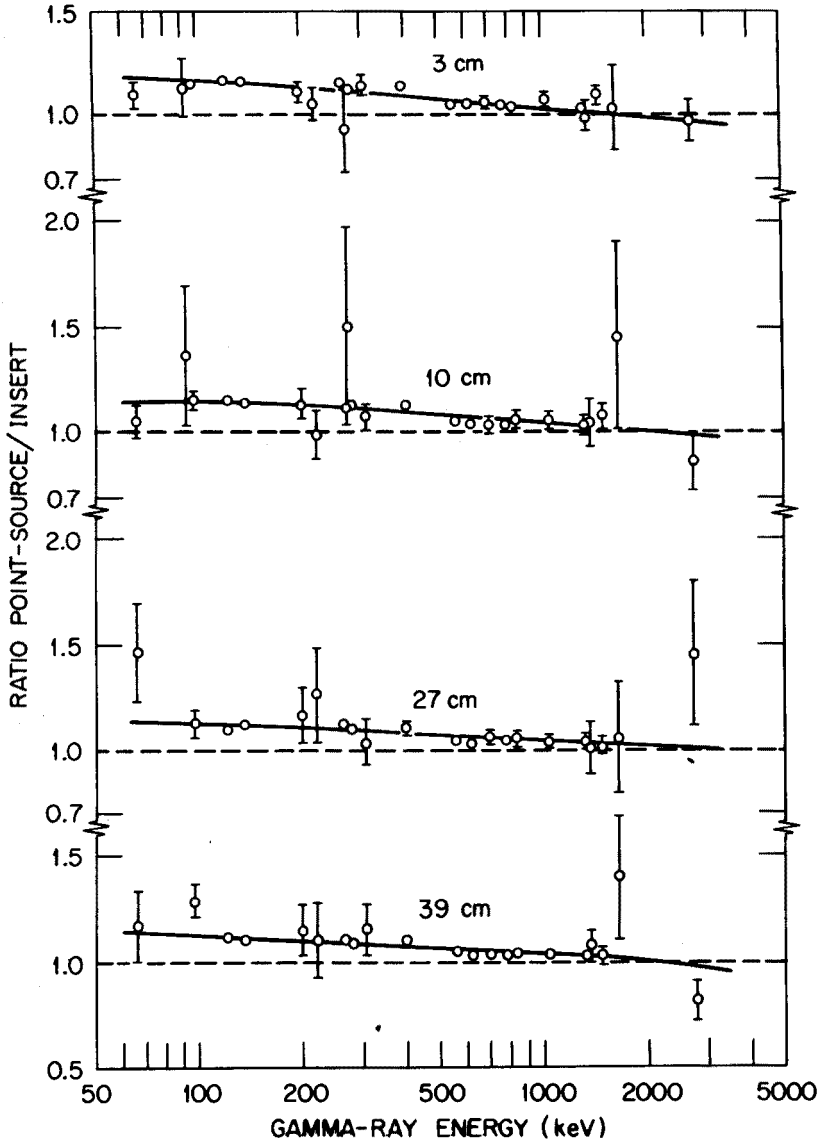

Fig. 2. Counting ratio of point-source/insert *vs.* γ-ray energy for the four detector–sample distances 3, 10, 27 and 39 cm.

a polyethylene insert for a rabbit, showed a total width variation of 4.6—5.8 %. Longitudinal variations (top to bottom of insert) were 0.33 % and 1.4 %, respectively, in activation experiments with chromel (Ni—Cr) and titanium [7] wires.

Stability of sample composition under bombardment

Bombardment at the h.f.i.r. subjects samples to *ca* 6 $W g^{-1}$ of γ-ray heating, and this causes darkening (wood, plastics) and sometimes disintegration (filter paper) of samples into a sticky powder. While Nuclepore filters only darken and become brittle under irradiation. Millipore filters evaporate, often causing explosion of the rabbits with crippling consequences for the pneumatic system.

To investigate the possibility of elemental losses during bombardment in sealed inserts, five similar (0.1-g) samples of Bowen's Kale Standard [9] were irradiated under normal conditions, but for increasing times of 15, 31, 45, 61 and 121 s. Counting was done normally, except for the last sample which had to be allowed to decay for 23.5 min -- the normal decay time is 5—7 min — before the first (short-lived product) count could be made. Results are listed in Table II, which also includes values obtained in conventional 5-s and 5-min (301-s) bombardments. Except for the chlorine results no trends are apparent. Furthermore, most maximum deviations from the average are consistent with the counting errors including those for bromine, the other volatile halogen. Even for chlorine, a 13 % deviation is well within the uncertainty of the method. No losses are thus apparent.

Effect of travel time of rabbits near the core

For most pneumatic transfer systems, the time spent by the rabbit in transit

TABLE II

Results of instrumental absolute n.a.a. for the Bowen Kale Standard [9] versus time of bombardment

Element	Multielement results (p.p.m.) for times of							Max. devn. [a] (%)	Error range [b] (%)
	5 s	15 s	31 s	45 s	61 s	121 s	301 s		
Na	2007	2348	2295	2160	2176	2145	2144	8.0	0.50–
Mg	1480	1925	1675	1647	1734	1666		14	5.2—1
Al	43	55	56	51	58			18	4.0—1
Cl	3570	4415	4024	3884	3834	3758		13	0.65–
K	22,888	26,417	25,116	24,691	24,728	23,538	23,830	8.0	1.5—2
Ca		47,919	45,109	44,256	43,428	46,074	45,000	5.8	2.2—1
V	0.53	0.47	0.51	0.42	0.51			14	12—19
Mn	13	14	15	13	14	13		9.8	4.3—1
Zn		28	28	21	28	33	28	24	2.0—1
Br		22	22	21	21	22	20	6.2	2.6—1
Rb		50	51	52	51	51	50	2.3	1.5—
Sr	107	137	115	104	115	103		21	13—2[illegible]

[a] Maximum deviation from the average.
[b] Range of error from counting statistics.

near the reactor core is negligible in comparison with the bombardment time. The high flux of the present reactor makes bombardments of a few seconds quite frequent, however, particularly during flux measurements. Figure 3 shows how the error of this determination increases for short bombardments when the travel time near the core is ignored. The error for the thermal flux (Φ_t) becomes acceptable (*ca.* 5 %) only for irradiations of 7 s or longer.

To calculate the travel time near the core, eqn. (1) can be reduced, for short bombardments ($t << T$) to:

$$A_s = A/(cg) = \frac{aN_0 \ln 2}{WT} (\Phi_t \sigma_0 + \Phi_r I_0) t = R t \qquad (2)$$

where A_s is the specific activity, and R is a constant combining all the activation constants. During short bombardments, the travel time near the core, τ, is comparable to t. If τ is assumed to be constant, and if in a given irradiation the sample sees approximately the same reactor flux during both τ and t, then eqn. (2) must be corrected to:

$$A_s = R(t + \tau) = R\tau + R t \qquad (3)$$

a straight line with slope R and intercept $R\tau$. Figure 3 shows plots of A_s *vs.* t for ^{56}Mn and ^{198}Au induced in the flux monitors. For a bombardment where $T \gg t \gg \tau$, eqn. (3) reduces to eqn. (2). Since t = 15 s in Fig.3 represents these conditions, we can obtain $R = 8.34 \cdot 10^4$ μg^{-1} s^{-1} /15 s = $5.56 \cdot 10^3$ μg^{-1} s^{-2} for ^{56}Mn. The intercept of this line is found graphically to be $R\tau = 5.2 \cdot 10^3$ μg^{-1} s^{-1}, and then τ = 0.94 s. Figure 3 shows this value on the t axis, after extrapolation to A_s(Mn) = 0; *i.e.*, $\tau = -t$ in eqn. (3). Thus, to avoid systematic error a minimum bombardment length of 10—11 s is established (see Φ_t curve in Fig.3).

The A_s(Mn) plot is a straight line, proving that the assumptions made for eqn. (3) are correct for activation of manganese. The slight upward curvature of the A_s(Au) plot indicates · because of the large resonance integral of gold — that eqn. (3) is not strictly correct when resonance activation is significant. However, the error is small for gold and negligible for most elements (with relatively smaller resonance integrals) because of the 35—45 flux ratio of the facility (see above).

Background impurities in accessory materials

High-flux bombardment results in high sensitivity, but it also creates the need for counting samples sealed in their irradiation inserts. Because impurities in the polyethylene inserts must be subtracted, their concentrations must be very low if the purpose of high-sensitivity n.a.a. is not to be defeated. The same applies to other materials such as filters in the analysis of filtrates. Impurity levels and other properties of Whatman, Millipore, polystyrene and cellulose acetate filters have been reported [10], but Millipore filters could not be

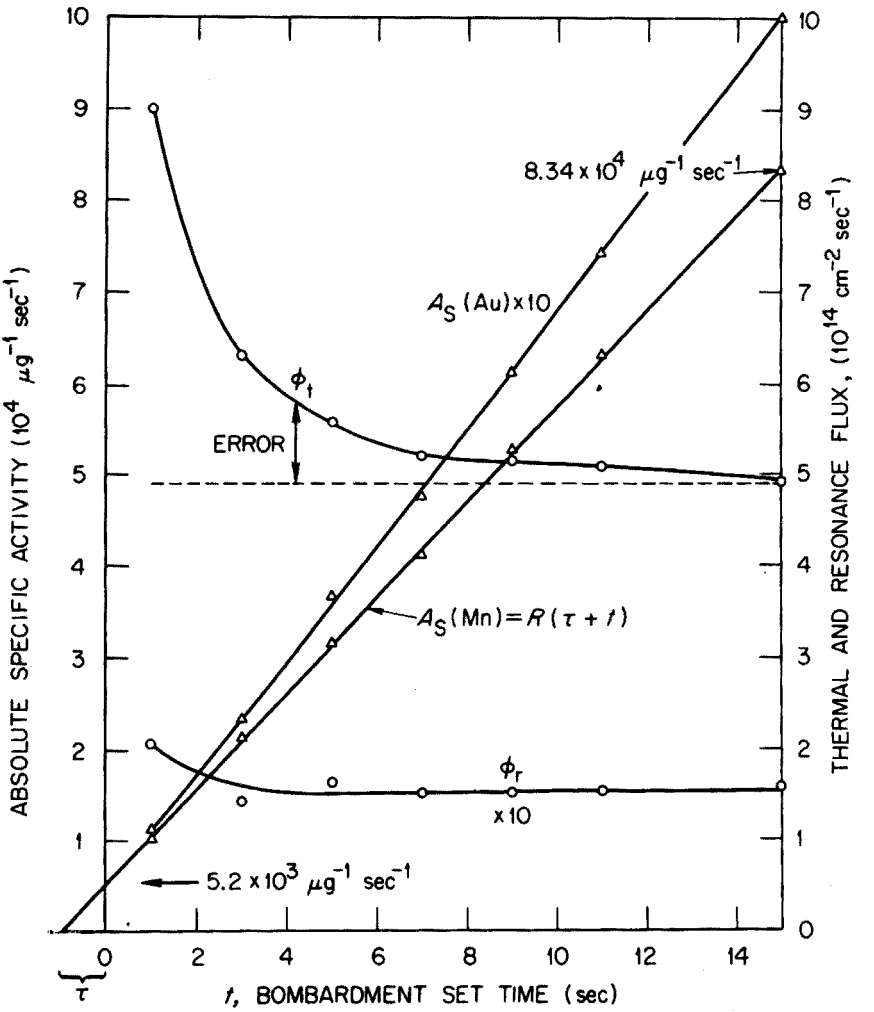

Fig.3. Influence of travel time of rabbit near the core on thermal and resonance flux determinations (○) and on induced specific activity at the end of bombardment (△).

irradiated in the facility used here, and Nuclepore filters were not included in the earlier study.

Duplicate samples of inserts and of 47-mm diameter Nuclepore filters of 0.8-μm pore size were analyzed for 15 elements. Table III shows that the elemental contents are quite acceptable. The impurities of Nuclepore filters are compared with values published by the manufacturer and with results for Millipore filters of the same diameter and pore size [10]. The results agree generally with those from the manufacturer except for Al, Cl, V and Zn, which show contents several times greater than those claimed. However, the greater bombardment stability and consistently lower impurity concentrations

TABLE III

Background impurities in polyethylene inserts (plus lids) and in 47-mm diameter filters

Element	This work [a]				Other	
	Inserts		Nuclepore		Nuclepore [b]	Millipore [c]
	Total (μg)	s_r (%)	Total (μg)	s_r (%)	Total (μg)	Total (μg)
Na	0.24	9.6	0.75	0.4	0.1–0.5	6.9
Al	0.27	9.7	0.73	0.6	0.05–0.1	0.17
Cl	1.3	14	0.68	3.6	-	17.3
K	ND [d]	—	ND	—	0.005—0.01	1.7
Ti	ND	—	ND	—	0.01—0.05	< 0.2
V	ND	—	0.30	1.7	—	< 0.001
Cr	0.26	1.3	0.05	17	0.01–0.05	0.26
Mn	0.008	78	0.004	18	0.01–0.05	0.03
Fe	ND	-	ND	—	0.1—0.5	0.69
Ni	ND	—	ND	—	0.05—0.1	< 0.35
Cu	ND	—	ND	—	0.01—0.05	1.0
Zn	0.38	21	0.44	5.4	0.05—0.1	0.12
As	ND	—	0.03	38	—	—
Br	0.004	20	0.02	32	—	0.03
Hg	ND	—	0.012	0.2	< 0.01	0.009

[a] Two samples analyzed in each case.
[b] Manufacturer's data from emission spectroscopy, atomic absorption, and n.a.a.
[c] From Ref.10.
[d] Not detected.

(Table III) of Nuclepore compared to Millipore filters make the former more suitable for high-flux n.a.a. Table III also shows that the polyethylene inserts are satisfactory; only seven trace impurities are present in small amounts.

Accuracy and precision

The reliability of the method was tested with three widely accepted multi-element standards: the NBS Standard Reference Materials No. 1571 (Orchard Leaves) and No. 1632 (Coal), and the Bowen Kale Standard [9]. Table IV shows that the present results agree well with the certified values for the coal and reasonably well with those for orchard leaves. Deviations from the kale standard values are somewhat larger, but do not show any trends or systematic errors. In general, for any one row (element) in the Table, either good agreement or deviations of opposite sign are apparent among the three standards. Accuracy is 10 % or better for most elements; only a few show greater deviations.

Table IV also shows that precision, measured as standard deviation, is

TABLE IV

Analysis of NBS orchard leaves, coal, and of Bowen's Kale Standards [a]

Orchard leaves			Coal		Bowen's Kale	
Element	Certified value	This work [b]	Certified value	This work [c]	Certified value	This work [d]
Na	82 ± 6	83 ± 5	414 ± 20 [e]	325 ± 6	2500	2144 ± 7
Mg	6200 ± 200	7830	2000 ± 500 [e]		1600	1500 ± 200
Al		378 ± 13	18,500 ± 1300 [e]	17,200 ± 900	37	43 ± 3
Cl	(700)	750 ± 19	890 ± 125 [e]	866 ± 40	3450	3570 ± 91
K	14,700 ± 300	13,800 ± 400	2800 ± 300 [e]	2660 ± 20	25,000	23,800 ± 200
Ca	20,900 ± 300	21,300 ± 900	4300 ± 500 [e]		40,000	45,000 ± 1600
Sc		0.065 ± 0.003	3.7 ± 0.3 [e]	3.7 ± 0.1	0.0086	0.014 ± 0
V		0.58 ± 0.07	35 ± 3	37 ± 3		0.53
Cr	(2.3)	2.8 ± 0.2	20.2 ± 0.3	17 ± 1	0.33	0.50 ± 0.19
Mn	91 ± 4	92 ± 3	40 ± 3	41 ± 1	14.9	13 ± 1
Fe	300 ± 20	283 ± 23	8700 ± 300	7800 ± 200	120	133 ± 15
Co	(0.2)	0.42 ± 0.47	(6)		0.056	0.10 ± 0.02
Zn	25 ± 3	21 ± 2	37 ± 4		32	28 ± 4
As	14 ± 2	9.7 ± 0.4	5.9 ± 0.6	4.5 ± 0.4		•
Se			2.9 ± 0.3	3.2 ± 0.3		
Br	(10)	7.4 ± 0.2	19.3 ± 1.9 [e]	19 ± 4	27	20.4 ± 0.5
Rb	12 ± 1	10.3 ± 0.7	21 ± 2 [e]		53	50.0 ± 0.1
Sr			161 ± 16 [e]		98	107 ± 29
Hg		0.19		0.51 ± 0.17	0.16	0.10 ± 0.02

[a] Results are given as averages with standard deviations. Despite various drying methods, no appreciable differences were observed between results of individual samples.
[b] Two samples were oven-dried at 90 °C for 24+ h (NBS method); the third was vacuum-dried at room temperature over P_2O_5 for 44 h. The results are the average of three determinations.
[c] One sample was oven-dried at 105 °C for 5 h; the other was vacuum-dried as in (b). The results are the average of two determinations.
[d] One sample was vacuum-dried as in (b); the other was oven-dried at 90 °C for 20 h (Bowen's method). Results are the average of two determinations.
[e] Reference 11; value not certified by the NBS.

similar to or better than that of the certified standards. Thus, the proposed high-flux multielement absolute instrumental n.a.a. technique appears to be reliable.

CHRONOLOGY OF ENVIRONMENTAL MULTIELEMENT BASELINES BY TREE-CORE ANALYSIS

To illustrate the usefulness of the method, an application to environmental science is described. Tree rings correspond to years of tree life; thus, tree-core sample impurities can be correlated to past environmental conditions. Chronological variations of environmental baselines and contamination levels over a century were studied by analyzing core samples from two similar Shortleaf Pines (*Pinus Echinata*) located in the Walker Branch Watershed — a relatively unpopulated area — and in the city of Knoxville. The results obtained indicate the potential of this type of approach.

With a 12-mm diameter bore, three cores were obtained from each tree 137 cm above ground and at approximate intervals of 120° around the trunk. The cores were immediately refrigerated in plastic bags, and then cut into portions corresponding to successive 4-year growth periods; the portions were kept in clean corked Pyrex tubes until bombardment. Core increments No.20 (years 1872—76), No.8 (1932—38), No.3 (1958—63) and No.1 (1968—72) were analyzed from both trees. The three cores from the Watershed tree were analyzed for 18 elements, while 16 elements were determined in two cores of the Knoxville tree.

The results are listed in Tables V and VI — 216 results for the Watershed tree and 128 for the Knoxville tree. Obviously, no clear conclusions can be drawn before a detailed statistical study has been made. However, to illustrate the power of this method, Fig. 4 shows the results of a simple data treatment, in which results for all cores were averaged for individual elements in each increment of each tree. The chronological dependence of these averages determined the curves of Fig.4. Standard deviations of these averages were often large, and sometimes larger than the averages; curves were not plotted when the latter occurred for most increments, which explains the absence of some elements in Fig.4, particularly the Knoxville tree curves for chlorine, cobalt and vanadium. These standard deviations reflect variations among cores of one of the trees rather than method uncertainties; and so do the error bars in the figure, as they represent the average of the standard deviations for each curve. Finally, elements thought to be naturally present in trees (left curves) were arbitrarily separated from those considered contaminants (right curves).

The above treatment is arbitrary, yet some preliminary observations may be made. First, a general increasing trend is apparent for the "natural components" (except magnesium) against a decreasing tendency of the "contaminants" (except vanadium). Evidence of this is strong for chlorine and potassium among the former, and for manganese and barium among the latter, because of their relatively small average standard deviations. Secondly, both concentration

TABLE V

Analysis of Walker Branch Watershed tree-core samples [a]

Element	Increment no.20 (1872-76)			Increment no.8 (1932-38)		
	Core number			Core number		
	1	2	3	1	2	3
Na	5.74 (1.3)	8.76 (0.96)	17.1 (1.5)	10.8 (1.0)	20.3 (0.73)	77.0 (
Mg	[c]	180 (13) [b]	[c]	120 (13) [b]	90 (20) [b]	120 (2
Al	ND	12.4 (3.1)	5.7 (11)	10.5 (4.3)	7.8 (5.3)	11.5 (
Cl	ND	ND	20 (6.1)	49 (6.0)	42 (5.4)	125 (3
K	147 (2.4)	144 (2.0) [b]	154 (4.0)	420 (1.2) [b]	414 (1.2) [b]	448 (1
Ca	1600 (12)	ND	ND	ND	ND	ND
V	ND	0.04 (30) [b]	ND	ND [b]	ND [b]	ND [b]
Cr	0.20 (> 30)	ND [b]	ND	0.3 (> 30) [b]	0.4 (> 30) [b]	ND [b]
Mn	120 (0.31)	94.2 (0.26)	95.2 (0.24)	113 (0.58)	122 (0.24)	136 (
Fe	ND	ND	ND	16 (14)	ND	ND
Co	ND	0.06 (> 30)	0.05 (> 30)	0.03 (> 30)	0.05 (> 30)	ND
Zn	ND	9 (20)	7.1 (4.0)	9.7 (2.4)	5.4 (4.9)	7.9 (2
Br	0.07 (18)	ND	ND	ND	ND	ND
Rb	ND	ND	ND	0.6 (17)	0.5 (24)	0.6 (2
Ag	ND	ND	ND	ND	0.1 (23)	ND
Ba	12.3 (8.6)	13.2 (7.8)	14.2 (7.9)	8.0 (7.9)	4.9 (13)	6.7 (1
W	ND	ND	ND	0.07 (34)	ND	ND
Hg	ND	ND	ND	ND	ND	ND

[a] Results in p.p.m. followed by (per cent counting statistical error).
[b] Computer forced result. Also Se, Sr, Sb, Cs and Au (forced) were not detected (ND).
[c] Element possibly present but missed by peak-finding routine.

levels and chronological variations are remarkably similar for the Watershed and the Knoxville trees. Clearly a detailed statistical study is essential; the large error bars of Fig.4 indicate that possibly meaningful differences among individual cores can be found.

CONCLUSIONS

An accurate, precise and sensitive method for multielement absolute n.a.a. based on high-flux bombardments has been developed. Because it is entirely instrumental, 15—20 elements can be determined simultaneously with little effort. The stringent requirements inherent in absolute n.a.a. are naturally enhanced when high-flux bombardments are used for high sensitivity. These difficulties can be overcome by a thorough methodology which involves, apart from calibration of detector efficiency, five possible causes of error. These steps can be adapted to analogous techniques developed for other similar facilities. Analysis of well-known standards showed that it was possible to ob-

TABLE V (continued)

Increment no.3 (1958–63)			Increment no.1 (1968–72)			Element
Core number			Core number			
1	2	3	1	2	3	
6.79 (1.1)	15.8 (0.82)	30.5 (0.64)	13.6 (1.3)	65.2 (0.50)	62.9 (0.80)	Na
50 (33) [b]	ND [b]	60 (32) [b]	[c]	70 (24) [b]	[c]	Mg
16.0 (3.9)	7.7 (8.4)	13.0 (4.1)	32 (7.7)	12.6 (3.6)	13.9 (4.5)	Al
27 (5.1)	34 (5.2)	47 (6.2)	168 (2.5)	215 (2.3)	155 (2.6)	Cl
529 (0.90) [b]	420 (1.2) [b]	378 (1.4) [b]	1631 (0.96)	958 (0.92) [b]	775 (1.6)	K
ND	ND	ND	1980 (8.7)	ND	ND	Ca
0.07 (26) [b]	ND [b]	0.05 (30) [b]	ND	0.07 (21) [b]	ND	V
0.7 (> 30) [b]	0.3 (> 30) [b]	0.9 (> 30) [b]	0.2 (> 30)	1.6 (> 30) [b]	ND	Cr
91.6 (0.59)	92.6 (0.24)	101 (0.64)	21.7 (0.28)	67.0 (0.31)	77.2 (0.27)	Mn
35 (9.4)	ND	14 (15)	38 (16)	35 (19)	26 (15)	Fe
0.3 (> 30)	0.05 (> 30)	0.02 (> 30)	0.05 (> 30)	0.08 (> 30)	0.03 (> 30)	Co
8 (18)	5.2 (5.2)	7.1 (3.2)	2.8 (9.9)	6.5 (6.5)	3.8 (6.4)	Zn
ND	0.049 (12)	ND	0.30 (11)	0.20 (5.5)	ND	Br
0.79 (0.79)	0.5 (23)	0.4 (24)	ND	ND	0.9 (20)	Rb
0.14 (19)	0.22 (14)	0.13 (15)	ND	0.28 (15)	ND	Ag
7.0 (12)	4.2 (16)	6.1 (12)	5.8 (17)	2 (35)	4 (23)	Ba
0.1 (22)	ND	ND	0.15 (18)	0.16 (17)	ND	W
0.05 (23)	ND	0.03 (29)	ND	ND	ND	Hg

tain the same or better precision than the certified values, and the accuracy of the method was shown to be 10–15 % for most elements.

We are indebted to W.F. Harris and D.E. Reichle of the ORNL Environmental Sciences Division for obtaining and providing the tree-core samples and for useful discussions, and to L.C. Bate and J.F. Emery for assistance in applying the MONSTR program.

This work was supported by the U.S. Energy Research and Development Administration under contract with the Union Carbide Corporation.

SUMMARY

Multielement determinations by high-flux absolute n.a.a. require careful methodology to avoid systematic error. The ORNL high-flux facility with a thermal flux of $5 \cdot 10^{14}$ cm^{-2} s^{-1} and a thermal-to-resonance flux ratio of

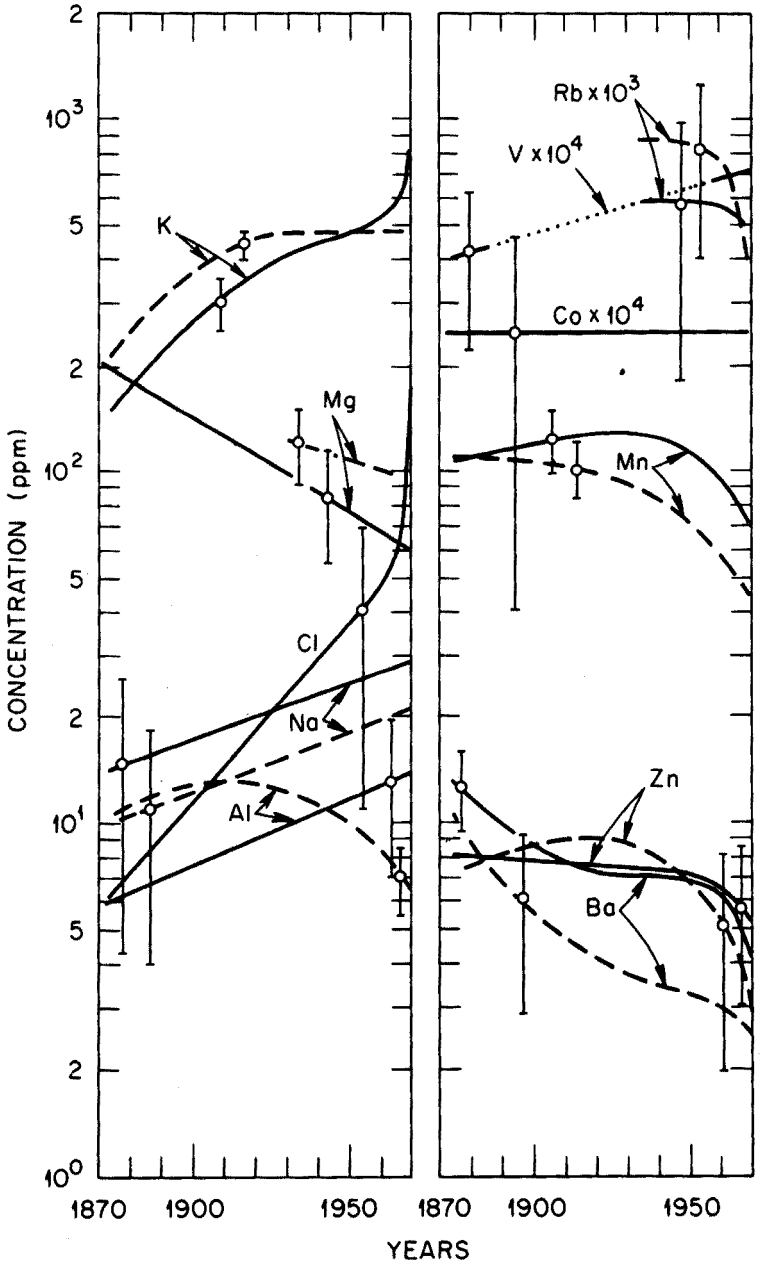

Fig.4. Chronological variation of environmental baselines and contamination levels by analysis of tree core samples (preliminary study). Solid and dashed lines correspond to data from Walker Branch Watershed and from Knoxville tree, respectively.

TABLE VI

Analysis of Knoxville tree-core samples [a]

Element	Increment no.20 (1872–76)		Increment no.8 (1932–38)		Increment no.3 (1958–63)		Increment no.1 (1968–72)	
	Core number 1	3	Core number 1	3	Core number 1	3	Core number 1	3
Na	12.9 (1.1)	2.67 (3.3)	33.8 (1.0)	11.2 (1.6)	15.6 (1.5)	31.4 (1.2)	22.4 (0.93)	9.9 (1.8)
Mg	[c]	[c]	160 (12) [b]	80 (27) [b]	100 (21) [b]	100 (30) [b]	[c]	[c]
Al	15.2 (5.4)	5.6 (6.1)	12.5 (3.8)	11.0 (4.4)	7.8 (6.6)	8.4 (7.4)	6.5 (14)	6.6 (6.2)
Cl	15.4 (9.1)	ND	66 (5.4)	ND	ND	55 (6.1)	26 (5.5)	22 (5.1)
K	205 (2.6)	223 (3.3)	493 (1.8) [b]	457 (1.9) [b]	478 (1.9) [b]	439 (2.1) [b]	449 (1.8)	570 (1.7)
Ca	1600 (11)	ND	ND	ND	ND	ND	ND	ND
Cr	ND	ND	ND [b]	ND [b]	0.3 (> 30) [b]	0.6 (> 30) [b]	0.6 (> 30)	ND
Mn	109 (0.30)	107 (0.23)	64.1 (0.42)	108 (0.32)	46.7 (0.51)	66.8 (0.44)	38.9 (0.39)	45.0 (0.34)
Fe	ND	ND	ND	ND	ND	19 (19)	25 (18)	ND
Co	ND	0.02 (> 30)	ND	ND	ND	ND	0.03 (> 30)	ND
Zn	7.2 (7)	7.4 (4.2)	13.0 (2.4)	9.2 (3.3)	5.6 (4.0)	4.5 (4.7)	ND	2.4 (8.8)
Br	0.10 (20)	ND	0.07 (12)	ND	0.024 (13)	ND	0.04 (> 30)	ND
Rb	ND	ND	0.9 (13)	0.8 (18)	0.8 (15)	0.7 (17)	ND	1.1 (18)
Ag	ND	ND	1.06 (3.0)	15.3 (0.71)	0.15 (15)	0.69 (4.8)	0.11 (28)	ND
Ba	11 (7.3)	10 (13)	3.2 (16)	ND	3.0 (15)	2.9 (18)	ND	3 (32)
W	ND	ND	ND	ND	ND	ND	0.06 (29)	ND

[a] Results in p.p.m. followed by (per cent counting statistical error).

[b] Computer forced result. Also V, Se, Sr, Sb, Cs and Au (forced) were not detected.

[c] Element possibly present but missed by peak-finding routine.

35—45, was used in developing an instrumental absolute multielement method. The detector was calibrated for absolute counting with two independent sets of radioactivity standards for four detector—source distances; the absolute activities of the standards were reproducible within accuracies of 9%. Five sources of systematic error were investigated: (a) correction for counting of cylindrical sources for 26 γ-ray energies reached 14—17% for photon energies below 500 keV; (b) flux variation during bombardment and within the irradiation capsule volume was not significant; (c) samples were sufficiently stable during high-flux bombardment; (d) multi-element impurities in accessory materials (polyethylene and "Nucleopore" filters) were not significant; (e) correction for sample activation during rabbit transfer was necessary for short bombardments, *e.g.*, 8.6 % for 6 s and 19.6 % for 4 s. This methodology resulted in accuracies of 10—15 % for most elements, as determined by analysis of N.B.S. orchard leaves and coal and of Bowen's kale standards. The method was applied to a preliminary chronological study of environmental baselines and contamination levels, based on tree ring samples, covering a period of 100 years.

REFERENCES

1 H.M. Clark and R.T. Overman, USAEC Report MDDC-1329, 1947.
2 G.E. Boyd, Anal. Chem., 21 (1949) 335.
3 T.I. Taylor and W.W. Havens, Jr. in W.G. Berl (Ed.), Physical Methods in Chemical Analysis,Vol. III, Academic Press, New York, 1956, p.557.
4 W.S. Lyon, E. Ricci and H.H. Ross, Anal. Chem., 44 (1972) 438R; 46 (1974) 431.
5 F. De Corte, A. Speecke and J. Hoste, J. Radioanal. Chem., 3 (1969) 205.
6 M. Okada and N. Tamura, JAERI-M-4900, Tokyo, 1972.
7 E. Ricci, T.H. Handley and F.F. Dyer, J. Radioanal. Chem., 19 (1974) 141.
8 J.F. Emery and F.F. Dyer, Proc. 2nd Int. Conf. Nucl. Methods Environ. Res., July 29- 31, 1974, Columbia, Mo.
9 H.J.M. Bowen in J.M.A. Lenihan and S.J. Thomson (Eds.), Advances in Activation Analysis,Vol.I, Academic Press, London, 1969, p.107.
10 R. Dams, K.A. Rahn and J.W. Winchester, Environ. Sci. Technol., 6 (1972) 441.
11 J.M. Ondov, W.H. Zoller, I. Olmez, N.K. Aras, G.E. Gordon, L.A. Rancitelli, K.H. Abel, R.H. Filby, K.R. Shah and R.C. Ragaini, Anal. Chem., 47 (1975) 1102.

Analytica Chimica Acta, 79 (1975) 125—137

THE PRECISE AND ACCURATE DETERMINATION OF SILICON IN ROCKS BY 14-MeV NEUTRON ACTIVATION ANALYSIS

D.M. BIBBY*

NIM-WITS Activation Analysis Research Group, Nuclear Physics Research Unit, University of the Witwatersrand, Johannesburg (South Africa)

(Received 2nd April 1975)

Silicon, with a concentration of about 27 % [1], is the second most abundant element in the earth's crust, and the most important in full major element geochemical analyses. Classical chemical methods for the determination of silicon are generally lengthy and require a high degree of skill if accurate results are to be obtained. The main instrumental method for the determination of silicon is x-ray fluorescence, but considerable matrix corrections have to be made unless the samples are fused with a heavy absorber. All these methods require prior dissolution or fusion of the rock; this can be a source of error, and is time-consuming with refractory materials.

The determination of silicon by fast neutron activation analysis (f.n.a.a.) is essentially non-destructive, and requires little or no sample preparation. The determination of silicon in a wide variety of matrices has been investigated by many authors [2], but only a limited amount of work [3] has been published on the potential accuracy and precision of this method.

This paper details an investigation into the precise and accurate determination of silicon in a number of well-characterized silicate rocks.

Nuclear data

The irradiation of silicon with fast neutrons gives the reactions summarized in Table 1. The most commonly used nuclide in analysis for silicon is aluminium-28 which has a single prominent photopeak at 1.778 MeV, and a convenient short half-life of 2.24 min. Interfering elements commonly found in silicate rocks are magnesium, aluminium, phosphorus and iron; these give rise either to direct nuclear interferences or to γ-ray spectral interference, and are included in Table 1.

EXPERIMENTAL

Apparatus

The neutron generator used was a Picker Nuclear Accelerator 1, operated

*Present Address: Chemistry Division, DSIR, Private Bag, Petone, New Zealand.

TABLE 1

Fast neutron reactions on silicon and interfering reactions from magnesium, aluminium, phosphorus and iron

Reaction	Isotopic abundance	Half-life [4]	γ-Ray energy (and abundance) [4]
$^{28}Si(n,p)^{28}Al$	92.21	2.24 min	1.778(100)
$^{29}Si(n,p)^{29}Al$	4.7	6.60 min	1.273(94), 2.425(6)
$^{30}Si(n,\alpha)^{27}Mg$	3.09	9.50 min	0.171(0.7), 0.844(72), 1.014(28)
$^{31}P(n,\alpha)^{28}Al$	100	2.24 min	1.778(100)
$^{27}Al(n,\gamma)^{28}Al$	100	2.24 min	1.778(100)
$^{27}Al(n,\alpha)^{24}Na$	100	15.00 h	1.369(100), 2.754(99.9)
$^{56}Fe(n,p)^{56}Mn$	91.66	2.57 h	0.847(99), 1.811(30), 2.113(15.5)
$^{24}Mg(n,p)^{24}Na$	78.7	15.00 h	1.369(100), 2.754(99.9)

to produce a neutron output of ca. 10^{11} ns^{-1}. Sample and monitor were irradiated simultaneously in a dual-axis rotator attached to the cooling jacket of the target, and were counted in single axis rotators held rigidly in front of 125 × 125 mm NaI(Tl) detectors (Bicron) with resolutions of ca. 7 %. These detectors were coupled to Ortec 276 preamplifiers and Elscint CAV-N-4 amplifiers modified to have a time constant of 0.4 μs. The outputs of the amplifiers were stabilized by Canberra 1520 Analog stabilizers and analysed with Canberra 1431 single-channel analysers (SCA's) and Tennelec 456P scalers.

Determination of counting losses

The losses suffered in SCA systems arise mainly from random coincidence between pulses, and are small compared with the losses suffered in multi-channel analysers. However, these must still be allowed for if the most accurate results are sought, and they were determined in a separate experiment by a modified version of a dead-time correction system, which measures [5] the loss of a known number of pulses injected into the counting system. The apparatus is shown schematically in Fig. 1. A second output from the analog stabilizer was taken to a pulse-rate divider (÷64) and to the external trigger input of a tail pulser (BNC-BHl). Tail pulses, taken to the test input of the preamplifier, appeared as a narrow peak in the γ-ray spectrum with an apparent energy of 6.05 MeV. The number of pulses in this peak was measured by a SCA having a window from 6.0 MeV to 6.1 MeV (this range covered any drift occurring during the counting period). Trigger pulses produced simultaneously with the tail pulse were taken directly to a scaler. The number of pulses lost could be measured by comparing the readings on the two scalers and a correction factor was then calculated.

The correction factor was plotted as a function of the total number of

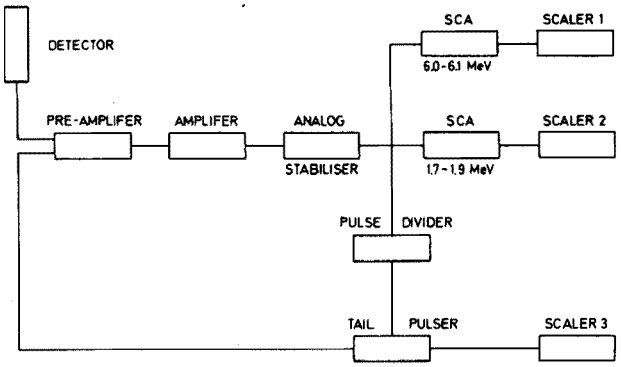

Fig. 1. Schematic diagram of instrumentation for the determination of count loss in a single-channel analyser system.

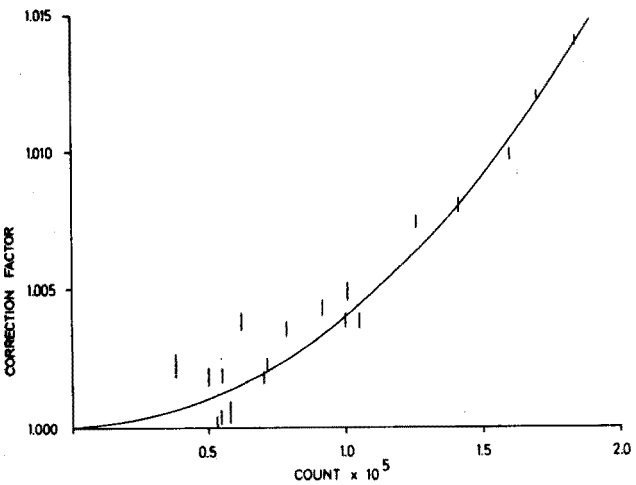

Fig. 2. Correction factor for count loss versus count, with curve obtained from eq. (1).

counts recorded in the 1.778-MeV photopeak during the counting time used, and a curve was fitted to the points (see Fig. 2). The background recorded by the SCA covering the pulser peak at 6.05 MeV was small (0.04 counts s^{-1}), but the statistical variations in this background resulted in large errors when the correction factor was calculated at low count-rates. The error bars shown in Fig. 2 were calculated for one standard deviation in the background count. The curve obtained can be described by:

$$C = \exp(4.0 \times 10^{-13} \times P^2) \quad (1)$$

where C is the correction factor, and P the total photopeak count. This equation was used to correct all results obtained.

Preparation of samples, standards and monitors

The rock samples analysed were supplied as powders and were mixed well before a sample portion was separated and dried at 110 °C for 16 h to remove H_2O^-. They were packed into small polyethylene vials, 10 mm i.d. by 19.7 mm long (sample volume, 1.55 cm^3), by a press with a spring-loaded plunger to obtain a uniform packing density. This small vial was held with polyethyler spacers at the bottom centre of the larger polyethylene rabbit used in the pneumatic transfer system.

Eleven samples of silica were packed as above for use as standards. The silica was prepared from the pure quartz tubing used to encapsulate samples for thermal neutron irradiation, by crushing to -120 mesh in an agate bowl using the Seibtechnik. The powder was heated to 1000 °C for 16 h before use to remove all adsorbed water.

Monitors of silica were used so that any variations in neutron intensity during the irradiation period would affect both sample and monitor equally, and could thus be ignored. A number of monitors was prepared from the same quartz tubing as the standards. These were carefully weighed so that monitor activity could be corrected for these small weight differences.

Unless otherwise stated, samples were irradiated with monitors selected in rotation so that any possible systematic errors from differences between the monitors could be avoided.

Precision of analysis

The standard deviation s of the method can be regarded as the combinatior of individual standard deviations arising from different independent sources of error:

$$s^2 = s_1^2 + s_2^2 + \ldots s_n^2 \qquad (2)$$

It is possible to identify and estimate the magnitude of various sources of error in the present method by a separate set of experiments. In these, each measurement is the normalization of the activity of the sample A to that of a monitor B to give the ratio R. It is necessary to use, instead of the standard deviation s, the percentage relative standard deviation $s_r = 100s/R$ (coefficien of variation). Then for each measurement the counting error s_{rC} arising from the random nature of radioactive decay, is given by:

$$s_{rC}^2 = s_{rA}^2 + s_{rB}^2$$

If these experiments are carried out in such a way that the ratio R is approxi-mately the same for each determination, then eq (2) can be divided throughor by $R^2/10^4$ to give:

$$s_r^2 = s_{r1}^2 + s_{r2}^2 + \ldots s_{rn}^2$$

Other sources of error can be identified:

(1) instrumental error, e.g. from irreproducible positioning of the sample during irradiation or counting, and (2) sample preparation and packing error, e.g. from variations in sample geometry or density variations through the sample.

These sources of error were investigated by taking the eleven silica standards and pairing them to eleven monitors. Each sample—monitor pair was irradiated and counted eleven times, and the results were analysed to give the average relative standard deviation for:

1 sample analysed 11 times: $s_r^1 = 0.59$ %

11 samples analysed 1 time: $s_r^{11} = 0.70$ %

The value of s_{rC} in this experiment was 0.48 %.

The error s_r^1 is made up of counting and instrumental errors, and the error s_r^{11} includes the sample preparation error, and also any systematic errors from sample—monitor pairing. Therefore, the instrumental error is:

$$s_{ri} = ((s_r^1)^2 - s_{rC}{}^2)^{1/2} = 0.34\ \% \qquad (3)$$

and the sample preparation error, plus monitoring error, is:

$$s_{rs} = ((s_r^{11})^2 - (s_r^1)^2)^{1/2} = 0.38\ \% \qquad (4)$$

To reduce the overall error it is clearly insufficient to improve the counting statistics only. The instrumental error would only be reduced significantly by rebuilding the equipment. Possible modifications which can be considered are:

(a) increasing the target—sample distance, which would require an increase in beam current to produce the same flux density at the sample;

(b) introducing beam scanning over the target to obtain a more uniform flux distribution; or

(c) decreasing the tolerances in the irradiation and counting rotators so that the rabbits could be more reproducibly positioned.

Sample preparation and monitoring errors were reduced as much as possible by taking care to control the packing geometry and density uniformity of samples and monitors. This source of error would be reduced further by dividing each sample into portions; analysing each portion fewer times would give the same counting error as the above procedure, but a smaller sample preparation error. With the limited quantities of international rock standards available, this replicate procedure was not practicable here.

Previous work [7] on the determination of oxygen in these samples showed that the sample preparation error was negligible. However, the effect of sample preparation errors can be expected to be more severe for the less energetic γ-rays from aluminium-28 than for the more energetic γ-rays from nitrogen-16.

Analysis of the data obtained for the rock samples showed that an average relative standard deviation for a single determination was about 0.85 %. This is higher than was obtained for the silica standards, because there was a smaller amount of silicon in the samples, resulting in larger counting errors. The relative standard deviation of the mean of twelve separate determinations

was 0.25 %, which was taken as the precision of the method used here and combined with the sample preparation error of 0.38 % to obtain an expected accuracy of about 0.45 %. Comparison of the final experimental results obtained with the accepted values for the silica contents of these rock standards showed this to be a valid estimate of the accuracy of the method.

INTERFERENCES

NaI(Tl) detectors were used despite their lower resolution compared with Ge(Li) detectors, because of their higher efficiency. This lower resolution results in a high probability of interferences; fast neutron reactions producing interferences in the determination of silicon in rocks are given in Table 1. With NaI(Tl) detectors the 1.811-MeV photopeak of manganese-56 cannot be distinguished completely from the 1.778-MeV photopeak of aluminium-28, and the relatively long half-life of manganese-56 results in a build-up of activity on repeated irradiations. Part of the Compton continuum from sodium 24 falls in the energy window of the 1.778-MeV photopeak of aluminium-28. The magnitude of the interference from aluminium by the production of aluminium-28 is determined by the thermal neutron flux; measures to reduce the amount of thermalization taking place in the sample vicinity will reduce this interference. The most serious nuclear interference is from phosphorus and this cannot be reduced.

The degree of interference from these elements was determined by irradiating pure samples of Fe_2O_3, MgO, Al and a variety of phosphates ($Ca_2HPO_4.2H_2O$, KH_2PO_4, K_2HPO_4 etc.) The following results were obtained:
100 % Mg is equivalent to 0.23 % Si
100 % Al is equivalent to 0.25 % Si
100 % P is equivalent to 49.4 % Si
100 % Fe is equivalent to 0.21 % Si.

Except for the phosphorus interference, these levels are considerably lower than found elsewhere [3]. Possible reasons for these discrepancies are: (a) the thermal neutron flux for aluminium is probably lower than that usually found since there is little thermalizing material surrounding the target and the production of aluminium-28 from aluminium is reduced; (b) the interferences from magnesium and iron depend largely on the width of the SCA window used and on the resolution of the detectors. The good resolution of the present detectors and the use of analog stabilizers to eliminate drift enabled a narrower energy window than usual to be used, thus reducing the interference to a minimum. The level of interference found for phosphorus is in good agreement with other literature values [3].

Neutron and γ-ray absorption

To obtain accurate results, the small errors caused by different neutron and γ-ray absorption between samples and standards must be corrected. The

effects of neutron and γ-ray absorption have been studied [6,7] and can be expressed as a simple exponential absorption law of the form

$$f = f_0 \exp(-\mu d)$$

The total correction for both neutron and γ-ray absorption is thus:

$$I = I_0 \exp(-\mu_n d_1) \exp(-\mu_\gamma d_2), \quad (5)$$

where I_0 = activity without absorption
I = activity with absorption
μ_n = neutron absorption coefficient
d_1 = effective sample thickness for neutron absorption
μ_γ = γ-ray absorption coefficient
d_2 = effective sample thickness for γ-ray absorption.

This can be simplified by assuming that $d_1 = d_2$, which is approximately the case. Equation (5) reduces to:

$$I = I_0 \exp[-(\mu_n + \mu_\gamma)d]$$

where d is the effective sample thickness for neutrons and γ-rays. The thickness d was determined experimentally to be 0.3 cm, which is reasonable since the sample radius is 0.5 cm.

The absorption coefficient for neutrons can be related to the more usual cross-section, viz.

$$\mu_n = \frac{1}{V} \sum_{i=1}^{n} \frac{\sigma_i W_i N}{M_i}$$

where V = volume of sample
σ_i = cross-section for element i
W_i = mass of element i
M_i = atomic mass of element i
N = Avogadro's number.

γ-Ray attenuation is a very similar phenomenon, and the factor μ_γ can be rewritten

$$\mu_\gamma = \sum_{i=1}^{n} \frac{\mu_i}{\rho_i} \cdot \frac{W_i}{V}$$

where μ_i/ρ_i = mass attenuation factor for element i.

The γ-ray absorption coefficients were calculated by interpolating the data of Davisson [8]. The variation of γ-ray absorption with sample density is shown in Fig. 3, together with lines showing the absorption of SiO_2 and Fe_2O_3. A reasonably good line is obtained, as expected from the similarity in composition of the samples analysed. The neutron absorption coefficients were calculated from the total neutron cross-sections at 14.7 MeV taken from Goldberg et al. [9]. The variation with sample density is shown in Fig. 4, together with lines showing the absorption of SiO_2 and Fe_2O_3. In this case there is a general trend,

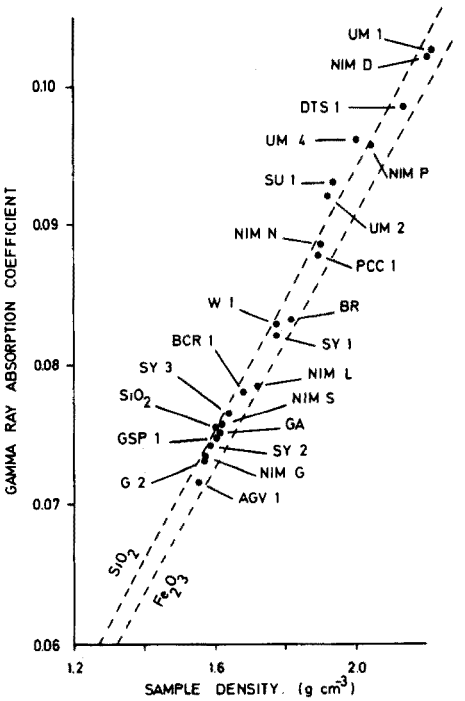

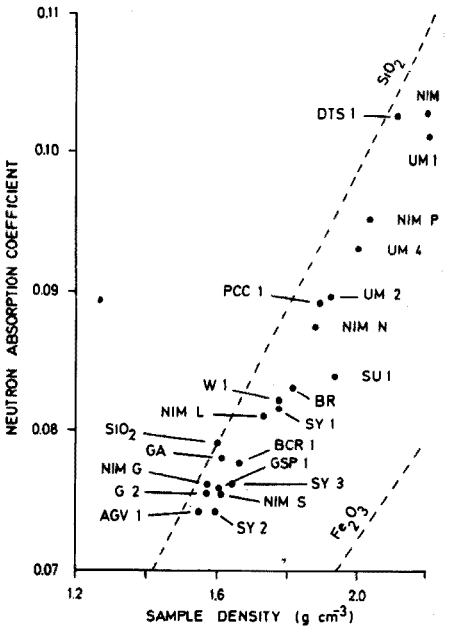

Fig. 3. γ-Ray absorption coefficient versus sample density for the standard rocks analysed. Dashed lines show the absorption of SiO_2 and Fe_2O_3.

Fig. 4. Neutron absorption coefficient versus sample density for the standard rocks analysed. Dashed lines show the absorption of SiO_2 and Fe_2O_3.

but the effects of different compositions are more severe than for γ-ray absorption. Figure 5 shows the overall correction factor vs, sample density; a good straight line is obtained, and a least-squares fit gives:

$$C^1 = 0.0281\rho + 0.9529 \qquad (6)$$

where C^1 is the total correction factor for neutron and γ-ray absorption, and ρ is the sample density.

Calculation of results

The samples and standards were analysed 12 times, and a mean and relative standard deviation were calculated. No results were significantly removed from the mean and significant differences were not found between the different relative standard deviations. The final errors given in Table 2 are calculated from these relative standard deviations and include the small error in the silica standard value.

Table 2 gives the data corrected for count loss, corrected for neutron and

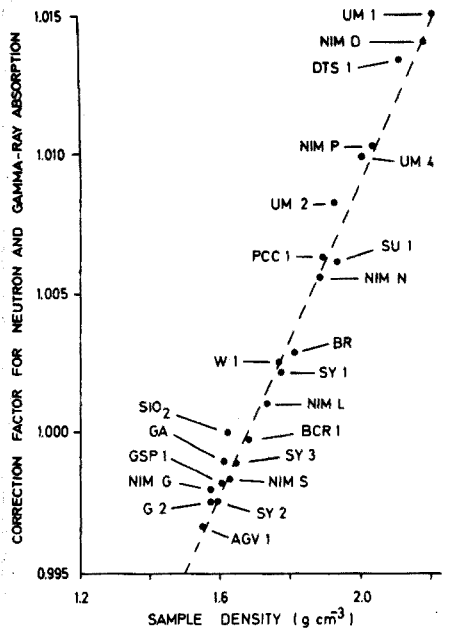

Fig. 5. Overall correction factor for neutron and γ-ray absorption versus sample density for the standard rocks analysed. Dashed line is a least-squares fit for the data.

γ-ray absorption, and corrected for interferences from magnesium, aluminium, phosphorus and iron. Corrections for inter-element interferences vary from 0.05 % for NIM G to 0.59 % for BR, with an average of 0.18 %.

The final results obtained are compared with various recommended and experimental values in Table 3, together with the percentage deviations between recommended and experimental results.

Procedure

The procedure used was to irradiate for 15—20 s, to allow a decay of 100 s, and to count for 120 s. The rock samples and silica standards were analysed 4 times per week, and a minimum of 24 h decay was allowed between irradiations. This allowed a substantial amount of the relatively long-lived isotopes (manganese-56 and sodium-24) to decay.

RESULTS AND DISCUSSION

The final results obtained are given in Table 3, on a dry weight basis, together with the various values reported for these standards [3,10—12].

The differences between the accepted values and the experimental results obtained here are, in general, of the same order as the errors found (0.45 %), which makes it meaningless to give the results obtained here to more than

TABLE 2

Silicon results (as silica) with corrections

Sample	Corrected for count loss	Corrected for n and γ abs	Mg	Al	P	Fe	Final value
NIM-G[a]	75.75	75.59	—	0.034	0.014	0.006	75.54
	75.98	75.82					75.77
NIM-S	64.04	63.93	0.001	0.049	0.060	0.004	63.82
	64.38	64.29					64.18
NIM-L	52.36	52.41	0.001	0.039	0.032	0.030	52.31
	51.86	51.89					51.79
NIM-N	52.78	53.13	0.022	0.047	0.018	0.028	53.01
	52.53	52.83					52.71
NIM-P	50.67	51.19	0.076	0.012	0.018	0.038	51.05
	50.92	51.46					51.32
NIM-D	38.44	38.98	0.130	0.001	0.014	0.053	38.78
	38.64	39.24					39.04
W-1[b]	52.90	53.04	0.020	0.042	0.065	0.034	52.88
G-2	69.85	69.69	0.002	0.043	0.065	0.008	69.57
GSP-1	67.47	67.35	0.003	0.043	0.129	0.013	67.16
AGV-1	59.80	59.60	0.005	0.048	0.226	0.021	59.30
BCR-1	55.27	55.25	0.010	0.038	0.114	0.042	55.05
PCC-1	42.41	42.68	0.130	0.002	—	0.026	42.52
DTS-1	40.34	40.88	0.149	0.001	—	0.027	40.70
GA[c]	70.77	70.70	0.003	0.041	0.055	0.009	70.59
BR	38.99	39.11	0.040	0.029	0.479	0.040	38.52
SY-1[d]	60.28	60.41	0.012	0.027	0.069	0.027	60.28
SY-2	60.82	60.67	0.006	0.032	NA[e]	0.023	60.61
SY-3	60.45	60.38	0.008	0.032	0.203	0.023	60.11
UM-1	36.86	37.41	0.108	0.003	—	0.060	37.24
UM-2	38.99	39.31	0.076	0.020	0.009	0.045	39.16
UM-4	38.71	39.09	0.068	0.025	0.009	0.045	38.95
SU-1	34.54	34.76	0.012	0.027	0.042	0.103	34.57

[a]National Institute for Metallurgy.
[b]United States Geological Survey.
[c]Centre de Recherches Petrographiques et Geochimiques.
[d]Canadian Department of Energy, Mines and Resources, Mines Branch.
[e]NA: not available.

three figures. In general, most of the major element analyses given for the standards analysed here are probably only accurate to three figures, perhaps w exception of the preferred values of Abbey [11].

There is an overall positive bias in the results of 0.13 %. If only the USGS and NIM rock standards are considered, this positive bias is 0.21 %, which, although small, may be significant, since other results obtained by f.n.a.a.

TABLE 3

Comparison of silica results

Sample	Reference					This work	% Δ
	10	11	12	3	10[a], 11[a]		
NIM-G	75.59[b]					75.7	+0.15
NIM-S	63.72[b]					64.0	+0.44
NIM-L	52.52[b]					52.1	−0.81
NIM-N	52.43[b]					52.9	+0.90
NIM-P	50.88[b]					51.2	+0.63
NIM-D	38.86[b]					38.9	+0.10
W-1	52.64				52.72[b]	52.9	+0.34
G-2	69.11	69.22		69.34	69.30[b]	69.6	+0.43
GSP-1	67.38	67.27		67.92	67.31[b]	67.2	−0.16
AGV-1	59.00	58.97		59.49	59.69[b]	59.3	−0.66
BCR-1	54.50	54.36		54.17	54.85[b]	55.1	+0.46
PCC-1	41.90	41.90		42.81	42.15[b]	42.5	+0.83
DTS-1	40.50	40.66		40.90	40.68[b]	40.7	+0.05
GA	69.90[b]					70.6	+1.00
BR	38.20[b]					38.5	+0.79
SY-1	59.5[b]					60.3	+1.34
SY-2			60.8[b]			60.6	−0.33
SY-3			60.3[b]			60.1	−0.33
UM-1			37.6[b]			37.2	−1.08
UM-2			39.2[b]			39.2	0
UM-4			39.35[b]			39.0	−0.90
SU-1			34.7[b]			34.6	−0.29

[a]Corrected for H_2O^-

[b]Percentage Δ from this figure.

also show a positive bias [3]. This may be the result of a previously noted [11] systematic error arising from the incomplete recovery of silica in conventional chemical methods of rock analysis.

The corrections for interfering elements necessary for these rock samples were generally small, averaging about 0.18 %. In general, phosphorus is the most important interfering element, although the average correction found (equivalent to 0.08 % SiO_2) is still small compared with the analytical errors found.

Neutron and γ-ray absorption corrections are, to a greater or lesser extent, proportional to sample density, as seen in Figs. 3 and 4. The overall correction factor, for both neutron and γ-ray absorption, is closely related to sample density (see Fig. 5). As for oxygen determination by f.n.a.a. in rocks [7], a simple correction factor, based on the sample density, can be used for neutron and γ-ray absorption corrections.

The average deviation between the experimental and recommended values for the NIM and USGS rock standards was 0.46 %. This figure agrees well with that (0.45 %) calculated for the accuracy of the method.

In general, the method used is rapid and accurate. The average relative standard deviation for a single silica determination in a silicate rock is about 0.85 %, and this compares well with that found by x-ray fluorescence [13], the main instrumental method used for silica determinations.

CONCLUSIONS

Analysis of 22 international rock standards has shown the determination of silicon in rocks by f.n.a.a. to be quick and accurate. Little sample preparation is required other than powdering and drying.

Corrections to the experimental data obtained are minimal: count-rate losses in the single-channel analysers are small, and a formula for this correction can be obtained by an experimental method described. Corrections for neutron and γ-ray absorption are also simple to apply: matrix effects in silicate rocks are shown to be closely related to the density of the packed sample, and a simple density-related correction can be used. Interferences from aluminium, magnesium, phosphorus and iron are on average equivalent to 0.18 % SiO_2; that from phosphorus is generally the most serious, averaging 0.08 % SiO_2.

The sources of error in the analysis have been investigated. Errors arising from instrumentation and the statistical nature of radioactive decay can be reduced by repeated analysis of a single sample; the error from sample preparati could, in principle, be reduced by analysis of replicate samples.

The final results show that the relative standard deviation on a single determination of silicon in a silicate rock is 0.85 %; after 12 determinations this is reduced to 0.25 %. The accuracy of the results obtained was about 0.45 %, in good agreement with the average deviation obtained between the experimental values found and the recommended values for the silica contents of the NIM and USGS international rock standards.

The author would like to thank H.M. Marques for technical assistance and Professor J.P.F. Sellschop and Mr. T.W. Steele for helpful discussions and critical reading of this manuscript. The paper is published by permission of the Director-General of the National Institute for Metallurgy.

SUMMARY

The errors associated with the measurement of silicon in silicate rocks by fast neutron activation analysis have been investigated. The accuracy has been determined by comparing the values obtained with the accepted values for 22 silicate rock standards. Precisions of 0.25 % and accuracies of about 0.45 % are possible.

REFERENCES

1 B. Mason, Principles of Geochemistry, Wiley, New York, 3rd edn., 1966.
2 R. van Grieken, J. Hoste, Annotated Bibliography on 14 MeV Neutron Activation Analysis, Eurisotop Office Information Booklet No. 65, Bibliographies-8, Brussels, 1972.

3 K. Huysmans, R. Gijbels and J. Hoste, Talanta, 20 (1973) 843.
4 F.F. Dyer and L.C. Bate, Oak Ridge National Laboratory Report, ORNL-TM-4095.
5 H.H. Boloton, M.G. Strauss and D.A. McClure, Nucl. Instrum. Methods, 83 (1970) 1.
6 S.S. Nargolwalla, M.R. Crambs and J.R. DeVoe, Anal. Chem., 40 (1968) 666.
7 D.M. Bibby and J.P.F. Sellschop, J. Radioanal. Chem., 20 (1974) 677.
8 C.M. Davisson, in K. Siegbahn (Ed.), Beta and Gamma-ray Spectroscopy, Vol. I, Interscience, Amsterdam, 1965, p. 827.
9 M.D. Goldberg, S.F. Mughabghab, B.A. Magurno and V.M. May, Brookhaven National Laboratory Report, BNL-325, 2nd edn., 1966.
10 F.J. Flanagan, Geochim. Cosmochim. Acta, 37 (1973) 1189.
11 S. Abbey, Can. Spectrosc., 15 (1970) 10.
12 G.H. Fay, Can. Dep. Energy, Mines, Resour., Mineral Sci. Div. Inform. Circular, IC.309 (1973).
13 E.B. Buchanan and Foo-Chung Tsai, Anal. Chem., 46 (1974) 1701.

Analytica Chimica Acta, 79 (1975) 139—148

THE DETERMINATION OF Pd, Pt, Au, Ag and Ir IN COPPER BY NEUTRON ACTIVATION ANALYSIS

A. GOVAERTS*, R. GIJBELS and J. HOSTE

Institute for Nuclear Sciences, Ghent University, Ghent (Belgium)

(Received 3rd April 1975)

During the production of noble metals, accurate, sensitive, precise and fast analytical techniques are required, and industrial laboratories are using instrumental methods to a much greater extent. As these are usually relative and influenced frequently by matrix effects, there exists a growing need for standard reference materials. The Bureau Eurisotop (Brussels) is now sponsoring the development of a copper metal matrix containing standardized platinum metal contents (in the first instance 100, 10 and 1 $\mu g\ g^{-1}$ palladium—copper and platinum—copper alloys). The proposed standards are prepared by successive dilutions, with high-frequency levitation melting [1], of palladium or platinum metal in a copper metal matrix (dilutions made by the Central Bureau for Nuclear Measurements (C.B.N.M.), Geel, Belgium). The analysis of the alloys was carried out in about twenty laboratories by methods such as gravimetry, spectrophotometry, emission spectrography, x-ray fluorescence, atomic absorption, spark-source mass spectrometry, and neutron, γ- and charged particle activation analysis. This paper deals with the n.a.a. of Pd, Pt, Au, Ag, Ir, Se, Sb and As in copper samples of various origins, from which one was chosen for the preparation of the alloys. The precise n.a.a. of palladium and platinum in the proposed standard reference materials will be described in due course.

Gijbels and Hoste [2] have recently reviewed the application of neutron activation analysis in the production and industrial use of noble metals. Several authors have already described the "radiochemical n.a.a." of traces of gold and silver in copper metal [3—7]. After a cooling time of 7—14 days and after chemical separation, ^{198}Au and ^{110m}Ag activities were usually counted with a NaI(Tl) detector. For the determination of palladium, platinum and rhodium in lead sponge, Park *et al.* [8] have used a pre-separation of these elements by spontaneous electrodeposition on amalgamated copper powder. After irradiation, mercury, gold and silver were removed and palladium and platinum were precipitated as palladium dimethylglyoximate and ammonium hexachloroplatinate. Platinum and palladium concentrations in lead sponge of

*Research fellow of the I.I.K.W.

10—100 $\mu g\ g^{-1}$ were determined (equivalent to 50—500 $\mu g\ g^{-1}$ in copper); the method allows the determination of less than 1 $\mu g\ g^{-1}$. The determination of iridium in copper slime by i.n.a.a., with coincidence spectrometry, has been described [9].

EXPERIMENTAL

Determination of palladium, platinum and gold in copper by r.n.a.a.

Before the preparation of the alloys was started, an inexpensive copper dilution matrix with a low platinum and palladium content had to be chosen. The most sensitive reactions for the determination of Pd and Pt by n.a.a. are $^{108}Pd(n,\gamma)^{109}Pd(\beta^-)\ ^{109m}Ag$ and $^{196}Pt(n,\gamma)^{197}Pt$ or $^{198}Pt(n,\gamma)^{199}Pt(\beta^-)^{199}Au$. In the latter reaction, ^{198}Au and ^{199}Au, produced via $^{197}Au(n,\gamma)^{198}Au(n,\gamma)^{199}A$ will also be present in the gold fraction if the sample contains gold. The second order interference for thermal neutron activation was calculated with the Bateman—Rubinson equations for two neutron fluxes and various irradiation times (see Table I).

In the present experimental conditions (irradiation for 7 h at a thermal neutron flux of 10^{12} n $cm^{-2}\ s^{-1}$ plus an epithermal neutron flux of *ca.* $3 \cdot 10^{10}$ n $cm^{-2}\ s^{-1}$ per unit lethargy) ^{199}Au photopeaks could not be detected in the ^{198}Au spectra of irradiated gold monitors, indicating that the second-order interference was below 0.6 $\mu g\ g^{-1}$ platinum per $\mu g\ g^{-1}$ of gold. In these conditions, the limiting factor for the determination of platinum via ^{199}Au, in the presence of gold by γ-spectrometry, is not the second-order interference but the Compton continuum and the backscatter peak (158 keV) of the 411.8-keV γ-ray of ^{198}Au. As some of the matrices contain up to 300 ng g^{-1} gold, the determination of platinum had to be based on ^{197}Pt.

As the copper matrix becomes quite active and as the half-lives of ^{109}Pd (13.47 h) and ^{197}Pt (18 h) are comparable with that of ^{64}Cu (12.8 h), an instrumental determination is not possible and a chemical separation with a high copper decontamination is required. Cation exchange was chosen for the retention of copper from dilute hydrochloric acid medium. Tracer experiments showed that less than 10^{-3} % copper passes through the column in the present working conditions. Gold was also determined: for some of the samples, ^{198}Au was the major activity passing through the column and had to be separated from Pt and Pd.

Irradiation

The copper samples (made by the C.B.N.M.) were disks (diameter 10 mm; thickness 1.5 mm; weight *ca.* 1 g) and were irradiated for 3 h at a flux of *ca.* 10^{12} n $cm^{-2}\ s^{-1}$ ($\phi_{th}/\phi_{epi} \approx 30$). Standards were prepared by spotting 50 μl (1 μg Au, 10 μg Pd and 30 μg Pt) of a standard solution (prepared from "SpecPure" Pd, Pt and Au metal) on 5 mg of high-purity silica powder in quartz vials. The solutions were evaporated carefully and the vials were sealed.

TABLE I

Apparent platinum content ($\mu g\ g^{-1}$) per $\mu g \cdot g^{-1}$ of gold

		β^- 2.7 d ↑		
(100 %) ^{197}Au	(n,γ) 98.8 barn	^{198}Au	(n,γ) ^{199}Au (β^-) 25800 barn	3.15 d
(7.21 %) ^{198}Pt	(n,γ) 4 barn	^{199}Pt (β^-) 31 min	^{199}Au (β^-) 3.15 d	
Irradiation time (h)	3	7	30	300
$\phi_{th} = 10^{12}$ n cm^{-2} s^{-1}	0.047	0.11	0.44	2.5
$\phi_{th} = 10^{14}$ n cm^{-2} s^{-1}	4.6	10.7	41	147

Procedure

After a cooling time of 40 min (decay of ^{66}Cu), the sample was dissolved in 10 ml of 10 *M* nitric acid in the presence of 1 mg Au, 10 mg Pd and 30 mg Pt carrier. Nitric acid was removed by three additions of 12 *M* hydrochloric acid followed by evaporation to a syrupy consistency on a hotplate. The final residue was dissolved in 50 ml of 0.03 *M* hydrochloric acid and the solution was passed through a Dowex 50W-X8 cation-exchange column (diam. 2 cm; height 12 cm). The resin was washed with 150 ml of 0.03 *M* hydrochloric acid. The eluate was stirred vigorously and heated to 80 °C. The noble metals were precipitated by addition of a few g of zinc powder (a rapid volume-reduction step). After precipitation, the excess of zinc metal was dissolved by adding hydrochloric acid. The precipitate was filtered off and dissolved in a few ml of aqua regia. Nitric acid was removed as described above with 12 *M* hydrochloric acid. The final residue was dissolved in 40 ml of 1 *M* hydrochloric acid. Gold was extracted with ethyl acetate (3 × 20 ml). The organic phases were combined and diluted with ethyl acetate to 100 ml in a standard flask. A 1 % solution of dimethylglyoxime in ethanol (3 ml) was added to the aqueous solution. The precipitate was collected on a Millipore filter (diam. 25 mm), dried under an infrared lamp, covered with a second Millipore filter, sandwiched between two Millipore foils, and mounted on an aluminium standard counting tray. The filtrate was heated to 80 °C and platinum was precipitated as ammonium hexachloroplatinate by the addition of 4 g of ammonium chloride. After 30 min, the precipitate was collected on a Millipore filter, dried, and mounted for counting as described for the $Pd(DMG)_2$ precipitate.

Treatment of the standards

The quartz ampoules were broken and boiled with aqua regia in the

presence of Au, Pd and Pt carrier (1, 10, and 30 mg, respectively). After conversion to 12 *M* hydrochloric acid medium, the solution was evaporated to dryness. The residue was dissolved in 40 ml of 1 *M* hydrochloric acid and Au was extracted; Pd and Pt were precipitated as for the sample.

Countings

The platinum and palladium precipitates were measured for 15 h, and for 10 and 25 h respectively, after irradiation, with a Ge(Li) low-energy photon detector described in detail by Hertogen and Gijbels [10] ("l.e.p.d.", window 0.13 mm Be, FWHM 245 eV for the 5.90-keV Mn $\bar{K}_\alpha$ peak).

For the determination of palladium, the Ag $\bar{K}_\alpha$ x-ray photopeak (internal conversion of the 88.04-keV γ-ray of ^{109m}Ag) was used. Figure 1 shows the l.e.p.d. spectrum of the palladium precipitate separated from a Lab.I copper sample, containing 1.6 ng Pd g^{-1}. The Pd K x-rays arise from fluorescence of the carrier. The self-absorption of the Ag $\bar{K}_\alpha$ radiation in the measuring direction for a typical palladium dimethylglyoximate precipitate amounts [11] to *ca.* 2 %; differences in chemical yield for the sample and the standard will therefore not produce an appreciable systematic error.

For the determination of platinum, the 77.4-keV γ-photopeak of ^{197}Pt was used. The spectra of the platinum precipitates from the Lab.I and Lab.III copper samples were essentially background spectra with Pt K x-ray photopeaks (fluorescence of the carrier). The ammonium chloride precipitation is not specific for platinum and can also be used for the precipitation of iridium. As the iridium concentration of the Lab.II samples was relatively high (*ca.* 5 ng g^{-1}) the precipitates were contaminated with ^{192}Ir and ^{194}Ir (γ-photopeaks at 295.9, 308.4, 316.5 and 293.6, 328.5 keV + Os and Pt x-rays).

The determination of the net peak area of the 77.4-keV γ-photopeak

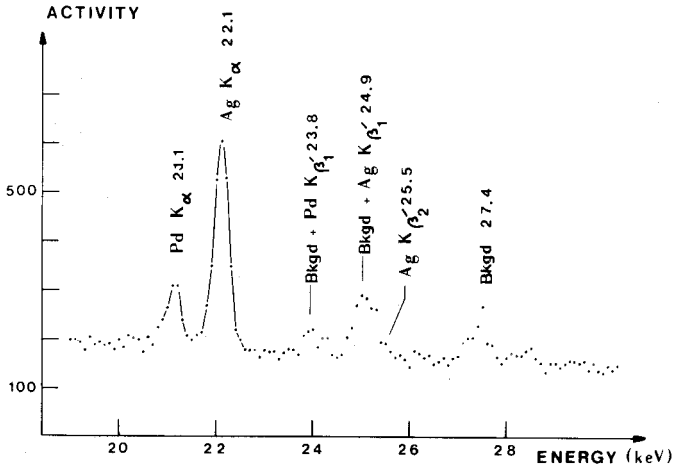

Fig.1. L.e.p.d. spectrum of the Pd(DMG)$_2$ precipitate, separated from a Lab I—8 Ag sample and counted for 15 h, 8 h after irradiation (1.6 ng g^{-1} Pd; Bkgd = background peaks).

became complicated; Fig. 2 shows an l.e.p.d. spectrum of the platinum precipitate of a Lab. II sample containing 90 ng g^{-1} Pt.

$A(77.4) = A(77) - A(\text{Bi } K_{\alpha 1}) - A(\text{Au } K_{\beta'1}) - A(\text{Pt } K_{\beta'2})$;
$A(77.4)$ = net peak area of the 77.4-keV γ-photopeak of ^{197}Pt;
$A(77)$ = total peak area of the complex 77-keV photopeak;
$A(\text{Bi } K_{\alpha 1})$ = peak area of the background Bik$_{\alpha 1}$ photopeak;
$A(\text{Au } K_{\beta'1})$ = peak area of the Au $K_{\beta'1}$ photopeak (from ^{197}Pt and from fluorescence of the l.e.p.d. gold electrode);
$A(\text{Pt } K_{\beta'2})$ = peak area of the Pt $K_{\beta'2}$ photopeak (from ^{192}Ir, ^{194}Ir, ^{195m}Pt, ^{193m}Pt and from fluorescence of the carrier).

The Bi $K_{\alpha 1}$ contribution can be calculated from background spectra, and the Au $K_{\beta'1}$ and Pt $K_{\beta'2}$ contributions from the gold and platinum K_{α} photopeaks.

The ratios of the x-ray photopeaks measured with the l.e.p.d. depend on the intrinsic relative intensities of the emitted x-rays and on the variation of the detection efficiency of the l.e.p.d. as a function of the photon energy. The influence of this variation was checked by measuring the relative intensities of Os and Pt K x photopeaks of a thin ^{192}Ir source:

		$K_{\alpha 2}$	$K_{\alpha 1}$	$K_{\beta'1}$	$K_{\beta'2}$
Os	*a*	57	100	33	8
	b	54	100	34	9
Pt	*a*	56	100	32	8
	b	55	100	34	9

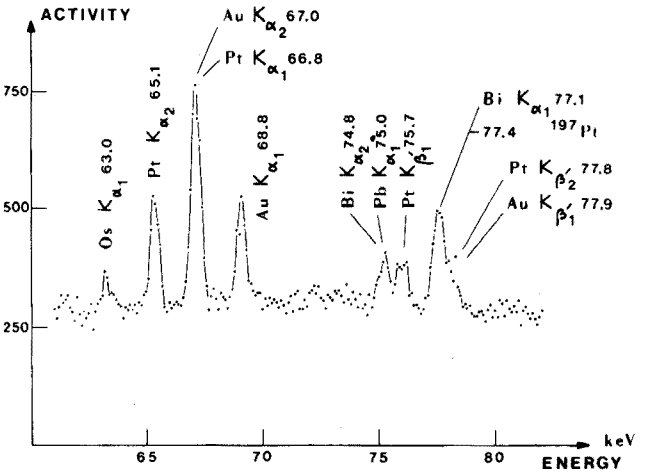

Fig. 2. L.e.p.d. spectrum of the $(NH_4)_2PtCl_6$ precipitate, separated from a Lab II—I sample and counted for 15 h, 10 h after irradiation (90 ng g^{-1} Pt).

where a indicates the measured values and b the intrinsic relative intensities taken from Wapstra *et al.* [12].

For the calculation of the Au $K_{\beta'1}$ and Pt $K_{\beta'2}$ corrections, the measured platinum ratios were used.

The ratios of the photopeaks also depend on self-absorption in the source as a function of the photon energy. This effect can be neglected as the platinum precipitates are thin (*ca.* 10 mg Pt cm^{-2}) and as the attenuation coefficients for photon energies lower than the Pt K absorption edge (78.4 keV) are quite small ($\mu/\rho < 4$ cm^2 g^{-1} above 60 keV [11]).

$$
\begin{aligned}
A(\text{Au } K_{\beta'1}) &= 0.32 \cdot A(\text{Au } K_{\alpha1}) \\
A(\text{Pt } K_{\beta'2}) &= 0.14 \cdot A(\text{Pt } K_{\alpha2}) \\
\text{or} \quad A(\text{Pt } K_{\alpha1}) &= A(\text{tot. } 67 \text{ keV}) - 0.56 \cdot A(\text{Au } K_{\alpha1}) \\
A(\text{Pt } K_{\beta'2}) &= 0.08 \cdot A(\text{Pt } K_{\alpha1})
\end{aligned}
$$

The gold fraction of the sample was measured a few days after irradiation for 1—15 h with a conventional 40-cm^3 Ge(Li) detector (FWHM 2.2 keV for the 1332-keV γ-ray of ^{60}Co). The 411.8-keV γ-photopeak of ^{198}Au was used for the determination of gold. For the Lab. III copper samples a detection limit for platinum could also be determined via ^{199}Au, as the gold content of these samples is very low.

Chemical yield determination

The chemical yields were determined by reactivation. The palladium and platinum precipitates were dissolved in 5 ml of aqua regia and the solutions were diluted with water to 50 or 100 ml; 50 μl of the noble metal solutions were spotted on 5 mg of high-purity silica powder in polyethylene vials. The solutions were evaporated carefully and reactivated for 7 h at a flux of $5 \cdot 10^{11}$ n cm^{-2} s^{-1} together with noble metal monitors prepared in the same way. The samples were counted the next day with a 40-cm^3 Ge(Li) detector. Palladium was determined via ^{109}Pd—^{109m}Ag (88 keV), platinum via ^{199}Au (158.4 keV) and gold via ^{198}Au (411.8 keV). Chemical yields were typically 80 % for palladium and gold, and 65—80 % for platinum.

Instrumental determination of Au, Ag, Ir, Se, Sb and As in copper

The copper samples were irradiated together with Au, Ag, Ir, Se, Sb and As standards for 3—7 h at a neutron flux of *ca.* 10^{12} n cm^{-2} s^{-1}. The standards were prepared by spotting the appropriate standard solutions on high-purity silica powder in polyethylene vials (typically: 0.2 μg Ir, 30 μg Se, 0.5 μg Au, 30 μg Ag, 20 μg Sb and 20 μg As). After a cooling time of 10—20 d (decay of ^{64}Cu), the samples were measured with a conventional Ge(Li) detector. Gold was determined via ^{198}Au (411.8 keV), silver via ^{110m}Ag (657.6, 884.5, 937.3 keV), iridium via ^{192}Ir (316.5 keV), selenium via ^{75}Se (264.6 keV), antimony

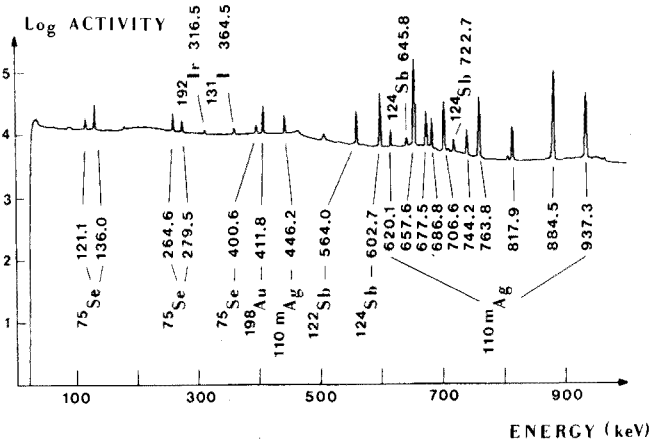

Fig. 3. γ-Ray spectrum of an irradiated and etched copper sample taken from the section of a Lab I—8 Ag ingot (irradiated for 15 h at 2.10^{12} n cm^{-2} s^{-1}, etched for 50 % of the orginal weight and counted for 40 h, 20 d after irradiation).

via ^{122}Sb (564.0 keV), and arsenic via ^{76}As (559.1 keV). Figure 3 shows the γ-spectrum of an irradiated copper sample measured 20 days after irradiation.

RESULTS AND DISCUSSION

Systematic errors from neutron self-shielding are estimated to be less than 10 %. Thermal neutron self-shielding in the disks can be computed with reasonable accuracy by the approximation given by Gilat and Gurfinkel [13] (f_{th} = 0.93, = 0.94 taking scattering into account) or by Monte—Carlo calculations (f_{th} = 0.95, = 0.95 taking scattering into account). Experimentally, f_{th} was evaluated by extrapolation. Samples of 1, 0.1 and 0.01 g were irradiated in a well-thermalized irradiation position ($CR_{Cu} \approx 150$) and counted via the annihilation radiation of ^{64}Cu. The 1- and 0.1-g samples consisted of stacks of copper foils in order to count the annihilation radiation in reproducible conditions.

	Mean specific activity
1 g (10 × 100-mg foils; diam. 10 mm)	0.960 ± 0.005
100 mg (10 × 10-mg foils; diam. 10 mm)	0.995 ± 0.005
10 mg (diam. 10 mm)	1

As it is reasonable to assume that thermal self-shielding does not occur at the 10-mg level, an experimental value for f_{th} of 0.96 was accepted.

As most irradiations were carried out in positions where $\phi_{th}/\phi_{epi} \approx 30$, an important fraction of the induced noble metal activity arises from epithermal activation. The systematic error from epithermal neutron self-shielding is believed to be of the same order of magnitude as that from thermal neutron

TABLE II

Pd, Pt and Au contents of proposed copper dilution matrices by r.n.a.a.

Sample	Pd(ng g^{-1})	Pt(ng g^{-1})	Au(ng g^{-1})
Lab. I [a]			
27 Ag	4.2	<100	18
8 Ag	1.3	<100	350 [b]
8 Ag	1.8	<25	86 [b]
8 Ag	1.6	<25	84 [b]
Lab. II			
I	82	90	76
II	32	50	40
III	34	50	87
Lab. III			
I	<1	<25 <5 via ^{199}Au	<0.2
II	<1	<25 <5 via ^{199}Au	<0.2

[a] 8 and 27 Ag: silver concentrations in $\mu g\ g^{-1}$ determined by the manufacturer.
[b] See text for discussion.

TABLE III

Au, Ag, Ir, Se, Sb and As contents of proposed copper dilution matrices by i.n.a.a.

Sample	Au (ng g^{-1})	Ag ($\mu g\ g^{-1}$)	Ir (ng g^{-1})	Se ($\mu g\ g^{-1}$)	Sb ($\mu g\ g^{-1}$)	As ($\mu g\ g^{-1}$)
Lab. I — 8 Ag	94	8.0	<1	—	0.37	1.1
Lab. I — 8 Ag	175	7.0	<1	—	0.34	1.6
50 % Etched	14					
75 % Etched	15					
Lab. I — 8 Ag ingot [a]	12.8±1.7	7.5±0.7	0.2	0.26±0.03	0.34±0.04	—
Etched	13.8±1.5	7.4±0.8	0.3	0.32±0.03	0.35±0.04	—
Lab. I — 27 Ag	16	28	<2	—	0.63	2.2
Lab. I — 27 Ag	16	29	<2	—	0.64	2.7
Lab. I — 27 Ag	20	27	0.3	0.28	0.59	—
25 % Etched	19	24	0.3	0.30	0.61	—
50 % Etched	18	32	0.3	0.40	0.60	—
Lab. III — I	0.5	0.028	0.1	<0.05	0.009	—
25 % Etched	<0.3	0.028	<0.05	<0.05	0.010	—

[a] Mean of thirteen analyses of samples taken from a section of a Lab. I — 8 Ag ingot received directly from the manufacturer.

self-shielding, since the resonance peaks are in an energy region where the copper neutron absorption cross-section is constant and small (*ca.* 8 barn).

The concentrations obtained by r.n.a.a. (see Table II), should be considered as upper limits, since no attempt was made to eliminate possible superficial noble metal contaminations after irradiation. Surface contamination can be neglected for the Lab. III copper samples as detection limits were obtained. For the Lab. II samples relatively high apparent concentrations (*ca.* 0.05 $\mu g\ g^{-1}$ for each element) were found, while the Lab. I samples contain less than 2 and 5 $ng\ g^{-1}$ Pd, and less than 25 and 100 $ng\ g^{-1}$ Pt, respectively. The gold values for the Lab. I — 8 Ag matrix were inconsistent: they varied from 80 to 300 $ng\ g^{-1}$ and were much higher than the concentration found for the 27 Ag matrix (18 $ng\ g^{-1}$). This may arise from surface contamination or inhomogeneity. As gold concentrations of 0.3 $\mu g\ g^{-1}$ were considered to be too high by the manufacturer and as gold could also be determined by i.n.a.a., the inconsistent results were checked by the instrumental method (see Table III).

For the preparation of the alloys the Bureau Eurisotop has chosen the Lab. I — 8 Ag matrix.

For the samples analyzed by i.n.a.a., systematic errors from γ-ray attenuation could be kept under control since an error of *ca.* 10 % can be calculated for the lowest γ-ray energy used (^{75}Se 264.6-keV).

Although etching with acids might not be effective for the removal of superficial noble metal contaminations (re-deposition on the residual lump is possible), some of the samples, analyzed by i.n.a.a., were etched with 10 ml of concentrated nitric acid (10—20 s in concentrated nitric acid, then decantation of the supernatant liquid and immediate washing of the copper residue with streaming water). After drying, the residual lump was weighed and measured again.

The gold results given by i.n.a.a. for the Lab. I — 8 Ag matrix samples, as received from the C.B.N.M., confirmed the varying and high results obtained by r.n.a.a. After the first etching the gold concentration decreased to 14 $ng\ g^{-1}$, and remained practically constant after the second etching. This suggests that etching with 14 M nitric acid is effective for the removal of gold surface contamination, that the 8 silver samples were contaminated, and that the matrix itself is homogeneous for gold. For control purposes, a section (10 × 10 cm) of a Lab. I — 8 Ag ingot received directly from the manufacturer was analyzed. The section was etched with 2 *M* nitric acid, dried, and divided into 1-g samples (1 × 1 cm) by sawing. Thirteen random samples were analyzed, with and without etching; practically constant Au, Ag, Sb and Se concentrations were obtained. The same gold concentration was found as for the etched sample received from the C.B.N.M. All other results were consistent.

A sample of a fourth Lab. II copper matrix was analyzed by i.n.a.a. (Table IV). After a cooling time of 30 d the sample was reactivated and etched with concentrated nitric acid; Pd, Pt and Au were determined in the etched fraction, and in the copper residue, by the r.n.a.a. method described above. It appears that possible palladium or gold surface contaminations for the Lab. II samples can be neglected in comparison with the actual concentrations.

TABLE IV

Au, Ag, Ir, Pd and Pt contents of a Lab. II(IV) copper matrix

I.n.a.a.	Au (ng g^{-1})	Ag (μg g^{-1})	Ir (ng g^{-1})
	53	2.2	5.4
R.n.a.a.	Au (ng g^{-1})	Pd (ng g^{-1})	Pt (ng g^{-1})
Etched fraction (30 %)	43	20	<100
Copper residue	59	23	< 50
Total	55	22	< 50

Thanks are given to the I.I.K.W. and the I.W.O.N.L. for financial support.

SUMMARY

The determination of palladium, platinum and gold in copper metal by neutron activation analysis is described. The matrix activity was separated from the noble metals by cation-exchange adsorption. Gold was extracted; palladium and platinum were precipitated. The precipitates were counted with a low-energy photon detector. The gold results were checked by instrumental neutron activation analysis. Silver, iridium, selenium, antimony and arsenic were also determined simultaneously.

REFERENCES

1 J. Van Audenhove and J. Joyeux, Nucl. Instrum. Methods, 102 (1972) 409.
2 R. Gijbels and J. Hoste, Report ITE-66-E, Bureau Eurisotop, Brussels, November 1971.
3 M. Cuypers, Ann. Chim. (Paris), 9—10 (1964) 509.
4 F. Lihl, P. Patek and H. Sorantin, Z. Anal. Chem., 221 (1966) 176.
5 A. Mizuike, Y.K. Yamada and S. Hirano, Anal. Chim. Acta, 32 (1965) 428.
6 T. Nakai, Y. Kamemoto and Ming-Tong Wey, Nippon Kagaku Zasshi, 83 (1962) 1194.
7 S. Yajima, Y. Kamemoto, K. Shiba and Y. Onoda, Nippon Kagaku Zasshi, 82 (1961) 38.
8 K.S. Park, R. Gijbels and J. Hoste, J. Radioanal. Chem., 5 (1970) 31, 43.
9 E.M. Lobanov and R.I. Khusnutdinov, Izv. Akad. Nauk Uzb.SSR, Ser. Fiz.-Mat. Nauk, 9 (1965) 72.
10 J. Hertogen and R. Gijbels, Anal. Chim. Acta, 56 (1971) 61.
11 E. Storm and H.I. Israel, Photon Cross-sections from 1 keV to 100 MeV for Elements 1 through 100, Academic Press, New York, 1970.
12 A.H. Wapstra, G.J. Nijgh and R. van Lieshout, Nuclear Spectroscopy Tables, North-Holland, Amsterdam, 1959.
13 J. Gilat and Y. Gurfinkel, Nucleoni, 21(8) (1963) 143.

Analytica Chimica Acta, 79 (1975) 149—159

COPPER MINING AND MILL ANALYSES BY γ-RAYS FROM CAPTURE OF CALIFORNIUM-252 NEUTRONS

DICK DUFFEY
Nuclear Engineering, University of Maryland, College Park, Maryland 20742 (U.S.A.)
J.P. BALOGNA
Los Alamos Scientific Laboratory, Los Alamos, New Mexico 87544 (U.S.A.)
P.F. WIGGINS
Naval Systems Engineering Department, U.S. Naval Academy, Annapolis, Maryland 21402 (U.S.A.)
A.A. ELKADY
Atomic Energy Establishment, United Arab Republic, Cairo (Egypt)

(Received 11th February 1975)

Copper production is a major metallurgical effort in the United States involving annually about 200 million tons of ore averaging 10—15 lb of copper per ton [1]. In exploration for copper and in outlining deposits for mining, many analyses are required, particularly drill hole information. Later in a typical process, copper ore (0.7 % Cu) is crushed and then transported as chunks to the grinding circuit, where it is ground as a water slurry and treated by froth flotation to a sulfide concentrate of 20—30 % Cu and a tailing. The subsequent smelting yields a copper matte of 30—45 % Cu, which goes through a converter [2] to a product of 98 % Cu; the converter slag might contain 2 % copper and 47 % iron oxides [3]. In electrolytic refining, the copper electrolyte might contain [4] 30—50 g Cu l^{-1}. All these process streams, as well as liquid and gaseous wastes, require prompt analyses to assist in mill operations.

Several nuclear spectrometric studies have shown the possibility of using neutrons as an analytical probe into mineral materials and then sensing the emitted radiation to determine the contained elements. Copper, because of its response and industrial importance, has been of interest. Neutron activation analysis with generator neutrons and decay γ-rays based on measurement of the 0.51-MeV peak from copper-64 has been applied on a pilot-plant scale [5,6]. Metallurgical applications of the decay γ-rays, *e.g.* for silicon in iron ore and iron in taconite, have been described by Rhodes [6]. The nuclear reactions utilized with copper are: ^{63}Cu (n, γ) ^{64}Cu; ^{65}Cu (n,γ) ^{66}Cu; and ^{63}Cu (n,2n)^{62}Cu. For these decay techniques, the product half-lives are: ^{64}Cu, 12.7 h; ^{66}Cu, 5.1 min; and ^{62}Cu, 9.78 min.

Recently, neutron capture γ-ray techniques have been applied to taconite ore, concentrate, and tailing samples from the Minnesota operations of

Reserve Mining with ^{252}Cf as the neutron source, and initial tests have been done with copper materials [7].

The nuclear spectrometric methods depend first on neutron absorption and then on γ-ray yield of the excited nuclei; when a neutron is absorbed, capture γ-rays are emitted immediately, but some elements become radioactive and emit decay γ-rays later. In general, neutron activation analysis has been concerned with decay radiation, which is analytically convenient because time is available for transportation and chemical procedures, the γ-ray spectra are simpler, and the relatively low-energy photons from decay (under about 2MeV) have been easier to measure. Such activation methods usually involve taking samples to a nuclear reactor or to a neutron generator with chemical steps before or after irradiation.

Capture γ-rays are of much higher energy (to about 10 MeV) and have become analytically useful only recently with the advent of high-resolution Ge (Li) detectors. Advantages of capture γ-rays are that problems of build-up of radioactivity and decay are eliminated; that the higher energies allow more penetration of the γ-signal in the sample and surrounding medium and hence larger sample sizes; and that interferences from decay γ-rays are minimi

Analytical sensitivity

The sensitivity of the capture γ-ray techniques depends on the neutron absorption or cross-section (σ in barns), and on the capture γ-ray intensity I (γ-rays per 100 neutrons absorbed). The product $I\sigma/A$, where A is the mass number, gives a sensitivity index [8,9]. Table 1 lists the sensitivity values for elements of interest in copper ore. These indicate that copper should respond well; other ore constituents of importance, e.g. Fe, Ca, and Si and Na, have a significant response. Additional elements which are favorable for the capture γ-ray methods and are of economic and environmental interest in metallurgical processes are Ti,V,Cr, Mn, Co, Ni, Au and Hg.

Because of pair production processes with high-energy γ-rays, Ge (Li) detectors provide three peaks for each energy, namely, a full (f) energy line, a more intense single escape (s) at 0.51 MeV lower, and a still more prominent double escape (d) at 1.02 MeV lower. These multiple peaks are an advantage because interferences by lines of other elements may sometimes be avoided.

On the basis of sensitivities and preliminary experiments on pure elements, all the process streams of a copper mill should respond to the capture γ-ray technique. Consequently, two experimental assemblies with ^{252}Cf as the neutro source were built at Los Alamos Scientific Laboratory. First, spectra were obtained from pure samples of the elements that occur in the ores; this established the significant spectral lines and their relative response. Then experiments were made on materials representative of metallurgical practice in the Western United States.

TABLE 1

Capture γ-ray sensitivity for elements in copper ores

Element	Cross-section (barns)	Atomic mass (A)	Energy (MeV)	Intensity I	Sensitivity ($I\sigma/A$)
Mn	13.3	54.938	7.244	12.05	2.92
			7.160	6.06	1.47
			7.058	11.35	2.75
Fe	2.62	55.847	7.646	22.14	0.18
			7.632	27.19	1.27
			6.018	8.08	0.38
			5.921	8.29	0.39
Cu	3.85	63.54	7.915	28.40	1.72
			7.637	14.47	0.88
			7.306	7.45	0.45
Na	0.534	22.9898	6.395	25.69	0.597
			5.616	5.99	0.139
			3.982	21.58	0.513
Si	0.160	28.086	8.472	2.31	0.0132
			7.199	7.16	0.0407
			6.380	12.62	0.072
			4.934	70.55	0.401
Ca	0.430	40.08	6.419	28.09	0.301

EXPERIMENTAL

Copper materials

To establish standards relating response to concentration, a mixture simulating a monzonite rock typical of large copper deposits was made of sand, oxides, carbonates, and free sulfur; the components and per cent by weight were 73 % SiO_2, 11 % Al_2O_3, 6 % K_2O, 1 % Na_2O, 4 % Fe_2O_3, 2 % MgO, 2 % CaO and 1 % S. To this synthetic monzonite, copper oxide was added to give concentrations of 0.5, 1.0 and 1.5 % Cu; these three mixtures served as standards. For the mill studies, several ores from Utah and Nevada were obtained. One was a monzonite porphyry ore, and its flotation concentrate and tailing were also tested. The compositions reported as average for these particular mill materials are in Table 2. The vein ores are representative of the high sulfur minerals in which copper is of less importance than lead, zinc, silver, or gold. The rhyolite copper ore represents oxidized deposits with little sulfide remaining. The monzonite porphyry is typical of the large deposits of low-grade copper ores in the Western United States, which are processed by froth flotation.

TABLE 2

Percentage composition of copper mill materials

	Cu	Pb	Zn	Fe	Si	Al	Ca	Na	K	S
Sulfide vein (Midvale, Utah)	0.48	9	5.3	11.4						
Sulfide vein (Park City, Utah)	0.93	5.4	2.9							
Rhyolite Dyke (oxide copper) (Yerrington, Nevada)	0.66									
Monzonite Porphyry (Sulfide copper) (Utah)	0.7			2	28	7	0.8	1	5	2
Flotation concentrate (Utah)	27	0.15	0.3	25	4	1.5	0.3		0.7	29
Flotation tailing (Utah)	0.08			2.6	33	7				0.7

In addition to these mill samples, several runs were made, as part of another research project, with core drill specimens from the Barley Canyon drill hole of the Valles Grande Caldera, New Mexico; this hole was for geothermal power studies at the Los Alamos Scientific Laboratory. Two of these core specimens were identified as augengneiss; chemical analysis of this granite (not necessarily the cores tested) showed about 0.2 % Cu. Three other core specimens were an amphybolite, and chemical analysis showed no copper present.

Irradiation

Two experimental arrangements were used. First, a small ^{252}Cf source and its storage drum was easily adapted by the help of shielding blocks of lead, polyethylene, and polyethylene with boron; this assembly was used to irradiate pure materials to establish spectral lines and relative intensity. Quantitative data can be obtained from such small sources (many of which are now in laboratories). However, it was more convenient to build a second arrangement with a larger source for the studies with the metallurgical materials.

The first arrangement, for standard spectra of pure elements, used a 10-μg ^{252}Cf source (yielding $2.3 \cdot 10^7$ n s^{-1}) fabricated by the Oak Ridge National Laboratory. The ^{252}Cf was placed in a double-walled capsule of type 304 stainless steel (overall 3/4-in. diameter and 3-in. long with a 2-in. stem for handling). The storage drum for the source was adapted for irradiations by building a sample cavity on the top (Fig. 1). After a sample (about a pound) usually a pure

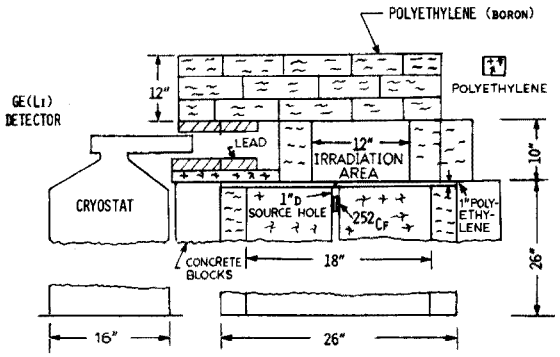

Fig. 1. ^{252}Cf storage drum irradiation arrangement.

metal, an oxide or a carbonate, in a polyethylene bag had been placed in the irradiation area shielded with polyethylene blocks (8 × 6 × 4 in.) containing about 5 % boron, the source was raised into the irradiation position by a string sliding through a crack in the shielding. The 1-in. thick slab of polyethylene between the source top and the sample provided moderation of the fission neutrons from the source and assured reproducible positioning of the raised source. (A small hole was placed over the source for passage of the string). Irradiation times for an energy calibration spectrum varied from one hour to perhaps several hours for the less sensitive elements. The Ge (Li) detector, located at the side, shielded with lead bricks to reduce the γ-ray background and with Boral to reduce neutrons, measured the γ-rays from the sample. The spectrum obtained for iron is shown in Fig. 2. Iron has proved to be one of the best energy calibration standards because of its good response over a long range from 9.3 MeV to the 1.21-MeV double escape peak of hydrogen of the polyethylene.

The second arrangement, for the copper mineral studies, used a 3.4-mg ^{252}Cf source (yielding about 10^{10} n s^{-1}) in a shielded cell; the ^{252}Cf had the same encapsulation as the source described. The irradiation container for the crushed sample materials was a polyethylene cup (about 2¼ × 3¼ in.) holding about 200 g. The cup was positioned about an inch from the 3.4-mg source in a polyethylene block (Fig. 3); the neutron moderation gave a maximum thermal flux in the samples of about 10^8 n cm^{-2} s^{-1}. The solid drill cores from the geothermal hole, which were about 2.25 in. in diameter and 3-in. long and weighed 200—400 g, were enclosed in a polyethylene covering and positioned similarly. The lead bricks surrounding the block structure reduced the scattered γ-ray background to the detector. The γ-ray contribution from the ^{252}Cf and encapsulating stainless steel was shielded from the detector by the 4-in. thick lead bricks directly in front of the source. Capture γ-rays from the source can be reduced by encapsulation with zirconium rather than stainless steel [10,11]. For a run, the assembly was loaded with the sample while the source was in its storage drum; then with the cell closed the source was moved into the irradiating position remotely.

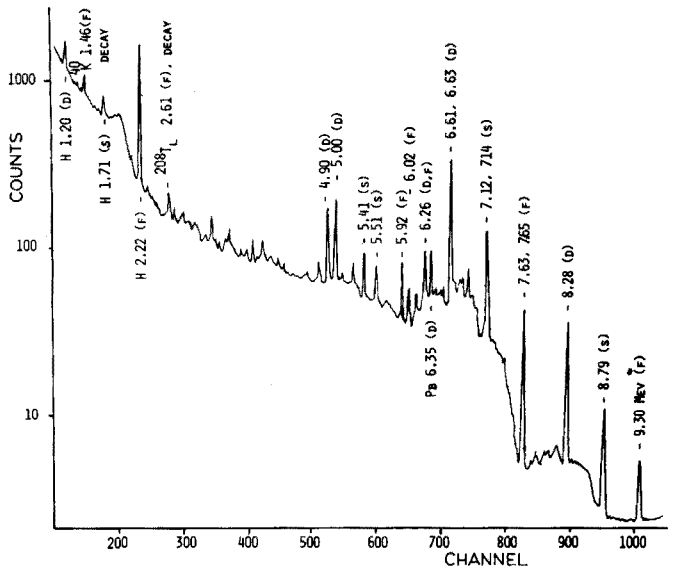

Fig. 2. Capture γ-ray spectrum for iron plate. 133-min ^{252}Cf, 10^7 n s^{-1}.

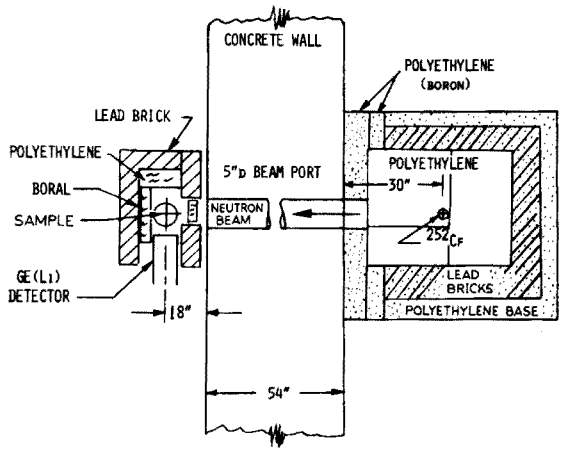

Fig. 3. ^{252}Cf internal irradiation arrangement.

The capture γ-rays from the irradiated sample passed through the polyethyle of the assembly, and through a 6-in. diameter port in the concrete shield wall of the cell. The beam was collimated to a 1.25-in. diameter beam by several lead pieces and measured by the Ge (Li) detector. The cell used had been designed for reactor work; this ^{252}Cf source assembly would not have required as much shielding as the cell wall provided. The detector was shielded by a block of polyethylene with boron and a Boral sheet in the γ-ray beam in front

of the detector. This detector shielding reduced the γ-ray signal somewhat; nevertheless, this limited the entry of neutrons to the detector and prevented damage to the Ge(Li) crystal.

The 20-cm^3 Ge(Li) detectors were used to measure the γ-rays from both irradiation arrangements. The resolution of the detector at the 1.33-MeV ^{60}Co γ-ray peak was 2 KeV (FWHM). A 1024-channel analyzer served the detector. A punched tape from the analyzer was processed in a PDP-9 computer to provide spectral data and plots.

RESULTS

Good spectra were obtained from all samples; those from the synthetic monzonite mixture, the monzonite porphyry ore, and the flotation concentrate are shown in Figs. 4—6, respectively. The synthetic monzonite and the monzonite copper ore gave similar spectra; the Fe, Cu, Si, Ca, Na, K and Al can be readily identified. The flotation concentrate shows very clearly the Fe, Cu, and S. The tailing gave disappointing results because chlorine, presumably from nearby brackish waters, had contaminated the sample, and caused some peak interference. Had this been recognized earlier, steps could have been taken, by washing, to eliminate the chlorine problem. With the lead and zinc ores, the iron and sulfur of the pyrite and the silicon were the prominent lines. For the rhyolite oxidized copper ore, the iron was clear with no sulfur line. The granite core samples gave spectra similar to that of the monzonite, and

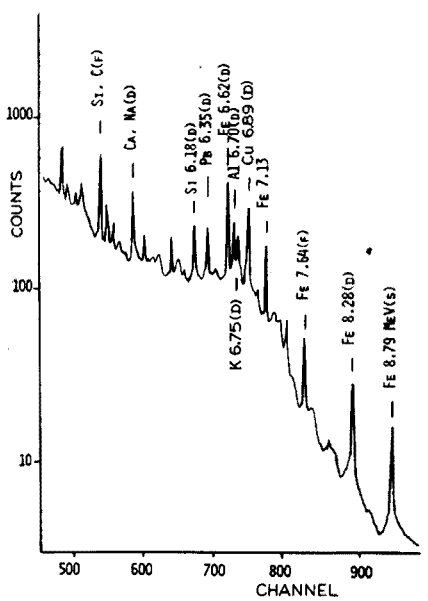

Fig. 4. Capture γ-ray spectrum for monzonite mixture. 174 g containing ca. 1.5 % Cu. ^{252}Cf source at 10^{10} n s^{-1}; 120-min irradiation.

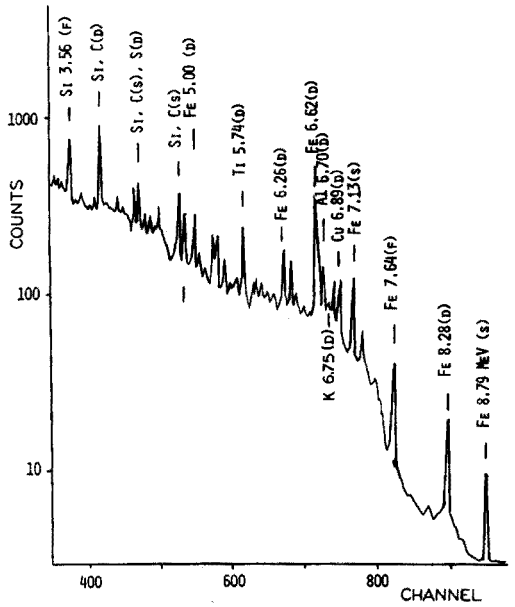

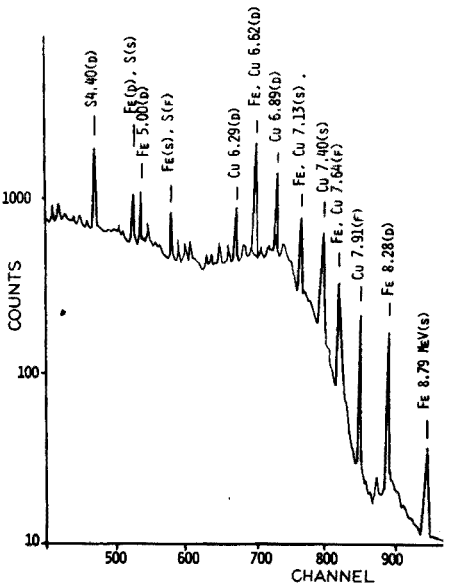

Fig. 5. Capture γ-ray spectrum for monzonite porphyry ore (Utah) 202 g containing ca. 0.7 % Cu. ^{252}Cf source at 10^{10} n s^{-1}; 60-min irradiation.

Fig. 6. Capture γ-ray spectrum for flotation concentrate (Utah) 250 g containing ca. 27 % Cu. Irradiation conditions as in Fig. 5.

the copper peak was clear. The amphybolite cores showed much iron, as expected, but no copper.

This study of copper materials, as well as related studies of rocks, show that the best peaks for quantitative results are: Cu 6.89 MeV (d); Fe 6.62 MeV (d), a doublet; Si 3.54 MeV (f); Ca 5.40 MeV (d); Na 2.96 MeV (d); K 6.75 MeV (d); Al 6.70 MeV (d); Mg 2.90 MeV (d). This order of response correspond generally to the sensitivities shown in Table 1, and to the elemental concentration.

A plot of the signal for copper (6.89 MeV, d) against copper concentration for the several materials is shown in Fig. 7. The three synthetic monzonite mixtures show linearity between counts and concentration. The copper signals of the ores and of the core material from the geothermal drill hole are plotted against the copper concentrations which have been reported for those materials (Table 2) but are not necessarily the actual contents of the samples tested. For all these heterogeneous materials tested, the agreement with the line for the known mixtures is fair. The spectral results with Fe, Si, Al, and S were in general accord with the concentrations in the materials; although not of interest in this study, the method could, presumably be applied in analyses for Fe, Si, Al, and S.

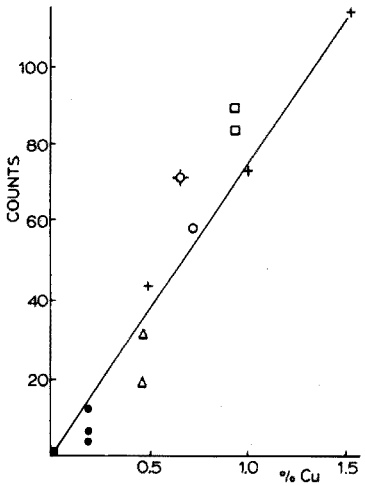

Fig. 7. Plot of copper concentration vs. counts at 6.89 MeV for 200-g samples. Irradiation conditions as in Fig. 5. (+) Synthetic monzonite standards; 0.5, 1.0, and 1.5 % Cu. (o) Monzonite porphyry; Utah: 0.73 % Cu. (⊕) Rhyolite Dyke, Nevada: 0.66 % Cu. (□) Sulfide vein 1, Utah: 0.93 % Cu. (△) Sulfide vein 2, Utah: 0.48 % Cu. (•) Granite, Barley Canyon, N. Mexico: 0.2 % Cu. Amphibolite, Barley Canyon, N. Mexico: —.

METALLURGICAL APPLICATION

Exploration for a copper deposit and outlining an ore body before mining must be supported by much analytical work. A field unit of ^{252}Cf with a Ge(Li) detector, perhaps in a laboratory or a truck, might assist a central analytical laboratory. In addition, drill hole exploration with an analytical probe of a ^{252}Cf source and a detector may be attractive [12,13]. Such a device might reduce expensive core drilling and laboratory analyses.

In metallurgical plants, an analytical assembly with a ^{252}Cf source in or adjacent to a processing stream with a Ge (Li) detector nearby (Fig. 8) could monitor the flow and give the concentration information necessary for mill operation and inventories. A single-channel analyzer set for a peak of the required element, e.g. the 6.89-MeV(d) peak of copper, could provide the signal which might assist in additions of chemical reagents and general process control. Several analytical units might be utilized in the plant. Possible locations for the units would be at conveyor belts with crushed copper ore, in slurries of ground ore in flotation circuits, in solutions in electrolytic plants, and in gaseous and liquid effluent streams.

Although copper was the subject of this study, other elements which respond well might also be monitored for process control. In such plant applications, the shielding of personnel must be given particular attention. Immersion of the source in a water slurry or solutions assists in shielding and also provides moderation for the neutrons. For other than immersion geometries, a moderating material, e.g. polyethylene, can be arranged around the source.

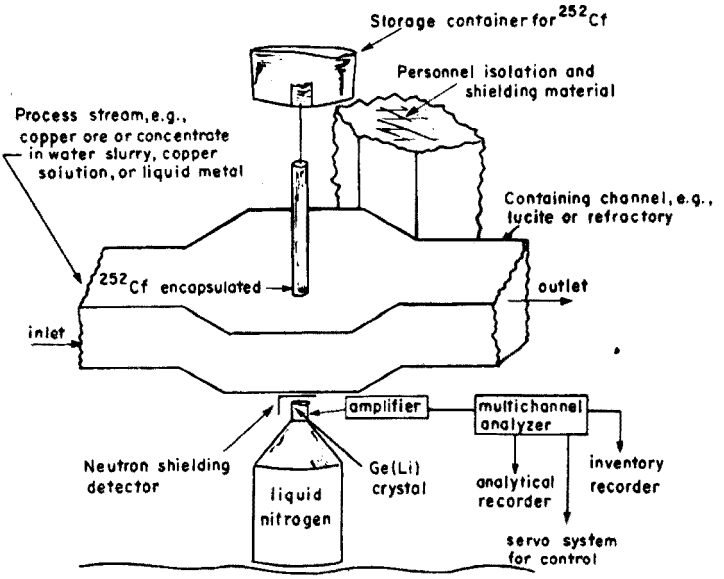

Fig. 8. Process control arrangement.

Although this paper is orientated towards capture γ-rays, decay γ-ray information is available and may be of use; for example, the 2.75-MeV decay line of sodium provides a means of determining that element.

In conclusion, the results with commercial copper ores and other copper-containing materials discussed in this paper, indicate that applications to the copper industry are possible, not only in exploration for copper deposits but in process control of milling and smelting.

SUMMARY

Copper mill materials from Utah and Nevada and rock cores from a geothermal drill hole at the Valles Grande Caldera in New Mexico were irradiated at the Los Alamos Scientific Laboratory with neutrons from a californium-252 source (about 10^{10} n s^{-1}), and the capture γ-rays were measured. The copper response, based on the 6.89-MeV double escape line, agreed sufficiently well with the known chemical composition of the materials to indicate usefulness of this technique for exploring copper deposits and for monitoring metallurgical extraction processes.

REFERENCES

1 Minerals Yearbook, Vols. I, II, U.S. Bureau of Mines, 1968, pp. 463, 769.
2 G. Hayward, Outline of Metallurgical Practice, Van Nostrand, New York, 3rd edn., 1964, p. 24.
3 G. Hayward, Outline of Metallurgical Practice, Van Nostrand, New York, 3rd edn., 1964, p. 70.

4 A. Butts, Copper, American Chemical Society Monograph, Rheinhold, New York, 1954, p. 176.
5 J.R. Rhodes, Isotopes and Radiation Technology (Atomic Energy Commission) 6 (1969) 359.
6 J.R. Rhodes, American Nuclear Society, Topical Meeting, Augusta, Georgia, Savannah River Lab Report Conf. 710402, Savannah River Lab., Aiken, S. Carolina, April 19—21, 1971, Vol. III, p.-IV.
7 D. Duffey, P.F. Wiggins and F.E. Senftle, Trans. Soc. Min. Engineers, AIME, 254 (1973) 112.
8 D. Duffey, A. ElKady and F.E. Senftle, Nucl. Instrum. Methods, 80 (1970) 149.
9 P.F. Wiggins, Ph.D. Thesis, University of Maryland, 1970.
10 F.E. Senftle, A.G. Evans, D. Duffey and P.F. Wiggins, Nucl. Technol., 10 (1971) 204.
11 P. Philbin, F.E. Senftle, D. Duffey, P. Wiggins and A.G. Evans, Nucl. Technol., 12 (1971) 404.
12 H.J. Paap and H.D. Scott, The Use of ^{252}Cf as a Neutron Source for Well Logging, see ref. 6, p. III—30.
13 A.B. Tanner, R.M. Maxham, F.E. Senftle and J.A. Baickes, Borehole Sonde Using a ^{252}Cf Source and a Ge(Li) Detector Cooled by a Melting Cryogen, see ref. 6, p. III—1.

Analytica Chimica Acta, 79 (1975) 161—173

MULTI-REACTION PROTON ACTIVATION ANALYSIS FOR TRACES OF MOLYBDENUM

V. KRIVAN

Max-Planck-Institut für Metallforschung Stuttgart, Institut für Werkstoffwissenschaften, Laboratorium für Reinststoffe, 7070 Schwäbisch Gmünd, Katharinenstrasse 17 (Federal Republic of Germany)

(Received 21st March 1975)

Molybdenum is a significant impurity in several high-purity materials such as special metals, *e.g.*, niobium, hafnium, tantalum, rhenium and tungsten, and also sometimes — depending on the origin and preparation procedure — in other metals such as iron, cobalt, copper, etc.

There exist many chemical and physical methods for the determination of molybdenum which have been excellently compiled by Elwell and Wood [1]. Reviewing these methods one can see that, for different reasons, very few of them can detect molybdenum at the lower p.p.m. range and below in metallic matrices; the detection limit often depends very strongly on the matrix. For most of the above-mentioned metallic matrices, radiochemical neutron activation analysis is the most sensitive method, despite the fact that the cross-sections of the principal reactions and/or the γ-ray intensities of the indicator radionuclides are rather low. The daughter technetium radionuclides ^{99m}Tc and ^{101}Tc formed by decay from the product radionuclides of the ^{98}Mo(n,γ) ^{99}Mo and ^{100}Mo(n,γ) ^{101}Mo reactions have often been detected. A detection limit down to about 0.1 p.p.m. can be achieved for the determination of molybdenum in difficult matrices [2—5]. However, neutron activation analysis is not very suitable for instrumental performance of the analysis. Even in matrices as suitable for instrumental neutron activation analysis as niobium and aluminium, experience has shown that molybdenum cannot be determined instrumentally at concentration levels much lower than 10 p.p.m.

Recently, molybdenum was included in the instrumental multi-element proton activation analysis of tantalum [6] and niobium [7]. From these two applications it is evident that proton activation analysis is, generally, a very interesting technique for the determination of molybdenum.

In the work described here, the application of all relevant proton-induced reactions to the determination of molybdenum was systematically investigated at proton energies of 12 MeV and 15 MeV. The following reactions were studied: ^{92}Mo(p,n)^{92}Tc, ^{94}Mo(p,n)^{94g}Tc + ^{95}Mo(p,2n)^{94g}Tc, ^{95}Mo(p,n)^{95m}Tc + ^{96}Mo(p,2n)^{95m}Tc, ^{95}Mo(p,n)^{95g}Tc + ^{96}Mo(p,2n)^{95g}Tc, ^{96}Mo(p,n)^{96g}Tc + ^{97}Mo(p,2n)^{96g}Tc and ^{100}Mo(p,2n)^{99m}Tc. In addition to a high sensitivity, an

advantage of this technique is that several principal reactions yielding indicator radionuclides with different half-lives can be used simultaneously for the determination. This is demonstrated by using the determination of molybdenum in cobalt as an example.

EXPERIMENTAL

Targets

Thick targets of pure molybdenum were used for measuring the analytical sensitivities and for standardization. Analyses were performed on cobalt samples of VP grade (Materials Research GmbH, Eching by München, West Germany). A pre-irradiation chemical etch of the molybdenum targets was accomplished with a nitric acid—hydrofluoric acid mixture (4:1) and the etch of samples with dilute (1 + 1) nitric acid.

Irradiation

Irradiations were performed with 12- and 15-MeV protons at the Karlsruhe isochronous cyclotron. For measuring the analytical sensitivities and for standardization, the beam currents were 5—200 nA of protons for 20—60 s. Cobalt samples for analysis were irradiated with 12-MeV protons in a water-cooled target holder at beam intensities of 3—5 μA for 5—60 min.

Counting equipment

γ-Rays were observed with a 30-cm^3 or a 55-cm^3 Ge(Li) detector coupled with a 4096-channel Northern or Nuclear Data pulse-height analyser. The energy resolutions of the two detectors were 2.3 keV and 2.1 keV FWHM, respectively, at the 1.332-MeV photopeak of ^{60}Co. The peak-to-Compton ratio were 26 : 1 and 29 : 1, respectively. The low-energy γ-rays were counted with an Elscint germanium low-energy detector (200 mm^2 area and 7 mm depth). The output signals from the detector were passed through an Elscint CA-N-1/1 preamplifier, a Canberra 1713 amplifier and a Canberra 1764 spectrum enhancer. The total system resolution was 495 eV at 122 keV. The detector was coupled to one of the two analysers.

Nuclear data used

Recent compilations and tables were used to obtain Q-values [8], threshold energies [9], excitation functions [10], isotopic abundance in natural elements [11], and the decay data [12,13].

RESULTS AND DISCUSSION

Choice of analytical reactions

Preliminary considerations and experiments showed that, of the various charged-particle activation techniques, proton activation analysis is most suitable for the determination of molybdenum. Proton activation gives the

benefit of a great choice of analytical reactions yielding indicator radionuclides with half-lives varying between 4.4 min and 61 days. In a given case, either the most suitable reactions can be chosen for the determination, or several or even all possible reactions can be used simultaneously. The latter way may be important in checking the accuracy of the determination. Only deuteron activation would offer similar possibilities with respect to the choice of analytical reactions and their sensitivities. However, the deuteron activation technique is less suitable for instrumental analysis than proton activation, because of the greater probability of activation of the matrix elements. For example, an instrumental determination of molybdenum in cobalt, which matrix was used as an example of the feasibility of the proton activation technique, would not be possible owing to the high activation of cobalt by the $^{59}Co(d,p)^{60}Co$ reaction. The same is true for many other matrix elements. If ^{3}He and α-particles are used, similar activation can occur, in the case of cobalt by the $^{59}Co(^{3}He,2p)^{60}Co$ and $^{59}Co(\alpha,2pn)^{60}$ reactions, respectively. In general, the activation of elements by means of deuterons, ^{3}He and α-particles is more complex than proton activation. Proton-induced nuclear reactions suitable for the determination of molybdenum are listed in Table I along with the pertinent nuclear data. In the energy range considered here, some of the indicator radionuclides can be produced via both the (p,n) and the (p,2n) reactions, because of the polyisotopic composition of the natural molybdenum. In these cases, the (p,n) type represents the main reaction while the contribution of the (p,2n) type to the production of the indicator radionuclide is generally much lower.

Sensitivity

The measured sensitivities, expressed as disintegrations per min per p.p.m. of molybdenum for a beam intensity of 1 μA, are summarized for six proton-induced reactions and for proton energies of 12 MeV and 15 MeV in Table II; the values given are averages of two or three runs. However, these results are valid only for matrices with an atomic number close to that of molybdenum. In other cases, because of matrix effects, the sensitivities will differ somewhat from those given in the Table. Figure 1 shows the dependence of the correction factor for 12-MeV and 15-MeV proton energies. As has recently been shown [6,7,14—17], the most interesting energy region for multielement proton activation analysis is that between 11 MeV and 15 MeV. To provide information about the dependence of the sensitivity on proton energy, data were obtained for two different energies: 12 MeV and 15 MeV. Increasing the proton energy from 12 MeV to 15 MeV increases the sensitivities differently for the individual proton-induced reactions, as can be seen from Table II. The increase varies by a factor of from 2.2 for the $Mo + p \rightarrow {}^{95g}Tc$ reaction to 5.9 for the $^{100}Mo(p,2n)^{99m}Tc$ reaction. In cases where the indicator radionuclide is produced by both (p,n) and (p,2n) reactions, as outlined above, the contribution of the latter to the increase of the sensitivity may vary from negligible to substantial depending on the appropriate Q-values, excitation functions and

TABLE I

Production and properties of the indicator radionuclides in activation of molybdenum via nuclear (p,n) and (p,2n) reactions

Nuclear reaction	Isotopic abundance (%)	Threshold energy (MeV)	Half-life	Major γ-rays (keV)	Absolute intensity (%)
^{92}Mo(p,n)^{92}Tc	15.84	8.8	4.4 min	147.9	55.0
				243.7	15.0
				329.3	78.0
				773.1	97.0
				1509.6	100.0
^{94}Mo(p,n)^{94m}Tc	9.04	5.1	52.0 min	870.9	91.0
^{95}Mo(p,2n)^{94m}Tc	15.72	12.5		1522.0	5.4
				1868.8	5.3
^{94}Mo(p,n)^{94g}Tc	9.04	5.1	4.88 h	702.6	100.0
^{95}Mo(p,2n)^{94g}Tc	15.72	12.5		849.7	100.0
				870.9	100.0
				916.2	6.8
^{95}Mo(p,n)^{95m}Tc	15.72	2.5	61.0 d	203.9	80.3
^{96}Mo(p,2n)^{95m}Tc	16.53	11.8		582.1	44.2
				786.2	12.0
				835.1	36.1
^{95}Mo(p,n)^{95g}Tc	15.72	2.5	20.0 h	765.8	94.0
^{96}Mo(p,2n)^{95}Tc	16.53	11.8		1074.1	4.0
^{96}Mo(p,n)^{96g}Tc	16.53	3.8	4.35 d	778.3	100.0
^{97}Mo(p,2n)^{96g}Tc	9.46	10.6		812.8	82.0
				850.3	99.0
				1127.2	15.0
^{100}Mo(p,2n)^{99m}Tc	9.63	7.8	6.02 h	140.5	85.0

TABLE II

Analytical sensitivities of different proton-induced reactions on molybdenum

Reactions	Sensitivity, d.p.m./p.p.m. μA[a]	
	E_p = 12 MeV	E_p = 15 MeV
^{92}Mo(p,n)^{92}Tc	$5.87 \cdot 10^3$	$1.23 \cdot 10^4$
Mo + p → ^{94g}Tc	$7.03 \cdot 10^2$	$3.39 \cdot 10^3$
Mo + p → ^{95m}Tc	12.5	30.2
Mo + p → ^{95g}Tc	$2.06 \cdot 10^3$	$4.60 \cdot 10^3$
Mo + p → ^{96g}Tc	$4.73 \cdot 10^2$	$1.17 \cdot 10^3$
^{100}Mo(p,2n)^{99m}Tc	$1.12 \cdot 10^3$	$6.67 \cdot 10^3$

[a] For an irradiation time of one half-life or a maximum of 2 h, at the end of the irradiation.

abundances for both reactions. Activation curves for the Mo(p,xn)^{96g}Tc and the Mo(p,xn)^{94g}Tc reactions (Figs.2 and 3) illustrate these circumstances.

From Table II, it is evident that the ^{92}Mo(p,n)^{92}Tc reaction is the most sensitive of the listed reactions. However, the disadvantage of this reaction may be the short half-life of ^{92}Tc (4.4 min). High sensitivities of the order of

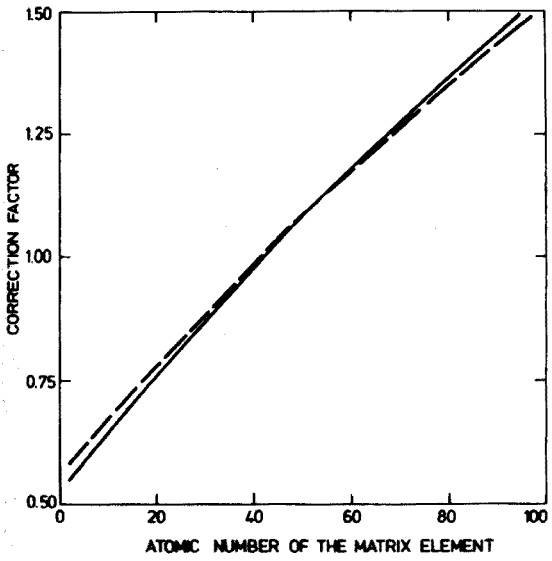

Fig.1. Sensitivity correction factors for the matrix effect in proton activation of molybdenum as a function of the atomic number of the matrix element.(——)12 MeV.(– – –)15 MeV.

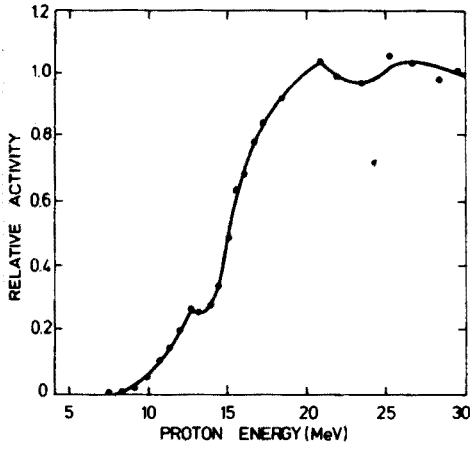

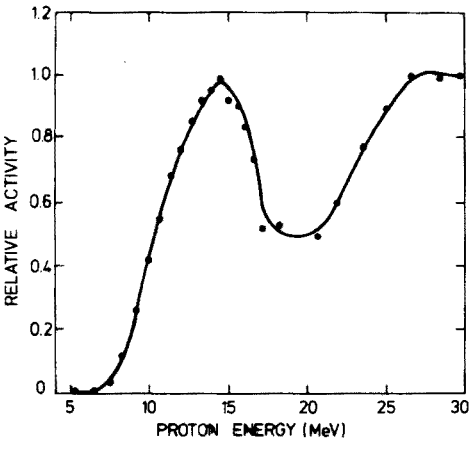

Fig.2. Activation curve for the Mo(p,xn)^{96g}Tc reactions.

Fig.3. Activation curve for the Mo(p,xn)^{94g}Tc reactions.

10^3 d.p.m./p.p.m. μA, can be achieved by using the Mo + p → ^{94g}Tc, Mo + p → ^{95g}Tc, Mo + p → ^{96g}Tc, and ^{100}Mo(p,2n)^{99m}Tc reactions. The half-lives of the indicator radionuclides produced by these reactions vary between 4.88 h and 4.35 days. The ^{95}Mo(p,n)^{95m}Tc reaction gives the lowest sensitivity; under certain circumstances, however, *e.g.* if medium or high trace concentratic must be determined and the counting can be done only after a long decay time, this reaction may be of interest.

Interferences

Table III summarizes primary interfering reactions which are energetically possible with proton energy up to 15 MeV. With only one exception — in the ^{100}Mo(p,2n)^{99m}Tc reaction — they are nuclear reactions induced on ruthenium. If the molybdenum and ruthenium concentrations are equal, the interfering reaction yields much lower activities of the indicator radionuclide than the principal reaction does. This may be caused by the very low cross-sections of the given interfering reactions up to proton energies of 15 MeV, and by the low isotopic abundance of the ruthenium nuclide in question. Ruthenium may also be determined via (p,xn) reactions, with ^{99m}Rh, ^{99g}Rh, ^{100}Rh and ^{101m}Rh as the indicator radionuclides [18]; thus the presence of ruthenium as possible interfering element in the determination of molybdenum can be checked easily and any necessary corrections can be made.

If instrumental proton activation analysis is considered, attention must be paid to interferences arising from overlapping γ-rays from other activation

TABLE III

Possible primary interfering reactions

Principal reaction	Interfering reaction	Threshold energy (MeV)	Isotopic abundance (%)
^{92}Mo(p,n)^{92}Tc	^{96}Ru(p,αn)^{92}Tc	10.5	5.51
^{94}Mo(p,n)^{94m,g}Tc	^{96}Ru(p,^{3}He)^{94m,g}Tc	9.7	5.51
	^{98}Ru(p,αn)^{94m,g}Tc	7.4	1.87
^{95}Mo(p,n)^{95m,g}Tc	^{96}Ru(p,2p)^{95m,g}Tc	7.4	5.51
	^{98}Ru(p,α)^{95m,g}Tc	0.0	1.87
	^{99}Ru(p,αn)^{95m,g}Tc	4.9	12.72
	^{100}Ru(p,α2n)^{95m,g}Tc	14.6	12.62
^{96}Mo(p,n)^{96g}Tc	^{99}Ru(p,α)^{96g}Tc	0.0	12.72
	^{100}Ru(p,αn)^{96g}Tc	6.6	12.62
	^{101}Ru(p,α2n)^{96g}Tc	13.5	17.07
^{100}Mo(p,2n)^{99m}Tc	^{100}Ru(p,2p)^{99m}Tc	9.3	12.62
	^{101}Ru(p,^{3}He)^{99m}Tc	16.2	17.07
	^{102}Ru(p,α)^{99m}Tc	0.0	31.61
	^{104}Ru(p,α2n)^{99m}Tc	12.1	18.58
	^{103}Rh(p,αp)^{99m}Tc	3.1	100.0

products. For ^{95g}Tc and ^{96g}Tc, data on such interferences have already been summarized [7]. The interferences for all other indicator radionuclides were investigated and are listed in Table IV. For γ-energies below 1 MeV, all those γ-rays were considered whose energy differs from that of the analytical γ-ray by up to ± 5 keV; and for γ-energies above 1 MeV, up to ± 7 keV. In the cases of the 147.9-keV γ-ray of ^{92}Tc, the 203.9-keV γ-ray of ^{95m}Tc, and the 140.4-keV γ-ray of ^{99m}Tc, counting with a low-energy detector is assumed. Consequently, γ-rays differing in their energy up to ± 800 eV from the energy of the analytical γ-ray were considered as interferences. The half-lives of the interfering radionuclides considered were limited to the interval between 1 min and 1000 times the half-life of the indicator radionuclide.

A comparison of the individual indicator radionuclides and their γ-rays shows that the possibilities of avoiding instrumental interferences are very different. Apparently the most suitable for instrumental analysis are the 140.4-MeV γ-ray of ^{99m}Tc produced by the ^{100}Mo(p,2n) reaction where only zirconium can interfere, and the 778.3-keV γ-ray of ^{96g}Tc produced mainly by the ^{96}Mo(p,n) reaction where only selenium interferes. In both cases, the difference between the half-lives of the indicator radionuclide and of the interfering radionuclide is great enough to permit analysis of the decay curve. In the first case, the 140.5-keV analytical γ-ray and the 141.2-keV interfering γ-ray can be resolved by using a good low-energy detector and a suitable computer program for peak analysis. When any of the other γ-rays are used for the determination, two or more elements can interfere. At any rate, it is absolutely necessary to check if the counted γ-rays are free of interference; for this purpose, a combination of procedures may be used as discussed recently [7,12].

Analysis of samples

The applicability of the analytical reactions listed in Table I to the determination of traces of molybdenum is shown by using the analysis of cobalt as an example. In 12-MeV proton activation of cobalt, practically no radioactivity is produced from the matrix so that the sample can be counted immediately after the end of the irradiation, *i.e.*, any indicator radionuclide can be counted. Table V gives the results of analysis of VP-purity cobalt obtained by using six different analytical reactions. The results and the deviations given are average values of three determinations on replicate samples. Experimental examination ensured that there were no detectable nuclear interferences; the γ-rays counted were carefully checked for instrumental interferences by following their decay curves to determine the half-lives, and, where possible, by examining the ratios of peak intensities of different γ-rays of the given indicator radionuclide. Only those γ-rays were considered which were in any case free of interference, or could be obtained so during the period of counting. Table V also shows the limits of detection obtained under optimal experimental conditions with regard to irradiation, decay and counting time;

TABLE IV

Possible instrumental interferences in the determination of molybdenum by γ-ray spectrometry

	γ-Ray measured (keV)	Interferences						
		γ-Ray (keV)	Intensity (%)	Nuclide	Half-life	Possible formation	Isotopic abundance	Threshold energy
^{92}Mo(p,n)^{92}Tc	*reaction (T_{y_2} = 4.4 min)*							
	147.9[a]	146.7	40.0	^{182m}Ta	16.0 m	^{186}W(p,αn)	28.41	0.0
		147.1	1.7	^{189}Re	24.0 h	^{192}Os(p,α)	41.0	0.0
		147.7	37.0	^{196m}Au	9.7 h	^{196}Pt(p,n)	25.3	2.3
						^{197}Au(p,pn)	100.0	8.1
						^{199}Hg(p,α)	16.84	0.0
		148.9	15.0	^{182}Re	64.0 h	^{182}W(p,n)	26.41	3.7
						^{186}Os(p,αn)	1.59	0.8
	329.3	324.4	11.0	^{97}Ru	2.88 d	^{98}Ru(p,pn)	1.87	10.4
		325.7	95.0	^{178}Ta	2.1 h	^{178}Hf(p,n)	27.14	2.7
						^{182}W(p,αn)	26.41	0.9
		326.6	4.4	^{149}Nd	1.8 h	^{150}Nd(p,pn)	5.62	7.4
		327.6	?	^{108}In	58.0 m	^{108}Cd(p,n)	0.87	6.0
						^{112}Sn(p,αn)	0.96	7.8
		328.5	60.9	^{194}Au	39.5 h	^{194}Pt(p,n)	32.9	3.3
						^{198}Hg(p,αn)	10.02	2.0
		331.9	25.0	^{178}Ta	2.1 h	^{178}Hf(p,n)	27.14	2.7
						^{182}W(p,αn)	26.41	0.9
		333.9	4.0	^{150}Eu	12.8 h	^{150}Sm(p,n)	7.44	3.1
						^{151}Eu(p,pn)	47.82	8.0
						^{154}Gd(p,αn)	2.15	2.2
		333.9	70.0	^{150}Pm	2.68 h	^{150}Nd(p,n)	5.62	0.9
						^{154}Sm(p,n)	22.71	2.1
	773.1	770.0	?	^{60}Cu	23.4 m	^{60}Ni(p,n)	26.23	7.0
						^{64}Zn(p,αn)	48.89	11.0
		773.1	?	^{186}Ir	15.0 h	^{186}Os(p,n)	1.59	4.6
		776.5	83.2	^{82}Br	35.4 h	^{82}Se(p,n)	9.19	0.9
		777.4	22.4	^{86}Y	14.6 h	^{86}Sr(p,n)	9.86	6.1
						^{90}Zr(p,αn)	51.46	12.9

TABLE IV (*continued*)

	γ-Ray measured (keV)	Interferences						
		γ-Ray (keV)	Intensity (%)	Nuclide	Half-life	Possible formation	Isotopic abundance	Threshold energy
	1509.6	1502.8	6.5	^{84}Y	43.0 h	^{84}Sr(p,n)	0.56	7.8
		1507.7	7.0	^{116m}In	54.0 m	^{116}Cd(p,n)	7.58	1.3
						^{119}Sn(p,αn)	8.58	3.8
		1508.0	6.7	^{89m}Zr	4.18 m	^{90}Zr(p,pn)	51.46	12.1
						^{89}Y(p,n)	100.0	3.7
						^{93}Nb(p,αn)	100.0	5.6
		1508.0	25.0	^{91m}Mo	66.0 s	^{92}Mo(p,pn)	15.84	12.8
		1509.0	?	^{70}As	52.0 m	^{70}Ge(p,n)	20.52	7.1
						^{74}Se(p,αn)	0.87	11.2
		1511.9	2.6	^{170}Lu	2.0 d	^{170}Yb(p,n)	3.03	4.2
						^{174}Hf(p,αn)	0.18	1.7
		1514.9	4.0	^{200}Tl	26.1 h	^{200}Hg(p,n)	23.13	3.3
						^{204}Pb(p,αn)	1.45	1.3
^{92}Mo(p,n)^{94m}Tc	*reaction (T_{y_2} = 52.0 min)*							
	870.9	866.6	?	^{57}Ni	36.0 h	^{58}Ni(p,pn)	67.88	12.4
		870.5	3.2	^{135}Ce	17.0 h	^{131}Ce(p,pn)	0.19	10.3
		870.9	100.0	^{94}Tc	4.88 h	^{94}Mo(p,n)	9.04	8.8
						^{98}Ru(p,αn)	1.87	7.4
		871.5	12.3	^{160}Ho	25.0 m	^{160}Dy(p,n)	2.29	3.7
		872.0	9.5	^{69}Ge	39.0 h	^{69}Ga(p,n)	60.4	3.1
						^{70}Ge(p,pn)	20.52	11.7
		872.5	5.8	^{129m}Ba	2.13 h	^{130}Ba(p,pn)	0.10	10.5
		873.8	5.2	^{91}Mo	15.5 m	^{92}Mo(p,pn)	15.84	12.8
^{94}Mo(p,n)^{94g}Tc	*reaction (T_{y_2} = 4.88 h)*							
	702.6	698.6	28.0	^{82}Br	35.4 h	^{82}Se(p,n)	9.19	0.9
		700.6	2.4	^{129m}Ba	2.13 h	^{130}Ba(p,pn)	0.10	10.5
		701.7	100.0	^{53m}Fe	2.53 m	^{54}Fe(p,pn)	5.82	13.6
		703.1	4.6	^{106m}Ag	8.5 d	^{106}Pd(p,n)	27.33	3.8
						^{107}Ag(p,pn)	51.35	9.6
						^{110}Cd(p,αn)	12.39	6.7

TABLE IV (*continued*)

	γ-Ray measured (keV)	Interferences						
		γ-Ray (keV)	Intensity (%)	Nuclide	Half-life	Possible formation	Isotopic abundance	Threshold energy
		703.3	15.4	^{84}Y	14.4 h	^{86}Sr(p,n)	9.86	6.1
						^{90}Zr(p,αn)	51.46	12.9
		706.3	16.0	^{166}Tm	7.7 h	^{166}Er(p,n)	33.41	3.8
						^{170}Yb(p,αn)	3.03	2.1
		707.4	31.2	^{110m}In	4.9	^{110}Cd(p,n)	12.39	7.4
						^{114}Sn(p,αn)	0.66	4.8
	849.7	846.7	99.9	^{56}Co	77.3 d	^{56}Fe(p,n)	91.66	5.6
						^{60}Ni(p,αn)	26.23	11.8
		847.3	3.6	^{106m}Ag	8.5 d	^{106}Pd(p,n)	27.30	3.8
						^{107}Ag(p,pn)	51.35	9.6
						^{110}Cd(p,αn)	12.39	6.7
		848.4	3.2	^{52}Mn	5.6 d	^{52}Cr(p,n)	83.76	5.6
						^{56}Fe(p,αn)	91.66	13.3
		850.3	99.9	^{96}Tc	4.35 d	^{96}Mo(p,n)	16.53	3.8
						^{99}Ru(p,α)	12.72	0.0
		852.7	3.6	^{171}Lu	8.3 d	^{171}Yb(p,n)	14.31	2.7
						^{174}Hf(p,αn)	0.18	1.7
	870.9[b]	870.9	91.0	^{94m}Tc	52.0 m	^{94}Mo(p,n)	9.04	5.1
						^{98}Ru(p,αn)	1.87	7.4
		874.8	6.6	^{185}Os	94.0 d	^{186}Os(p,pn)	1.59	8.3
						^{185}Re(p,n)	37.07	1.8
^{95}Mo(p,n)^{95m}Tc	*reaction (T_{y_2} = 61.0 d)*							
	203.9[a]	202.3	21.8	^{129m}Ba	2.13 h	^{130}Ba(p,pn)	0.10	10.5
		202.8	58.2	^{127}Xe	36.4 d	^{127}I(p,n)	100.0	1.5
		203.4	5.3	^{172}Lu	6.7 d	^{172}Yb(p,n)	14.31	4.1
						^{176}Hf(p,αn)	5.20	1.8
		204.1	14.6	^{177m}Lu	155.0 d	^{180}Hf(p,α)	35.24	0.0
		205.8	3.3	^{192}Ir	74.2 d	^{192}Os(p,n)	41.0	1.8
						^{193}Ir(p,pn)	62.7	7.8
						^{195}Pt(p,α)	33.8	0.0

	γ-Ray measured (keV)	Interferences						
		γ-Ray (keV)	Intensity (%)	Nuclide	Half-life	Possible formation	Isotopic abundance	Threshold energy
	582.1	579.3	14.0	^{200}Tl	26.1 h	^{200}Hg(p,n)	23.13	3.3
						^{204}Pb(p,αn)	1.48	1.3
		579.4	2.8	^{77}Br	56.0 h	^{77}Se(p,n)	7.58	2.2
		580.6	4.8	^{86}Y	14.6 h	^{86}Sr(p,n)	9.86	6.1
						^{90}Zr(p,αn)	51.46	12.9
		582.0	9.0	^{110}In	4.9 h	^{110}Cd(p,n)	12.39	4.8
		584.0	6.6			^{114}Sn(p,αn)	0.66	7.4
		584.4	?	^{186}Ir	15.0 h	^{186}Os(p,n)	1.59	4.6
		585.9	1.3	^{77}Br	56.0 h	^{77}Se(p,n)	7.58	2.2
	835.1	831.8	12.3	^{150}Pm	2.68 h	^{150}Nd(p,n)	5.62	0.9
		832.4	?	^{86}Y	14.6 h	^{86}Sr(p,n)	9.86	6.1
						^{90}Zr(p,αn)	51.46	12.9
		833.6	2.8	^{129m}Ba	2.13 h	^{130}Ba(p,pn)	0.10	10.5
		833.6	5.9	^{66}Ga	9.4 h	^{66}Zn(p,n)	27.81	6.0
						^{70}Ge(p,αn)	20.52	10.2
		833.9	76.6	^{72}As	26.0 h	^{27}Ge(p,n)	27.43	5.2
						^{76}Se(p,αn)	9.02	10.4
		833.9	100.0	^{72}Ga	14.1 h	^{76}Ge(p,αn)	7.76	7.9
		834.8	99.9	^{54}Mn	312.5 d	^{54}Cr(p,n)	2.38	2.2
						^{55}Mn(p,pn)	100.0	10.4
						^{57}Fe(p,α)	2.19	0.0
		835.7	4.4	^{86}Y	14.6 h	^{86}Sr(p,n)	9.86	6.1
						^{90}Zr(p,αn)	51.46	12.9
		839.8	4.6	^{171}Lu	8.3 d	^{171}Yb(p,n)	14.31	2.7
						^{174}Hf(p,α)	0.18	0.0
^{100}Mo(p,2n)^{99m}Tc	*reaction (6.02 h)*							
	140.5[a]	141.2	67.0	^{90}Nb	14.6 h	^{90}Zr(p,n)	51.46	7.0
						^{94}Mo(p,αn)	9.04	9.1

[a] Counting with a low-energy detector is assumed.
[b] Interferences given for the 870.9-keV γ-ray of the ^{94m}Tc as indicator radionuclide must also be added.

TABLE V

Results of analysis of VP-purity cobalt for molybdenum obtained by various proton-induced reactions

Analytical reaction	Concentration determined (p.p.m.)	Detection limit (p.p.m.)
$^{92}Mo(p,n)^{92}Tc$	87.6 ± 7.1	9.2
$Mo + p \rightarrow {}^{94g}Tc$	87.0 ± 4.2	1.1
$Mo + p \rightarrow {}^{95m}Tc$	85.1 ± 6.9	5.2
$Mo + p \rightarrow {}^{95g}Tc$	93.4 ± 3.8	0.09
$Mo + p \rightarrow {}^{96g}Tc$	89.1 ± 3.9	0.1
$^{100}Mo(p,2n)^{99m}Tc$	91.1 ± 5.2	1.2

these limits were calculated by reducing the peak intensities in the γ-ray spectra of the cobalt sample to the minimal detectable values by means of the "working expressions" of Currie [19]. As can be seen, the limits of detection of the individual analytical reactions, even of those giving very similar absolute sensitivities (Table II), differ considerably. The high limit of detection of the $^{92}Mo(p,n)^{92}Tc$ reaction is caused mainly by the high Compton background in the counting of 4.4-min ^{92}Tc; this background originates predominantly from 23.4-min ^{60}Cu produced by the $^{60}Ni(p,n)$ reaction from the nickel present in the sample at a concentration of 570 p.p.m. Moreover, counting could be started only after 1.5—2 half-lives of ^{92}Tc had elapsed after the en of the irradiation. Similarly, the presence of nickel and other impurities yieldin relatively short-lived radionuclides, *e.g.* chromium, tin and zinc, are the reason for the relatively high limits of detection for the $Mo + p \rightarrow {}^{94g}Tc$ and $^{100}Mo(p,2n)^{99m}Tc$ reactions. In the $Mo + p \rightarrow {}^{95m}Tc$ reaction, the limit of detection is determined mainly by the low saturation factor which arises from the long half-life of ^{95m}Tc (61 d). Thus, for cobalt samples of this grade of purity, the best sensitivity for the determination of molybdenum is achieved by the $Mo + p \rightarrow {}^{95g}Tc$ and the $Mo + p \rightarrow {}^{96g}Tc$ reactions. From Table II it is evident that all considered reactions give much better sensitivities if radiochemical separation of the indicator radionuclide is performed.

Conclusions

Molybdenum can be determined with high sensitivity via five proton-induced principal reactions. One of the important features of this multi-reaction activation technique is the possibility of checking the accuracy of the analysis with regard to nuclear and instrumental interferences as well as with regard to the depth distribution of molybdenum in the sample. Distribution studies are possible because the distribution of the indicator radionuclide activity with depth differs for the individual principal reactions.

SUMMARY

The application of proton activation analysis to the determination of molybdenum is described. Thick molybdenum targets were bombarded with 12-MeV and 15-MeV protons. The reactions studied were $^{92}Mo(p,n)^{92}Tc$, $^{94}Mo(p,n)^{94g}Tc + {}^{95}Mo(p,2n)^{94g}Tc$, $^{95}Mo(p,n)^{95m}Tc + {}^{96}Mo(p,2n)^{95m}Tc$, $^{95}Mo(p,n)^{95g}Tc + {}^{96}Mo(p,2n)^{95g}Tc$, $^{96}Mo(p,n)^{96g}Tc + {}^{97}Mo(p,2n)^{96g}Tc$ and $^{100}Mo(p,2n)^{99m}Tc$. Except for the Mo + p → ^{95m}Tc reaction, all these reactions give high analytical sensitivities. For 12-MeV protons and an irradiation time of one half-life or a maximum of 2 h, the sensitivities range from $5 \cdot 10^2$ to $6 \cdot 10^3$ d.p.m./p.p.m. μA, and for 15-MeV protons and the same irradiation conditions from 10^3 to 10^4 d.p.m./p.p.m. μA. In addition to the high sensitivity, the great advantage of proton activation is that different principal reactions yield indicator radionuclides with half-lives between 4.4 min and 61 d. Simultaneous determinations by these reactions are of value for checking the accuracy. For each reaction, detailed data are given on nuclear and instrumental interferences. Analytical application of this multi-reaction proton activation analysis is illustrated by the instrumental determination of molybdenum in cobalt.

REFERENCES

1 W.T. Elwell and D.F. Wood, Analytical Chemistry of Molybdenum and Tungsten, Pergamon, Oxford, 1971.
2 J. Starý, A. Zeman and J. Růžička, Anal. Chim. Acta, 29 (1963) 103.
3 H. Grosse-Ruyken and H.G. Doge, Talanta, 12 (1965) 73.
4 R.A. Nadkarni and B.C. Haldar, Talanta, 16 (1969) 116.
5 N.K. Baisha and R.B. Heslop, Anal. Chim. Acta, 50 (1970) 209.
6 V. Krivan, D.L. Swindle and E.A. Schweikert, Anal. Chem., 46 (1974) 1626.
7 V. Krivan, Anal. Chem., 47 (1975) 469.
8 K.A. Keller, H. Münzel and J. Lange, in K.-H. Hellwege (Ed.), *Q*-values for Nuclear Reactions, Landolt-Börnstein, New Series, Group I, Vol. 5, Part a, Springer, Berlin, 1973.
9 K.A. Keller, J. Lange and H. Münzel, in K.-H. Hellwege (Ed.), Estimation of Unknown Excitation Functions and Thick Target Yields for p, d, ^{3}He and α Reactions, Landolt-Börnstein, New Series, Group I, Vol. 5, Part c, Springer, Berlin, 1974.
10 K.A. Keller, J. Lange, H. Münzel and G. Pfennig, in K.-H. Hellwege (Ed.), Excitation Functions for Charged-Particle Induced Nuclear Reactions, Landolt-Börnstein, New Series, Group I, Vol. 5, Part b, Springer, Berlin, 1973.
11 W. Seelmann-Eggebert, G. Pfennig and H. Münzel, Chart of the Nuclides, Bundesministerium für Bildung und Forschung, Bonn, 3rd edn., 1968.
12 C.M. Lederer, J.M. Hollander and I. Perlman, Table of Isotopes, Wiley, New York, 6th edn., 1967.
13 G. Erdtmann and W. Soyka, Die Gamma-Linien der Radionuklide, Band 1—3, Jül-1003-AC, Jülich, West Germany, September 1973.
14 S.M. Kormali and E.A. Schweikert, J. Radioanal. Chem., 22 (1974) 139.
15 J.N. Barrandon, J.L. Debrun and A. Kohn, J. Radioanal. Chem., 16 (1973) 617.
16 N.H. Krasnov, Yu.G. Sevastyanov, I.O. Konstantinov, V.G. Vinogradova and V.V. Malukhin, J. Radioanal. Chem., 16 (1973) 395.
17 V. Krivan, J. Radioanal. Chem., 26 (1975) 151.
18 To be published.
19 L.A. Currie, Anal. Chem., 40 (1968) 586.

Analytica Chimica Acta, 79 (1975) 175—183

THE HIGH-PRESSURE LIQUID CHROMATOGRAPHIC SEPARATION OF COPPER(II) AND NICKEL(II) SCHIFF BASE CHELATES ON MICROPARTICULATE SILICA

PETER C. UDEN and FREDERICK H. WALTERS
Department of Chemistry, University of Massachusetts, Amherst, Mass. 01002 (U.S.A.)
(Received 28th April 1975)

The rapid development of high-pressure liquid chromatographic (h.p.l.c.) column separation techniques in recent years has greatly extended the range of chemical systems amenable to high-resolution chromatography. Since the wide range of substrates available in liquid chromatography can be utilized, h.p.l.c. has outstanding possibilities. The availability of partition, adsorption, ion-exchange and exclusion mechanisms in the high-pressure mode, coupled with the development of sensitive detection systems, has prompted considerable interest in instrumental development [1] and analytical applications [2—5]. The recent advent of microparticulate ($\leqslant$ 10-μm diameter) substrates has greatly increased h.p.l.c. column efficiencies, making the results comparable in many cases with those of gas chromatography.

While h.p.l.c. techniques have been applied to a very wide range of organic compounds, little attention has so far been paid to ionic metallic species, metal complexes or organometallic systems. This lack of application scarcely reflects the wide use of classical low-pressure liquid chromatographic column procedures and paper and thin-layer adsorption and partition methods [6]. Of the h.p.l.c. studies which have been made, the most definitive data are those of Huber *et al.* [7], who used a ternary liquid—liquid partition system for the separation of the acetylacetonates and trifluoroacetylacetonates of a range of metals including beryllium(II), copper(II), zinc(II), aluminium(III), cobalt(III) and zirconium(IV). A water: 2,2,4-trimethylpentane: ethanol system was employed, the water-rich phase being employed as the stationary medium and the water-poor phase as the eluant. The addition of traces of chelating agent to the solvent was found to suppress hydrolysis of the chelates. Recently, Heizmann and Ballschmiter [8] have reported adsorption h.p.l.c. of the mercury(II) and copper(II) chelates of bisacetyl-bisthiobenzoylhydrazones on silica with benzene as the mobile phase. Good HETP values (1—3 mm) and R_s values (0.7—1.74) were obtained, and satisfactory correlation with t.l.c. data was reported, 'Forced flow' ion-exchange chromatography has been used by Seymour and Fritz [9] for the separation of a range of metal ions. The few reported studies in the organometallic area include those of Veening and coworkers [10] on the liquid—liquid partition separation of arenetricar-

bonylchromium complexes, Graf and Lillya [11] on the reversed-phase separation of isomeric tricarbonyl(dieneone)iron complexes and Evans and Hawthorne [12] who resolved cobalt metallocarboranes.

All of the foregoing results were obtained on columns containing substrates of relatively large mesh with results which, although important, were not generally comparable with those found for systems amenable to gas chromatography in terms of column efficiency and resolution.

A key feature of recent h.p.l.c. development has been the commercial production of reproducible microparticulate substrates ($\leqslant 10\ \mu m$ diameter) from which much greater column efficiencies may be obtained. Thus silica in the 5—10-μm diameter range is available for adsorption studies and permanently bonded microparticulate substrates are available for normal and reverse phase partition chromatography. Some of these systems seem worthy of study for the separation of a range of neutral metal complexes of considerable analytical importance. The present paper describes studies on microparticulate silica; partition studies will be reported in future papers.

The adsorption h.p.l.c. characteristics of tetradentate β-ketoamine and salicylaldimine chelates of copper(II) and nickel(II) with the structures shown below, were studied.

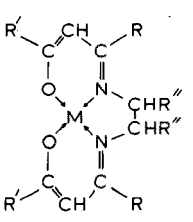

(A)

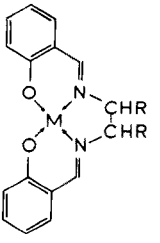

(B)

The representative ligands considered were N,N′-ethylenebis(acetylacetonei [bis(acetylacetone)ethylenediamine; $H_2(enAA_2)$; R = R′ = methyl and R″ = H and N,N′-ethylenebis(salicylaldimine)[$H_2(enSal_2)$; R = H in B]. These ligands are obtained by condensation of two molecules of acetylacetone or salicylaldehyde with ethylenediamine.

EXPERIMENTAL

Preparation of ligands

$H_2(enAA_2)$ was prepared from acetylacetone and ethylenediamine as described previously [13,14] and purified by recrystallization from n-hexane. $H_2(enSal_2)$ was prepared by reacting salicylaldehyde and ethylenediamine in ethanolic solution followed by recrystallization from aqueous ethanol.

Preparation of metal complexes

The copper(II) and nickel(II) chelates were prepared by reacting ammoniacal metal ion solutions with the purified crystalline ligands. The precipitated complexes were filtered and washed with water; they were then purified by recrystallization from methanol—water or acetonitrile—water solutions. The complexes gave single spots in t.l.c. and single peaks in h.p.l.c.; their mass spectra showed predicted fragmentation patterns with authentic molecular ion parent peaks.

High-pressure liquid chromatography

A Tracor-Chromatec model 3100 liquid chromatograph was employed: the pumping system consisted of an electronically driven reciprocating piston giving a maximum pressure of 1000 p.s.i. A u.v. detector with a single detection wavelength of 254 nm, a full-scale sensitivity of 0.01 A (absorbance units) and flow-cell with a volume of 8 μl was used. The 30 cm × 4 mm i.d. column employed contained Partisil (10-μm diameter; Reeve Angel Inc.). Certified (ACS grade) solvents (Fisher Scientific Corporation) were used without further purification.

Mass spectrometry

Mass spectra of the chelates and eluted samples were obtained on a Hitachi Perkin-Elmer RMU.6L single focussing mass spectrometer operating at an ionizing voltage of 70 eV. The source temperature was maintained at 210 ± 5 °C and solid samples were evaporated into the source by means of a direct insertion probe.

Electron spin resonance spectroscopy

A Varian E-9 instrument was used; the operating frequency range was 8.8—9.6 GHz and the modulation field intensity was 50 mgauss to 40 gauss peak-to-peak. Cu(enSal$_2$) was confirmed in the eluted peaks, no sample concentration being needed. Spectra obtained at room temperature yielded the same characteristic four-peak spectrum for eluted Cu(enSal$_2$) as for the pure complex and the referenced sample [15].

Ultra-violet spectrophotometry

A Hitachi-Coleman EPS-3T instrument was employed in the range 210—360 nm, with a deuterium source and a photomultiplier setting of 2; 1-cm quartz cells were used. Solutions were made up in 1 % methylene chloride in diethyl ether and run against similar blanks.

RESULTS AND DISCUSSION

Bidentate and tetradentate β-ketoamine ligands have been shown to be particularly suited to gas chromatographic (g.c.) separation of divalent transition metals, since in contrast to the β-diketonates, their chelates have little tendency to oxidize, polymerize, solvate or form stable base adducts, all of which features give rise to analytical difficulties [13,14]. In g.c. studies, particular attention has been given to the resolution of analogous copper(II) and nickel(II) chelates, since these show closely similar chemical and structural properties. While progress has been made in the determination of copper and nickel mixtures at trace levels [16], improved resolution is still a matter of primary concern.

The β-ketoamines and related Schiff base ligands are of considerable potential in quantitative analysis for metals since reactions are rapid and quantitative at all concentration levels and are relatively free from interferences provided that a pH of 10 or above is maintained. Further, the ligands and pure chelates are readily obtainable in a high state of purity to set up standard calibrations.

The results obtained from previous g.c. studies indicated that h.p.l.c. might be applied successfully to these chelates. The adsorption mode, with silica as substrate, has the advantage that correlation is possible with t.l.c. data obtained on silica plates. In addition, t.l.c. indicates the polarity and type of solvent system appropriate for h.p.l.c. Of the solvents tried for t.l.c. of the complexes on silica, acetonitrile was found to give optimal resolution, R_F values being obtained as follows: Cu(enAA$_2$), 0.79; Ni(enAA$_2$), 0.86; Cu(enSal$_2$), 0.16; and Ni(enSal$_2$), 0.40. From general observations on t.l.c. and h.p.l.c. on silica, however, it might be predicted that a solvent system of lower polarity would give better resolution of chelate pairs than acetonitrile in h.p.l.c.

A solvent system consisting of 20 % acetonitrile in methylene chloride was found suitable for the resolution of both pairs of copper and nickel chelates. Figure 1(a) shows the separation of Cu(enAA$_2$) and Ni(enAA$_2$) with this solvent, while Fig. 1(b) shows that for Cu(enSal$_2$) and Ni(enSal$_2$). Both chelate systems clearly demonstrate adequate resolution for qualitative and quantitative analysis of the copper and nickel complexes. Somewhat improved resolution for the enAA$_2$ complexes was possible when lower percentages of acetonitrile were used, but the same solvent is depicted here for better comparison between the two chelate types. For the enAA$_2$ complexes, peak shape and resolution are comparable with that obtained gas chromatographically [17], while for the enSal$_2$ system no g.c. elution has been achieved. The resolution between the components for each of the two pairs bears a distinct relationship to the R_F data given above. Resolution factors calculated are 1.42 for Ni/Cu(enAA$_2$) and 4.87 for Ni/Cu(enSal$_2$). Theoretical plates calculated are as follows: Cu(enAA$_2$), 493; Ni(enAA$_2$), 361; Cu(enSal$_2$), 447; Ni(enSal$_2$), 309.

In order to ensure that the peaks observed corresponded to the species

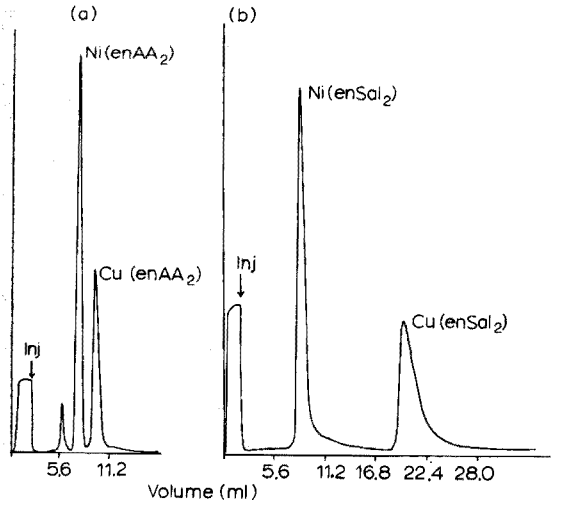

Fig.1. High pressure liquid chromatograms of chelates. (a) $Ni(enAA_2)$ and $Cu(enAA_2)$; (b) $Ni(enSal_2)$ and $Cu(enSal_2)$. Column, 30 cm × 4 mm i.d., 10-μm diameter Partisil. Solvent 4 : 1 CH_2Cl_2—CH_3CN. Flow rate, 2.8 ml min^{-1}.

chromatographed, the chelates were collected from the eluant and after concentration by evaporation were analysed by a number of methods. Qualitative integrity of eluates was established by mass spectrometry, a heated solids probe being used for sample introduction. Spectra identical to those of the pure chelates were obtained in each case, with characteristic molecular ions and fragmentation patterns as shown in Table I.

Ultraviolet spectrophotometry, in the range 220—360 nm, was employed for both qualitative and quantitative confirmation of elution. Spectra of the four chelates are shown in Fig.2. In all cases, the wavelength of 254 nm available for detection gave high sensitivities although it was not optimal. Molar absorptivities calculated for the chelates at 254 nm are: $Cu(enAA_2)$, 11,600; $Ni(enAA_2)$, 13,085; $Cu(enSal_2)$, 22,700; and $Ni(enSal_2)$, 49,800.

TABLE I

Principal features of chelate mass spectral fragmentation patterns
(P indicates the parent ion, L the ligand and M the metal. R.I. = relative intensity. Most fragment ions below P^{2+} are not included. Based on Ni (58) and Cu (63).)

Chelate	$Ni(enSal_2)$		$Cu(enSal_2)$		$Ni(enAA_2)$		$Cu(enAA_2)$	
Ion	m/e	R.I.	m/e	R.I.	m/e	R.I.	m/e	R.I.
P^+	324	100	329	100	280	78	285	61
$(M + \frac{1}{2}L)^+$	191	51	196	69	169	100	174	100
P^{2+}	162	13	164.5	8	140	38	142.5	2
$(\frac{1}{2}L)^+$	132	22	132	68	—	—	—	—
M^+	58	26	63	20	58	27	63	9

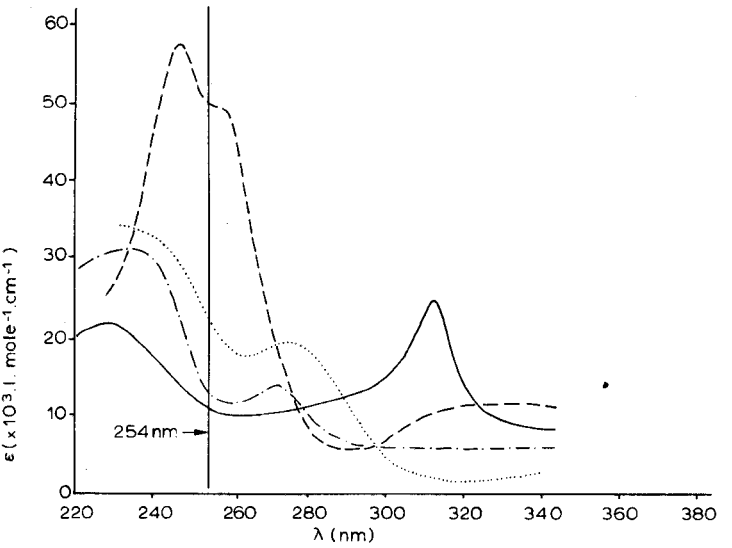

Fig. 2. Plot of molar absorptivity against wavelength for chelates. (a) (——) $Cu(enAA_2)$; (b) (— · — · —) $Ni(enAA_2)$; (c) (· · · · ·) $Cu(enSal_2)$; (d) (– – –) $Ni(enSal_2)$.

These values are in close agreement with literature values [18,19].

Sample recoveries were studied for $Cu(enAA_2)$, the least stable of the four chelates, to determine whether elution was quantitative. Collection of a number of different samples, absorbance measurement and correlation with the amount injected showed recoveries in the range 98—102 % with a precision of *ca.* ± 5 %.

Further confirmation of elution for $Cu(enSal_2)$ was made by electron spin resonance spectroscopy, the characteristic four-peak spectrum for the copper(II) chelate at room temperature [15] being noted in the eluate.

Quantitative studies were carried out for each chelate to determine the linearity of detector response and the approximate limits of detection. Figure 3 shows a plot of peak areas against weight of chelate for $Cu(enAA_2)$ and $Ni(enAA_2)$ over the range 25 ng—20 μg. Good linearity of response was maintained up to *ca.* 5 μg, above which a diminution of response was indicated. Comparative studies carried out for organic compounds having similar absorbances at 254 nm indicated a similar curvature above the 5—10 μg level, which proved the effect to be the result of non-linear detector response. The detection limits of *ca.* 25 ng are taken at a signal-to-noise ratio of 2 : 1. The precision of the data in the present study is insufficient to show an appreciable difference between the calibration plots for the two chelates whose molar absorptivities differ by approximately 10 %.

Figure 4 shows similar plots for $Cu(enSal_2)$ and $Ni(enSal_2)$. In this case, the difference in molar absorptivities is large enough to separate the logarithmic calibration plots. Detection limits are *ca.* 10 ng for $Cu(enSal_2)$ and *ca.* 5 ng

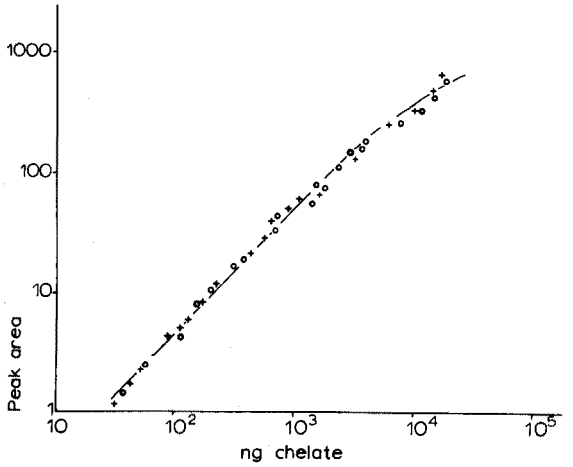

Fig.3. Plot of peak area against weight of chelate for Ni(enAA$_2$) (○) and Cu(enAA$_2$) (+). Column conditions as for Fig.1.

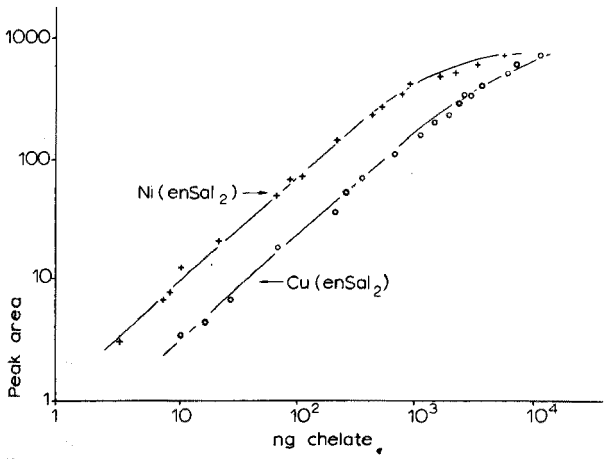

Fig.4. Plot of peak area against weight of chelate for Ni(enSal$_2$) and Cu(enSal$_2$). Column conditions as for Fig.1.

for Ni(enSal$_2$), being directly related to their absorptivities. Linearity is maintained up to the microgram level, which is again consistent with the absorbance limits of linearity for the detector. Intercepts of the plots on the peak area axis are also in fair agreement with the absorptivity ratio for the complexes.

These results indicate that a linearity range of somewhat under 3 orders of magnitude is obtainable by u.v. detection under the conditions specified. Provided that the chelate has a molar absorptivity of 10,000 or above at the detection wavelength, quantitative determinations corresponding to low nanogram levels of metal are possible. It may be noted that these limits are

comparable to the lowest limits for flame ionization detection in gas chromatography for chelates of appropriate volatility and thermal stability.

It appears that the techniques of g.c. and h.p.l.c. may prove complementary for metal determinations. The latter can provide separations for species such as the salicylaldimine complexes which are not sufficiently thermally stable or volatile for gas chromatography, but have advantages in terms of rapid quantitative formation in aqueous solution. Determinations of copper, nickel and palladium by this and similar h.p.l.c. techniques are currently being investigated and comparisons with g.c. methods made.

The h.p.l.c. characteristics of a range of fluorinated and unfluorinated β-ketoamine and β-thioketone chelates on microparticulate substrates in both adsorption and partition modes will be reported in future publications.

We acknowledge support for the acquisition of equipment from a National Institutes of Health, Biomedical Sciences Support grant (RR 07048) to the University of Massachusetts. We are also grateful to Professor Hans Veening for discussions and advice.

SUMMARY

The separation of neutral copper and nickel chelates of two representative Schiff base ligands, N,N′-ethylenebis(acetylacetoneimine) and N,N′-ethylenebis(salicylaldimine) is reported on a column of 10-μm diameter silica. Both pairs of chelates are well resolved with good peak shape and efficiencies when the mobile phase is 4 : 1 methylene chloride—acetonitrile. The u.v. detector response at 254 nm is linear over approximately three orders of magnitude of quantity of chelate injected; the detection limits are in the low nanogram range. Qualitative and quantitative elution of undegraded chelates was demonstrated by u.v. spectrophotometry, mass spectrometry and electron spin resonance spectroscopy.

REFERENCES

1 H. Veening, J. Chem. Educ., 50 (1973) 9,A429; 10,A481; 11,A529.
2 J.J. Kirkland (Ed.), Modern Practice of Liquid Chromatography, Wiley-Interscience, New York, 1971.
3 L.R. Snyder and J.J. Kirkland, Introduction to Modern Liquid Chromatography, Wiley-Interscience, New York, 1974.
4 P.R. Brown, High Pressure Liquid Chromatography, Biochemical and Biomedical Applications, Academic Press, New York, 1973.
5 F. Baumann *et al.* (Eds.), Basic Liquid Chromatography, Varian Aerograph, Walnut Creek, Calif., 1971.
6 J. Michal, Inorganic Chromatographic Analysis, Van Nostrand Reinhold Company, New York, 1973.
7 J.F.K. Huber, J.C. Kraak and H. Veening, Anal. Chem., 44 (1972) 1554.
8 P. Heizmann and K. Ballschmiter, Z. Anal. Chem., 266 (1973) 206.

9 M.D. Seymour and J.S. Fritz, Anal. Chem., 45 (1973) 1632.
10 J.M. Greenwood, H. Veening and B.R. Willeford, J. Organometal. Chem., 38 (1972) 345.
11 R.E. Graf and C.P. Lillya, J. Organometal. Chem., 47 (1973) 413.
12 W.J. Evans and M.F. Hawthorne, J. Chromatogr., 88 (1974) 187.
13 R. Belcher, K Blessel, T. Cardwell, M. Pravica, W.I. Stephen and P.C. Uden, J. Inorg. Nucl. Chem., 35 (1973) 1127.
14 R. Belcher, D.E. Henderson, A. Kamalizad, R.J. Martin, W.I. Stephen and P.C. Uden, Anal. Chem., 45 (1973) 1197.
15 G.O. Carlisle and W.E. Hatfield, Inorg. Nucl. Chem. Lett., 6 (1970) 633.
16 P.C. Uden, D.E. Henderson and A. Kamalizad, J. Chromatogr., Sci., 12 (1974) 591.
17 P.C. Uden and D.E. Henderson, J. Chromatogr., 99 (1974) 309.
18 K. Ueno and A.E. Martell, J. Phys. Chem., 61 (1957) 257.
19 S.M. Crawford, Spectrochim. Acta, 19 (1963) 255.

Analytica Chimica Acta, 79 (1975) 185—197

STRUCTURAL ANALYSIS OF THE GUM POLYSACCHARIDE FROM *ANACARDIUM OCCIDENTALE**

D.M.W. ANDERSON and P.C. BELL
Department of Chemistry, The University, Edinburgh EH9 3JJ (Scotland)
(Received 3rd March 1975)

Plant gum exudates are the most complex acidic heteropolysaccharides known, and investigations of their composition and structure present a formidable challenge. Some fifty different plant gums from a variety of botanical genera have now been studied; although xylose and mannose have been found in a few cases, galactose, arabinose, rhamnose, galacturonic acid, and glucuronic acid and/or its 4-O-methyl ether are the sugars that are almost always involved.

Recently, *Anacardium occidentale* (the cashew-nut tree) was found [2] to contain glucose. In addition, a previous study [3] of this gum was found to be incorrect: the major uronic acid present is glucuronic acid [2], not galacturonic acid [3]. Although very little is known about exudates from taxa within *Anacardiaceae*, the exudate from *Anacardium occidentale* has recently become of considerable industrial interest, and the need arose for the structural location of the glucose in the complex molecule to be identified. The analyses that were carried out for this purpose are reported below.

EXPERIMENTAL

Origin and purification of the gum sample

Gum from *A. occidentale* was collected in October, 1969, by the Forest Department Utilisation Officer, Tamilnadu, Madras. The crude gum was soluble in cold water, and was purified as reported previously [2]; its analytical parameters were very similar to those of a Papuan specimen of the gum [2].

Analytical methods

Standard methods of gum analysis were used [4,5]. Paper chromatography was carried out on Whatman No. 1 paper with the following solvent systems (v/v); (a) benzene, butan-1-ol, pyridine, water (1:5:3:3, upper layer); (b) acetic acid, ethyl acetate, formic acid, water (3:18:1:4); (c) acetic acid, ethyl acetate, formic acid, water (8:18:3:9); (d) butan-1-ol, ethanol, water (4:1:5); (e) ammonia (0.88), butan-2-one, water (1:200:17); (f) butan-1-ol, ethanol, 0.1 *M* hydrochloric acid (1:10:5). Before solvent (f) was used, the paper was

* Part 48 of the series "Studies of Uronic Acid Materials". For Part 47, see ref. 1.

pretreated with 0.3 *M* sodium dihydrogenphosphate solution and allowed to dry. Glucose was detected by the conventional glucose oxidase spray. Unless otherwise stated, methylation of polysaccharides was carried out by the combined Haworth and Purdie procedures [6,7]. G.l.c. of mixtures of O-methyl sugars was carried out with a Pye Argon Chromatograph at argon flow-rates of *ca.* 100 ml min^{-1} on columns (120 × 0.5 cm) of (1) 15 % by weight of poly(ethylene glycol adipate) on 45—60 mesh Gas-Chrom Z at 176 °C and (2) 15 % by weight of poly(butan-1,4-diol succinate) on 80—100 mesh Gas-Chrom P at 176 °C. Retention times (*T*) are quoted relative to that of methyl 2,3,4,6-tetra-O-methyl-β-D-glucopyranoside.

RESULTS

Homogeneity of the gum

Zone electrophoresis of the gum on cellulose acetate film in 0.1 *M* ammonium carbonate buffer (pH 8.9) and 0.1 *M* sodium acetate buffer (pH 4.7), and thin-layer electrophoresis on "Phoroslides" in 0.1 *M* ammonium carbonate buffer and 0.05 *M* sodium borate buffer (pH 9.2) showed one broad distinct band. Ion-exchange chromatography on a DEAE cellulose column (45 × 1.3 cm) with a sodium chloride gradient (0.0—0.5 *M*) in 0.02 *M* acetate buffer gave a single symmetric peak, as did ultracentrifugation at 44 700 r.p.m. Molecular-sieve chromatography on a Bio-gel A5m column showed a small peak at the void volume in addition to a much larger symmetric peak. This small component has been shown [2] to be due to molecular aggregation.

The neutral and acidic components

Purified gum (3 g) was hydrolysed with 0.5 *M* sulphuric acid (150 ml) for 8 h at 100 °C. After cooling, and neutralization with barium carbonate, the solution was deionized with Amberlite IR-120(H^+) resin, concentrated, and fractionated on a column (41 × 2.6 cm) of Duolite A-4 resin in the formate form. Elution with water and then 5 % formic acid yielded the neutral and acidic fractions, respectively.

After concentration to a syrup, the neutral fraction was chromatographed in solvents (a) and (b) against authentic standards. A large amount of galactose was detected along with smaller amounts of arabinose, glucose, and rhamnose. Trace amounts of mannose and xylose were also found.

The acidic fraction was concentrated and, after removal of formic acid by the repeated addition of water followed by concentration to a syrup, paper chromatography was carried out in solvents (b) and (c). Galactose was observed along with two acidic components which had R_{gal} values of 0.28 in solvent (b) and 0.61 in solvent (c) [major component]; and 0.62 in solvent (b) and 0.83 in solvent (c) [minor component]. The acidic components were fractionated on Whatman 3MM papers in solvent (b).

The major component had $[\alpha]_D$ + 20°, which indicated a β-D-linkage. The syrup (8 mg) was hydrolysed with 1 *M* sulphuric acid for 8 h at 100 °C.

Chromatography in solvents (a), (b) and (f) indicated the presence of galactose and glucuronic acid only. The aldobiuronic acid (6 mg) was methylated [8]; g.l.c. of the methanolysate on column (1) indicated the presence of 2,3,4-tri-O-methyl-D-glucuronic acid (*T* 2.59, 2.99), 2,3,5-tri-O-methyl-D-galactose (*T* 4.12, 4.74) and 2,3,4-tri-O-methyl-D-galactose (*T* 6.28). Reduction of the methanolysate with sodium borohydride followed by removal of the methyl glycosides by mild hydrolysis with 0.5 *M* sulphuric acid for 4 h at 100 °C and chromatography in solvent (d) showed 2,3,4-tri-O-methyl-D-galactose (R_G 0.72, red spot), 2,3,5-tri-O-methyl-D-galactose (R_G 0.83, brown/black spot) and 2,3,4-tri-O-methyl-D-glucose (R_G 0.88, red spot). This identified the aldobiuronic acid as 6-O-(β-D-glucopyranosyluronic acid)-D-galactose.

The other aldobiuronic acid was not present in sufficient quantity for complete characterization. It had $[\alpha]_D + 10°$ (*c* 0.7) and was identical chromatographically in solvent (b) (R_{gal} 0.60) and solvent (c) (R_{gal} 0.90) with a specimen of 6-O-(4-O-methyl-β-D-glucopyranosyluronic acid)D-galactose characterized [9] in a previous study.

Preparation of degraded gum A

Purified gum (6.4 g) was hydrolysed with 0.005 *M* sulphuric acid (350 ml) for 96 h at 100 °C. After cooling, neutralization with barium carbonate and filtration, the solution was deionized with Amberlite IR-120(H^+) resin, concentrated, and dialysed against distilled water (1 l) for 24 h. After further dialysis against running tap water for 48 h, degraded gum A was recovered as a pale brown product (3.2 g, 50 %). The dialysate was concentrated and chromatographed in solvents (a) and (b). Galactose, arabinose, rhamnose, and trace amounts of mannose and xylose were detected. A chromatogram developed with glucose oxidase spray gave a negative result. Also present were small amounts of the neutral disaccharide 6-O-β-D-galactopyranosyl-D-galactose [R_{gal} 0.31 in solvent (a); 0.28 in solvent (b)] and trace amounts of 3-O-β-D-galactopyranosyl-D-galactose [R_{gal} 0.50 in solvent (a); 0.46 in solvent (b)]. Arabinose disaccharides (pink spots) were not detected.

Examination of degraded gum A. Degraded gum A had $[\alpha]_D + 29.1°$. An equivalent weight determination allowed the total uronic acid content to be calculated as 8.7 %, of which 2.2 % was 4-O-methylglucuronic acid if all the methoxyl content is located in this acid. Degraded gum A (30 mg) was hydrolysed with 0.5 *M* sulphuric acid for 7.5 h at 100 °C; paper chromatography of the resulting syrup in solvents (a) and (b) indicated the presence of galactose, glucose, and the two aldobiuronic acids identified previously. Mild hydrolysis with 0.25 *M* sulphuric acid for 1 h at 100 °C showed 3-O-β-D-galactopyranosyl-D-galactose to be the only disaccharide present. Degraded gum A (198 mg) was methylated to give a product (120 mg) (found: 40.2 % OMe). Methanolysis of a portion of this, followed by g.l.c. examination, gave the results shown in Table I. Hydrolysis of the methyl glycosides, followed by paper chromatography in solvents (d) and (e), indicated the presence of substantial amounts of 2-O-methyl-D-galactose in addition to the O-methyl sugars already identified as their methyl glycosides by g.l.c.

TABLE I

Examination of methanolysis products from methylated degraded gums A and B

Relative retention time (T) of methyl glycosides		R_G in solvent (e)	O-Methyl sugar identified	Relative amounts	
Column (1)	Column (2)			Degraded gum A	Degraded gum B
1.00, 1.39	1.00, 1.41	0.99	2,3,4,6-Tetra-O-methyl-D-glucose	5	—
1.62	1.72	0.80	2,3,4,6-Tetra-O-methyl-D-galactose	35	13
(2,89), (3.57), (3.89)	(3.03), (3.88), (4.35)	0.56	2,3,6-Tri-O-methyl-D-galactose	1	4
(3.57), (3.89)	(3.88), (4.35)	0.47	2,4,6-Tri-O-methyl-D-galactose	24	70
6.42	6.64	0.41	2,3,4-Tri-O-methyl-D-galactose	6	—
9.24	9.48	0.25	2,6-Di-O-methyl-D-galactose	1	7
14.8, 16.0	15.36, 16.95	0.16	2,4-Di-O-methyl-D-galactose	20	6
2.32, (2.89)	2.42, (3.03)	—	2,3,4-Tri-O-methyl-D-glucuronic acid[a]	8	—

[a] As methyl ester methyl glycoside.

Preparation of degraded gum B by Smith-degradation of degraded gum A

Degraded gum A (1.7 g) was dissolved in water (50 ml) and 0.5 *M* sodium metaperiodate (50 ml) was added. After 72 h in darkness at room temperature, the reaction was stopped by the addition of ethylene glycol (4 ml). (The amounts of periodate reduced and formic acid released are shown in Table III). The solution was dialysed against running tap water for 48 h, sodium borohydride (1 g) was added, and after 30 h at room temperature, the solution was dialysed for a further 48 h and made 0.5 *M* with respect to sulphuric acid, and the polyalcohol was hydrolysed for 48 h at room temperature. After dialysis for 48 h, degraded gum B was isolated as the freeze-dried product (0.6 g, 31 %).

Examination of degraded gum B. Degraded gum B had $[\alpha]_D$ + 38.3°. Hydrolysis with 0.5 *M* and with 1 *M* sulphuric acid showed that galactose was the only sugar present. Partial acid hydrolysis with 0.25 *M* sulphuric acid for 1 h at 100 °C, followed by chromatography in solvent (a), indicated the presence of 3-O-β-D-galactopyranosyl-D-galactose. Degraded gum B (182 mg) was methylated to give a product (139 mg) (found: 40.7 % OMe). After methanolysis of a portion of this product, g.l.c. examination gave the results shown in Table I. Hydrolysis of the mixture of methyl glycosides, followed by paper chromatography in solvents (d) and (e), indicated the presence of 2-O-methyl-D-galactose in addition to the methyl glycosides found from g.l.c. examination.

Partial acid hydrolysis and methylation of A. occidentale gum

Hydrolysis of the gum (100 mg) with 0.25 *M* sulphuric acid (10 ml) for 1 h at 100 °C, followed by paper chromatography in solvent (a), showed the presence of the disaccharides 3-O-β-D-galactopyranosyl-D-galactose (major component) and 6-O-β-D-galactopyranosyl-D-galactose (minor component) together with other higher oligosaccharides. Arabinose-containing disaccharides were not detected. The pure gum (287 mg) was methylated to give a product (178 mg) (found: 42.6 % OMe). After methanolysis of a portion of this, g.l.c. examination gave the methyl glycosides shown in Table II. Hydrolysis of the methyl glycosides, followed by paper chromatography in solvents (d) and (e), also indicated the presence of 2-O-methyl-D-galactose.

Preparation of polysaccharide I

Preliminary small-scale experiments indicated that 0.25 *M* sodium metaperiodate solution and an oxidation time of 72 h were required for *A. occidentale* gum. The gum (40.7 g) was then dissolved in water (1125 ml), 0.50 *M* sodium metaperiodate (1125 ml) was added, and the solution was kept in darkness at room temperature. The oxidation was followed by measuring the release of formic acid with time. After 72 h the amounts of periodate reduced and formic acid released were as shown in Table III. The reaction was stopped by the addition of ethylene glycol (23.9 ml), and the solution was dialysed for 48 h against running tap water. Sodium borohydride (13.3 g) was added, and after 30 h at room temperature, followed by dialysis

TABLE II

Methyl glycosides from methylated *A. occidentale* gum

Relative retention time (T)[a] of methyl glycosides		R_G after hydrolysis		O-Methyl sugar identified	Estimated relative amounts
Column (1)	Column (2)	Solvent (e)	Solvent (f)		
(0.45)	(0.46)	1.02	1.03	2,3,4-Tri-O-methyl-L-rhamnose	(9)
(0.45), (0.54)	(0.46), (0.56)	1.02	1.03	2,3,4-Tri-O-methyl-D-xylose	
(0.99), (1.38)	(1.00), (1.42)	0.99	0.98	2,3,4,6-Tetra-O-methyl-D-glucose	(10)
(1.38)	(1.42)	0.87	0.83	2,3,4,6-Tetra-O-methyl-D-mannose	
(0.54), 0.67	(0.56), 0.71	0.94	1.03	2,3,5-Tri-O-methyl-L-arabinose	(9)
(0.97)	(1.02)	0.80	0.74	2,3,4-Tri-O-methyl-L-arabinose	(4)
1.14, (2.59)	1.18, (2.45)	0.80	0.74	3,5-Di-O-methyl-L-arabinose	(3)
1.91	2.13	0.80	0.74	3,4-Di-O-methyl-L-arabinose	(2)
1.59	1.68	0.87	0.77	2,3,4,6-Tetra-O-methyl-D-galactose	(25)
(2.90), (3.60), (3.90)	(2.98), (3.85), (4.18)	0.75	0.61	2,3,6-Tri-O-methyl-D-galactose	
(3.60), (3.90)	(3.85), (4.18)	0.75	0.43	2,4,6-Tri-O-methyl-D-galactose	(20)
6.45	6.42	0.75	0.37	2,3,4-Tri-O-methyl-D-galactose	(3)
9.43	9.48	0.55	0.20	2,6-Di-O-methyl-D-galactose	
15.5, 16.4	15.36, 16.95	0.49	0.13	2,4-Di-O-methyl-D-galactose	(10)
(2.59), (2.90)	(2.45), (2.98)	—	—	2,3,4-Tri-O-methyl-D-glucuronic acid[b]	(7)

[a] Figures in parenthesis indicate T values of components which are not completely resolved.
[b] As methyl ester methyl glycoside.

TABLE III

Data for *Anacardium occidentale* gum and its degradation products

Polysaccharide	Yield (%)	$[\alpha]_D$ (degrees)	Constituent sugars (%)						Uronic acid	Periodate reduced (mmol g^{-1})	Formic acid released (mmol g^{-1})
			Gal	Ara	Rha	Glu	Man	Xyl			
A. occidentale gum	54	+24.6	61	14	7	8	2	2	6.2	9.79	3.89
Degraded gum A	49	+29.1	84	Trace	—	7	—	—	8.7	13.2	6.14
Degraded gum B	31	+38.3	100	—	—	—	—	—	—	N.d.	N.d.
Polysaccharide I	29	+41.6	76	22	—	—	—	—	1.8	2.50	2.32
Polysaccharide II	77	+39.9	90	10	—	—	—	—	—	1.46	1.25
Polysaccharide III	53	+35.2	97	3	—	—	—	—	—	1.30	1.58
Polysaccharide IV	48	+38.1	100	Trace	—	—	—	—	—	2.01	0.98
Polysaccharide V	8	N.d.	100	—	—	—	—	—	—	N.d.	N.d.

N.d., not done.

for a further 48 h, the solution was made 0.5 *M* with respect to sulphuric acid. After hydrolysis of the polyalcohol for 48 h at room temperature, followed by dialysis for a further 48 h, polysaccharide I was obtained as the freeze-dried product (11.6 g, 28.5 %).

Examination of polysaccharide I. Polysaccharide I had $[\alpha]_D$ + 41.6° and $\bar{M}_w$ = 38,800 (light scattering, SOFICA 42000 photogoniodiffusometer). Polysaccharide I (50 mg) was hydrolysed with 0.5 *M* sulphuric acid for 7.5 h at 100 °C. Paper chromatography of the hydrolysate in solvents (a) and (b) indicated the presence of galactose (major component) and arabinose. Glucose was not present, but hydrolysis with 1 *M* sulphuric acid, followed by chromatography, showed that a small amount of glucuronic acid was present. Partial acid hydrolysis (0.25 *M* sulphuric acid for 1 h at 100 °C) showed 3-O-β-D-galactopyranosyl-D-galactose to be present in large amounts. Polysaccharide I (270 mg) was methylated to give a product (153 mg) (found: 40.8 % OMe). Methanolysis of a portion of this, followed by g.l.c. examination of the mixture of methyl glycosides, gave the results shown in Table IV. Hydrolysis of the methyl glycosides, followed by paper chromatography in solvents (d) and (e), indicated the presence of small amounts of 2-O-methyl-D-galactose in addition to those methyl glycosides already identified.

TABLE IV

Methylation data and relative molar proportions of O-methyl sugars present in methylated polysaccharides I—V

	Polysaccharides				
	I	II	III	IV	V
Methylation data					
Weight of polysaccharide used (mg)	270	208	253	110	30
Weight of product (mg)	153	130	152	59	n.i.[a]
$[\alpha]_D$ of product (degrees)	−1.8	−8.2	−8.2	−8.9	—
OMe of product (%)	40.8	42.8	41.6	41.4	—
O-Methyl sugars identified					
2,3,5-Tri-O-methyl-L-arabinose	12	6	2	1	—
2,3,4-Tri-O-methyl-L-arabinose	Trace	—	—	—	—
3,5-Di-O-methyl-L-arabinose	11	5	1	—	—
3,4-Di-O-methyl-L-arabinose	2	—	—	—	—
2,3,4,6-Tetra-O-methyl-D-galactose	17	16	14	14	12
2,3,6-Tri-O-methyl-D-galactose	4	2	2	2	3
2,4,6-Tri-O-methyl-D-galactose	37	52	66	73	77
2,3,4-Tri-O-methyl-D-galactose	4	Trace	—	—	—
2,6-Di-O-methyl-D-galactose	3	13	13	10	8
2,4-Di-O-methyl-D-galactose	8	5	3	Trace	Trace
2,3,4-Tri-O-methyl-D-glucuronic acid	4	—	—	—	—

[a] Not isolated.

Preparation of polysaccharides II—V by sequential Smith-degradations

The following weights of polysaccharides, in a sequence of Smith-degradations, were oxidized with 0.125 *M* sodium periodate, reduced with borohydride and hydrolysed with sulphuric acid, and the corresponding products were recovered, all as described previously for polysaccharide I. Polysaccharide I (9.2 g) gave polysaccharide II (7.8 g); polysaccharide II (4.6 g) gave polysaccharide III (2.8 g); polysaccharide III (2.2 g) gave polysaccharide IV (1.03 g); polysaccharide IV (494 mg) gave polysaccharide V (48 mg). The percentage yields and analytical data for polysaccharides II—V are shown in Table III.

Examination of polysaccharides II—V. Hydrolysis of polysaccharide II with 0.5 *M* and with 1 *M* sulphuric acid for 7.5 h at 100 °C showed galactose and arabinose only, with galactose the major component. Polysaccharides III and IV contained progressively less arabinose; polysaccharide V was a galactan. Partial acid hydrolysis (0.25 *M* sulphuric acid for 1 h at 100 °C) of polysaccharides II—V indicated the presence in each of large amounts of 3-O-β-D-galactopyranosyl-D-galactose. All the Smith-degradation products were methylated in the normal way; data for the products are shown in Table IV. Portions of each product were methanolysed and examined by g.l.c. The methyl glycosides found, together with their relative amounts, are shown in Table IV. Hydrolysis of the methyl glycosides, followed by chromatography in solvents (d) and (e), indicated the presence of 2-O-methyl-D-galactose in addition to the other methyl glycosides identified by g.l.c.

DISCUSSION

Purified gum from *Anacardium occidentale* was examined by zone electrophoresis, thin-layer electrophoresis, ion-exchange chromatography and ultracentrifugation; each of these experiments indicated a one-component system. Molecular-sieve chromatography on a Bio-gel A5 m column showed a small peak at the void volume in addition to a large symmetric peak at a greater elution volume; the small peak was found to be a time-dependent molecular self-aggregation as has been found [10] in molecular-sieve experiments with *Acacia* gums. *A. occidentale* gum therefore behaves as a homogeneous system similar to that of many *Acacia* gum exudates [11—13] and the gum from *Lannea humilis* [9].

Galactose is the major sugar present in the gum. Substantial amounts of arabinose, rhamnose, glucose, and uronic acid are also present, with trace amounts of mannose and xylose. The two aldobiuronic acids present are 6-O-(β-D-glucopyranosyluronic acid)-D-galactose and its 4-O-methyl analogue.

Mild acid hydrolysis of the gum gave degraded gum A together with major amounts of galactose, arabinose, and rhamnose, and trace amounts of mannose and xylose. Also liberated were the disaccharides 6-O-β-D-galactopyranosyl-D-galactose and 3-O-β-D-galactopyranosyl-D-galactose; the former was by far the major component. Glucose was not released. Degraded gum A contained galactose, glucose, and uronic acid only. Partial acid hydrolysis of degraded

gum A showed the presence of only 1,3-linked galactobiose residues; all the 1,6-galactobiose residues present in the gum had therefore been removed by mild treatment with acid. Methylated degraded gum A on methanolysis and hydrolysis indicated the presence of end-group galactose (large amount), glucose, and glucuronic acid in addition to 2,4,6-, and 2,3,4-tri-, and 2,4-di-O-methyl-D-galactose. The 2,3,6-tri-, 2,6-di-, and 2-O-methyl-D-galactose may have arisen through incomplete methylation.

Periodate oxidation of degraded gum A gave degraded gum B, which was a galactan. Methanolysis and hydrolysis of degraded gum B indicated the presen of 2,4,6-tri-O-methyl-D-galactose and 2,3,4,6-tetra-O-methyl-D-galactose as th major components; as for degraded gum A, 2,3,6-tri-, 2,6-di-, and 2-O-methyl-D-galactose may have arisen through incomplete methylation. Degraded gum I therefore contains chains of 1,3-linked galactose residues, linked 1,6- to each other.

Attempts to determine the molecular weights, $\bar{M}_n$, of degraded gums A and B by end-group analysis [14] gave low results. End-group analysis is based on the assumption that each reducing end-group produces one molecule of formaldehyde. Since extensive fragmentation of the gum occurred during mild acid hydrolysis, fragments too large to be removed by dialysis may have formed, as suggested by the large consumption of periodate during oxidation of degraded gum A. More than one reducing end-group would therefore be present to yield formaldehyde, hence indicating low values of $\bar{M}_n$. This effect has been found previously during mild acid hydrolysis of *Acacia* gums [12,13]

Anacardium occidentale gum, on partial acid hydrolysis, showed only two galactobioses. Arabinobioses and galactoarabinobioses were not detectable, implying that arabinose residues and chains are not bound strongly to the main gum structure. Methylation of the gum showed that rhamnose, xylose, mannose, glucose, arabinofuranose, arabinopyranose, galactose and glucuronic acid were present as end-groups. To accommodate such a large proportion of end-groups, the gum must have a very highly branched structure. This is consistent with the very low viscosity (6.3 ml g^{-1}) found for a polymer of $\bar{M}_w$ 260,000.

Anacardium occidentale gum was subjected to five successive Smith-degradations, giving polysaccharides I—V. The first degradation was drastic, as indicated by the large amount of periodate reduced and the low yield obtained; all the xylose, mannose, glucose and rhamnose, together with considerable amounts of galactose, arabinose and glucuronic acid, were removed. The presence of 2,3,4-tri-O-methyl-D-glucuronic acid in the methylated polysaccharide from *A. occidentale* gum indicated that all glucuronic acid residues should be removed during the first degradation, but a small amount of glucuronic acid was found in polysaccharide I; this is attributed to incomplete oxidation through steric hindrance. Since all 1,6-linked galactose residue were removed in the first Smith-degradation, such units may be present as end groups.

Five Smith-degradations were required to remove all the arabinose, but the small amounts of 2,3,5-tri- and 3,5-di-O-methyl-L-arabinose in polysaccharide III, and the trace amount of 2,3,5-tri-O-methyl-L-arabinose in polysaccharide IV, indicate that the number of chains containing five arabinose units is small.

The fact that only 3,4- and 3,5-di-O-methyl-L-arabinose were found in the methanolysates of the gum and its degradation products indicates that the arabinose chains contained 1,2-linkages, in contrast to arabinose side-chains in the *Acacia* genus, which are 1,3-linked and apparently more resistant to mild acid hydrolysis, since arabinobioses are observed in partial acid hydrolysates of *Acacia* gums and in dialysates from the corresponding degradation products.

The values of $[\alpha]_D$ for polysaccharides I—IV were almost identical. This indicates that, after the first Smith-degradation, the basic structure of the gum remained virtually unchanged. *Anacardium occidentale* gum therefore has a highly branched structure similar in degree of branching to that of group I *Acacia* exudates [16].

The structural information obtained therefore indicates a highly branched galactan framework in which β-1,3-linkages are closely interspersed with β-1,6-branch points. With such a closely branched structure it appears reasonable to postulate that incomplete methylation of 2,4-di-O-methyl-D-galactose would occur, resulting in the formation of the 2-O-methyl-D-galactose observed.

A possible structural fragment of *Anacardium occidentale* gum is shown in Fig.1, although it must be emphasized that this is not intended to represent any repeating structural unit within the molecule. The structure consists of a branched galactan core with β-1,3 and β-1,6 linkages; the ends of these galactose chains are terminated by rhamnose, glucose, glucuronic acid, arabinose, short arabinose chains of not more than 5 units, or galactose itself. All the glucuronic acid is linked to C_6 of galactose residues. The mode of attachment of glucose and rhamnose is unknown. Because 2,3-di-O-methyl-D-glucuronic acid was not found in the methylated gum, rhamnose cannot be joined [17] to the 4-position of glucuronic acid, as occurs [11—13] commonly in *Acacia* gum exudates.

We thank Rowntree-Mackintosh Ltd. (York) and Laing-National Ltd. (Manchester) for financial support, and Mr T.P. Baskaradoss, Utilisation Officer, Forest Department, Tamilnadu, for supplying the specimen of gum.

SUMMARY

The gum exudate from *Anacardium occidentale* contains galactose (61 %), arabinose (14 %), rhamnose (7 %), glucose (8 %) and glucuronic acid (5 %) in addition to small amounts (<2 %) of each of mannose, xylose and 4-O-methylglucuronic acid. Contrary to earlier findings, the main aldobiuronic acid present is 6-O-(β-D-glucopyranosyluronic acid)-D-galactose; smaller amounts of the 4-O-methyl analogue are also present. Mild acid hydrolysis showed only two galactobioses, 3-O-β-D-galactopyranosyl-D-galactose (major

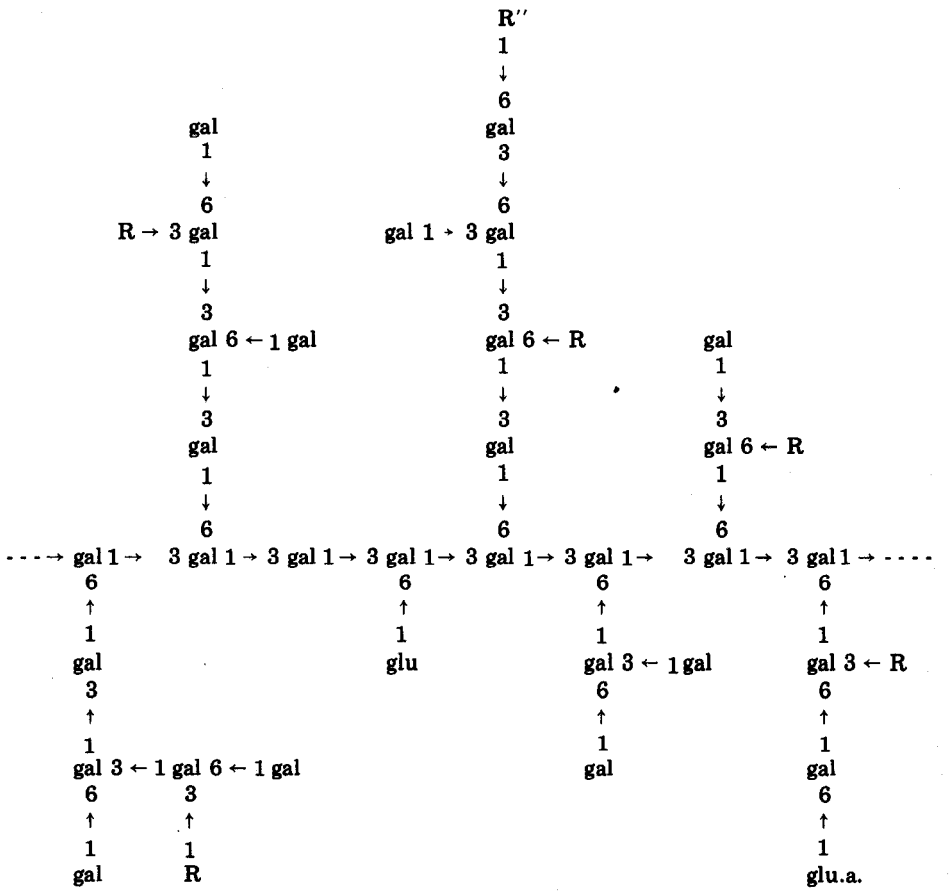

Fig.1. A possible structural fragment from *A. occidentale* gum. *R* represents D-mannose, D-xylose, L-rhamnose, L-arabinose or 1,2-linked arabinose chains. *R''* represents D-glucose or D-glucuronic acid.

component) and 6-O-β-D-galactopyranosyl-D-galactose (minor component). Degraded gum A, prepared by controlled acid hydrolysis, contained galactose, glucose, and uronic acid. A Smith-degradation of degraded gum A gave degraded gum B, which contained only galactose. Sequential Smith-degradations of *Anacardium occidentale* gum, and methylation analyses of the gum and of its degradation products indicated a highly-branched galactan framework consisting of chains of β-(1—3)-linked D-galactose residues branched and interspersed with β-(1—6) linkages. Arabinose is present as end-groups or in short (1—2)-linked chains up to five units long. Glucose, rhamnose, mannose xylose, and uronic acid are all present as end-groups.

REFERENCES

1 D.M.W. Anderson and M.C.L. Gill, Phytochemistry, 14 (1975) 739 (Part 47).
2 D.M.W. Anderson, P.C. Bell and J.R.A. Millar, Phytochemistry, 13 (1974) 2189.
3 M. Biswas and S. Bose, Indian J. Biochem., 7 (1970) 68.
4 D.M.W. Anderson and J.F. Stoddart, Carbohyd. Res., 2 (1966) 104.
5 D.M.W. Anderson and A.C. Munro, Carbohyd. Res., 11 (1969) 43.
6 W.N. Haworth, J. Chem. Soc., London, 107 (1915) 8.
7 T. Purdie and J.C. Irvine, J. Chem. Soc., London, 83 (1903) 1021.
8 R. Kuhn, I. Löw and H. Trischmann, Angew. Chem., 67 (1955) 32.
9 D.M.W. Anderson and A. Hendrie, Carbohyd. Res., 22 (1972) 265.
10 D.M.W. Anderson, A. Hendrie and A.C. Munro, Carbohyd. Res., 9 (1969) 363.
11 D.M.W. Anderson, E.L. Hirst and J.F. Stoddart, J. Chem. Soc. C, (1966) 1959.
12 D.M.W. Anderson, I.C.M. Dea and R.N. Smith, Carbohyd. Res., 7 (1968) 320.
13 D.M.W. Anderson and A.C. Munro, Carbohyd. Res., 12 (1970) 9.
14 W.D. Annan, E.L. Hirst and D.J. Manners, J. Chem. Soc., London, (1965) 220.
15 H. Klostermann and F. Smith, J. Amer. Chem. Soc., 74 (1952) 5336.
16 D.M.W. Anderson and P.C. Bell, to be published.
17 G.O. Aspinall, A.J. Charlson, E.L. Hirst and R. Young, J. Chem. Soc., London, (1963) 1696.

Analytica Chimica Acta, 79 (1975) 199—206

QUANTITATIVE MEASUREMENTS OF INORGANIC AND METHYL ARSENICALS BY GAS-LIQUID CHROMATOGRAPHY

E. HUNTER DAUGHTREY, JR., ARTHUR W. FITCHETT and PAUL MUSHAK*

Department of Pathology, University of North Carolina at Chapel Hill, Chapel Hill, North Carolina 27514 (U.S.A.)

(Received 17th February 1975)

At present, most analytical procedures employed to assess arsenic levels routinely in various media involve total arsenic measurement, without regard to the specific chemical form(s) of arsenic present. Recent reports in the literature, however, point to the advisability, in at least certain cases, of assessing arsenic in its various forms, particularly as the methylated derivatives. Arsenic has been shown to undergo microbial methylation to various stages, including the generation of trimethylarsine [1—3]. Furthermore, Braman and Foreback [4] have reported that methyl arsenicals are excreted in selected human subjects and appear in various environmental samples; their method involves [4] the selective and sequential generation of these arsenicals as the volatile hydrides, which are trapped in liquid nitrogen-cooled vessels and analysed by atomic absorption spectrometry.

This paper presents a straightforward gas—liquid chromatographic procedure for the measurement of inorganic and methylated arsenic as the diethyldithiocarbamate complexes.

EXPERIMENTAL

Apparatus

A Hewlett-Packard Model 5755B gas-liquid chromatograph, and a Glowall Model 320 dual-oven instrument equipped with electron-capture detection (^{3}H foil) and glass-coil columns. were used.

The column packing consisted of 5 % OV-17 on 80/90 mesh Anakrom AS (Analabs, Inc. North Haven, Conn.) prepared with a fluidizing apparatus (Applied Science Laboratories, State College, Pa.). Columns were exhaustively silanized with an ether solution (3 %) of DMCS at the outset, and were so maintained periodically (weekly or bi-weekly) to ensure high performance. The carrier gas was a 95 : 5 mixture of argon/methane. Chromatographic conditions were as follows: for inorganic arsenic diethyldithiocarbamate, column

*To whom correspondence should be directed.

170 °C, injector port 200 °C, detector 190 °C; for monomethylarsenic diethyldithiocarbamate, column 110 °C, injector port and detector as above; for dimethylarsenic diethyldithiocarbamate, column 80 °C, injector port and detector as above.

Synthesis of arsenic standards

Pure samples of the diethyldithiocarbamate derivatives of inorganic, mono- and dimethylarsenic were prepared via reactions of the corresponding iodides (arsenic triiodide and diiodomethylarsine, Ventron-Alfa Inorganics, Beverly, Mass.) and cacodyl iodide (prepared as described by van der Kelen [5]) with diethylammonium diethyldithiocarbamate. Acetonic solutions of the iodides, in the appropriate stoichiometric ratio, were added to acetonic solutions of the ligand and heated for several hours. Water was added to precipitate the crude solids (inorganic or monomethylarsenic derivatives) or the crude oil (dimethylarsenic). Purification of the former two products was achieved by recrystallization from hot benzene; dimethylarsenic was taken up in hexane and manipulated carefully in a dry ice—acetone bath. Thin-layer chromatography was employed to ascertain homogeneity. Tris(diethyldithiocarbamato)arsenic, m.p. 140 °C, lit. [6], 135 °C; bis(diethyldithiocarbamato)methylarsenic, m.p. 105 °C, lit. [6] 102 °C; (diethyldithiocarbamato)dimethylarsenic, m.p. 40 °C, lit. [6] 45 °C.

Reagents and glassware

A.C.S.-certified reagents were employed. Pesticide-grade solvents, benzene and hexane, and reagent-grade toluene served as extraction solvents.

Glassware included glass screw-cap 2-dram vials which were prepared for first-time use and routine use by cleaning procedures described elsewhere [7] as well as 25-ml specimen tubes which were worked up similarly for analytical use.

Analytical procedures

Inorganic arsenic in water and urine. Transfer samples of water or urine (5.0 ml) to acid-washed specimen tubes (*vide supra*), the necks of which are wrapped with several turns of teflon tape to preclude leakage on sealing and warming. Add concentrated hydrochloric acid (10.0 ml), mix gently and warm the vessels for *ca.* 1 h in a water bath at 60—70 °C. Cool and add 1.0 ml of saturated potassium iodide (1.0 g ml^{-1}) solution; after mixing keep the tubes at room temperature for 10 min. After adding toluene (5.0 ml) seal the vessels and agitate with a Vortex-Genie apparatus for 1 min at maximum speed. Centrifuge at 2000 r.p.m. for 5 min and remove to a 2-dram acid-washed vial containing 1.0 ml of a freshly-prepared buffered diethyldithiocarbamate solution (0.1 g of diethylammonium diethyldithiocarbamate dissolved in 10.0 ml

of 0.05 *M* potassium hydrogenphthalate buffer, pH 4). Agitate for 1 min, allow to stand for 5 min, and then centrifuge at 3000 r.p.m. for 5 min. Open the vessels, and transfer a portion of the organic layer to a second vial containing anhydrous sodium sulfate for drying. Introduce an aliquot (5 μl) into the gas chromatograph. Handle reagent blanks and external standard samples similarly.

For quantitative purposes, the level of arsenic per ml of toluene is in a 1 : 1 ratio to that of the original water or urine sample and is then related to the water or urine standards containing arsenic.

Methylated arsenicals in water or urine. To 2.0 ml of water or urine in acid-washed 2-dram vials add concentrated sulfuric acid (0.2 ml), seal and warm at 60—70 °C for *ca.* 1 h. Wrap the vessel necks with teflon tape to ensure sealing. Cool, and add potassium iodide solution (0.5 ml) and 5 % sodium metabisulfite solution (0.2 ml). Agitate the samples briefly by hand and set aside for 1 min; then add 0.1 ml of an aqueous 2 % solution of diethylammonium diethyldithiocarbamate (freshly prepared). For the analysis of monomethylarsenic, add benzene (2.0 ml); use 2.0 ml of hexane for dimethylarsenic analysis. Agitate the vessels with a Vortex-Genie mixer for 1 min, centrifuge at 3000 r.p.m. for several minutes, and remove portions for drying over sodium sulfate. Introduce aliquots (3 μl) into the gas chromatograph. For quantitative work, proceed as described for inorganic arsenic, the arsenic content of benzene or hexane also being in a 1 : 1 ratio to the sample level.

RESULTS AND DISCUSSION

Thermal conductivity and flame-ionization detectors were used by Gudzinowicz and Martin [8] to investigate the chromatographic behavior of arsenic(III) bromide and some organic derivatives of arsenic, but analytical applications were not described. Arsenate and arsenite, as the trimethylsilyl (TMS) derivatives, were chromatographed by Butts and Rainey [9]. The hydrolytic instability of these derivatives largely precludes any direct assay scheme for arsenic. Inorganic arsenic was assessed in soft tissue by Schwedt and Ruessel [10] by extraction of arsenic as the diethyldithiocarbamate complex, followed by arylation with phenyl Grignard reagent and g.l.c. analysis of the resulting triphenylarsine with a flame-ionization detector. Determination of dimethylarsenic, as cacodyl iodide, was recently noted by Soderquist *et al.* [11]; this iodide is highly labile, requiring rapid sample work-up and chromatography.

In addition to the marked chemical stability of the diethyldithiocarbamate complexes of inorganic arsenic and various organoarsenicals, this group of arsenic complexes was evaluated since the dithiocarbamate moiety should also be amenable to sensitive electron-capture detectors. Consideration of the literature dealing with the comparative stability of various sub-classes of dithiocarbamates indicated that the diethyl analogs led to arsenical complexes of high stability [12]; this ligand was therefore studied exclusively.

Preliminary g.l.c. studies of pure samples of inorganic, mono- and dimethylarsenic diethyldithiocarbamates led to the choice of a 5 % loading of OV-17 on Anakrom AS as column material. An interesting feature of the chromatographic behavior of these complexes is the necessity for extensive silanization of the packing and column wall to permit satisfactory results. Unsilanized or lightly silanized packing did not permit the elution of any inorganic arsenic material, and high temperatures and high sample concentrations of the methylated arsenic complexes were necessary for the elution of the latter. This may account in part for the surprising paucity of data relating to g.l.c. studies of various classes of dithiocarbamate complexes; exhaustive silanizing at the outset and periodic treatment, weekly or biweekly as necessary, is required for satisfactory handling of the arsenicals.

The trapping of effluents from the column to which the various complexes were applied and subsequent analysis for arsenic via flameless atomic absorption spectrometry indicated that arsenic-containing species were being eluted, although no effort was made to characterize their chemical nature by mass spectrometric or other means.

The inorganic arsenic derivative has a considerably higher detection limit (73 ng ml^{-1}) than the methylated derivatives; the dimethyl derivative has a corresponding value (15 ng ml^{-1}) lower than that of monomethylarsenic (40 ng ml^{-1}). This trend is in the opposite direction to that predicted on the basis of the number of dithiocarbamate moieties, and reflects the extent of adsorption and/or decomposition on the column. This is supported by the observation that the amount of arsenic-containing eluates trapped from the columns is least, relative to the levels applied, for inorganic arsenic.

The comparatively low elution temperature of dimethylarsenic on highly-silanized columns creates peak-overlap problems with a number of solvents, including chromatographic-grade benzene. This has necessitated the use of hexane, for which overlap is not a problem, but this complicates the possibility of a common solvent extraction step for the assessment of mixed arsenicals in media, as will be noted below.

Solutions of the various arsenic complexes, even at low concentrations, appeared to be stable for considerable periods of time. Take-up on the walls of transfer vessels, however, appears to occur with the dimethyl derivative and it is necessary to avoid the use of glass pipettes in making up sub-p.p.m. solutions a more concentrated stock solution, and Hamilton micro syringes of 10—25 μl capacity, should be used.

The evolution of procedures for the determination of inorganic, mono- and dimethylarsenic in water and urine by g.l.c. was studied. The assessment of inorganic arsenic was found to require a procedure somewhat different from that for the methylated derivatives; sample treatments were necessary to liberate arsenic in a form suitable for reaction with diethyldithiocarbamate and ready extractability. When hydrochloric acid and iodide were used to generate arsenic(III) iodide, optimal results were obtained with 5 ml of water or urine to 10 ml of concentrated hydrochloric acid. Sample manipulation in-

volved mild warming of the samples with hydrochloric acid to assist the liberation of any arsenic, by hydrolysis, bound to biomolecules present in urine. The iodide solution, serving to reduce arsenate to arsenite and to generate arsenic triiodide, is introduced after warming; prior addition leads to extensive formation of iodine. Since the reaction vessels are sealed on warming, loss of volatile arsenic trihalide is minimized.

The chelating agent decomposes rapidly on exposure to the acidic medium, necessitating a study of the optimal concentration of reagent and time of exposure. When chelation-extraction of inorganic arsenic was attempted directly from the acidified medium, recovery of 60—70 % of the added arsenic was achieved. A marked improvement was brought about by the initial isolation of arsenic as the triiodide in toluene, followed by agitation with a volume of buffered (pH 4.0) diethyldithiocarbamate solution; recoveries in excess of 80 % were repeatedly observed (Table I).

Problems of recovery are not encountered with mono- and dimethylarsenic when a simplified version of the procedure developed for inorganic arsenic is used. The warming step is retained but the volume of sample is reduced to several ml and a small volume of sulfuric acid (0.2 ml) is used, thus permitting the use of 2-dram vials as reaction vessels. Cleavage of arsenic—carbon bonds did not create any problems, which is to be expected from the known stability of this linkage [4].

Benzene is used as the extracting solvent for monomethylarsenic, since hexane is inferior in extraction efficiency, but hexane is employed with dimethylarsenic to avoid solvent overlap problems. Furthermore, the procedure for inorganic arsenic, as described for simultaneous removal of all three arsenicals as the iodides into toluene, cannot be used because of the interfering peak and solvent overlap problems for mono- and dimethylarsenic respectively.

Figure 1 shows chromatograms for a typical analysis of inorganic arsenic in

TABLE I

Recovery and precision data for various arsenicals in water and urine

Medium	Arsenical amount taken	(p.p.m.)	No. of samples	Recovery (%)	s_r
Urine	Inorganic	1.0	7	82.6	7.5
Urine	Inorganic	2.0	5	91.0	7.7
Urine	Monomethyl [a]	0.5	5	81.6	4.2
Urine	Monomethyl	2.0	5	93.6	3.8
Water	Monomethyl	0.5	5	91.5	7.0
Water	Monomethyl	1.0	6	99.7	3.0
Urine	Dimethyl [b]	0.5	6	103.9	4.0
Water	Dimethyl	0.5	6	101.4	2.4

[a] Diiodomethylarsine added.
[b] Cacodylic acid added.

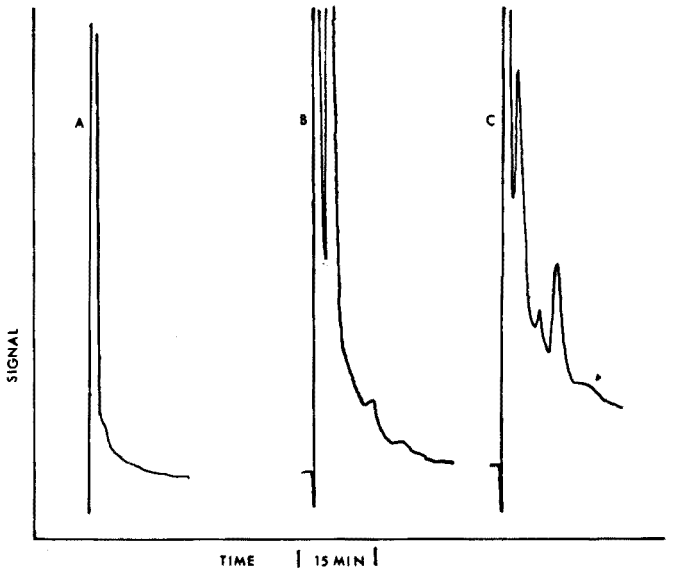

Fig.1. Chromatograms of (A) urine sample, carried through procedure without added inorganic arsenic; (B) Tris(diethyldithiocarbamato)arsenic in toluene; (C) urine sample carried through procedure with added inorganic arsenic (2.0 p.p.m.).

urine; corresponding data are given in Figs.2 and 3 for mono- and dimethylarsenic.

Working standard curves were linear over the range of arsenical levels covered (up to 2.0 p.p.m.) in both water and urine.

The recovery and precision data are given for all three arsenicals in Table I at several selected levels of arsenic addition. Recovery is essentially quantitative for dimethylarsenic in water and urine as well as for monomethylarsenic in water.

Generous support of this study by the National Institutes of Health, Grant No. ES-00481, and partial support by the National Institutes of Health, Training Grant No. GM-92, is gratefully acknowledged.

SUMMARY

Procedures are described for determinations of inorganic and methylated arsenicals in urine and water by gas—liquid chromatography of the corresponding diethyldithiocarbamate complexes. Silanized 5 % OV-17 on Anakrom AS as packing is used in an instrument equipped with electron-capture detection (^{3}H foil). Samples of water or urine are treated to generate the iodides of inorganic, mono- and dimethylarsenic and these are treated with diethyldithiocarbamate, followed by isolation into various organic solvents. Recovery and precision s_r data for the analysis of the arsenicals in urine include: inorganic (1.0 p.p.m.), 82.6 %, ± 7.7; monomethylarsenic (0.5 p.p.m.), 91.5 %, ± 7.0; dimethylarsenic (0.5 p.p.m.), quantitative, ± 4.0.

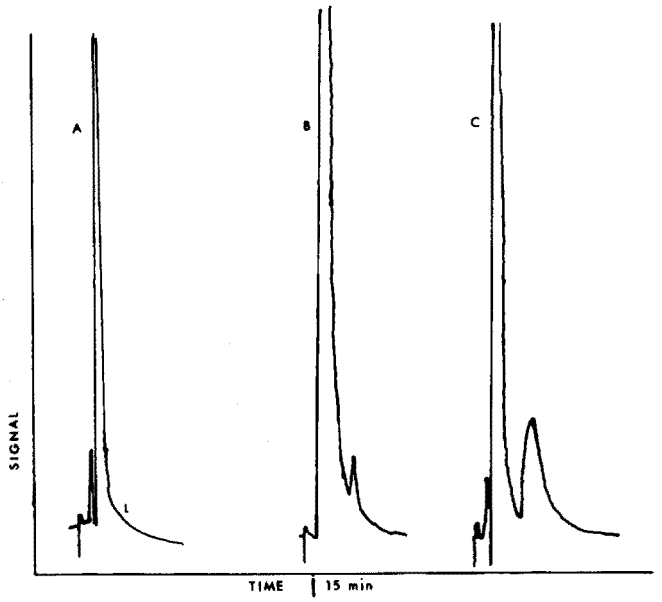

Fig.2. Chromatograms of: (A) urine sample, carried through procedure without added monomethylarsenic; (B) Bis(diethyldithiocarbamato)methylarsenic in benzene; (C) urine sample carried through procedure with added monomethylarsenic (0.5 p.p.m.).

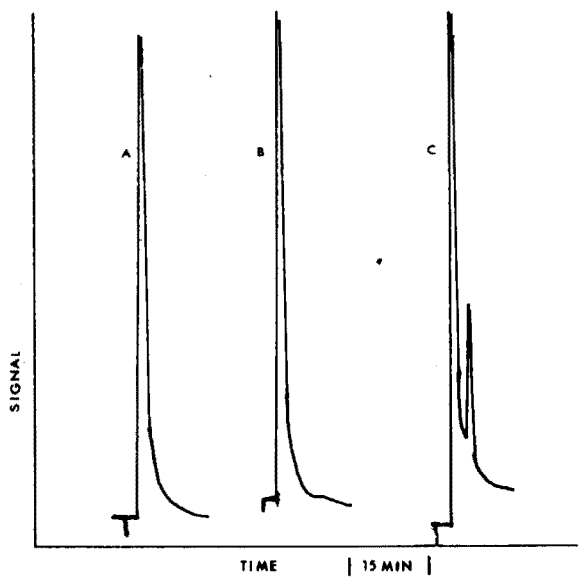

Fig.3. Chromatograms of: (A) urine sample, carried through procedure without added dimethylarsenic; (B) (Diethyldithiocarbamato)dimethylarsenic in hexane; (C) urine sample with added dimethylarsenic (0.5 p.p.m.).

REFERENCES

1 F. Challenger, Chem. Rev., 36 (1945) 315.
2 B.C. McBride and R.S. Wolfe, Biochemistry, 10 (1971) 4312.
3 D.P. Cox and M. Alexander, Appl. Microbiol., 25 (1973) 408.
4 R.S. Braman and C.C. Foreback, Science, 182 (1973) 1247.
5 G.P. van der Kelen, Bull. Soc. Chim. Belg., 65 (1956) 343.
6 L. Bourgeois and J. Bolle, Mem. Serv. Chim. Etat., 34 (1948) 411.
7 P. Zarnegar and P. Mushak, Anal. Chim. Acta, 69 (1974) 389.
8 B.T. Gudzinowicz and H.F. Martin, Anal. Chem., 34 (1962) 648.
9 W.C. Butts and W.T. Rainey, Anal. Chem., 43 (1971) 538.
10 G. Schwedt and H.A. Ruessel, Chromatographia, 5 (1972) 242.
11 C.J. Soderquist, D.G. Crosby and J.B. Bowers, Anal. Chem., 46 (1974) 155.
12 G.D. Thorn and R.A. Ludwig, The Dithiocarbamates and Related Compounds, Elsevier, New York, 1962, and references therein.

Analytica Chimica Acta, 79 (1975) 207—218

DETERMINATION OF SEVEN TRACE ELEMENTS IN NATURAL WATERS AFTER SEPARATION BY SOLVENT EXTRACTION AND ANION-EXCHANGE CHROMATOGRAPHY

J. KORKISCH and A. SORIO

Institute for Analytical Chemistry, Analysis of Nuclear Raw Materials Division, University of Vienna, Währingerstrasse 38, A-1090 Vienna (Austria)

(Received 18th March 1975)

Determinations of toxic elements in natural waters, including snow and sea water, are gaining importance as a method of ascertaining the degree of pollution of the environment. For this purpose, analytical techniques based on atomic absorption spectrometry are often employed [1], frequently in combination with liquid—liquid extraction and/or ion-exchange [1] to pre-concentrate toxic metals such as cadmium, copper, lead etc., so that improved detection limits and accuracy can be achieved. In this paper, a combination of these methods is described for the assay of cadmium, cobalt, copper, manganese, lead, uranium, and zinc in water samples.

EXPERIMENTAL

Solutions and reagents

Ion-exchange resin. The strongly basic anion-exchange resin Dowex 1 (Bio-Rad AG1-X8; 100—200 mesh; chloride form) was used. Slurry the resin (4 g) with 100 ml of 6 *M* hydrochloric acid and wash it several times with a total of 100 ml of 1 *M* nitric acid to remove trace elements which may contaminate the resin (*e.g.* Zn, Pb and Cu). Take up the resin in about 20 ml of the THF—MG—HCl mixture (see below), let stand for 8—10 h and pour into an ion-exchange column. Subsequently wash the resin bed with 50 ml of the same mixture to complete the pretreatment of the anion exchanger.

Standard solutions. Dilute aliquots of stock solutions containing 500 μg each of Cd, Co, Cu, Mn, Pb, U and Zn per milliliter of 6 *M* hydrochloric acid with 0.1 *M* hydrochloric acid to obtain standard solutions containing from 0.04 to 100 p.p.m. of the elements.

Extractant. Prepare a mixture of acetone and chloroform (2:5, v/v).

THF—MG—HCl mixture. Prepare a mixture 5:4:1 (v/v) of tetrahydrofuran (THF), methyl glycol (MG, monomethyl ether of ethylene glycol) and 6 *M* hydrochloric acid.

Methanolic HBr. Prepare a mixture 9:1 (v/v) of methanol and 1.5 *M* hydrobromic acid.

Apparatus and operating conditions

A Perkin-Elmer atomic absorption spectrophotometer 303 (equipped with a Hitachi-Perkin-Elmer Recorder 56 connected to a read-out accessory) was used with the following instrumental settings:

Grating:	Ultraviolet (Cd, Co, Cu, Mn, Pb and Zn).
Wavelength:	228.8 nm (Cd), 241 nm (Co), 342.7 nm (Cu), 280.1 nm (Mn), 284 nm (Pb) and 213.8 nm (Zn).
Scale expansion:	Up to 10× (Cd, Co, Cu, Mn, Pb, and Zn).
Slit:	3(0.3 mm; 0.2 nm bandpass)(Co), 4(1 mm; 0.7 nm bandpass) (Cd, Cu, Mn and Pb) and 5(3 mm; 2 nm bandpass)(Zn).
Source:	Hollow-cathode lamps (Cd, Co, Cu, Mn, Pb, and Zn).
Lamp current:	8 mA (Cd and Pb), 15 mA (Cu and Zn), 20 mA (Mn) and 30 mA (Co).
Burner:	Standard burner head (flat) (Cd, Co, Cu, Mn, Pb, and Zn).
Acetylene pressure:	8 p.s.i.g.; 7.0 on flow meter (arbitrary scale) (Cd, Co, Cu, Mn, Pb, and Zn).
Air pressure:	30 p.s.i.g.; 9.0 on flow meter (arbitrary scale) (Cd, Co, Cu, Mn, Pb, and Zn).
Noise suppression:	Up to 4 (Cd, Co, Cu, Mn, Pb, and Zn).

When the methanolic HBr solution is used, the following sensitivities for 1 % absorption are obtained:

Cd = 0.033 p.p.m.; Co = 0.109 p.p.m.; Cu = 0.04 p.p.m.; Mn = 0.058 p.p.m.; Pb = 0.28 p.p.m.; and Zn = 0.01 p.p.m.

The fluorimetric determinations of uranium were carried out with a Galvanek—Morrison fluorimeter, Mark V (Jarrel-Ash). The separations of Cd, Co, Cu, Mn, Pb, U and Zn were performed in ion-exchange columns of the type and dimensions described earlier [2].

Determination of distribution coefficients

The weight distribution coefficients (K_d values on Dowex 1) of Cd, Co, Cu, Mn, Pb, U, and Zn were determined by the batch method [3].

Separation procedure

Acidify 1 l of the water sample with 8.5 ml of 12 *M* hydrochloric acid. (If a different volume of sample is required for analysis, the amounts of reagents added are altered accordingly). Filter through a dense filter and to the filtrate add 10 g of sodium acetate. Mix thoroughly until this reagent has dissolved and adjust the solution to *ca.* pH 5 by adding 25 % sodium hydroxid

solution (about 15 ml of this alkaline solution are required). Transfer the solution to a 2-l separatory funnel and saturate the aqueous phase by shaking it for *ca.* 30 s with 15 ml of the extractant. Add 1 g of sodium diethyldithiocarbamate and, almost simultaneously, add another 15-ml portion of the extractant. Shake for about 1 min and separate the organic extract. (If the separation of the phases is not satisfactory, as was observed when analysing some samples from the Danube, the extract is passed through dry filter paper to remove contaminants adhering to the organic phase.) Repeat the extraction with two 10-ml portions of the extractant, shaking for about 1 min during each extraction. Combine the organic extracts and evaporate to dryness with an infrared lamp. To the residue of diethyldithiocarbamates add 20 ml of the THF—MG—HCl mixture and evaporate to dryness under the same conditions as the original extract. Dissolve the residue in 30 ml of the THF—MG—HCl mixture and pass the solution (sorption solution) through a column containing 4 g of the pretreated anion-exchange resin at a flow-rate which corresponds to the back-pressure of the resin bed (about 45 ml h^{-1}). Wash the resin bed with 60 ml of the THF—MG—HCl mixture. Elute Co, Cu, Mn and Pb with 100 ml of 6 *M* hydrochloric acid (first eluate), uranium with 50 ml of 1 *M* hydrochloric acid (second eluate), and Cd and Zn with 100 ml of 2 *M* nitric acid (third eluate).

Determination of trace elements

Co, Cu, Mn and Pb. Evaporate the first eluate to dryness under an infrared lamp and dissolve the residue in 25 ml of methanolic HBr solution. Aspirate the solution into the air—acetylene flame and construct the calibration curve by aspirating suitable Co, Cu, Mn and Pb standard solutions (prepared in exactly the same way as the samples) before and after each batch of samples.

Cd and Zn. Evaporate the third eluate (see above) to dryness under an infrared lamp and continue as described above for the determination of Co, Cu, Mn, and Pb.

Uranium. Evaporate the second eluate (see above) to dryness and continue as described earlier [4]. Uranium is determined fluorimetrically.

In the determination of extremely small quantities, run a reagent blank through the whole procedure (starting with the addition of concentrated hydrochloric acid; see above) and finally deduct the concentrations of Cd, Co, Cu, Mn, Pb, U, and Zn found from those apparently present in the water sample.

RESULTS AND DISCUSSION

Liquid—liquid extraction of trace elements

Investigations with respect to the suitability of the 2:5 mixture of acetone and chloroform as an extractant for metal diethyldithiocarbamates [5] showed that quantitative extraction of Cd, Co, Cu, Mn, Pb, U, and Zn is achieved under the conditions described in the Separation procedure. Thus, the extraction is best performed at *ca.* pH 5 in the presence of acetate. The

sodium diethyldithiocarbamate is added to the water sample immediately after this has been saturated with the extractant in order to take full advantage of the extraction efficiency of the chelating agent. At pH 5 the rate of decomposition of diethyldithiocarbamate was relatively high [5].

Anion-exchange separation

The THF—MG—HCl mixture used previously in the anion-exchange separation of uranium from natural waters [4] can also be employed effectively for the fractionation of metal ions after extraction of their diethyldithiocarbamat under the conditions described in the Experimental part of the present paper. Following evaporation of the extractant, the diethyldithiocarbamate complexes must be destroyed by evaporation in the presence of THF—MG—HCl (see Procedure), otherwise many of the elements are retained incompletely on subsequent passage of the THF—MG—HCl sorption solution through the ion-exchange column, *e.g.* cobalt is not adsorbed at all, and only 5, 10, 80 and 85 % of copper, lead, manganese, and zinc, respectively, are adsorbed. After destruction of the diethyldithiocarbamates, all of the elements investigated, *i.e.* Cd, Co, Cu, Mn, Pb, U, and Zn, are retained quantitatively by the anion-exchange resin; the distribution coefficients shown in Table I were measured in the various media used for adsorption and elution. These results show that successive applications of 6 *M* hydrochloric acid, 1 *M* hydrochloric acid and 2 *M* nitric acid give eluates which contain Co, Cu, Mn and Pb, uranium, and Cd and Zn respectively (see Procedure).

TABLE I

Distribution coefficients

(1 g Dowex 1; 1 mg load)

Ion	THF—MG—HCl mixture	6 *M* HCl	2 *M* HNO_3	1 *M* HNO_3
Cd(II)	705	130	700	<1
Co(II)	6030	<10	<1	<1
Cu(II)	75	12	<1	<1
Mn(II)	200	<10	<1	<1
Pb(II)	250	<10	65	<10
UO_2(II)	3510	250	<1	<1
Zn(II)	305	125	195	<1

Effect of volume

To investigate the effect of volume of the water sample on the recovery and accuracy of the determinations of the trace elements, varying volumes of tap water were analysed for these 7 elements: The results in Table II show that the volume of water has no effect in the volume range investigated but for accurate determinations of most elements not less than 1 l of water

TABLE II

Effect of the volume of water sample on determination of trace elements in Vienna tap water

A, Determination after preliminary isolation by extraction and anion-exchange. B, Results obtained after preliminary isolation by extraction and anion-exchange and deduction of known amounts of the trace elements added as spikes before the separations. The number in parentheses gives the amount of spike (in $\mu g\ l^{-1}$) used.

Vol. of water taken (l)[a]	Contents found ($\mu g\ l^{-1}$)													
	Cd		Co		Cu		Mn		Pb		U		Zn	
	A	B	A	B	A	B	A	B	A	B	A	B	A	B
0.25	—	0.1 (0.1)	—	0.15 (4.9)	13.6	12.8 (3.8)	—	0.2 (5.5)	18.5	19.2 (4.1)	0.15	0.2 (0.2)	20.1	21.0 (2.9)
0.50	—	0.1 (0.1)	—	0.15 (4.9)	12.1	12.5 (3.8)	0.1	0.15 (5.5)	18.5	18.6 (4.1)	0.20	0.4 (0.2)	18.9	19.5 (2.9)
0.75	0.15	0.1 (0.1)	0.15	0.1 (4.5)	12.6	13.0 (3.8)	0.15	0.15 (5.5)	18.3	18.9 (4.1)	0.30	0.3 (0.2)	18.8	19.6 (2.9)
1.00	0.10	0.1 (0.1)	0.10	0.1 (4.9)	11.6	11.9 (3.8)	0.15	0.20 (5.5)	19.1	18.5 (4.1)	0.27	0.33 (0.2)	18.5 18.9[b]	18.8 (2.9)

[a] On November 24, 1974, the water sample was taken immediately after opening the tap. A sample taken 20 min afterwards contained much lower contents of copper, lead and zinc, *i.e.* 4.9, 13.6 and 5.8 $\mu g\ l^{-1}$ respectively.

[b] Results obtained after anion-exchange separation of zinc thiocyanate [6].

sample should be used. As mentioned in footnote[a] of Table II, the amounts of some trace elements in tap water are dependent on the technique used for collecting the sample, because these elements are constituents of the water pipes (*i.e.* Pb, Cu and Zn).

Effect of iron

Since iron is the only major constituent of natural waters extractable as the diethyldithiocarbamate under the conditions employed, the effect of foreign metal ions on the extraction and anion-exchange separation of the trace elements was studied with respect to the behaviour of iron only. The results (Table III) show that up to 10 mg of iron did not affect the results

TABLE III

Effect of iron on extraction and anion-exchange separation

Fe added[a]	Contents found ($\mu g\ l^{-1}$)[b]						
	Cd	Co	Cu	Mn	Pb	U	Zn
0.0	0.1	0.1	9.2	0.1	11.8	0.28	7.0
0.2	10.0	12.4	8.9	13.6	10.8	0.20	7.8
	(10.2)	(12.2)	(9.6)	(13.7)	(10.2)	(0.20)	(7.25)
2.0	9.8	12.1	9.0	12.8	10.4	0.16	7.8
	(10.2)	(12.2)	(9.6)	(13.7)	(10.2)	(0.20)	(7.25)
10.0	9.8	12.4	8.8	12.5	10.4	0.09	7.6
	(10.2)	(12.2)	(9.6)	(13.7)	(10.2)	(0.20)	(7.25)

[a] Amount of Fe (in mg) added to 1 l of tap water.
[b] Results obtained after addition of the amounts (in $\mu g\ l^{-1}$) of spike shown in parentheses and deduction of the natural trace element contents (see first row of results).

obtained for the trace elements, except for uranium, of which much lower contents were found in the presence of 2 and 10 mg of iron. This is because 60 ml of the THF—MG—HCl mixture (see Procedure) are not sufficient to remove iron completely from the anion exchanger so that some iron accompanies uranium into the 1 *M* hydrochloric acid eluate and causes quenching of the uranium fluorescence. Complete removal of iron can be achieved by increasing [4] the volume of THF—MG—HCl solution to 100—200 ml. Some of the copper will then pass into the effluent, however, because of its relatively low distribution coefficient (see Table I).

Effect of concentration

Experiments with respect to the effect of the concentrations of the trace elements on their recovery from 1-l samples of tap water gave the results presented in Table IV; in all cases the elements were recovered quantitatively.

TABLE IV

Effects of concentration on the recovery of trace elements

(Contents found in $\mu g\ l^{-1}$)[a]

Cd	Co	Cu	Mn	Pb	U	Zn
0.15	0.1	4.9	0.1	13.6	0.23	5.6
4.0	4.9	3.8	5.6	4.5	0.05	2.8
(4.1)	(4.9)	(3.85)	(5.5)	(4.1)	(0.04)	(2.9)
7.9	9.2	7.5	11.3	8.7	0.07	5.6
(8.15)	(9.8)	(7.7)	(11.0)	(8.2)	(0.08)	(5.8)
40.0	48.8	38.4	55.7	42.1	0.3	28.6
(40.5)	(49.0)	(38.5)	(55.0)	(40.5)	(0.4)	(29.0)
81.0	99.0	75.9	109.0	84.1	0.7	60.3
(81.5)	(98.0)	(77.0)	(110)	(81.5)	(0.8)	(58.0)

[a]Results obtained after addition, to 1.0-l samples of tap water, of the spike-amounts (in $\mu g\ l^{-1}$) shown in parentheses and deduction of the natural trace element contents (see first row of results).

Application to natural waters

Table V shows the results of determinations of trace elements in Austrian waters by the recommended procedure. These results indicate clearly that cadmium, cobalt and lead cannot be determined without preliminary isolation by the extraction and anion-exchange methods (see column A of Table V).

The results for the four snow samples (see Table VI) show that the trace element contents decrease invariably with increasing distance from the highway except for uranium which shows virtually the same concentration in all the snow samples, because uranium is not contained in the exhaust fumes of cars; its presence in the samples can be attributed to its removal (with the dust) from the air by the snow-fall.

In order to investigate if the method is also applicable to the analysis of saline waters, a sample of sea water from the Adriatic Sea was analysed by the recommended procedure. The results (Table VII) indicate that none of the trace elements in the sample can be determined by direct atomic absorption measurements (see column A of Table VII). The uranium determinations agreed very well with those obtained after anion-exchange separation of uranium thiocyanate [7].

It should be mentioned finally that, in place of the solvent extraction procedure, the trace elements can also be concentrated quantitatively on a 4-g column of the cation exchanger Dowex 50 from 1 l of the water sample which is 0.1 *M* in hydrochloric acid. Following adsorption, the trace elements (together with the co-adsorbed main constituents) are eluted with 6 *M* hydrochloric acid and, after evaporation of the eluate, the anion-exchange separation described here is carried out. However, this cation-exchange method was abandoned in favour of the more rapid extraction method so that this tech-

TABLE V

Results of determination of trace elements in samples of Austrian waters

A, Direct atomic absorption determination without preliminary separation by extraction and anion-exchange. B, Determination after preliminary isolation by extraction and anion-exchange. C, Results obtained after preliminary isolation by extraction and anion-exchange and deduction of the known amounts of trace elements added as spikes before the separations. The number in parentheses gives the amount of spike used.

Sample no., origin and sampling date	Contents ($\mu g\ l^{-1}$)				
	Element	A	B	C	
1. Danube near Pischelsdorf (11.2.1975)	Cd	N.d.[a]	0.37	0.4	(1.0)
	Co	N.d.	0.42	0.5	(0.5)
	Cu	N.d.	13.8	11.2	(10)
	Mn	44.0	36.8	35.1	(30)
	Pb	N.d.	10.0	9.7	(10)
	U	—	0.83	0.65	(1.0)
	Zn	56.3	53.8	55.2	(50)
2. Danube near Kronau (near Donau-Chemie Co.) (11.2.1975)	Cd	N.d.	1.8	1.7	(1.0)
	Co	N.d.	0.1	0.7	(0.5)
	Cu	N.d.	13.8	10.9	(10)
	Mn	29.0	26.1	27.5	(30)
	Pb	N.d.	9.0	9.5	(10)
	U	—	1.48	1.55	(1.0)
	Zn	61.9	53.2	56.0	(50)
3. Danube near Tulln (near a sugar refinery) (11.2.1975)	Cd	N.d.	0.49	0.45	(1.0)
	Co	N.d.	0.10	0.10	(0.5)
	Cu	N.d.	14.5	13.6	(10)
	Mn	37.0	33.9	31.8	(30)
	Pb	N.d.	1.5	2.3	(10)
	U	—	0.85	0.92	(1.0)
	Zn	61.5	54.9	53.1	(50)
4. Danube near Klosterneuburg (Ferry) (11.2.1975)	Cd	N.d.	0.49	0.50	(1.0)
	Co	N.d.	0.10	0.10	(0.5)
	Cu	17.5	16.1	17.0	(20)
	Mn	28.0	25.3	26.0	(30)
	Pb	N.d.	18.9	17.8	(20)
	U	—	1.41	1.35	(1.0)
	Zn	56.5	53.9	55.0	(50)
5. Danube Canal near Friedensbrücke (11.2.1975)	Cd	N.d.	0.49	0.48	(1.0)
	Co	N.d.	0.32	0.40	(0.5)
	Cu	20.0	18.0	18.5	(20)
	Mn	28.0	24.1	24.7	(30)
	Pb	N.d.	9.5	10.2	(10)
	U	—	1.08	1.16	(1.0)
	Zn	73.1	56.2	58.5	(50)

Sample no., origin and sampling date	Contents ($\mu g\ l^{-1}$)			
	Element	A	B	C
6. Danube Canal near Atominstitut der Österreichischen Hochschulen, Vienna (11.2.1975)	Cd	N.d.	0.83	0.90 (1.0)
	Co	N.d.	0.53	0.48 (0.5)
	Cu	20.0	18.8	18.5 (20)
	Mn	28.0	25.2	26.1 (30)
	Pb	N.d.	6.4	6.9 (10)
	U	—	3.20	3.05 (3)
	Zn	85.6	57.6	61.3 (50)
7. Intersection of Danube Canal with Danube (Lobau) (11.2.1975)	Cd	N.d.	0.49	0.50 (1.0)
	Co	N.d.	0.37	0.45 (0.5)
	Cu	22.9	26.9	25.7 (20)
	Mn	37.0	35.4	36.2 (30)
	Pb	N.d.	9.0	9.3 (10)
	U	—	2.35	2.10 (3)
	Zn	61.3	55.4	56.1 (50)
8. Frauensbach near Schwechat (near a brewery) (11.2.1975)	Cd	N.d.	0.54	0.50 (1.0)
	Co	N.d.	0.42	0.40 (0.5)
	Cu	57.0	47.6	49.7 (50)
	Mn	46.0	33.9	35.1 (30)
	Pb	N.d.	5.0	5.2 (10)
	U	—	1.32	1.35 (1.0)
	Zn	118	59.8	63.2 (50)
9. Ziegelswasser near Mannswörth (near an oil refinery and brewery) (11.2.1975)	Cd	N.d.	0.70	0.80 (1.0)
	Co	N.d.	0.48	0.55 (0.5)
	Cu	55.0	46.8	48.1 (50)
	Mn	32.0	26.8	29.4 (30)
	Pb	N.d.	12.5	12.7 (10)
	U	—	1.11	1.05 (1.0)
	Zn	120	58.2	66.7 (50)
10. Branch of Danube near Fischamend (ground water) (11.2.1975)	Cd	N.d.	0.49	0.52 (1.0)
	Co	N.d.	0.39	0.45 (0.5)
	Cu	15.8	18.1	17.6 (20)
	Mn	260.	229.	241. (120)
	Pb	N.d.	10.5	11.1 (10)
	U	—	1.46	1.50 (1.0)
	Zn	55.6	58.1	57.5 (50)

[a] N.d. = not detectable.

TABLE VI

Results of determinations of trace elements in snow samples[a]

(For explanation of A, B and C, see Table V)

Distance (m) of sampling site from highway	Metal content (p.p.b.)			
	A	B	C	
Cadmium				
10	N.d.[b]	1.07	1.12	(1.0)
20	N.d.	0.82	0.80	(1.0)
50	N.d.	0.39	0.42	(0.5)
300	N.d.	0.26	0.22	(0.5)
Cobalt				
10	N.d.	0.78	0.75	(0.5)
20	N.d.	0.30	0.28	(0.5)
50	N.d.	0.19	0.20	(0.5)
300	N.d.	0.10	0.10	(0.5)
Copper				
10	30.3	29.4	30.1	(30.0)
20	7.5	18.8	19.2	(15)
50	N.d.	12.6	12.2	(15)
300	N.d.	11.3	11.5	(15)
Manganese				
10	165	153	151	(100)
20	45	39	40	(50)
50	21	22	22	(25)
300	9.4	9.7	9.5	(12.5)
Lead				
10	283	290	291	(100)
20	55	82	80	(100)
50	32	49	50	(50)
300	N.d.	36.2	35.5	(50)
Uranium				
10	N.d.	0.12	0.14	(0.2)
20	N.d.	0.11	0.14	(0.2)
50	N.d.	0.13	0.12	(0.2
300	N.d.	0.14	0.13	(0.2)
Zinc				
10	172	187	185	(100)
20	54	132	130	(100)
50	53	120	120	(100)
300	52	108	109	(100)

[a] The samples of aged snow were collected on 12.2.1975 in the Salzachtal at various distances from highway No. 157 near Kuchl, Salzburg.
[b] N.d. = not detectable.

TABLE VII

Results of determinations of trace elements in a sample of sea water[a]

(For explanation of A, B and C, see Table V)

Element	Contents ($\mu g\ l^{-1}$)		
	A	B	C
Cd	22.1	0.10	0.05 (0.5)
Co	98.4	0.15	0.15 (0.5)
Cu	26.7	2.30	2.10 (4.5)
Mn	28.6	3.80	4.20 (5.0)
Pb	95.2	0.35	0.37 (0.5)
U	0.9[c]	2.35	2.40 (2.5)
		2.25[b]	2.36 (1.0)[b]
Zn	28.8	0.55	0.75 (1.0)

[a] Sample taken from the Adriatic Sea in October 1974 at the shore near Lignano Pineta, Italy.
[b] Results obtained after anion-exchange separation of uranium thiocyanate [7].
[c] Determination by direct fluorimetry.

nique is more suitable for the routine determination of trace elements in natural waters.

This research was sponsored by the Fonds zur Förderung der wissenschaftlichen Forschung, Vienna, Austria. The generous support from this Fund is gratefully acknowledged.

SUMMARY

A method is described for the determination of cadmium, cobalt, copper, manganese, lead, uranium, and zinc in samples of natural waters. After acidification with hydrochloric acid the water sample is filtered and the diethyldithiocarbamates of the trace elements are isolated by extraction with acetone—chloroform (2:5) at pH 5. Following this preconcentration step the metal ions are adsorbed on a column of the strongly basic anion-exchange resin Dowex 1-X8 (chloride form) using as sorption solution a mixture (5:4:1, v/v) of tetrahydrofuran, methyl glycol and 6 *M* hydrochloric acid. Successive elution is effected with 6 *M* hydrochloric acid (Co, Cu, Mn and Pb), 1 *M* hydrochloric acid (U) and 2 *M* nitric acid (Cd and Zn); the metal ions in the eluates are determined by atomic absorption spectrophotometry (except uranium, which is determined fluorimetrically). The procedure was used to determine the trace metals in water and snow samples collected in Austria and to analyse a sample of sea water from the Adriatic Sea.

REFERENCES

1 J. Korkisch and A. Sorio, Anal. Chim. Acta, 76 (1975) 393.
2 W. Koch and J. Korkisch, Mikrochim. Acta, (1972) 687.
3 J. Korkisch, Modern Methods for the Separation of Rarer Metal Ions, Pergamon, Oxford, 1969.
4 J. Korkisch and L. Gödl, Anal. Chim. Acta, 71 (1974) 113.
5 A.K. De, S.M. Khopkar and R.A. Chalmers, Solvent Extraction of Metals, Van Nostrand Reinhold, London, 1970.
6 J. Korkisch and L. Gödl, Talanta, 22 (1975) 281.
7 J. Korkisch and I. Steffan, Anal. Chim. Acta, 77 (1975) 312.

Analytica Chimica Acta, 79 (1975) 219—227

SELECTIVE SEPARATIONS BY REACTIVE ION EXCHANGE

PART III. PRECONCENTRATION AND SEPARATION OF OXO ANIONS

JOYCE W. LIN and GILBERT E. JANAUER

Department of Chemistry, State University of New York at Binghamton, Binghamton, New York 13901 (U.S.A.)

(Received 14th February 1975)

The combination of ion exchangers with redox reactions has been explored by several authors. Cassidy [1] first developed the idea of using "electron exchange-polymers", and with his coworkers [2—4] prepared and studied various polymers such as vinylhydroquinone. These polymers were capable of oxidizing or reducing certain organic and inorganic species directly. Sansoni [5] adsorbed iron(II) and leuco methylene blue on cation-exchange resins and hydroquinone on anion-exchange resins, the separation of radioruthenium from uranium fission products by means of a redox resin was achieved recently [6]. More redox reactions were studied by Inczédy, who among other reactions carried out the reduction of iron(III) on cation-exchange resin with ascorbic acid [7—9]. Dalibor [10] reduced organic substances on titanium(III) and chromium(II) forms of cation-exchange resins and on the thiosulfate form of an anion-exchange resin.

Reactive ion exchange with redox systems was applied in this laboratory [11, 12], for a study of toxic chromium(VI) traces in a natural-water system. Janauer *et al.* [13] recently proposed reactive ion exchange as a general approach based on thermodynamic considerations, and predicted selective separations for various ionic species. Application of the method to the preconcentration and analysis of complex iron cyanides was also described recently [14]. The results to be discussed here were obtained with the oxo anions permanganate, chromate, vanadate, and molybdate, most of which form positively charged species in their lower oxidation states. Their behavior was studied during reduction/adsorption on suitable cation- or anion-exchange resins and during elution in the form of complexes. As the reactive adsorption and elution steps were carefully chosen and combined, the separation of these anions was achieved without the resins being attacked or damaged by the strongly oxidizing species. The present method not only permits efficient and convenient preconcentration, separation, and determination of these ions at the trace level, but may also prove applicable to laboratory-scale separations and waste-water treatment for pollution control.

EXPERIMENTAL

Equipment

A Perkin-Elmer 303 Atomic Absorption Spectrophotometer with a Honeywell Electronix 194 recorder was used for chromium and manganese determinations. A Beckman DBG was used for spectrophotometric determination of vanadium and molybdenum. An automatic fraction collector "Fractomat" from Buchler Instruments with siphon delivery tubes of 3 and 5 ml was used whenever continuous collection of eluates was needed. All pH measurements and adjustments were done on a Beckman Expandomatic pH meter.

Materials

All chemicals used were reagent grade. The cation-exchange resin, Dowex 50W-X4 (Bio-Rad Laboratories, 100–200 mesh) in the hydrogen form, was used for separation procedures and preliminary tests; the strongly basic anion-exchange resin AG 1-X4 (Bio-Rad Laboratories; 100—200 mesh) in the chloride form, was only used for preliminary tests.

Stock solutions of the oxo anions were prepared at concentrations of 5000 p.p.m. of the required elements (chromium, manganese, vanadium, and molybdenum). Sample solutions were diluted from stock solutions daily with distilled–deionized water and were adjusted to the required pH with nitric acid.

Resin pretreatment

Weighed amounts of cation-exchange resin (hydrogen form) or anion-exchange resin (chloride form) were allowed to swell for at least two days in deionized—distilled water before treatment. Solutions containing iron(II) (from $Fe(NH_4)_2(SO_4)_2 \cdot 6H_2O$) or tin(II) (from $SnCl_2 \cdot 2H_2O$) for treating cation-exchange resin, and sulfite ion (from Na_2SO_3) or thiosulfate ion (from $Na_2S_2O_3 \cdot 5H_2O$) for treating anion-exchange resin, were prepared and added to the resins in Erlenmeyer flasks. A twofold molar excess of the electrolytes with reference to the capacity of the resin samples was always used for batch equilibration with the standard resins. After two days of shaking, the resins were filtered off, washed, and filled into columns (as aqueous slurries). The resins ($\overline{Fe^{2+}}$, $\overline{Sn^{2+}}$, $\overline{SO_3^{2-}}$, and $\overline{S_2O_3^{2-}}$) have been kept for longer than one month with retention of most of their reducing capacity.

Preliminary experiments

Columns of 0.7-cm inner diameter were packed with about 0.5 g of treated or standard resins (the latter were used for blanks). Then 10 ml of sample

TABLE I

Results of preliminary experiments

Reactive resin	Original ion	Adsorbed ion	pH	Column process [a]	Elution behavior [b]	
					1 *M* H_2SO_4	1 *M* NaOH
$\overline{Fe^{2+}}$	MnO_4^-	Mn^{2+}	1.0	RAD	+ + +	
	CrO_4^{2-}	Cr^{3+}	1.0	RAD	+ + +	
	VO_3^-	VO^{2+}	1.0	RAD	+ +	
	MoO_4^{2-}	–	1.0	None		
$\overline{Sn^{2+}}$	MnO_4^-	Mn^{2+}	5.5	RAD	+ + +	
	CrO_4^{2-}	Cr^{3+}	7.6	RAD	+ + +	
	VO_3^-	VO^{2+}	7.1	RAD	+ +	–
	MoO_4^{2-}	—	6.6	RAD	+	
$\overline{SO_3^{2-}}$	MnO_4^-	Complex?	6.8	RAD [c]	–	–
		Complex?	5.5	RAD [c]	+ +	
	CrO_4^{2-}	CrO_4^{2-}	8.5	AD	+ +	
		CrO_4^{2-}	7.6	AD	+	
		Complex?	2.1	RAD [c]	+ + +	
	VO_3^-	?	7.1	(AD)	+ + +	
		?	1.1	(AD)	–	–
	MoO_4^{2-}	?	6.6	(AD)	+ + +	
$\overline{S_2O_3^{2-}}$	MnO_4^-	Complex?	6.8	RAD [c]	–	–
		Complex?	5.5	RAD [c]	+ +	
	CrO_4^{2-}	CrO_4^{2-}	8.5	AD	+	+
		CrO_4^{2-}	7.6	AD	+	
	VO_3^-	?	7.1	(AD)	+ + +	
	MoO_4^{2-}	?	6.6	(AD)	+ +	

[a] RAD = reactive adsorption. AD = adsorption. (AD) indicates uncertain adsorption.
[b] The symbol + + + stands for "quantitative elution", + + for "major fraction eluted", + for "small fraction eluted", and – for "no elution".
[c] The original color of the MnO_4^- and CrO_4^{2-} species was no longer visible after adsorption had occurred.

solutions at different pH values containing 5 p.p.m. of either permanganate ($KMnO_4$), chromate (K_2CrO_4), vanadate ($NaVO_3$) or molybdate ($Na_2MoO_4 \cdot 2H_2O$) were passed through each type of column, followed by the eluant, 1 *M* sulfuric acid; 10-ml fractions were collected for analysis by atomic absorption for manganese and chromium, and by spectrophotometry for vanadium (peroxide method) [15] and for molybdenum (thiocyanate method) [15]. In a few cases, 1 *M* sodium hydroxide was also tried as an eluant. The results are shown in Table I. Standard addition was later used in all quantitative work.

Separation procedure

The column setup was similar to that described by Pankow and Janauer [11] except that the cartridge (into which the resin was packed) was removable so that the dead volume below the cartridge was reduced to a negligible amount during elution.

Permanganate, chromate, and vanadate solutions were mixed and diluted to 1 l in order to obtain the required final concentration (usually 100 p.p.b.) of each oxo anion, and the pH was adjusted to 3.7. The treated resin (0.5 g; $\overline{Fe}^{2+}$ in most later experiments) was packed into cartridges and the solutions to be preconcentrated were passed through at a flow rate of about 2 ml min^{-1} (usually overnight). Elution was done at a flow rate of 0.5 ml min^{-1}. A volume of 10 ml of 0.3 % hydrogen peroxide in 0.01 *M* nitric acid solution eluted the reduced vanadium(IV). Then manganese(II) was eluted with 25 ml of 0.3 *M* hydrochloric acid, and chromium(III) with 25 ml of 4 *M* hydrochloric acid. Vanadium(IV) was determined by the phosphotungstate method [15]. Ammonium hydrogen fluoride (1 %) and 0.2 % ammonium sulfate were added to the final chromium(III) eluate as a releasing reagent in order to obtain a better atomic absorption signal [16].

Interference study

"Samples" (100 ml) were prepared so that they contained not only the three oxo anions at the 100 (or 50) p.p.b. level, but also 200 p.p.m. calcium, 355 p.p.m. chloride ($CaCl_2 \cdot 2H_2O$); 100 p.p.m. sodium, 250 p.p.m. nitrate ($NaNO_3$); and 50 p.p.m. magnesium, 190 p.p.m. sulfate ($MgSO_4 \cdot 7H_2O$). The pH was adjusted to 3.7 as before and the procedure was the same as above, except that 1.5 g of iron(II) resin was used. The increased amount of resin was needed, because the greater electrolyte concentrations used resulted in depletion of iron(II) (by exchange) along the column as sample was passed through.

RESULTS

Table I shows some representative results of preliminary experiments on the reactive adsorption behavior of the four anions studied and elution results for the same systems.

Table II illustrates the effects on recovery of Mn, Cr, and V of both pH (during adsorption) and acid anion or acid concentration (0.3–0.4 *M* HCl for manganese) in eluants.

Table III shows the results of recovery studies with very dilute mixtures under the optimal conditions selected (from Table II).

Table IV gives the results of a study of (potential) interferences in a simulated hard fresh water at two concentration levels of the analytes.

DISCUSSION

While the simultaneous separation of the oxo anions chromate, vanadate, and molybdate is still difficult, some successful ion-exchange separations have been reported [18]. Newer separation procedures have been reviewed by Korkisch [19], but resin attack by ions such as vanadate remains a problem [19]. During recent work in this laboratory, the use of intermediate to neutral

TABLE II

Effect of adsorption pH and eluant compositions on recovery of Mn, Cr, and V from iron(II) and tin(II) resins
(100 p.p.b. mixtures of the anions in triplicate runs.)

Resin	pH	Element	Eluant	Recovery (%)	s (%)
Sn^{2+}	5.5	V	0.3 % H_2O_2 in 0.01 *M* HNO_3	48	1
		Mn	0.30 *M* HCl	67	3
		Cr [a]	4.0 *M* HNO_3	37	4
	3.7	V	0.3 % H_2O_2 in 0.01 *M* HNO_3	50	2
		Mn	0.3 *M* HCl	89	2
		Cr [b]	4.0 *M* HNO_3	67	4
Fe^{2+}	5.5	V	0.3 % H_2O_2 in 0.01 *M* HNO_3	46	4
		Mn	0.35 *M* HCl	64	7
		Cr [b]	4.0 *M* HNO_3	54	5
	3.7	V	0.3 % H_2O_2 in 0.01 *M* HNO_3	95	6
		Mn	0.40 *M* HCl	101	3
		Cr [c]	4.0 *M* HCl	92	2

[a] No reagent was added for a.a.s. determination.
[b] Hydrogenfluoride and sulphate solution was added after elution of Cr [16].
[c] Oxine was added after elution of Cr [17]. Addition of HF and sulphate was equally efficient in averting AAS signal depression, and also gave more reproducible results.

TABLE III

Recovery studies at low concentrations
(Eluants: V – 10 ml of 0.3 % H_2O_2 in 0.01 *M* HNO_3; Mn – 25 ml of 0.40 *M* HCl; Cr – 25 ml of 4 *M* HCl; Fe(II) resin; pH 3, 7; 1-l samples.)

Species	Concentration (p.p.b.)	Recovery (%)	s (%)
V	50	95	2
Mn	50	99	7
Cr	50	94	5
V	25	95	4
Mn	25	98	4
Cr	25	93	5
V	10	90	4
Mn	10	99	4
Cr	10	93	5
V	5	[a]	–
Mn	5	91	5
Cr	5	89	8
V	2.5	[a]	–
Mn	2.5	86	5
Cr	2.5	87	5

[a] The value is uncertain because the concentration was too low to be detected.

TABLE IV

Ionic interference study

Species	Concentration (p.p.b.)	Recovery (%)	s (%)
V	100	93	3
Mn	100	91	5
Cr	100	93	4
V	50	93	6
Mn	50	92	2
Cr	50	92	4

(Concentration (p.p.m.): Ca^{2+} 200, Mg^{2+} 50, Na^{+} 100, Cl^{-} 355, SO_4^{2-} 190, NO_3^{-} 250. Eluants: as in Table III. Fe(II) resin; pH 3.7; 100-ml samples.)

pH during sorption, reduced resin contact times, and reductive elution proved successful in keeping losses caused by redox reactions within reasonable limits when traces of chromate were preconcentrated [12] on Dowex 1. It seemed reasonable to expect that the application of reactive ion-exchange resins treated with Fe^{2+} or Sn^{2+} would prevent completely any resin oxidation (even with permanganate) and at the same time permit quantitative preconcentration of permanganate, dichromate and vanadate on these cation exchangers after reduction to Mn^{2+}, Cr^{3+}, and VO^{2+}, respectively. Molybdate (and tungstate) would normally not be reduced or sorb on these cation-exchange resins and would, therefore, separate automatically. These expectations were fulfilled; sorption of Mn, Cr, and V was efficient, *i.e.*, the reduced metal ions were sorbed in a narrow zone of the tiny Fe^{2+} resin beds employed.

The intrinsic colors of permanganate, chromate, and chromium(III) species were used to detect the presence (or absence) of these species on the column ($\geq$ 5 p.p.m.) in preliminary experiments and the effluents and eluates were tested for manganese and chromium by a.a.s. (Table I). The peroxide and thiocyanate methods were used for vanadate and molybdate detection, respectively. Uncertain adsorption was sometimes noted when the resins were in the anionic form; reactive adsorption was noted when the resin was in the cationic form. In the latter case, the oxo anions must be repulsed by the resin fixed ions (same charge type) unless reduction occurs. The observation that positively charged reduced ions could be retained on anion-exchange resins can be explained by complex formation. Complex formation of manganese(II), chromium(III), vanadium(VI), and molybdenum(VI) with sulfate has been reported [20], so that reaction and retention of the oxo anions with the sulfite- and thiosulfate-treated resin would be possible; complex formation of the reduced metal ions with sulfate (produced by reaction) could occur because of the high local concentrations of these ligands in the resin bed. In some cases straight ion exchange of anions occurred apparently without reduction.

At pH 7.6 chromate was reduced and adsorbed on the tin(II) resin, but was

adsorbed as an anion on the sulfite and thiosulfate resins. The reduction on the tin(II) resin has the obvious advantage of changing electrostatistically repelled co-ions into attracted counter-ions. When the pH was lowered to 2.1, chromate was also reduced on the sulfite resin, which may be attributed to the pH effect on the oxidation potential of the system and/or the greater extent of displacement of reducing ions from the resins by the increased concentration of acid anions.

As illustrated in Table II, a pH of 3.7 resulted in a higher yield with both the iron(II) and the tin(II) resins. The low pH favors the reduction, and decreases the tendency of the tin and iron species to hydrolyze. However, too low a pH causes appreciable replacement of reducing counter-ions from the resin by protons. Hydrolysis of tin species may account for the poorer performance of the tin(II) resin compared to the iron(II) resin. The iron(II) resin was superior for separations of all four elements. It is easy to prepare and cheap. Molybdate is not adsorbed, so that only the other three oxo anions in the mixture have to be separated on the resin bed. However, the other three reducing resins have proved valuable in other reactive ion-exchange systems and various applications are being investigated.

Fritz *et al.* [21, 22] used 1 % hydrogen peroxide in dilute acid to elute vanadium and some other metal ions which form anionic complexes in the presence of peroxide, from cation exchangers. However, a 1 % peroxide solution produced gas bubbles and caused channelling in the present resin beds. When 0.3 % hydrogen peroxide in 0.01 *M* nitric acid was used as the eluant for vanadium(IV), bubble formation was avoided, and complete separation was achieved. As the peroxide solution percolated down the column, the light yellowish-orange iron(II) resin turned black because of oxidation and perhaps complex formation. (When the iron(II) resin was stored in air for some time, it also darkened gradually until it became black, without significantly losing its reducing ability.) No trace of manganese or chromium, nor even iron (which interferes in most methods of vanadium determination) was found in the 10 ml of eluate. Therefore, vanadium could be successfully preconcentrated and determined at levels as low as 10 p.p.b. at pH 3.7 on the iron(II) cation-exchange resin with recoveries of 90—95 % and standard deviations of 2—6 % (Tables II and III). The use of the spectrophotometric determination with PAR [23] might allow determination of vanadium at the sub-p.p.b. level after preconcentration by the described method.

Manganese(II) was eluted with 25 ml of 0.3–0.4 *M* HCl. The black resin turned back to orange as soon as the acid contacted it. Iron(III) was complexed and eluted with the chloride ions, as was manganese(II). Conventional a.a.s. makes possible the determination of manganese at a level of 2.5 p.p.b. with recoveries of 86—101 % and standard deviations of 3–7 %. The preconcentration and analysis of even lower concentration levels is possible with larger sample volumes. The presence of other ions at 100-p.p.m. levels did not interfere (Table IV).

With vanadium(IV) and manganese(II), (and all iron eluted), only

chromium(III) was left on the resin bed, which was eluted with 4 *M* HCl. The a.a.s. determination of chromium has always been a problem when an air—acetylene flame was used. Many "releasing reagents" have been suggested for eliminating various interferences, but only hydrogen fluoride and sulfate [16] were found satisfactory here. Oxine [17] also significantly enhanced the signal, but signals were not reproducible. Chromium(VI) was preconcentrated from samples containing 2.5 p.p.b. with recoveries from 87 % to 94 % and standard deviations of 2–8 %.

In additional experiments, an alternative way of isolating chromium was found by using 0.1 *M* disodium—EDTA as a complexing eluant. In this case 10 ml sufficed to elute all the vanadium, manganese, and iron, while chromium remained adsorbed quantitatively, because of the slow kinetics of the reaction between EDTA and chromium(III). After three days at room temperature, the purplish chromium—EDTA complex was visible on the column and was simply washed out with a few ml of distilled water. However, the iron present in the first eluate interfered with the determination of trace amounts of vanadium. Also, at the concentration used, EDTA precipitated even though the pH was controlled carefully. When vanadium was eluted first with the peroxide solution, and then EDTA was used as eluant for manganese, some chromium(III) was co-eluted. This may be due to an unknown catalytic effect on the kinetics of chromium(III) chelation in the presence of peroxide. Although the use of EDTA was not pursued further in this study, there will be other situations where kinetic differentiation between chromium(III) and other reduced oxo anions may permit elegant separations and determinations.

Conclusions

The *in situ* reduction with charge reversal of strongly oxidizing anions on resins treated with iron(II) or other suitable ions can be employed to preconcentrate trace concentrations of Mn, Cr, and V as reduced cations so that p.p.b. levels of permanganate, chromate and vanadate can be determined by conventional a.a.s. or u.v.—visible spectrophotometry in aqueous samples. In addition to the separation procedures described, reactive ion exchange offers a variety of ways of differentiating between oxo anions including the application of different rates of chelation for chromium(III).

J.W. Lin wishes to express her appreciation for helpful discussions and other assistance rendered by G.O. Ramseyer.

SUMMARY

A new procedure for simultaneous preconcentration, separation, and determination of permanganate, chromate and vanadate was developed for aqueous solutions containing p.p.b. levels of these anions (and molybdate). The presence of other (non-complexing) ions in p.p.m. concentrations did not inter-

fere. The procedure consisted of reactive adsorption of all three anions as their reduced cations, on iron(II)-treated resin, followed by elution of vanadium(IV) with 0.01 *M* HNO_3/H_2O_2, manganese(II) with 0.35 *M* HCl, and chromium(III) with 4 *M* HCl. Concentration factors of 40 were obtained with 1-l "samples"; 10 p.p.b. concentrations were determined with standard deviations of 4—5 % by a.a.s. and conventional spectrophotometry.

REFERENCES

1 H.G. Cassidy, J. Amer. Chem. Soc., 71 (1949) 402.
2 I.H. Updegraff and H.G. Cassidy, J. Amer. Chem. Soc., 71 (1949) 407.
3 M. Ezrin, I.H. Updegraff and H.G. Cassidy, J. Amer. Chem. Soc., 75 (1953) 1610.
4 H.G. Cassidy, M. Ezrin and I.H. Updegraff, J. Amer. Chem. Soc., 75 (1953) 1615.
5 B. Sansoni, Naturwissenschaften, 39 (1952) 281.
6 R. Winkler and B. Sansoni, Radiochim. Acta, 15 (1971) 65.
7 L. Erdey, J. Inczédy and I. Markovits, Talanta, 4 (1960) 25.
8 J. Inczédy, Acta Chim. (Budapest), 27 (1961) 185.
9 J. Inczédy, Z. Chem., 2 (1962) 302.
10 H. Dalibor, Chem. Ber., 91 (1961) 1955.
11 J.F. Pankow and G.E. Janauer, Anal. Chim. Acta, 69 (1974) 97.
12 J.F. Pankow, D. Leta, J.W. Lin and G.E. Janauer, In preparation.
13 G.E. Janauer, G.O. Ramseyer and J.W. Lin, Anal. Chim. Acta, 73 (1974) 311 (Part I).
14 G.O. Ramseyer and G.E. Janauer, Anal. Chim. Acta, 77 (1975) 133 (Part II).
15 E.B. Sandell, Colorimetric Determination of Traces of Metals, Interscience, New York, 3rd edn., 1965.
16 A. Purushottam, P.P. Naidu and S.S. Lal, Talanta, 20 (1973) 631.
17 J.M. Ottaway and N.K. Pradhan, Talanta, 20 (1973) 927.
18 O. Samuelson, Ion Exchange Separations in Analytical Chemistry, John Wiley, New York, 1963.
19 J. Korkisch, Modern Methods for the Separation of Rarer Metal Ions, Pergamon, Oxford, 1969.
20 L.G. Sillen and A.E. Martell, Stability Constants of Metal—Ion Complexes, Special Publication No.25, The Chemical Society, Burlington House, London, 1971.
21 J.S. Fritz and J.E. Abbink, Anal. Chem., 34 (1962) 1080.
22 J.S. Fritz and L.H. Dahmer, Anal. Chem., 37 (1965) 1272.
23 T. Yotsuyanagi, J. Ito and K. Aomura, Talanta, 16 (1969) 1611.

Analytica Chimica Acta, 79 (1975) 229—236

CHELATING ION-EXCHANGERS CONTAINING N-SUBSTITUTED HYDROXYLAMINE FUNCTIONAL GROUPS PART II. N-ACYLPHENYLHYDROXYLAMINES

F. VERNON and H. ECCLES
The Ramage Laboratories, Department of Chemistry and Applied Chemistry, University of Salford, Salford, M5 4WT, Lancs. (England)
(Received 21st February 1975)

The chelate-forming properties of the linear N-aroyl oxime polymer described earlier [1] appeared promising, and the work was therefore extended to the preparation of a cross-linked N-acyl oxime resin which would be insoluble in alkaline solution. Attempts to convert a cross-linked methacrylic acid bead polymer to the acid chloride, with varying degrees of success, have been described in the literature [2—5]. It was proposed, therefore, to produce the acid chloride of Zeo-karb 226 and to treat it with phenylhydroxylamine to yield an N-acyl oxime chelating resin. Several synthetic methods were tested, but the chelating abilities of the products were unsatisfactory, and alternative methods for the production of cross-linked acid chloride resins were developed. The preparation of the phenylhydroxylamine derivative of such a resin is described, and its chelating properties are compared with those of the N-acyl oxime polymer derived from cross-linked methacrylic acid.

Carboxylic acid chlorides can be produced by treating the acid or its sodium salt with thionyl chloride, benzoyl chloride, or phosphorus oxy-, tri-, and pentachloride. Of these, only thionyl chloride has been used to prepare cross-linked polymeric acid chlorides. Grubhofer and Schleith [2] used thionyl chloride and pyridine to convert a lightly cross-linked methacrylic acid to the acid chloride; analysis for chlorine indicated over 50 % conversion of acid to acid chloride groups. Cornaz and Deuel reported the conversion of a commercial polymethacrylic acid exchanger to the acid chloride form before reaction with hydroxylamine [3], and later discussed the difficulties caused by anhydride formation and suggested the use of a methacrylic acid—methyl methacrylate copolymer for improved acid chloride yields [4].

An attractive alternative is the polymerization of acryloylchloride with a suitable cross-linking agent such as divinylbenzene, for the resulting cross-linked acid chloride polymer will not then be contaminated by carboxylic acid or anhydride groups. A simple preparation of acryloyl chloride has been described by Brown [6], but the production of a cross-linked poly(acid chloride) by this route has not been reported previously. Possible bulk and solution polymerization techniques and catalysts were evaluated; the method

described below gave the best product with regard to both physical characteristics and acid chloride content.

EXPERIMENTAL

Preparation of resins

Conversion of cross-linked methacrylic acid bead polymer to the acid chloride. Vacuum-dried beads of Zeokarb 226 were refluxed with the chlorinating reagent for various times. Details of resin form, bead size and chlorination conditions are given in Table I for eight reactions. After refluxing the excess of thionyl chloride was distilled off under vacuum; for resins 7 and 8 the beads were soaked overnight in phosphorus oxychloride which was then removed by washing with carbon tetrachloride. All resins were washed thoroughly with sodium-dried ether, and then dried under vacuum for at least 2 days.

TABLE I

Conditions for the conversion of Zeo-karb 226 to the acid chloride

Resin	Resin bead mesh	Resin form	Ratio of chlorinating agent to resin	Reflux time (days)
1	14—52	H^+	$SOCl_2$ 5:1	3
2	14—52	Na^+	$SOCl_2$ 5:1	3
3	14—52	H^+	$SOCl_2$ 10:1	3
4	14—52	H^+	$SOCl_2$ 10:1	14
5	100—200	H^+	$SOCl_2$ / C_5H_5N 5:1	8
6	100—200	Na^+	$SOCl_2$ / C_5H_5N 10:1	3
7	100—200	Na^+	$POCl_3$ 20:1	4
8	100—200	H^+	PCl_5 / PCl_3 50:1	7

Conversion of resins 1—4 to acylphenylhydroxylamines. The vacuum-dried polymeric acid chloride was allowed to react with phenylhydroxylamine at room temperature for several days. The solvent, base, ratio of reactants, and reaction time are listed in Table II. After reaction the beads were filtered, washed with acetone, and extracted (Soxhlet) for 18 h with ethanol. The resins were then washed with water, 1 *M* sodium hydroxide, water, 1 *M* hydrochloric acid and water until chloride-free. Nitrogen contents of vacuum-dried samples were determined with a Perkin-Elmer 240 Elemental Analyzer.

Preparation of an acryloyl chloride—styrene—DVB copolymer. Acryloyl chloride (38.2 g), styrene (9.2 g) and divinylbenzene (6.1 g of 54 % solution) were mixed in a Pyrex tube which was then flushed with dry nitrogen and

TABLE II

Coupling conditions for polymeric acid chloride to phenylhydroxylamine

Resin	Solvent system	Base	Phenylhydroxylamine to resin ratio	Reaction time (days)
1	Water	$NaHCO_3$	1:1	2
2	Toluene	C_5H_5N	1:1	5
3	DMF	DMF	2:1	3
4	DMF	DMF	3:2	3

sealed. The tube was irradiated with ultraviolet light for 40 h. As polymerization progressed, the polymer changed from a straw colour to yellow; on breaking the tube in a dry-bag a white polymer surrounded by a glassy yellow polymer was obtained. The material was cooled in liquid nitrogen, and ground to a coarse powder in the dry-bag. A small sample was vacuum-dried over phosphorus pentoxide before determination of chlorine content and equivalent weight, but the bulk of the material was coupled to phenylhydroxylamine.

Coupling of poly(acryloyl chloride) copolymer. The polymeric material (0.3 mole) was suspended in 200 ml of dimethylformamide (previously dried over sodium hydride), 0.6 mole of phenylhydroxylamine was added and the mixture was stirred for 14 days at less than 5 °C. Dry methanol (100 ml) was added and stirring was continued for a further 7 days. The solution was then decanted, and the resin was washed with methanol and extracted (Soxhlet) with methanol for 18 h. Finally, the resin was washed with water, 1 *M* hydrochloric acid, and water until chloride-free, and allowed to air-dry before being crushed and sieved. A small sample was vacuum-dried for elemental analysis; the 30—60 mesh particles were used for metal ion capacity determinations.

Metal ion capacities

The capacities for iron(III), iron(II), vanadium, copper, nickel, cobalt, mercury and lead were determined for the oxime—carboxyl resin derived from acryloyl chloride. Conditions for the determination of the capacities for the first four ions were described previously [1]. The same technique was used for nickel and cobalt capacities, nickel being determined colorimetrically with dimethylglyoxime [7] and cobalt by the thiocyanate—acetone method [7]. For mercury(II) acetate and lead nitrate, both the metal ion and acetate concentrations were as before [1], but sodium nitrate was added to give a total ionic strength of 3.0. Mercury(II) was determined by the zincon method [8], whereas eluted lead(II) was determined by atomic absorption spectrometry. Mercury and lead ions were eluted from the resin with 6 *M* acetic acid; nickel was eluted with 2 *M* sulphuric acid as previously described for other ions; vanadium was eluted with 4 *M* sulphuric acid.

RESULTS

Preparation of resins

Attempts to convert a cross-linked methacrylic acid ion-exchanger to the acid chloride form in high yield were unsuccessful. Although published methods were followed exactly, reflux with thionyl chloride or thionyl chloride—pyridine mixtures gave very poor yields of acid chloride polymer (Tables III and IV, resins 1—6). Resins 1—4 were taken through the procedures to the expected oxime—carbonyl resins, the conditions being varied as indicated in the Tables to achieve the best yields, but these phenylhydroxylamine resins contained a large number of carboxylic acid groups and had virtually no chelating capacity. The capacity of a polymethacrylic acid for vanadium is negligible below pH 6, whereas the oxime—carbonyl unit shows a high affinity for vanadium; the vanadium capacity can thus be used as a measure of the oxime—carbonyl groups introduced. Resins 1—4 contain nitrogen, but the vanadium and iron capacities indicate that this is not present as oxime—carbonyl except for resin 1.

The conversion to a polymeric acid chloride was examined further (resins 5—8), and the products were analysed for chloride and equivalent weight. Table IV shows that treatment of a cross-linked polymethacrylic acid with

TABLE III

Analysis and properties of acyl—phenylhydroxylamine resins from Zeo-karb 226

Resin	Nitrogen content (%)	Free carboxylic acid groups (mmole g^{-1})	mmole g^{-1} of chelating unit (from nitrogen)	Vanadium capacity (mmole g^{-1})	Iron capacity (mmole g^{-1})
1	1.5	8.2	1.0	0.05	0.16
2	3.2	6.8	2.3	<0.01	<0.01
3	6.3	4.4	4.5	<0.01	<0.01
4	4.6	5.9	3.3	<0.01	<0.01

TABLE IV

Analysis of acid chloride resins produced from Zeo-karb 226

Resin	Chlorine content (%)	Total Na^+ capacity (mmole g^{-1})	Free carboxylic acid groups (mmole g^{-1})
5	0.64	10.1	10.0
6	2.1	10.8	9.6
7	2.1	10.9	9.7
8	16.1	9.0	0

thionyl chloride—pyridine did not yield an acid chloride polymer (theor. 34 % Cl). Grubhofer and Schleith [2] used this method and obtained a chloride content of 19.3 % for the product; Cornaz *et al.* [3,4] reported 5—17 % conversions to poly(acid chloride), but their products also contained free acid groups. Petrie *et al.* [5] used the acid chloride route to prepare hydroxamic acid resins by reaction with hydroxylamine, the product containing 3.9 % nitrogen (*i.e.* 28 % overall yield). However, resins 3 and 4 (Table III) contain higher percentages of nitrogen than this, but do not show any chelating ability. As a model, adipic acid was treated with thionyl chloride; the conversion to adipoyl chloride was only 25 %, and it is unlikely that conversion of polymeric acids to acid chlorides will approach this value. Only resin 1 showed any chelating ability for vanadium at pH 3.0, thereby proving the existence of the oxime—carbonyl unit in the polymer.

Of the other attempts to convert the poly(methacrylic acid) to the acid chloride, only resin 8 in Table IV is worth noting. This resin was prepared by heating with phosphorus pentachloride and trichloride, and washed thoroughly by the procedure described under Experimental. The high chlorine content (16.1 %) and the absence of residual carboxylic acid groups suggests that this may be the best technique for the preparation of poly(acid chlorides). However, the total sodium capacity of the product decreased to 9.0 mmole g^{-1} from 9.7 mmole g^{-1} for the original material; decarboxylation could have occurred at the reaction temperature of 150 °C, and the high chlorine content may be due in part to inadequate washing.

Polymerization of acryloyl chloride

Initial attempts to prepare an acryloyl chloride—DVB polymer in carbon tetrachloride with azobisisobutyronitrile (azoB) gave an 18 % yield, the polymer being an amorphous white powder. Bulk polymerization of an acryloyl chloride—DVB mixture with azoB was unsuccessful but the mixture polymerized readily under ultraviolet irradiation. A linear poly(acryloyl chloride) was produced in 95 % yield by this method (38.8 % Cl found, theor. 39.2 %; equivalent weight 44.7, theor. 45.3), but the bulk polymerized copolymer was too rubbery for practical use. Styrene was therefore incorporated to increase the rigidity. The acryloyl chloride—styrene—DVB copolymer described in the Experimental section, was treated under anhydrous conditions with phenylhydroxylamine below 5 °C to prevent degradation; treatment with anhydrous methanol then converted unreacted acid chloride groups to ester groups, so that the polymer should contain no free carboxylic acid units. Consequently, any chelating ability of this polymer should be due to oxime—carbonyl units.

Table V gives the capacities for copper, cobalt, iron and vanadium from acetate buffers alone and in the presence of citrate as a competing ligand; (for comparison, the capacities obtained for a cross-linked poly(methacrylic acid) are also listed.) The capacity *versus* pH contours were similar to those reported previously [1] for the aroylhydroxylamine polymer; but the capacities were

TABLE V

Metal capacities of a cross-linked styrene—acryloylphenylhydroxylamine copolymer (SAPHA) and of cross-linked poly(methacrylic acid) (PMA)

Ion	Metal capacities from acetate media (mmole g^{-1})		Metal capacities in the presence of citrate (mmole g^{-1})	
	SAPHA	PMA	SAPHA	PMA
Cu	3.1	3.6	0.8	0.01
Co	1.2	2.1	0.7	0.01
Fe(III)	0.2	1.0	0.1	0.01
V(V)	0.45	0.01	—	0.01

higher for copper and cobalt and lower for iron(III) and vanadium(V). The nitrogen content of the product (2.6 %) indicated a theoretical total capacity of 1.83 mmole g^{-1}, but the capacity for sodium ions was 5.3 mmole g^{-1}, showing that carboxylic acid groups were in fact still present. The nitrogen content of 2.6 % indicates that the coupling reaction with phenylhydroxylamir was only 38 % efficient.

The free carboxylic acid groups explain why the capacities for copper and cobalt were unusually high. In the presence of citric acid as a competing ligand at pH 6, the copper and cobalt capacities were much lower. The values given in Table V indicate that the acylphenylhydroxylamine polymer produced had total capacity values (from the oxime—carbonyl grouping) similar to those of the aroylphenylhydroxylamine polymer [1]. The effective oxime—carbonyl content was *ca.* 0.5 mmole g^{-1}, but the value obtained from vanadium capacity at pH 6 was 0.45 mmole g^{-1}.

Figure 1 shows the capacity *versus* pH contours for nickel, lead and mercury(II) ions, which were not studied with the previous oxime—carbonyl exchanger. The contour for nickel is almost identical with that for cobalt;

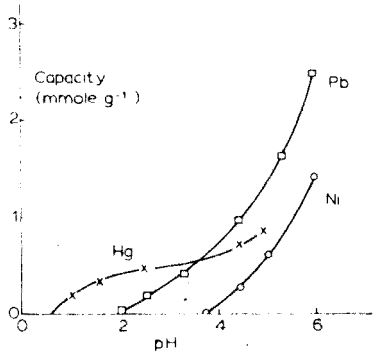

Fig.1. Resin capacity versus pH curves for nickel, mercury(II) and lead ions from acetate media.

the very slight displacement to lower pH indicates that the nickel complex has a slightly higher stability constant than the cobalt complex.

Column operation

Differences in the behaviour of mercury(II) and lead ions at low pH indicated that a separation of these ions should be possible. A sodium nitrate solution (1 l; total ionic strength 3.0) containing 5 mg of mercury as mercury(II) acetate and 10 mg of lead as lead nitrate was prepared and its pH adjusted to 1.5 with 1 *M* nitric acid. A 10-cm column of the resin was pre-equilibrated by allowing 1 l of a sodium nitrate—nitric acid solution, pH 1.5, to pass through the column. The mercury(II) and lead solution (1 l) was then passed through the column at a rate of 2.5 ml min^{-1}, after which the column was washed with 100 ml of the sodium nitrate—nitric acid blank. The washings and eluate were combined and lead was determined by atomic absorption spectrometry. The recovery of lead from the column was quantitative. The column was then washed with 50 ml of 6 *M* acetic acid followed by deionized water until the total volume of eluate was 100 ml. The recovery of mercury, determined by the zincon method, from the column was found to be 90 %. Further column washings, with 6 *M* acetic acid, were found to be mercury-free, demonstrating that the missing 10 % of mercury had passed through the column with the lead. It should therefore be possible, by more precise control of the flow rate, pH and column length, to separate mercury and lead quantitatively with this exchanger. Das and Shome [9] have reported that mercury is extractable with BPHA in chloroform above pH 2.8; these results indicate that the acryloyl derivative forms a mercury(II) complex of similar or greater stability than that formed by BPHA.

CONCLUSIONS

The preparation of a cross-linked polymeric chelate incorporating an N-acylphenylhydroxylamine group was partially successful. The polymer did, however, have free carboxylic acid groups which sometimes contributed towards and complicated the metal ion capacities. Capacities similar to those previously reported for a linear oxime—carbonyl polymer were observed; the vanadium capacity at pH 6 was taken as an assessment of the oxime—carbonyl function and was found to be 0.45 mmole g^{-1}. Anomalously high capacities for copper and cobalt can be explained in terms of the carboxylic acid content of the resin. In the presence of citrate as a competing ligand, the carboxylic unit would not be sufficient to remove ions from solution and the capacity values from citrate solution confirm this. The resin is capable of separating mercury(II) and lead ions at low pH with preferential retention of mercury by the column. It should be particularly suitable for column work as it has a relatively rapid rate of equilibration. The time to half-saturation (for copper ions) was 27 min whilst the $t_{½}$ of the Zeokarb 226 carboxylic acid

was found to be 42 min under similar conditions.

The conversion of polymeric acid chlorides to acyl—phenylhydroxylamine chelating ion exchangers appears to be limited by the slow rate of interaction of the solid acid chloride with a phenylhydroxylamine solution. Satisfactory conversions were not obtained, and the lengthy periods of interaction are limited by a certain lack of stability in phenylhydroxylamine, which tends to rearrange to an aminophenol.

The much more reactive parent compound, hydroxylamine, should react readily with the acid chlorides with the production of poly(hydroxamic acids) which should exhibit interesting ion-exchange properties and have high capacities. Work on the production of such chelating ion exchangers will be reported in Part III in this series.

SUMMARY

The problems associated with the conversion of commercial carboxylic acid ion exchangers to the acid chloride have been studied and a synthesis of a cross-linked poly(acryloyl chloride) is described. Reaction with phenylhydroxylamine produced a chelating ion exchanger, possessing acyl oxime functional groups, whose properties are compared with those of an aroyl oxime exchanger described earlier. Resin capacity from the acyl oxime group was 0.45 mmole g^{-1}, and the resin had a rapid equilibration rate. A column separation of mercury and lead is discussed.

REFERENCES

1 F. Vernon and H. Eccles, Anal. Chim. Acta, 77 (1975) 145.
2 N. Grubhofer and L. Schleith, Naturwissenschaften, 40 (1953) 508.
3 J.P. Cornaz and H. Deuel, Experimentia, 10 (1954) 137.
4 J.P. Cornaz, K. Hutschneker and H. Deuel, Helv. Chim. Acta, 40 (1957) 2015.
5 G. Petrie, D. Locke and C.E. Meloan, Anal. Chem., 37 (1965) 919.
6 H.C. Brown, J. Amer. Chem. Soc., 60 (1938) 1325.
7 M. Pinta, Detection and Determination of Trace Elements, IPST, Jerusalem, 1966.
8 A.G. Morris, Analyst (London), 82 (1957) 34.
9 B. Das and S.C. Shome, Anal. Chim. Acta, 35 (1966) 337.

Analytica Chimica Acta, 79 (1975) 237—241

EXTRACTION OF IRON(III) DITHIZONATE

Yu.A. ZOLOTOV, O.A. KISELEVA, N.V. SHAKHOVA and V.I. LEBEDEV

Vernadsky Institute of Geochemistry and Analytical Chemistry, Academy of Sciences, Moscow (U.S.S.R.)

(Received 11th March 1975)

It is believed that iron(III) does not form a complex with dithizone and that large amounts of iron(III) oxidize the reagent [1—4]. However, Carlton and Bradbury [5] who investigated the interaction of dithizone with elements in molten naphthalene, described a coloured reaction with iron(III). Zolotov *et al.* [6] assumed that the absence of iron(III) dithizonate extraction is explained by the formation of a cationic complex. In fact, when a large anion (tetraphenylborate) is introduced into the dithizone—iron(III) system at pH 7.0—8.5, iron passes into the organic phase. Extraction of iron(II) dithizonate is possible over the pH range 7—9; in the opinion of the authors [6], iron(III) is not reduced under the conditions used, and iron(III) dithizonate is extracted. Later, Marczenko and Mojski [7], on investigating iron(III) and (II) dithizonates, noted again the lack of a dithizone compound with iron(III). Hence, it seemed expedient to investigate in more detail the possibility of this dithizonate formation.

EXPERIMENTAL

Reagents and solutions

The initial $1.2 \cdot 10^{-3}$ *M* iron(III) solution was prepared by dissolving freshly precipitated iron hydroxide in 6 *M* hydrochloric acid [8], and standardized by a complexometric method. The ^{59}Fe radioisotope was purified by extraction with diethyl ether from 6 *M* hydrochloric acid. Solutions of other elements were prepared by dissolution of accurately weighed amounts of salts (reagent grade). Sodium tetraphenylborate solution (0.2 *M*) was prepared by dissolving the reagent in isoamyl alcohol. Standard dithizone solutions were prepared from purified dithizone [1] by dissolving precisely weighed amounts in the organic solvent, *e.g.* distilled chloroform solvents were purified by known procedures [9].

Procedure

To an aliquot of ^{59}Fe-labelled iron(III) solution, were added 2 ml of 0.01 *M* dithizone solution in an organic solvent, a solution of the compound providing

the required anion, a sodium hydroxide solution to obtain the necessary pH, and enough water to adjust the total volume of the aqueous phase to 2 ml. Extractions were done in 10-ml glass-stoppered test tubes for 30 min in an air thermostat at 25±1 °C. After phase separation, the γ-activity of aliquots of two phases was measured by a scintillation counter with a NaI(Tl) crystal. The percentage of iron extracted (R %) and the distribution coefficient (D) were calculated from the measurements.

RESULTS AND DISCUSSION

Extraction of iron

Extraction of iron in the presence of dithizone and a number of anion-partners was studied in order to check assumptions about the existence of iron dithizonate in the form of a complex cation. Capric, benzenesulfonic and 2-naphthalenesulfonic acids, sodium acetate, sodium tetraphenylborate and lithium chloride of different concentrations were used to provide the anions. Iron was extracted with carbon tetrachloride, chloroform, or 1,2-dichloroethane.

Addition of capric acid (0.2 M) ensured iron extraction at pH 5—7 (Fig.1). Capric acid alone was a reasonably good extractant for iron in the pH range investigated. However, the absorption spectra of the extracts showed that in the presence of dithizone iron passed into the organic phase as its dithizonate (the maximum of the absorption spectrum is at 520 nm, as for many other dithizonates).

Sodium acetate forms no extractable compound with iron, but in the presence of dithizone, the results were similar to those obtained with capric acid. In the presence of 0.2 M sodium acetate, iron was extracted almost completely (Fig.2). Iron extraction in the presence of acetate was investigated as a func-

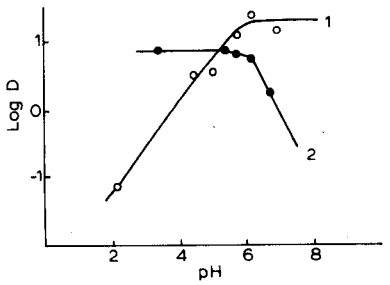

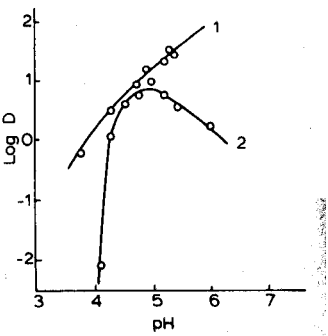

Fig.1. Iron extraction in the presence of 0.2 M capric acid by 0.01 M dithizone in dichloroethane (1) and by 0.2 M capric acid in dichloroethane (2).

Fig.2. Iron extraction in the presence of 0.2 M sodium acetate by 0.01 M dithizone in dichloroethane (1) and chloroform (2).

tion of dithizone concentration. The slope of the straight line obtained in the log D—log [H_2Dz] plot was 2.

In the presence of 0.2 M lithium chloride, iron was not extracted by dithizone. Addition of benzenesulfonic or 2-napthalenesulfonic acid, or of sodium tetraphenylborate -- all of which are large anions -- ensured extraction of iron, the percentage extraction increasing in the indicated sequence of compounds. Maximum extraction occurred in the presence of tetraphenylborate (Fig.3). Because of the poor solubility of sodium tetraphenylborate in water, this reagent was introduced as a solution in isoamyl alcohol, so that relatively high concentrations could be used. In the presence of sodium tetraphenylborate the percentage iron extraction increased in the series carbon tetrachloride < chloroform < 1,2-dichloroethane (Fig.4).

Equilibrium was attained in the systems during a phase contact of 30 min. If the phase contact exceeded 2 h, the complex began to decompose.

The data obtained suggest that in the reaction of iron(III) with dithizone, the cation $Fe(HDz)_2^+$ is formed, and this is extracted as an ion associate with a suitable anion. The fact that such ion associates can be extracted in systems containing acetate and sulfonates with inert solvents (chloroform, dichloroethane) apparently indicates that the cation does not contain coordinately bound water molecules.

Electrophoresis of the extracts confirmed that iron(III) was extracted in the cationic part of the ion associate. The iron activity in the cathodic space increased from 2 500 to 3 000 c.p.m. as the time of electrophoresis increased from 4 to 8 h, while the activity in the centre decreased from 1120 to 700 c.p.m. The activity in the anodic space decreased to zero.

Metal-containing anions can also act as the ion associate if this metal ion does not form stable dithizonates. Such metal-containing complex anions then

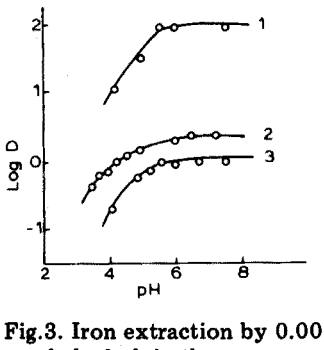

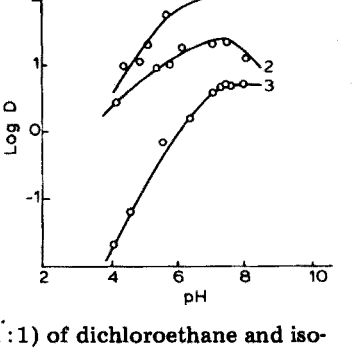

Fig.3. Iron extraction by 0.005 M dithizone in a mixture (1:1) of dichloroethane and isoamyl alcohol, in the presence of sodium tetraphenylborate (1), naphthalenesulfonic acid (2), and benzenesulfonic acid (3).

Fig.4. Iron extraction in the presence of 0.1 M sodium tetraphenylborate in isoamyl alcohol by 0.005 M dithizone in dichloroethane (1), chloroform (2), and carbon tetrachloride (3).

influence the extraction of iron. Perrhenate was selected as a suitable anion for testing; Fig.5 shows that the perrhenate ion indeed favours extraction of iron(III). Analysis of the organic phase proved that rhenium was coextracted with iron in a 1 : 1 ratio. In tests with different amounts of iron(III) varying from 0.6 to $6 \cdot 10^{-5}$ *M*, the Re : Fe ratios found varied from 0.9 to 1.2, with no significant trend in the results. Under the conditions for extraction of iron dithizonate, rhenium (without iron) is not extracted as the dithizonate, thus in the presence of iron(III), this element is probably extracted only as the perrhenate ion. The ion associate $Fe(HDz)_2^+ ReO_4^-$ is probably extracted.

Isolation and determination of iron

The possibility of isolation of iron(III) with dithizone is of importance as it increases the number of elements extractable with this widely used reagent. According to the data obtained here, iron(III) is most completely extracted by a 0.01 *M* solution of dithizone in chloroform at pH 7—8 in the presence of 0.1 *M* sodium tetraphenylborate, which is introduced as a solution in isoamyl alcohol. According to the literature, the dithizonates of Au, Bi, Cd, Co, Cu, Hg, Pb, Zn and Sn are extracted at pH 7—8. It is of interest to ensure the simultaneous isolation of iron(III) and of all these elements, with their subsequent determination by atomic-absorption spectrometry.

Because the isolation conditions for the dithizonates of Au, Bi, Cd, Co, Cu, Hg, Pb, Zn, and Sn are well known, only the extraction behaviour of iron(III) in the presence of these elements was examined. It was established that all the elements listed, at concentrations of 10^{-6}—10^{-4} *M*, did not interfere with the extraction of iron and its determination when the extract was introduced into the flame.

Procedures for the isolation of iron from solutions of sodium and potassium chlorides with its subsequent determination by atomic-absorption spectrometry were worked out. A 0.2 *M* solution (2.5 ml) of sodium tetraphenylborate in isoamyl alcohol and 2.5 ml of a 0.01 *M* solution of dithizone in

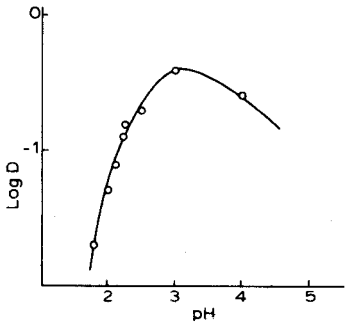

Fig.5. Iron extraction by 0.01 *M* dithizone solution in chloroform in the presence of 0.06 *M* NH_4ReO_4.

chloroform were added to 5 ml of 0.4 *M* sodium or potassium chloride solution, and the mixture was mechanically shaken for 30 min. Iron was determined in the extract with a Perkin Elmer model 403 atomic-absorption spectrophotometer. Standard solutions containing iron over the range 0.1—10 $\mu g\ ml^{-1}$ in the isoamyl alcohol—chloroform mixture were sprayed into an air — acetylene flame. The consumption of the solution was 2.2 ml min^{-1}, the air flow was 21 l min^{-1} and the acetylene flow was 4 l min^{-1}. To estimate the precision, 10 samples were analysed and the same number of blank measurements were carried out. A statistical treatment of the results showed that the data from the determination were quite satisfactory.

SUMMARY

The extraction of iron(III) with dithizone in the presence of different anions, was studied. The complex cation $Fe(HDz)_2^+$ formed is extracted in the presence of sodium acetate and tetraphenylborate or capric acid as an ion associate, $Fe(HDz)_2^+ X^-$, where X^- is the anion of the indicated compounds. In the presence of perrhenate ion, rhenium is coextracted with iron in a 1 : 1 ratio; the ion associate $Fe(HDz)_2^+ ReO_4^-$ is apparently extracted. The isolation of iron from alkali metal chlorides and its atomic-absorption determination is described.

REFERENCES

1 J. Starý. The Solvent Extraction of Metal Chelates, Pergamon Press, Oxford, 1964.
2 Z. Marczenko, Photometrichescoe Opredelenie Elementov (Photometric Determination of Elements), Mir, Moscow, 1971.
3 E.B. Sandell, Colorimetric Determination of Traces of Metals, Interscience, New York, 1959.
4 G. Iwantscheff, Das Dithizon und seine Anwendung in der Mikro- und Spurenanalyse, Verlag Chemie, Weinheim, 1958.
5 I.K. Carlton and W.C. Bradbury, Anal. Chem., 26 (1954) 1226.
6 Yu.A. Zolotov, O.M. Petrukhin and N.M. Kuzmin in I.P. Alimarin (Ed.), Chemicheskie Osnovy Extractzionnogo Metoda Razdeleniya Elementov (Chemical Bases of the Extraction Method of Element Separation), Nauka, Moscow, 1966, p.28.
7 Z. Marczenko and M. Mojski, Chem. Anal. (Warsaw), 53 (1971) 529.
8 V.I. Kuznetsov, Yu.A. Bankovsky and A.F. Ievinsh, Zh. Anal. Khim., 13 (1958) 267.
9 A. Weisberger, E.S. Proskauer, J.A. Riddick and E.E. Tups, Organic Solvents, Physical Properties and Methods of Purification, Interscience, New York, 1955.

Analytica Chimica Acta, 79 (1975) 243—256

ANALYTICAL INTERFERENCE EFFECTS ON LASER-INDUCED FLUORESCENCE OF ETHYLENE BY SELECTED MOLECULAR SPECIES

J.W. ROBINSON and N. KATAYAMA
Chemistry Department, Louisiana State University, Baton Rouge, Louisiana 70803 (U.S.A.)
(Received 17th February 1975)

Laser-induced infrared fluorescence has been proposed as a method of monitoring air pollution [1—3]. To date few applications have been reported because of lack of analytical instrumentation. Physicochemical applications of the technique have been reported [4—36], with the number of studies rapidly increasing since 1967.

Before the laser-induced infrared fluorescence technique can be used as a method of molecular analysis, possible analytical interferences must be studied. It is well known that vibrationally excited molecules transfer their vibrational energies to other molecules by collision [37—39], and that vibrational—vibrational and/or vibrational—rotational/translational energy transfers can occur intermolecularly. Collisional deactivation of excited molecules can cause quenching of the expected fluorescence. However, when the molecule of interest becomes excited through collision, an increased fluorescence signal may result. Studies of collisional deactivation of laser fluorescence have been made for ethylene [5,40], methane [6], fluoromethane [7,8], chloromethane [9], carbon monoxide [10—13], ozone [14,15], hydrogen fluoride [16—18], deuterium fluoride [17], hydrogen chloride [19—21], nitric oxide [22,23], nitrous oxide [24], carbonyl sulfide [25], and sulfur hexafluoride [26,27]. A few collisional activation studies have been reported [8,22,25,33,41—44]. All of these studies, except one [41], involved systems at very low pressures rather than at atmospheric pressure and all studies except two [40,41] considered the process from a physicochemical viewpoint.

The early collisional deactivation studies used either methane, triatomic molecules such as H_2O and CO_2, diatomic molecules such as N_2, O_2 and H_2, or a rare gas as a collision partner for the laser excited molecules. The aim was to understand the mechanism of the energy transfer between the two colliding molecules. The mechanism was deduced from the deactivation rate, obtained by observing the fluorescence decay curve of the excited molecules. Collisional deactivation of excited molecules can occur via vibrational—vibrational or vibrational—rotational/translational energy transfer. In the vibrational—vibrational process, the vibrational energy of excited molecules is transferred to vibrational energy in the colliding molecules as a result of their collision. In the second process, (vibrational—rotational/translational),

the vibrational energy of the excited molecules is transferred to the collision partner and appears as rotational or translational energy. In general, the two processes have similar deactivation rates [39] and are thus not easily separable.

When rare gases are used as collision partners, only vibrational—rotational/translational transfer can occur as these monoatomic species have no vibrational or rotational energy states. A deeper understanding of the mechanism can be achieved by using light diatomic molecules such as H_2 or D_2, especially since these molecules have quite different quenching effects [36]. The fluorescence decay curves become more complicated as the deactivating species become more complex. Seldom is it possible to obtain much information about the energy transfer process from complex decay curves. Since mechanisti studies would be prohibitively difficult for systems as complex as the atmosphere, more elementary interference studies were undertaken. Of interest were (a) how greatly the O_2 and N_2 in the air and (b) how other added compounds would effect the fluorescence of a fluorescing compound. To this end a study was made of the effect of twenty-three compounds on the 10.6-μm fluorescence of ethylene with three cell atmospheres, nitrogen, air, and vacuum

EXPERIMENTAL

Reagents

The reagents used as collision partners were as follows (the source and grade are given in brackets) and they were used without further purification: acetaldehyde (Matheson, Coleman, and Bell, reagent grade), acetylene (Matheson, C.P.), air (Woodward Wight Big Three, 20.90 % O_2, 78.13 % N_2, 0.93 % Ar, 67 p.p.m. H_2O, 8 p.p.m. CH_4, 1 p.p.m. H.C., 40 p.p.m. CO_2), argon (Woodward Wight Big Three, 99.985 %), benzene (Mallinckrodt, analytical reagent), 1-butene (Matheson, C.P.), carbon dioxide (Matheson, C.P.), carbon tetrachloride (Mallinckrodt, analytical reagent), chloroform (Mallinckrodt, analytical reagent), cyclohexane (Matheson, Coleman, and Bell, research grade), ethyl acetate (Mallinckrodt, analytical reagent), ethanol (U.S.I., reagent quality), ethylene (Matheson, C.P.), ethyl ether (Mallinckrodt, analytical reagent), helium (Matheson, C.P.), heptane (Matheson, Coleman, and Bell, research grade), hexane (Matheson, Coleman, and Bell, research grade), methane (Matheson, C.P.), methanol (Mallinckrodt, analytical reagent), nitric oxide (Matheson, C.P.), nitrogen (Woodward Wight Big Three, 99.993 %), nitrogen dioxide (Matheson, C.P.), oxygen (Woodward Wight Big Three, 99.9 %), propane (Matheson, C.P.), propylene (Matheson, C.P.), and sulfur dioxide (Matheson, anhydrous).

Equipment

A quasi-c.w. CO_2 gas laser (Perkin-Elmer Model 6200) with a principal lasing mode of 10.6 μm and a 10-mm beam diameter, was used as the excita-

tion source. The laser power was stabilized at 30 W. Fluctuation of the power during the experiments was less than 5 %.

A Beckman Model IR-10 with a Beckman thermocouple detector was employed. The preamplifier of the Beckman IR-10 and a Princeton Applied Research, Model 124, lock-in amplifier with a PAR, Model 116 preamplifier, were used.

Fluorescence cells

The Pyrex glass cell is shown in Fig.1. Laser beam transmission through this cell was provided by two 1-in. diameter Irtran-2 (Eastman Kodak) windows. Another Irtran-2 window (1.5-in. diameter) was provided for observation of fluorescence. This cell was used for the experiments with SO_2, NO, and NO_2, and the cell was externally cooled.

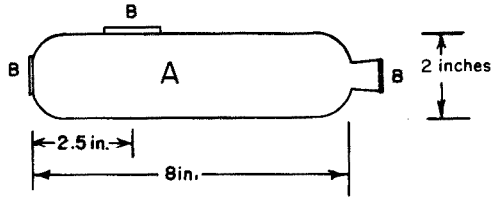

Fig.1. A, Glass cell body. B, Irtran windows.

For all experiments except with SO_2, NO, and NO_2, a water-cooled brass cell (Fig.2) was used. The brass cylindrical cell had a capacity of 490 ml and was fitted with a water cooling jacket. Irtran-2 windows (1.5-in. diameter) were employed for the entrance and exit of the laser beam as well as for the observation of fluorescence.

A Coherent Radiation, Model 201, was used to monitor the laser power.

The optical arrangement is shown in Fig.3.

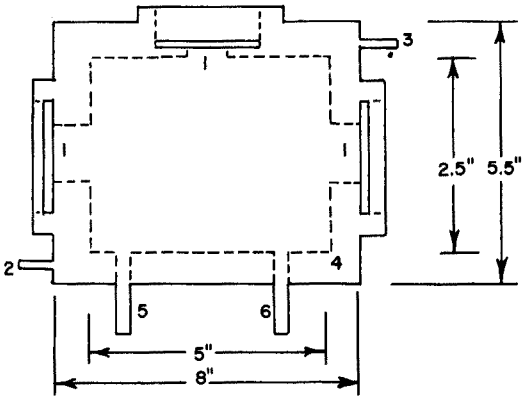

Fig.2. Water-cooled cell. (1) Irtran. (2) Windows. (2, 3) Water inlet and outlet. (4) Water jacket. (5, 6) Sample inlet and outlet.

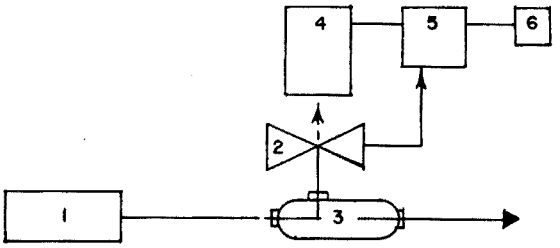

Fig.3. Optical arrangement. (1) Perkin—Elmer laser. (2) Chopper. (3) Fluorescence cell. (4) Monochromator and detector. (5) Amplifier. (6) Recorder. The chopper was placed between the fluorescence cell and monochromator, resulting in the total signal, both fluorescence and thermal radiation, being modulated.

Procedures

Experiments were conducted with atmospheres in the cell of nitrogen and air at atmospheric and at low pressure (≃0.5 torr). The nitrogen-filled cell was prepared by flowing nitrogen through activated charcoal to remove impurities and then through the cell for 10 min to ensure complete flushing. The cell wa then sealed and ethylene injected with a syringe. The air-filled cell was prepar in the same manner. For the vacuum system, the cell was evacuated, flushed with ethylene, and then re-evacuated for 10 min.

Ethylene fluorescence was measured at 10.4 μm. Ethylene concentration in all cases was adjusted to 0.4 % by volume, corresponding to 3 torr of ethylene for the vacuum experiments. First the fluorescence intensity of pure ethylene, I_{f_0}, was measured. Various amounts of a second compound were then added to the cell, and the fluorescence intensity of the ethylene in the gas mixture, I_f, was measured. Each measurement was made at least five times and I_f/I_{f_0} was calculated for each case.

In order to study quenching effects of some compounds on ethylene fluorescence more clearly, separate experiments on the foreign gas were done at higher pressure (up to atmospheric pressure). To the evacuated water-cooled cell, a pressure of 15 torr ethylene was introduced and the fluorescence intensity at 10.4 μm was recorded. Then various amounts of helium, methane, air, nitrogen, argon or propane were added to the cell until the total pressure of the cell was near atmospheric pressure. A calibrated pressure gauge was used to determine the pressure of added gases.

RESULTS AND DISCUSSION

Results showed that the fluorescence intensity obtained at reduced pressur was quite different from that obtained in the presence of nitrogen or air at atmospheric pressure. Table 1 shows that similar results were obtained whether nitrogen or air atmospheres were used. In these atmospheres, within experimental error, no interference was observed from propane, hexane,

TABLE 1

Fluorescence intensity ratio, I_f/I_{f_0}, for gases at various concentrations in different cell systems
(Ethylene concentration = 0.4 % by volume or 3 torr; fluorescence measured at 10.6 μm. Results are given for cells filled with nitrogen or air, or with sample at reduced pressure.)

Gas	% Gas phase vol. added	I_f/I_{f_0} (Nitrogen)	I_f/I_{f_0} (Air)	I_f/I_{f_0} (Low pressure)
CH_4	0	1	1	1
	0.2	0.91 ± 0.06[a]	0.93 ± 0.12	0.85 ± 0.09
	0.4	0.92 ± 0.06	0.92 ± 0.12	0.66 ± 0.08
	0.6	0.87 ± 0.06	0.89 ± 0.12	0.58 ± 0.08
	0.8	0.86 ± 0.06	1.00 ± 0.13	0.57 ± 0.07
	1.0	0.84 ± 0.06	0.76 ± 0.11	0.46 ± 0.07
Propane	0	1	1	1
	0.2	1.00 ± 0.09	0.95 ± 0.12	1.13 ± 0.17
	0.4	1.00 ± 0.09	1.01 ± 0.12	1.01 ± 0.16
	0.6	1.04 ± 0.09	0.96 ± 0.12	1.07 ± 0.16
	0.8	1.00 ± 0.09	0.90 ± 0.11	0.95 ± 0.05
	1.0	0.89 ± 0.09	0.98 ± 0.12	1.03 ± 0.16
Hexane	0	1	1	1
	0.2	0.97 ± 0.16	1.07 ± 0.07	0.99 ± 0.18
	0.4	1.00 ± 0.17	0.97 ± 0.06	0.79 ± 0.10
	0.6	1.07 ± 0.18	0.96 ± 0.06	0.80 ± 0.22
	0.8	0.98 ± 0.16	1.11 ± 0.06	0.52 ± 0.08
	1.0	0.99 ± 0.17	1.04 ± 0.07	0.47 ± 0.08
Heptane	0	1	1	1
	0.2	0.93 ± 0.10	0.96 ± 0.12	0.91 ± 0.07
	0.4	0.90 ± 0.10	0.99 ± 0.13	0.61 ± 0.06
	0.6	1.03 ± 0.11	0.96 ± 0.12	0.80 ± 0.08
	0.8	1.11 ± 0.11	0.99 ± 0.13	0.75 ± 0.07
	1.0	1.06 ± 0.09	1.03 ± 0.13	0.79 ± 0.07
Propylene	0	1	1	1
	0.2	1.52 ± 0.21	1.72 ± 0.22	2.00 ± 0.28
	0.4	2.29 ± 0.27	2.34 ± 0.28	2.76 ± 0.33
	0.6	2.90 ± 0.40	3.09 ± 0.42	3.55 ± 0.60
	0.8	3.60 ± 0.46	3.64 ± 0.47	3.86 ± 0.63
	1.0	4.19 ± 0.51	4.54 ± 0.54	4.76 ± 0.69
	1.2	—	5.23 ± 0.60	—
1-Butene	0	1	1	1
	0.2	1.31 ± 0.14	1.45 ± 0.22	1.56 ± 0.29
	0.4	1.53 ± 0.17	1.64 ± 0.24	2.09 ± 0.34
	0.6	1.83 ± 0.26	1.81 ± 0.26	2.78 ± 0.40
	0.8	2.06 ± 0.27	2.11 ± 0.29	3.57 ± 0.46
	1.0	2.45 ± 0.30	2.53 ± 0.32	3.76 ± 0.75
C_2H_2	0	1	1	1
	0.2	0.96 ± 0.09	1.04 ± 0.16	0.98 ± 0.10
	0.4	0.99 ± 0.10	1.06 ± 0.16	1.04 ± 0.11
	0.6	0.99 ± 0.10	0.99 ± 0.15	0.93 ± 0.10
	0.8	1.02 ± 0.10	1.02 ± 0.15	0.96 ± 0.10
	1.0	1.02 ± 0.10	1.02 ± 0.15	0.96 ± 0.10

TABLE 1 (*continued*)

Gas	% Gas phase vol. added	I_f/I_{f_0} (Nitrogen)	I_f/I_{f_0} (Air)	I_f/I_{f_0} (Low pressure)
Benzene	0	1	1	1
	0.2	0.99 ± 0.17	1.10 ± 0.21	0.79 ± 0.12
	0.4	1.01 ± 0.17	1.00 ± 0.20	0.62 ± 0.11
	0.6	0.97 ± 0.17	1.02 ± 0.20	0.56 ± 0.10
	0.8	1.01 ± 0.17	1.13 ± 0.21	0.53 ± 0.10
	1.0	0.99 ± 0.17	1.04 ± 0.22	0.52 ± 0.10
Cyclohexane	0	1	1	1
	0.2	0.99 ± 0.18	1.09 ± 0.21	0.91 ± 0.20
	0.4	1.02 ± 0.19	1.01 ± 0.20	0.65 ± 0.17
	0.6	1.01 ± 0.19	0.99 ± 0.20	0.50 ± 0.16
	0.8	0.98 ± 0.18	1.02 ± 0.20	0.48 ± 0.15
	1.0	1.01 ± 0.19	1.04 ± 0.20	0.51 ± 0.16
Acetone	0	1	1	1
	0.24	0.99 ± 0.11	1.00 ± 0.15	1.36 ± 0.18
	0.48	1.17 ± 0.13	0.95 ± 0.14	1.30 ± 0.18
	0.72	1.20 ± 0.13	0.95 ± 0.14	1.38 ± 0.18
	0.95	1.11 ± 0.24	1.09 ± 0.15	1.38 ± 0.18
$CHCl_3$	0	1	1	1
	0.2	0.94 ± 0.13	0.96 ± 0.13	0.82 ± 0.15
	0.4	1.03 ± 0.14	0.94 ± 0.13	0.85 ± 0.23
	0.6	1.10 ± 0.15	0.96 ± 0.13	0.67 ± 0.14
	0.8	1.05 ± 0.14	1.04 ± 0.14	0.59 ± 0.12
	1.0	—	1.00 ± 0.13	0.68 ± 0.14
CCl_4	0	1	1	1
	0.2	0.98 ± 0.04	0.98 ± 0.11	0.72 ± 0.15
	0.4	0.94 ± 0.04	0.89 ± 0.11	0.62 ± 0.14
	0.6	0.98 ± 0.04	0.98 ± 0.11	0.51 ± 0.13
	0.8	0.92 ± 0.04	0.91 ± 0.10	0.50 ± 0.13
	1.0	0.90 ± 0.04	0.84 ± 0.11	0.46 ± 0.13
CH_3OH	0	1	1	1
	0.2	1.27 ± 0.24	1.05 ± 0.22	1.68 ± 0.37
	0.4	1.27 ± 0.24	1.06 ± 0.22	2.39 ± 0.63
	0.6	1.59 ± 0.28	1.09 ± 0.22	4.34 ± 1.80
	0.8	1.71 ± 0.29	1.39 ± 0.25	4.82 ± 1.33
	1.0	2.00 ± 0.32	1.61 ± 0.28	5.62 ± 1.52
C_2H_5OH	0	1	1	1
	0.2	1.34 ± 0.43	1.03 ± 0.19	1.34 ± 0.20
	0.4	1.45 ± 0.16	1.34 ± 0.22	1.68 ± 0.23
	0.6	1.42 ± 0.15	1.55 ± 0.24	1.66 ± 0.23
	0.8	1.47 ± 0.16	1.38 ± 0.22	1.60 ± 0.22
	1.0	1.35 ± 0.15	1.57 ± 0.24	1.86 ± 0.24
SO_2	0	1	1	1
	0.2	1.16 ± 0.10	1.08 ± 0.17	0.91 ± 0.09
	0.4	1.19 ± 0.11	1.14 ± 0.17	0.97 ± 0.10
	0.6	1.14 ± 0.10	1.21 ± 0.20	0.93 ± 0.09
	0.8	1.19 ± 0.10	1.23 ± 0.18	0.92 ± 0.09
	1.0	1.14 ± 0.10	1.17 ± 0.18	0.89 ± 0.09

TABLE 1 (*continued*)

Gas	% Gas phase vol. added	I_f/I_{f_0} (Nitrogen)	I_f/I_{f_0} (Air)	I_f/I_{f_0} (Low pressure)
NO_2	0	1	1	1
	0.2	1.03 ± 0.04	1.02 ± 0.04	0.48 ± 0.09
	0.4	1.03 ± 0.05	1.03 ± 0.05	0.41 ± 0.08
	0.6	1.03 ± 0.05	1.00 ± 0.04	0.47 ± 0.09
	0.8	0.99 ± 0.04	1.02 ± 0.04	0.47 ± 0.09
	1.0	1.02 ± 0.05	1.00 ± 0.04	0.42 ± 0.08
NO	0	1	1	1
	0.2	0.97 ± 0.14	1.02 ± 0.14	0.95 ± 0.17
	0.4	1.00 ± 0.14	0.99 ± 0.14	0.99 ± 0.18
	0.6	0.95 ± 0.14	1.05 ± 0.14	0.99 ± 0.18
	0.8	1.02 ± 0.14	1.04 ± 0.14	1.03 ± 0.17
	1.0	1.03 ± 0.14	0.94 ± 0.14	0.95 ± 0.17
CO_2	0	1	1	1
	0.2	1.06 ± 0.13	0.97 ± 0.14	1.36 ± 0.29
	0.4	0.98 ± 0.12	1.00 ± 0.14	1.53 ± 0.32
	0.6	1.03 ± 0.13	1.09 ± 0.15	1.66 ± 0.32
	0.8	0.98 ± 0.12	1.06 ± 0.15	1.96 ± 0.36
	1.0	1.03 ± 0.13	1.06 ± 0.14	1.67 ± 0.33
Ar	0	1	1	1
	0.2	1.06 ± 0.10	1.05 ± 0.13	0.95 ± 0.13
	0.4	0.96 ± 0.09	1.03 ± 0.13	0.88 ± 0.13
	0.6	0.95 ± 0.10	1.06 ± 0.13	0.72 ± 0.11
	0.8	1.01 ± 0.10	1.03 ± 0.13	0.84 ± 0.12
	1.0	0.99 ± 0.09	0.96 ± 0.12	0.81 ± 0.12
He	0	1	1	1
	0.2	0.95 ± 0.15	0.99 ± 0.16	0.70 ± 0.11
	0.4	0.88 ± 0.15	0.97 ± 0.16	0.62 ± 0.10
	0.6	0.90 ± 0.15	0.92 ± 0.13	0.53 ± 0.09
	0.8	0.81 ± 0.15	0.90 ± 0.15	0.46 ± 0.09
	1.0	0.86 ± 0.15	0.84 ± 0.15	0.44 ± 0.09
N_2	0	—	—	1
	0.2	—	—	0.87 ± 0.09
	0.4	—	—	0.80 ± 0.09
	0.6	—	—	0.81 ± 0.09
	0.8	—	—	0.74 ± 0.08
	1.0	—	—	0.70 ± 0.08
Air	0	—	—	1
	0.2	—	—	0.95 ± 0.07
	0.4	—	—	0.87 ± 0.07
	0.6	—	—	0.81 ± 0.06
	0.8	—	—	0.76 ± 0.06
	1.0	—	—	0.72 ± 0.06
H_2O	0	1	1	1
	0.5	1.01 ± 0.15	1.04 ± 0.15	0.88 ± 0.22
	1.0	1.01 ± 0.15	1.93 ± 0.14	0.93 ± 0.22
	1.5	1.01 ± 0.15	1.97 ± 0.14	0.84 ± 0.21
	2.0	1.00 ± 0.17	0.98 ± 0.14	0.88 ± 0.22
	2.5	0.94 ± 0.15	1.00 ± 0.14	0.84 ± 0.21
	3.0	0.87 ± 0.14	0.99 ± 0.14	0.91 ± 0.22

[a]Standard deviation of at least 5 measurements.

heptane, acetylene, benzene, cyclohexane, acetone, chloroform, nitrogen dioxide, nitric oxide, carbon dioxide, argon or water. A small quenching of the fluorescence signal was seen for methane, carbon tetrachloride, and helium. Increased fluorescence signals resulted when propylene, 1-butene, methanol, ethanol, or sulfur dioxide was present.

Under low pressure conditions, for most compounds, either increased or decreased fluorescence signals were observed. Compounds for which quenching was observed were methane, hexane, heptane, benzene, cyclohexane, chloroform, carbon tetrachloride, nitrogen dioxide, argon, helium, nitrogen and air. Compounds causing a signal enhancement were propylene, 1-butene, acetone, methanol, ethanol and carbon dioxide. Five compounds had no effect, within experimental error, these being propane, acetylene, sulfur dioxide, nitric oxide and water. Table 2 lists several characteristics of the added compounds potentially important in characterizing their effect on ethylene fluorescence.

TABLE 2

Characteristics of interfering gases

Molecule	M.w.	Absorption[a] at				I_f/I_{f_0}[b]
		10.4 μm	7.0 μm	3.3 μm	Bands near 10.6 μm	
CH_4	16	—	s	s	—	0.46
Propane	44	v.w.	s	s	—	1.03
Hexane	86	v.w.	s	s	—	0.47
Heptane	100	v.w.	s	s	—	0.79
Propylene	42	s	s	s	—	4.76
1-Butene	56	s	s	s	—	3.76
Acetylene	26	—	v.w.	v.w.	—	0.96
C_6H_6	78	—	v.w.	s	9.8	0.52
Cyclohexane	84	—	s	s	11	0.51
Acetone	58	v.w.	s	m	11	1.38
$CHCl_3$	113	—	—	—	13.3	0.68
CCl_4	154	—	—	—	13	0.46
MeOH	32	v.w.	m	s	9.8	5.62
EtOH	46	v.w.	m.s.	s	9.7	1.86
SO_2	64	—	s	—	8.9	0.89
NO_2	46	—	—	—	11.3	0.42
NO	30	—[c]	—	—	—	0.95
CO_2	44	—	—	—	—	1.67
H_2O	18	—	w	—	—	0.93
Ar	40	—	—	—	—	0.81
He	4	—	—	—	—	0.44
N_2	28	—	—	—	—	0.70
Air		—	—	—	—	0.72

[a] v.w. = very weakly, w = weakly, m = moderately, m.s. = moderately strongly, s = strongly, — = none.

[b] Obtained from Table III for 1 % (or 7.6 torr) of the interfering gas in the vacuum experiments.

[c] Absorbs 10.6-μm laser energy from an excited state [29].

In a bimolecular system, where molecule A fluoresces from its excited state and B is the quenching species, the following relationship [39] exists:

$$\tau_{obs.}^{-1} = K_{AA} P_A + K_{AB} P_B + \tau_{rad.}^{-1} \quad (1)$$

where $\tau_{obs.}$ is the observed lifetime of excited state molecule A; K_{AA} the deactivation rate of pure A; K_{AB} the deactivation rate of A by B; P_A, P_B the partial pressures of A and B; and $\tau_{rad.}$ the radiative lifetime of A.

Furthermore [40,45]:

$$\frac{I_{f_0}}{I_f} = \frac{\tau_0}{\tau} \quad (2)$$

where I_{f_0} is the fluorescence intensity in the absence of a quencher; I_f the fluorescence intensity with a quencher; τ_0 the lifetime of the fluorescence of the pure gas; and τ the lifetime of the collisionally quenched fluorescence.

These equations indicate that when a collision partner has a large deactivation rate K_{AB} and/or is present at a high pressure, the observed fluorescence intensity, I_f, becomes small. Thus, in the low-pressure experiments an observed decrease in fluorescence intensity should be a direct measurement of the deactivation rate of each collision partner. A large deactivation effect is observed if vibrational—vibrational and/or vibrational—rotational/translational energy transfer readily occur [37]. An effective vibrational—vibrational energy transfer is expected if the colliding molecules have similar energy states; this is termed the near resonance effect [5,46,47]. With respect to vibrational—rotational/translational transfer, Stretton [37] and Tanczos [48] have developed modified vibrational—translational transfer theories in which molecular rotation is ignored and vibrational energy transfer depends mainly on the relative translational velocity of the collision pair. These theories predict that increasing deactivation probability, i.e. increasing numbers of collisions per unit time, will be found with a decrease in the reduced mass of the collision pair. In the vacuum experiments which are bimolecular systems, a large deactivation effect was observed for helium and nitrogen, and a relatively small effect for argon. These findings coincide with the theories of Stretton and Tanczos. The large quenching effect of methane on ethylene fluorescence can be explained by Stretton's and Tanczos' theories and by a near resonance effect.

Vibrational energy is rapidly redistributed among the vibrational modes of a molecule [5,7,27,34]. Thus, the 7-μm ethylene vibrational state will be populated by equilibration with the pumped state of ethylene at 10.6 μm. Energy can then be transferred to the 7.7-μm methane vibrational state through efficient near resonance vibrational—vibrational energy transfer. The large quenching effect observed for hexane, benzene, cyclohexane, chloroform, carbon tetrachloride, and nitrogen dioxide might come from a near resonance effect. All of these compounds have vibrational states near the vibrational states of ethylene. However, acetylene and nitric oxide did not affect the intensity of ethylene fluorescence, and they do not have vibrational states

overlapping those of ethylene. On the basis of near resonance effects, both sulfur dioxide and water would be expected to quench ethylene fluorescence strongly. In both cases, some quenching was observed, but it was not strong. In contrast, a strongly sensitized sulfur dioxide fluorescence has been shown in connected work here, but these observations have not yet been explained. Similar observations have been made in an ethylene—water system by Yuan and Flynn [5].

The deactivation rates of ethylene fluorescence by helium, argon, nitrogen and methane, based upon the measurement of fluorescence decay curves, have been reported [5]. The reported deactivation rates were $5.44 \cdot 10^3$ s^{-1} $torr^{-1}$ for helium, $0.47 \cdot 10^3$ for argon, $0.82 \cdot 10^3$ for nitrogen, and $17.1 \cdot 10^3$ and $8.0 \cdot 10^3$ for methane. The rate of ethylene self-deactivation was also reported [5] to be $7.23 \cdot 10^3$. From eqns. (1) and (2), I_f/I_{f_0} values for 7.6 torr, or 1 % in volume helium, argon, nitrogen and methane were calculated. Since $\tau_{rad.}^{-1}$ is very small in comparison with other terms in eqn. (1), it was neglected. The results of these calculations are compared to the experimentally determined I_f/I_{f_0} values in Table 3. The observed I_f/I_{f_0} values for helium, argon, and nitrogen are in good agreement with the calculated values. However, a large discrepancy between the observed and calculated values for methane was noted. In a later experiment, it was shown that helium was a better quencher than methane. This discrepancy has not been explained although increased collision rates must be a factor.

TABLE 3

Comparison of calculated and observed quenching efficiencies

Quenching molecule	K_{AB}[a] (s^{-1} $torr^{-1}$)	Calculated[b] I_f/I_{f_0}	Observed[c] I_f/I_{f_0}
He	$5.44 \cdot 10^3$	0.34	0.44 ± 0.09
Ar	$0.47 \cdot 10^3$	0.86	0.81 ± 0.12
N_2	$0.82 \cdot 10^3$	0.78	0.70 ± 0.08
CH_4	$17.1 \cdot 10^3$	0.078	0.46 ± 0.07
CH_4	$8.0 \cdot 10^3$	0.27	

[a] Obtained from Ref. 5.
[b] Values calculated from eqns. (1) and (2).
[c] Obtained for 1 % of the interfering gas in the vacuum experiments.

In the vacuum experiments, several compounds caused an increase in the fluorescence signal of ethylene. A characteristic of these compounds is that they either strongly or weakly absorb 10.6-μm laser radiation. The compound which either did not affect or quenched ethylene fluorescence did not absorb 10.6-μm radiation. Exceptions to these generalizations were hexane and heptane which were weak absorbers of 10.6-μm radiation and also quenched ethylene fluorescence.

Propylene, 1-butene, acetone, methanol, ethanol and carbon dioxide

enhanced ethylene fluorescence. Further experiments were performed to determine how the enhancement occurred. "Fluorescence" signals at 10.4-μm were measured for each compound without ethylene in the cell. It was found that the enhancement of the ethylene fluorescence was greater than the signal produced by the pure compounds, i.e., the effect must have been a sensitizing phenomenon. It was possible that these compounds absorbed the 10.6-μm laser radiation and transferred the energy to ethylene molecules thus enhancing the ethylene fluorescence. It was also possible, especially in the cases of propylene and 1-butene, for the energy transfer to be from ethylene to the added compound, with the increase in signal being due to fluorescence of the added species. Both propylene and 1-butene give strong fluorescence signals at 10.6-μm [49].

In the experiments with a nitrogen or air atmosphere, most of the compounds examined had no effect on ethylene fluorescence intensity. The data can be supported by consideration of eqns. (1) and (2). In the polymolecular system, eqn. (1) will be:

$$\tau_{\text{obs.}}^{-1} = K_{AA}P_A + K_{AB}P_B + K_{AC}P_C + K_{AD}P_D + \ldots + \tau_{\text{rad.}}^{-1} \quad (3)$$

where K_{AC}, K_{AD} are the deactivation rates of A by C and D, and P_C, P_D are the partial pressures of C and D. In the cases where the nitrogen and oxygen concentrations were large, further compounds added to the cell would contribute little to $\tau_{\text{obs.}}^{-1}$ in eqn. (3), and therefore I_f in eqn. (2). Thus,

$$K_{C_2H_4-B}P_B \ll K_{C_2H_4-N_2}P_{N_2} + K_{C_2H_4-O_2}P_{O_2}$$

unless $K_{C_2H_4-B}$ is large. Methane, carbon tetrachloride, and helium gave large deactivation effects in the low-pressure experiments and showed small quenching effects in experiments at atmospheric pressure. The deactivation of ethylene fluorescence by oxygen has been reported [5] as $1.43 \cdot 10^3$ s^{-1} torr^{-1} which is very similar but slightly larger than that by nitrogen. Thereeriments employing a nitrogen atmosphere should give similar experiments employing air atmosphere. This was observed to be

tensity of ethylene fluorescence was not affected by compounds which did not absorb 10.6-μm laser radiation when measured at atmospheric pressure. The fluorescence was quenched by these compounds in evacuated systems. However, compounds which absorb 10.6-μm radiation tended to give positive interference effects. These results have important analytical implications to the laser fluorescence technique as used for air pollution monitoring. Concentrations of atmospheric pollutants should be quite low when compared to the concentration of nitrogen or oxygen. Under such circumstances, the observed intensity of fluorescence signals would be fairly free from interferences by air pollutants which do not absorb the laser energy. Thus, if a tunable laser can be used which is specific for a single rotational—vibrational line of a molecule, no major interferences could occur. The results for water also indicate that changes in atmospheric humidity would not

affect the system. Another possible application of the technique is the monitoring of point sources, such as a stack or automotive exhaust pipes. In these cases, analytical interferences could be severe owing to the high concentration and varying nature of pollutants. Here careful calibration as well as careful interpretation of analytical data will be necessary.

Quenching of the ethylene 10.4-μm fluorescence by a foreign gas at higher pressure (up to atmospheric pressure)

In the foregoing experiments, ethylene at 3 torr (or 0.4 % gas phase volume was studied. In these studies, at higher pressures, sufficient ethylene was used, 15 torr, so that stronger ethylene fluorescence signals were produced. This allowed more accurate determination of possible quenching effects. The Stern—Volmer plots for the experiments on helium, methane, air, nitrogen, argon, and propane are shown in Fig.4. The Stern—Volmer quenching law is expressed [50] by $I_{f_0}/I_f = 1 + aC$, where I_{f_0} and I_f are defined as for eqn. (2), C is the known concentration or partial pressure of the quenching species,

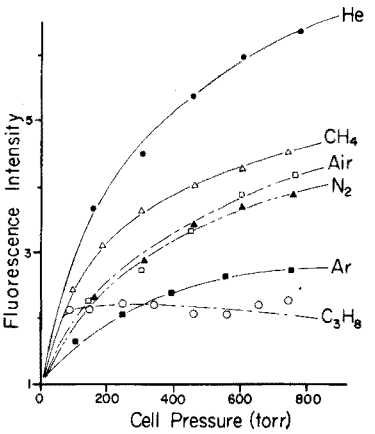

Fig.4. Collisional deactivation of ethylene fluorescence (Stern—Volmer plots).

and a is a constant. The expected linear Stern—Volmer plots were not observed in this study. In the experiments with nitrogen as a quencher, the CO_2 laser radiation was absorbed more strongly when the pressure of nitrogen was increased [5]. This resulted in pressure broadening of ethylene rotational lines associated with the 10.4-μm band. If corrections were made to the fluorescence intensities for the amount of the laser radiation absorbed, the Stern—Volmer plots would be more nearly linear. However for propane such a correlation would not give a linear plot. Propane absorbs 10.6-μm radiation and its fluorescence may have contributed to the signal observed. As seen in Fig.4, helium was the best quencher of the ethylene fluorescence. A large deactivation effect has generally been observed for helium, and has been attributed to vibrational energy transfer [5,7,9,27,29]. In general, the quenching effi-

ciencies observed in this experiment were in good agreement with those of the foregoing low-pressure studies.

This investigation was supported by research grant R 800697, Air Pollution Control Office, Environmental Protection Agency.

SUMMARY

The interference of numerous compounds on the laser-induced fluorescence of ethylene at 10.6-μm was studied. The compounds studied were methane, propane, hexane, heptane, propylene, 1-butene, acetylene, benzene, cyclohexane, acetone, chloroform, carbon tetrachloride, methanol, ethanol, sulfur dioxide, nitrogen dioxide, nitric oxide, carbon dioxide, water, argon, helium, nitrogen, and air. Only some of these, in low concentrations, interfered at atmospheric pressure, but most interfered in evacuated systems. Compounds which absorbed the excitation 10.6-μm radiation enhanced the fluorescence signals of ethylene, while non-absorbing compounds generally did not interfere. The quenching efficiencies of helium, argon, nitrogen, and methane on excited ethylene molecules were determined, and compared to values calculated from published data; good agreement was found except for methane. Quenching experiments with higher concentrations of added compounds were also performed.

REFERENCES

1 P.L. Hanst, Appl. Spectros., 24 (1970) 161.
2 L.R. Snowman and R.J. Gillmeister, AIAA Paper No. 71-1059, 1971.
3 H. Kildal and R.L. Byer, Proc. IEEE, 59 (1971) 1644.
4 L.O. Hocker, M.A. Kovacs, C.K. Rhodes, G.W. Flynn and A. Javan, Phys. Rev. Lett., 17 (1966) 233.
5 R.C.L. Yuan and G.W. Flynn, J. Chem. Phys., 57 (1972) 1316; 58 (1973) 649.
6 J.T. Yardley and C.B. Moore, J. Chem. Phys., 48 (1968) 14.
7 F.R. Grabiner and G.W. Flynn, J. Chem. Phys., 59 (1973) 2330.
8 S.M. Lee and A.M. Ronn, Chem. Phys. Lett., 24 (1974) 535.
9 J.T. Knudtson and G.W. Flynn, J. Chem. Phys., 58 (1973) 2684.
10 I. Burak, A.V. Nowak, J.I. Steinfeld and D.G. Sutton, J. Chem. Phys., 51 (1969) 2275.
11 P.E. Zittel and C.B. Moore, Appl. Phys. Lett., 21 (1972) 81.
12 R.C.L. Yuan, J.M. Preses and G.W. Flynn, J. Chem. Phys., 59 (1973) 6128.
13 J.C. Stephenson and E.R. Mosburg, Jr., J. Chem. Phys., 60 (1974) 3562.
14 D.I. Rosen and T.A. Cool, J. Chem. Phys., 59 (1973) 5824, 6097.
15 M.J. Kurylo, W. Braun and A. Kaldor, Chem. Phys. Lett., 27 (1974) 249.
16 J.K. Hancock and W.H. Green, J. Chem. Phys., 59 (1973) 6350.
17 R.A. Lucht and T.A. Cool, J. Chem. Phys., 60 (1974) 1026, 2554.
18 J.F. Bott and N. Cohen, J. Chem. Phys., 61 (1974) 681.
19 H. Chen and C.B. Moore, J. Chem. Phys., 54 (1971) 4072.
20 P.F. Zittel and C.B. Moore, J. Chem. Phys., 58 (1973) 2922.
21 R.V. Steele, Jr. and C.B. Moore, J. Chem. Phys., 60 (1974) 2794.
22 W.H. Green and J.K. Hancock, IEEE J. Quant. Electron., QE-9 (1973) 50.
23 J.C. Stephenson, J. Chem. Phys., 60 (1974) 4289
24 R.D. Bates, Jr., G.W. Flynn and A.M. Ronn, J. Chem. Phys., 49 (1968) 1432.
25 B.M. Hopkins, A. Baronarski and H.L. Chen, J. Chem. Phys., 59 (1973) 836.
26 R.D. Bates, Jr., J.T. Knudtson, G.W. Flynn and A.M. Ronn, J. Chem. Phys., 57 (1972) 4174.
27 J.T. Knudtson and G.W. Flynn, J. Chem. Phys., 58 (1973) 1467.

28 R.T. Bailey, F.R. Cruickshank and T.R. Jones, Nature (London), 234 (1971) 92.
29 C.B. Moore, R.E. Wood, B.L. Hu and J.T. Yardly, J. Chem. Phys., 46 (1967) 4222.
30 E. Weitz, G. Flynn and A.M. Ronn, J. Chem. Phys., 56 (1972) 6060.
31 E. Weitz and G.W. Flynn, J. Chem. Phys., 58 (1973) 2781.
32 F.R. Grabiner and G.W. Flynn, J. Chem. Phys., 60 (1974) 398.
33 A.B. Peterson and C. Wittig, Chem. Phys. Lett., 27 (1974) 442.
34 J.T. Yardley and C.R. Moore, J. Chem. Phys., 49 (1968) 1111; 45 (1966) 1066.
35 J.C. Stephenson, R.E. Wood and C.B. Moore, J. Chem. Phys., 54 (1971) 3097.
36 W.H. Green and J.K. Hancock, J. Chem. Phys., 59 (1973) 4326.
37 J.L. Stretton, Trans. Faraday Soc., 61 (1965) 1053.
38 E. Hirshlaff, Fluorescence and Phosphorescence, Methuen, London, 1938, Ch. IV.
39 R.N. Schwartz, Z.I. Slawsky and K.F. Herzfeld, J. Chem. Phys., 20 (1952) 1591.
40 J.W. Robinson and J.D. Dake, Spectrosc. Lett., 6 (1973) 377.
41 J.W. Robinson, C. Woodward and H.M. Barnes, Anal. Chim. Acta, 43 (1968) 119.
42 E.A. Ogryzlo and B.A. Thrush, Chem. Phys. Lett., 24 (1974) 314.
43 P.E. Zittel and C.B. Moore, J. Chem. Phys., 58 (1973) 2004.
44 I. Burak, Y. Noter and A. Szöke, IEEE J. Quant. Electron., QE-9 (1973) 541.
45 G.G. Guilbault, Fluorescence, M. Dekker, New York, 1967, Ch. 3.
46 E. Hirshlaff, Fluorescence and Phosphorescence, Methuen, London, 1938, p. 26.
47 J.W. Arnold, J.C. McCoubrey and A.R. Ubbelhode, Proc. Roy. Soc., Ser. A, 248 (1958) 445.
48 F.I. Tanczos, J. Chem. Phys., 25 (1956) 439.
49 J.W. Robinson and N. Katayama, Spectrosc. Lett., 8 (1975) 61.
50 J.I. Steinfeld, Accounts Chem. Res., 3 (1970) 313.
51 J.D. Dake, Dissertation, Louisiana State University, Baton Rouge, Louisiana, 1973.

Analytica Chimica Acta, 79 (1975) 257—263

THE SIMULTANEOUS SPECTROPHOTOMETRIC DETERMINATION OF NICKEL AND COBALT IN MIXTURES WITH 3-HYDROXYPICOLINEALDEHYDE AZINE

A. GARCIA DE TORRES, M. VALCARCEL and F. PINO

Department of Analytical Chemistry, University of Seville, Seville (Spain)

(Received 3rd April 1975)

The characteristics and analytical possibilities of 3-hydroxypicolinealdehyde azine (3-OH-PAA) have already been described [1], and this reagent has been compared with the salicylaldehyde and picolinealdehyde azines. The presence of both pyridine nitrogen atoms and phenolic groups is responsible for the high reactivity of 3-OH-PAA with metal ions.

The spectrophotometric determination of traces of cobalt with these azines has been also reported [2]. The 3-OH-PAA provides the most favourable reaction with cobalt (II), forming violet solutions of a 1:3 chelate at pH 4.5; the wavelength of maximal absorbance lies at 545 nm with a shoulder at 570 nm ($\epsilon = 3.04 \cdot 10^4$ l mol^{-1} cm^{-1}). The method is very sensitive and there are few interferences.

In this paper the properties of the nickel complex with 3-OH-PAA are described, and a photometric method for determining traces of nickel is proposed. A simultaneous spectrophotometric determination of traces of cobalt (II) and nickel (II) ions has also been developed.

EXPERIMENTAL

Reagents

A 0.05 % (w/v) solution of 3-hydroxypicolinealdehyde azine in dimethylformamide (DMF) was used. The reagent was prepared [1] by reaction of hydrazine with 3-hydroxypicolinealdehyde, which was obtained by controlled oxidation of 3-hydroxy-2-methoxypyridine hydrochloride with manganese dioxide in water in the presence of chloroform.

Solutions of cobalt (II) were standardized with EDTA, and solutions of nickel (II) with dimethylglyoxime. A 0.5 M acetic acid—sodium acetate buffer solution of pH 4.5 was prepared. All solvents and reagents were of analytical grade.

Apparatus

Unicam SP800, Unicam SP600, and Beckman DU spectrophotometers equipped with 1.0-cm glass or quartz cells, a Perkin-Elmer 503 atomic absorption spectrophotometer, and a Philips PW 9408 digital pH meter with glass-calomel electrodes, were used.

Determination of nickel

To the solution containing 10—25 μg of nickel, add 8 ml of acetate buffer p 4.5 and 5 ml of 0.05 % reagent solution. Heat the samples in a water bath at 100 °C for 15 min: transfer to 25.0-ml volumetric flasks and dilute to volume with 1:1 ethanol—water. Measure the absorbance at 480 nm against a reagent blank prepared in a similar way without nickel. Construct calibration graphs for standard solutions treated in the same way.

Determination of nickel and cobalt mixtures

To the solution of nickel and cobalt (5—25 μg of each), add 8 ml of acetate buffer pH 4.5 and 5 ml of 0.05 % reagent solution in DMF. Heat and dilute the solution as described above. Measure the absorbances at 480 and 540 nm against a reagent blank, and calculate the cobalt and nickel concentrations by solving two simultaneous equations.

Determination of nickel and cobalt in industrial catalysts

Weigh accurately a suitable amount (1.0—2.0 g) of catalyst and place in a flask fitted with a reflux condenser. Add 20 ml of concentrated nitric acid and 60 ml of concentrated hydrochloric acid, reflux for 3 h, and then concentrate to about 25 ml. Dilute the cooled solution with distilled water to 100 ml in a volumetric flask. Analyse suitable aliquots of this solution for nickel and cobalt as described above.

RESULTS AND DISCUSSION

Reaction of 3-hydroxypicolinealdehyde azine with nickel

When dilute solutions of nickel (II) and 3-OH-PAA were mixed, a yellow-orange complex was obtained. The absorption spectra of the coloured solution underwent bathochromic and hyperchromic shifts with temperature (Fig. 1) and time. The absorption spectrum of an unheated solution after 24 h was the same as that of a solution heated at 95—100 °C for 5 min. It was necessary to warm the solutions to avoid unstable measurements and to achieve high absorbances.

Several solutions containing 1.2 ppm of nickel, prepared by the method

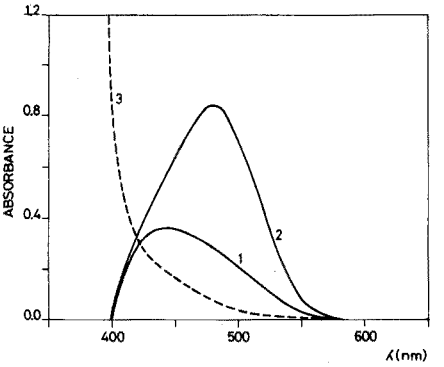

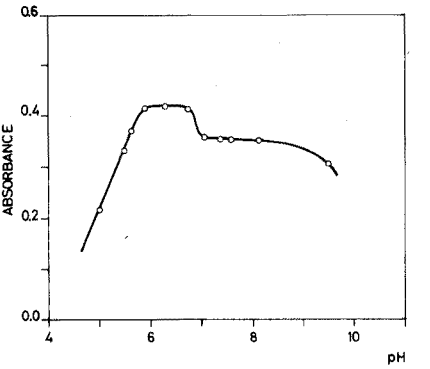

Fig. 1. Absorption spectra of the nickel complex. 1.0 ppm of nickel: 1, at 20 °C; 2, at 100 °C; 3, reagent alone (water blank).

Fig. 2. Effect of pH on the formation of the nickel complex. 0.6 ppm of nickel. 480 nm.

explained in the Experimental section were heated at different temperatures (50, 60, 70, 80, 90 and 100 °C) for various times (0.5, 1, 1.5, 2 and 3 h). The absorbances at 470 and 480 nm were measured at different times after heating. The numerous data obtained indicated that the absorbance increased by 0.1 unit/10 °C and that, at the same temperature, the absorbance increased by 0.04 units/h with the time of heating; however, when the solutions were heated in a water-bath at 100 °C, the time of heating did not affect the absorbance values, provided that it exceeded 10 min. In all experiments, the absorbances remained constant after the solutions had been heated.

To obtain the most sensitive, reliable results, the solutions were heated at 100 °C. When the temperature of heating was low, the method was not reliable because the absorbance was affected by small variations in the time and temperature of heating.

The effect of pH on the colour development was studied by preparing series of solutions with 0.6 ppm of nickel (II) varying from pH 1 to 11. The absorbance at 470—80 nm increased steeply in the pH range 4—6; no change in absorbance was observed over the pH range 5.9—6.7 or over the pH range 7.0—9.0 but the absorbance value in the latter range was lower (Fig. 2). For the analytical procedure, an acetate buffer was selected because the volume of DMF added in the preparation of the solutions increased the pH by over one unit.

The pH—absorbance curves for the nickel and cobalt (II) complexes of 3-OH-PAA are similar, although the permissible pH range for cobalt is narrower [2].

Stoichiometry of nickel complex

The results obtained by Job's method in acetate buffer for solutions of nickel (II) and 3-OH-PAA ($2.4 \cdot 10^{-4}$ M) heated in a boiling water bath are

shown in Fig. 3. The metal:ligand ratio of the nickel complex is 1:3, which is the same as for the cobalt complex. This forced configuration could be the cause of the slow formation of the complex and the positive influence of the temperature.

Spectrophotometric determination of nickel

The optimal experimental conditions for complex formation (temperature and time of heating, reagent concentration, influence of ionic strength, influence of order of reagent addition, etc.) were established empirically.

The calibration graph proved to be linear over the range 0.1—1.2 ppm of nickel. The molar absorptivity for the complex, calculated statistically from Beer's law, was $4.2 \cdot 10^4$ l mol^{-1} cm^{-1}. The optimal concentration range evaluated by Ringbon's method was 0.4—1.0 ppm of nickel. The relative error (P = 0.05) of the method was ± 0.30 % at 470 and 480 nm.

Numerous cations and anions were examined by applying the method to 0.5 ppm solutions of nickel. The interferences were similar to those found [2] in the determination of cobalt with 3-OH-PAA. The following ions in 200-fold amounts (w/w) did not interfere: aluminium, arsenic, barium, calcium, lead, lanthanides, magnesium, manganese, molybdenum, tungsten, rubidium, uranium thallium. Mercury ions did not interfere in 100-fold (w/w) amounts. Cobalt,

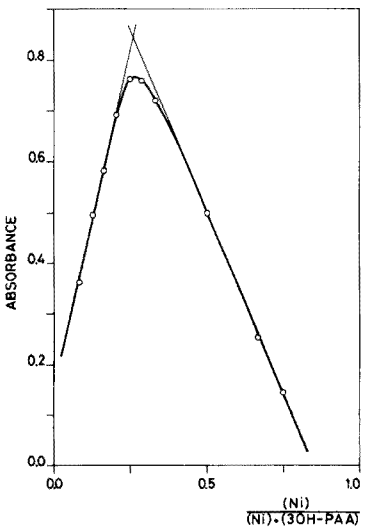

Fig. 3. Composition of 3-OH-PAA—Ni complex by the continuous variations method.

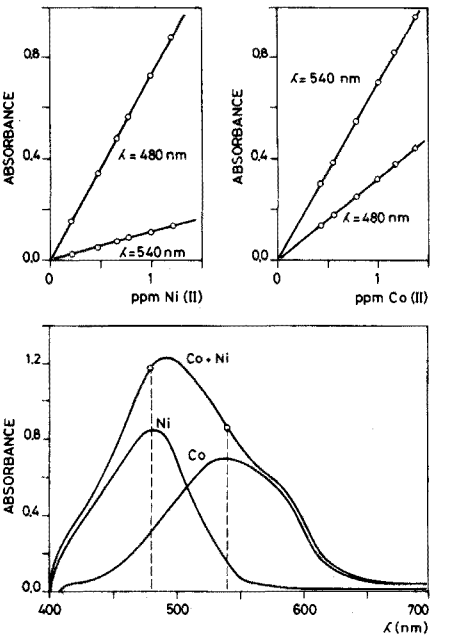

Fig. 4. Simultaneous spectrophotometric determination of traces of cobalt and nickel with 3-OH-PAA.

copper, iron, palladium, zinc, gold and chromium interfered when their concentrations exceeded twice that of nickel. Sodium fluoride, sodium sulphate, potassium nitrate, ammonium hydrogenphosphate, tartaric acid and citric acid did not interfere. EDTA produced a serious interference when present at the same concentration as nickel.

Simultaneous determination of nickel and cobalt

The absorption spectra of three acetate-buffered solutions, prepared as described under Experimental, with 1 ppm of nickel, 1 ppm of cobalt (II), and 1 ppm of nickel plus 1 ppm of cobalt (II), are shown in Fig. 4. The absorption spectrum of the mixed complexes is the sum of the two separate spectra.

Two analytical wavelengths were selected: 480 and 540 nm. To evaluate the molar absorptivities of the complexes at these wavelengths. calibration graphs were plotted as shown in Fig. 4. The values found are shown in Table 1.

To determine traces of cobalt and nickel in a solution, a single sample or solution is analysed as described in the Experimental part, and the results are evaluated by solving two simultaneous equations:

$$A_{480} = 4.20 \cdot 10^4 \; C_{Ni} + 1.90 \cdot 10^4 \; C_{Co}$$

$$A_{540} = 6.68 \cdot 10^3 \; C_{Ni} + 4.12 \cdot 10^4 \; C_{Co}$$

where C_{Ni} and C_{Co} are the unknown concentrations.

The results of the determination of nickel and cobalt in 18 samples, with Ni/Co ratios of 0.1—10, are shown in Table 2. These results prove the satisfactory nature of the 3-OH-PAA method.

Analysis of industrial catalysts

The techniques described above were applied to the determination of trace amounts of nickel and cobalt on aluminium oxide supports used in process catalysts, such as Unifining catalyst, Isomax-UOP-DHC-2 and Filtrol 475-8; all these supports are spherical particles of about 2-mm diameter, or small cylinders of similar dimensions. The results found are compared with those obtained

TABLE 1

Molar absorptivities of the cobalt and nickel complexes at the two analytical wavelengths

	ϵ (l mol^{-1} cm^{-1})	
	480 nm	540 nm
Ni—3-OH-PAA	$4.20 \cdot 10^4$	$6.68 \cdot 10^3$
Co(II)—3-OH-PAA	$1.90 \cdot 10^4$	$4.12 \cdot 10^4$

TABLE 2

Simultaneous determination of nickel and cobalt in mixtures[a]

Sample number	Ni/Co ratio	Amounts taken (ppm)		Ni found (ppm)	Difference	Co found (ppm)	Difference
		Ni	Co				
1	0.1	0.11	1.12	0.11	0.00	1.06	0.06
2		0.14	1.40	0.14	0.00	1.38	0.02
3	0.25	0.11	0.45	0.11	0.00	0.45	0.00
4		0.33	1.35	0.32	0.01	1.35	0.00
5	0.5	0.22	0.45	0.22	0.00	0.44	0.01
6		0.56	1.12	0.55	0.01	1.11	0.01
7	0.75	0.34	0.44	0.34	0.00	0.44	0.00
8		0.67	0.89	0.66	0.01	0.90	0.01
9	1	0.34	0.34	0.34	0.00	0.34	0.00
10		0.67	0.67	0.66	0.01	0.67	0.00
11	2.5	0.56	0.22	0.56	0.00	0.22	0.00
12		0.73	0.28	0.73	0.00	0.28	0.00
13	5	0.56	0.11	0.56	0.00	0.11	0.00
14		1.12	0.22	1.12	0.00	0.23	0.01
15	7.5	0.73	0.11	0.74	0.01	0.11	0.00
16		1.12	0.14	1.15	0.03	0.16	0.02
17	10	1.12	0.11	1.10	0.02	0.11	0.00
18		1.40	0.14	1.36	0.04	0.14	0.00

[a] Each result is the mean of 3 separate determinations.

TABLE 3

Analysis of industrial catalysts[a]

Sample	Ni found (%)				Co found (%)		
	A.a.s.	s	3-OH-PAA	s	A.a.s.	s	3-OH-PAA
Unifining catalyst	3.45	0.03	3.40	0.04	0.07	0.002	0.05
Isomax	1.44	0.02	1.40	0.02	0.03	0.003	—
Filtrol	0.02	0.003	—	—	2.16	0.01	2.00

[a] Each result is the mean of 6 separate determinations.

by atomic absorption spectrometry in Table 3. It should be noted that there is no interference from the large amount of aluminium oxide or from the molybdenum present in the catalysts (Unifining, 7.0 % Mo; Isomax, 12.6 % Mo; Filtrol, 11.5 % Mo).

SUMMARY

The properties of the nickel complex of 3-hydroxypicolinealdehyde azine are described (λ_{max} = 480 nm, $\epsilon = 4.2 \cdot 10^4$ l mol^{-1} cm^{-1}). The optimal conditions for a selective and sensitive spectrophotometric determination of nickel are discussed. The absorption spectra of the nickel and cobalt (II) complexes of 3-hydroxypicolinealdehyde azine are sufficiently different to permit the simultaneous spectrophotometric determination of both ions when the absorbances are measured at 480 nm and 540 nm. Mixtures containing nickel and cobalt in ratios from 0.1 to 10 can be analysed. The method has been applied to process catalysts on alumina supports.

REFERENCES

1 A. Garcia de Torres, M. Valcarcel and F. Pino, Talanta, 20 (1973) 919.
2 A. Garcia de Torres, M. Valcarcel and F. Pino. Anal. Chim. Acta, 68 (1974) 466.

Analytica Chimica Acta, 79 (1975) 265—272

SPECTROPHOTOMETRIC DETERMINATION OF TETRAPHENYLARSONIUM SALTS BY SOLVENT EXTRACTION WITH VANADIUM—PAR COMPLEX

M. ŠIROKI and Lj. MARIĆ

Laboratory of Analytical Chemistry, Faculty of Science, The University of Zagreb, Strossmayerov trg 14, 41000 Zagreb (Yugoslavia)

(Received 26th March 1975)

Studies of precipitation and solvent extraction processes involving tetraphenylarsonium salts require sensitive, accurate methods for their determination. The u.v. spectrophotometric method for the tetraphenylarsonium ion [1] has been used in establishing solubility [2] and extraction behaviour [3]. The absorbances in aqueous media are measured on the flat shoulder at 220 nm or at the 265-nm band; the absorption at 220 nm is strong but is not clearly perceptible in all solvents of interest, whereas the bands in the 260-nm region are so sharp that significant errors may be caused by change of solvents or the presence of impurities [4].

The extraction—visible spectrophotometric method described in this paper is more sensitive and less subject to interferences than the u.v. method.

EXPERIMENTAL

Apparatus

Beckman DU-2 and Perkin-Elmer Coleman 124 spectrophotometers with 1-cm cells, a Radiometer TTT 1d pH meter, and a Griffin flask shaker with a time switch were used.

Reagents

All the chemicals and solvents were of analytical grade and were used as received.

Aqueous and chloroform solutions of tetraphenylarsonium chloride ($1 \cdot 10^{-2}$ *M*) were standardized titrimetrically [5]. Lower concentrations were obtained by dilution and checked spectrophotometrically.

Buffered vanadium(V)—4-(2-pyridylazo)resorcinol complex solution ($2 \cdot 10^{-4}$ *M*) was prepared by mixing 100 ml of aqueous $1 \cdot 10^{-3}$ *M* ammonium vanadate solution, 100 ml of aqueous $1 \cdot 10^{-3}$*M* PAR (Na-salt) solution and

100 ml of 1 *M* acetic acid—sodium acetate buffer (pH 6), followed by dilution to 500 ml with distilled water. The solution remains stable for at least two weeks.

Procedures

Determination of tetraphenylarsonium in aqueous solution. Transfer an aliquot of aqueous solution (1—10 ml) containing 0.25—0.01 micromole of tetraphenylarsonium salt to a separatory funnel, and add 5 ml of the $2 \cdot 10^{-4}$ *M* vanadium—PAR solution and 5 ml of chloroform. Strongly acidic or alkaline solutions must be nearly neutralized before addition of the reagent. Shake for 2 min, separate the layers and measure the absorbance of the organic phase at 560 nm with the reagent blank as reference.

Alternatively, transfer the reaction mixture to a stoppered 50-ml flask and shake mechanically for 5—15 min.

Determination of tetraphenylarsonium in organic solution. Mix *x* ml of organic solution (chloroform, *o*-dichlorobenzene, dichloromethane, 1,2-dichloroethane or nitrobenzene) containing 0.25—0.01 micromole of tetraphenylarsonium salt, 5*x* ml of the same organic solvent, and 5 ml of the $2 \cdot 10^{-4}$ *M* vanadium—PAR solution. Then follow the procedure described above.

RESULTS AND DISCUSSION

The extraction of the ion-pairs formed between tetraphenylarsonium or phosphonium cation and highly coloured anionic metal—PAR complexes has been utilized for spectrophotometric determinations of several metal ions [6—9]. In considering the use of such systems for the determination of tetraphenyl onium cations, the vanadium—PAR complex appeared to be the most promising choice. Its solution is stable and easily prepared, the extraction of the ion-pairs is quantitative, and the vanadium—PAR complex alone is not significantly extracted into the solvents which are normally used in these ion-pair extraction systems.

Solvents

The results obtained with different extraction solvents are summarized in Table I. These solvents can be grouped as those that extract [Ph_4As] [V—PAR] ion-pairs but not the vanadium—PAR complex itself to any appreciable extent, and those that extract the vanadium—PAR complex as well as the ion-pair. A further group — carbon tetrachloride, benzene, cyclohexane, diethyl ether and petroleum ether — extracts neither. For the extraction of tetraphenylarsonium ion, the best solvent is chloroform.

TABLE I

Effect of solvents
(Aqueous phase: $2 \cdot 10^{-5}$ *M* $(C_6H_5)_4AsCl$, $1 \cdot 10^{-4}$ *M* vanadium—PAR, acetate buffer (0.2 *M*); $V_{org} = V_{aq}$)

Organic phase	λ_{max}	Absorbance (A)		ΔA
		$(C_6H_5)_4As$-extract	Reagent blank	
Chloroform	558	0.777	0.016	0.761
Dichloromethane	558	0.820	0.022	0.798
1,2-Dichloroethane	558	0.805	0.020	0.785
1,2-Dichlorobenzene	558	0.690	0.010	0.680
Nitrobenzene	558	0.880	0.130	0.750
Methyl isobutyl ketone	548	0.660	0.112	0.548
n-Amyl alcohol	555	1.327	1.320	0.007
Cyclohexanone	560	1.155	1.180	—

Absorption spectra

The visible spectra of the $[Ph_4As]$ [V—PAR] chloroform extract are shown in Fig.1(a). Absorption is maximal at 558 nm, the molar absorptivity being $3.8 \cdot 10^4$ l $mol^{-1} cm^{-1}$. The same maximum and nearly the same molar absorptivity values were obtained for the dichlorinated solvents and nitrobenzene (Table I). The u.v. spectra of tetraphenylarsonium chloride in chloroform are shown in Fig.1(b). In order to compare the intensity and sharpness of absorption bands, the spectra (a) and (b) were recorded with the same concentrations of tetraphenylarsonium ion and under the same recording parameters. The u.v. absorption maximum in chloroform occurs at 265.0 nm, the molar absorptivity being $3.5 \cdot 10^3$ l mol^{-1} cm^{-1}. The maximum must be located to within ±0.1 nm to obtain reliable absorbance values [4]. In the extraction—visible spectrophotometric method, the same absorbance values (within experimental error) were obtained in the wavelength range 555—562 nm.

Effect of pH and reagent concentration

The effect of pH on the extraction of tetraphenylarsonium with the vanadium—PAR complex was studied for a series of aqueous solutions buffered to various pH values. As shown in Fig.2 (curve 1), the absorbance of the extract was constant in the range pH 5—7. At lower pH values the extraction of the ion-pair decreased whereas the absorbance of reagent blank increased (curve 2), because of the pH-dependent equilibria between the anionic and neutral vanadium—PAR complex species. In alkaline solution, the vanadium—PAR complex decomposed.

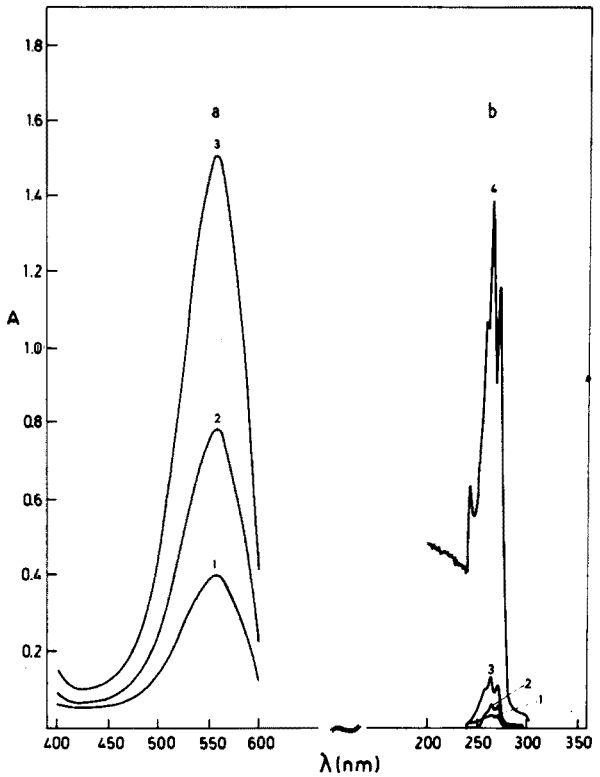

Fig.1. The visible spectra of $[(C_6H_5)_4As][V—PAR]$ extracts (a) and the u.v. spectra of $(C_6H_5)_4AsCl$ in chloroform (b). $[(C_6H_5)_4As^+]$: (1) $1 \cdot 10^{-5}$ *M*; (2) $2 \cdot 10^{-5}$ *M*; (3) $4 \cdot 10^{-5}$ *M*; (4) $4 \cdot 10^{-4}$ *M*.

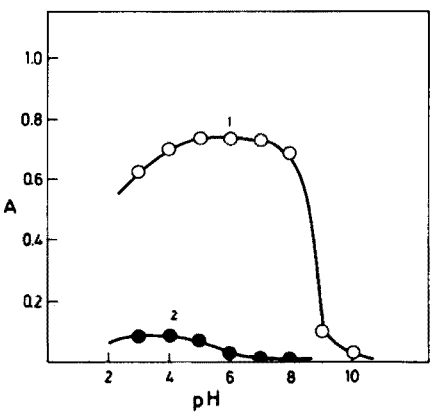

Fig. 2. The effect of pH. (1) $[(C_6H_5)_4As^+] = 2 \cdot 10^{-5}$ *M*; absorbance measured against the reagent blank. (2) Reagent blank.

In order to maintain the optimal pH range, acetate buffer was used and was added in a fixed amount to keep the ionic strength of the aqueous phase constant.

The maximal constant extraction was obtained with more than a 5-fold molar excess of the vanadium—PAR complex. Above this value the absorbance of the organic phase was independent of the reagent concentration as shown in Fig. 3.

Time of extraction and volume ratio

Fixed amounts of tetraphenylarsonium chloride and vanadium—PAR complex at pH 6 were shaken for times of 1—60 min; maximal extraction was achieved after a shaking period of 2 min, and further shaking up to 60 min produced no further change in absorbance. Results obtained with tetraphenylarsonium chloride initially present in the organic phase were identical with the results obtained when the salt was in the aqueous phase.

Equal volumes of aqueous and organic phase were used in most of the experiments described, but the same results were obtained with V_{org}/V_{aq} ratios up to 1:3, in single extractions. Thus, the lower limit of detection may be decreased by preconcentration.

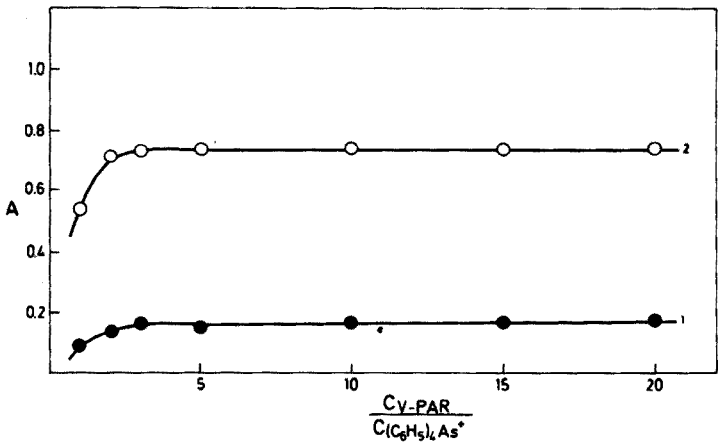

Fig. 3. The effect of reagent concentration. $[(C_6H_5)_4As^+]$ = (1) $5 \cdot 10^{-6}$ *M*; (2) $2 \cdot 10^{-5}$ *M*.

Stability of reagent solution and the extracts

Aqueous solutions of the vanadium—PAR complex were stable for at least two weeks. The colour intensity of the extracts was also very stable; no measurable change in absorbance of the chloroform phase occurred for 48 h.

Beer's law, sensitivity and precision

The calibration graph by the recommended procedure was linear over the range $1 \cdot 10^{-6}$—$5 \cdot 10^{-5}$ *M* tetraphenylarsonium ion in the extract. The effective molar absorptivity at 560 nm was $3.8 \cdot 10^4$ l $mol^{-1}cm^{-1}$.

The reproducibility was estimated from the results of twenty determinations with tetraphenylarsonium concentrations of $5 \cdot 10^{-6}$ and $2 \cdot 10^{-5}$ *M*. The mean absorbances measured in the 1-cm cell were 0.185 and 0.768, respectively, with an average deviation of 0.01 absorbance unit.

Effect of anions

The effect of the anions on the extraction of tetraphenylarsonium with vanadium—PAR complex was studied by the addition of the anion to the aqueous phase in excess over tetraphenylarsonium chloride, which was added later with the chloroform phase. There was no significant interference by moderate amounts of most of the anions studied, except for hexafluorophosphate and perchlorate (Table II), which decreased the absorbance of the chloroform phase at 560 nm, since they competed with the vanadium—PAR complex for the tetraphenylarsonium cation. However, when these ions were not present in excess, the method could be applied successfully.

The effect of triphenylarsine oxide

The coprecipitation of triphenylarsine oxide with tetraphenylarsonium salts during the standard method of synthesis [10] could hardly be avoided. When tetraphenylarsonium salts are determined by u.v. spectrophotometry, coprecipitated triphenylarsine oxide causes large spectrophotometric errors [4]. In contrast, no significant interference was found in the determination of tetraphenylarsonium salts by the proposed extraction—visible spectrophotometric method, even in the presence of relatively large amounts of triphenylarsine oxide (Table III).

Composition of the extracted species

The molar ratio for the tetraphenylarsonium—vanadium—PAR species in the organic phase, derived by application of the Job method, the mole-ratio and slope-ratio methods was found to be 1:1:1. An anionic vanadium(V)—PAR complex species, VO_2R^-, is present primarily in the reagent—buffer solution at pH 6, and the tetraphenylarsonium ion is extracted into the organic phase from the aqueous solution by ion-pair formation [6]:

$$[(C_6H_5)_4As]^+ + [VO_2R]^-_{aq} \rightleftharpoons [(C_6H_5)_4As][VO_2R]_{org}$$

TABLE II

Effect of anions

(Organic phase: $2 \cdot 10^{-5}$ *M* $(C_6H_5)_4AsCl$ in chloroform. Aqueous phase: $1 \cdot 10^{-4}$ *M* vanadium–PAR, acetate buffer (0.2 *M*) and anion added.)

Anion[a]	$[(C_6H_5)_4As]/[anion]$	A_{560}	Anion[a]	$[(C_6H_5)_4As]/[anion]$	A_{560}
—	—	0.760	PF_6^-	1 : 1	0.638
F^-	1 : 10	0.740		1 : 5	0.430
	1 : 100	0.740		1 : 50	0.135
	1 : 1000	0.730		1 : 500	0.030
Cl^-	1 : 1	0.760	MnO_4^-[b]	1 : 1	0.752
	1 : 50	0.758		1 : 10	0.740
	1 : 500	0.759		1 : 100	0.020
	1 : 5000	0.760	CrO_4^{2-}	1 : 10	0.748
Br^-	1 : 50	0.773		1 : 100	0.708
	1 : 500	0.770		1 : 1000	0.660
	1 : 5000	0.746	WO_4^{2-}	1 : 1	0.750
	1 : 15000	0.655		1 : 10	0.750
I^-	1 : 1	0.770		1 : 100	0.590
	1 : 5	0.764		1 : 1000	0.450
	1 : 50	0.736	MoO_4^{2-}	1 : 1	0.795
	1 : 500	0.550		1 : 10	0.770
	1 : 5000	0.280		1 : 100	0.792
SCN^-	1 : 1	0.771		1 : 1000	0.785
	1 : 5	0.770	$H_2PO_4^-$	1 : 50	0.765
	1 : 50	0.724		1 : 500	0.770
	1 : 500	0.575		1 : 5000	0.770
	1 : 5000	0.211	$C_2O_4^{2-}$	1 : 5	0.758
NO_3^-	1 : 5	0.764		1 : 50	0.757
	1 : 50	0.756		1 : 500	0.755
	1 : 500	0.770		1 : 5000	0.595
	1 : 5000	0.686	Ac^-	1 : 0	0.710[c]
ClO_4^-	1 : 1	0.760		1 : 10000	0.761
	1 : 10	0.675		1 : 20000	0.750
	1 : 100	0.330		1 : 40000	0.762
	1 : 1000	0.090		1 : 50000	0.755

[a] All anions were added as their sodium or potassium salts except for PF_6^- and MoO_4^{2-}, which were added as their ammonium salts.
[b] $KMnO_4$ at higher concentrations oxidizes PAR.
[c] Without acetate buffer.

TABLE III

Effect of triphenylarsine oxide

(Aqueous phase: $1 \cdot 10^{-4}$ *M* V—PAR in acetate buffer pH 6. Organic phase: tetraphenylarsonium chloride and triphenylarsine oxide in chloroform.)

$(C_6H_5)_3AsO$ added ($\cdot 10^{-5}$ *M*)	$(C_6H_5)_4AsCl$ ($\cdot 10^{-5}$ *M*)	
	Added	Found
0.2	—	0.00
—	2.0	2.00
0.2	2.0	2.01
2.0	2.0	2.03
10.0	2.0	2.04
20.0	2.0	2.09

The same equilibrium is reached when the tetraphenylarsonium salt is present initially in the organic solution.

SUMMARY

An extraction—visible spectrophotometric method for the determination of tetraphenylarsonium salts is described. The method is based on the extraction of the ion-pair formed between the tetraphenylarsonium cation and the anionic vanadium(V)—4-(2-pyridylazo)resorcinol complex, followed by the spectrophotometric measurements of the coloured organic phase at 560 nm. The method can be applied to micro amounts of tetraphenylarsonium salt or to very dilute solutions (10^{-6}—10^{-5} *M*). It is more sensitive and less subject to interferences than the direct u.v. method.

REFERENCES

1 C.N.R. Rao, J. Ramachandran and A. Balasubramanian, Can. J. Chem., 39 (1961) 171; R. Armstrong, N.A. Gibson, J.W. Hosking and D.C. Weatherburn, Aust. J. Chem., 20 (1967) 2771; A.I. Popov and R.E. Humphrey, J. Amer. Chem. Soc., 81 (1959) 2043.
2 H.E. Affsprung and V.S. Archer, Anal. Chem., 35 (1963) 1912; T. Okubo, F. Aoki and T. Teraoka, Nippon Kagaku Zasshi, 89 (1968) 432, Chem. Abstr., 69 (1968) 22500q.
3 N.A. Gibson and D.C. Weatherburn, Anal. Chim. Acta, 58 (1972) 149; 58 (1972) 159.
4 K.W. Loach, Anal. Chim. Acta, 45 (1969) 93.
5 H. Flaschka, Mikrochemie, 40 (1953) 21.
6 M. Široki and C. Djordjević, Anal. Chim. Acta, 57 (1971) 301; J. Less-Common Metals, 23 (1971) 228.
7 M. Široki and C. Djordjević, Anal. Chem., 43 (1971) 1377.
8 M. Široki, Lj. Marić, Z. Štefanac and M.J. Herak, Anal. Chim. Acta, 75 (1975) 101.
9 Lj. Marić, M. Široki and M.J. Herak, J. Inorg. Nucl. Chem., (1975) in press.
10 R.L. Shriner and C.N. Wolf, Org. Syn., Coll. Vol. IV (1963) 910.

Analytica Chimica Acta, 79 (1975) 273—278

TITRATION OF ANTIMONY(III) WITH CERIUM(IV) SULPHATE AND DIPHENYLAMINE AND ITS DERIVATIVES AS REVERSIBLE INDICATORS

G. GOPALA RAO, S.G. VISWANATH and MURALIKRISHNA GANDIKOTA
Department of Chemistry, Andhra University, Waltair (India)
(Received 20th March 1975)

The determination of antimony is of great importance in minerals and alloys of lead, tin, and copper, such as solder, bearing and type metals, etc. Antimony is also added to lead to increase its hardness for use as cable coverings and storage battery plates. Antimony oxide is an important constituent of some white pigments and enamels, and is also used in certain pharmaceuticals. Metallic antimony has been recommended for standardization of permanganate [1] and bromate [2]. The difficulties encountered in the determination of antimony(III) with permanganate, iodate and bromate have been well documented [3]. Rathsburg [4] was the first to employ cerium(IV) sulphate for the titration of antimony(III) at room temperature, in an approximately 1.8—3.7 *M* hydrochloric acid medium, using various irreversible indicators. This method was confirmed by Furman [5] and Petzold [6], but Willard and Young [7] found the oxidation too slow and proposed iodine monochloride as a catalyst. The end-point change with methyl orange is said to be very sluggish unless the hydrochloric acid concentration is 3—4 *M* at the end-point [8]. Methyl orange [5] and methyl red [6] have been preferred as the indicator; no satisfactory reversible indicators have so far been reported for this titration. Willard and Young [9] stated that ferroin is satisfactory at 50 °C in a medium containing 15 % (v/v) hydrochloric acid and iodine monochloride catalyst, but this has been disputed [10]. As irreversible indicators often cause trouble, especially in inexperienced hands, the use of diphenylamine and its derivatives has been investigated; the successful use of these reversible indicators in the titration of arsenic(III) with cerium(IV) has recently been reported [11]. The procedures described below for the determination of antimony(III) with diphenylamine-type indicators possess several advantages over earlier methods for this determination.

EXPERIMENTAL

Reagents

Antimony(III) solutions (0.05 N). Three solutions were prepared from analytical-grade reagents. *Solution A:* Antimony(III) chloride was dissolved

in 3 *M* hydrochloric acid and the solution was standardized against Analar potassium bromate as described by Vogel [12]. *Solution B*: Antimony(III) oxide was dissolved in hot concentrated sulphuric acid and the solution was cooled; sufficient hydrochloric acid was added to give a solution containing 2 *M* sulphuric acid and 0.7 *M* hydrochloric acid after dilution to 1 l. *Solution C*: An aqueous solution was prepared from tartar emetic.

Indicator solutions (0.01 M). Diphenylamine and diphenylbenzidine solutions were prepared in concentrated sulphuric acid, barium diphenylamine sulphonate in water, N-phenylanthranilic acid in sodium carbonate, and 2-nitrodiphenylamine in glacial acetic acid; 0.1 ml of indicator solution was used for 50 ml of titration mixture.

Catalyst mixture. This was prepared by mixing 20.8 ml of 0.1 *M* potassium iodide and 4.16 ml of 0.1 *M* potassium iodate and diluting to 250 ml; 1 ml of the catalyst mixture was added to 50 ml of titration mixture. Iodine monochloride was not found satisfactory. As the iodine catalyst is not affected by the titration, no correction is necessary.

A 0.05 *M* cerium(IV) sulphate solution in 0.5 *M* sulphuric acid was prepared and standardized as described previously [11].

Model procedure

Treat 5—9 ml of antimony(III) solution with enough water and sulphuric or hydrochloric acid to give the required acidity (in addition to that derived from the antimony solution) when diluted to 50 ml. Add 1 ml of the catalyst mixture and 0.1 ml of the indicator solution. Titrate with 0.05 *M* cerium(IV) sulphate solution at the usual speed for diphenylamine or diphenylbenzidine, and with a wait of 10—15 s between drops near the end-point for barium diphenylamine sulphonate.

RESULTS

Determination of antimony(III) in antimony trichloride in hydrochloric acid medium

Antimony solution A was titrated as indicated above in 1.0 *M* hydrochloric acid media. Diphenylamine and diphenylbenzidine proved satisfactory indicat N-Phenylanthranilic acid and 2-nitrodiphenylamine did not function as indicat in hydrochloric acid medium, being destroyed even in the initial stages of the titration. Even the other indicators were unsatisfactory if the concentration of hydrochloric acid added exceeded 1 *M*.

Determination of antimony(III) in sulphuric acid medium

Titrations were made as indicated above, with antimony solutions A and B in 0.5—2 *M* sulphuric acid media. Diphenylamine, diphenylbenzidine and

TABLE I

Titration of antimony(III) with cerium(IV) sulphate

Indicator	Antimony(III) (meq)		Indicator	Antimony(III) (meq)	
	Taken	Found		Taken	Found
Diphenylamine	0.2404	0.2402	Barium diphenylamine sulphonate	0.2404	0.2403
	0.3005	0.3000		0.3846	0.3850
	0.3605	0.3598		0.4206	0.4206
	0.4206	0.4189		0.4807	0.4804
	0.4807	0.4797			
Diphenylbenzidine	0.3005	0.2995			
	0.3185	0.3180			
	0.4507	0.4490			
	0.4807	0.4796			

barium diphenylamine sulphonate functioned satisfactorily. Typical results are presented in Table I. The reversibility of the indicators was excellent and the end-point colours were very vivid and stable. It is noteworthy that the colours of the oxidation products of diphenylamine and diphenylbenzidine were stable for over 3 h, whereas that of barium diphenylamine sulphonate was stable only for 15 min. Even the low concentration of hydrochloric acid derived from either of the antimony(III) solutions hampered the indicator action of N-phenylanthranilic acid and 2-nitrodiphenylamine.

When more dilute solutions (0.01 *N*) of antimony(III) solution A, containing 0.1 ml of diphenylamine solution as indicator and 1 ml of catalyst mixture, were titrated with 0.01 *M* solutions of cerium(IV) sulphate in 0.5 *M* sulphuric acid, irregular results were obtained. When 0.5 ml of catalyst solution and 0.1 ml of indicator solution were used, the consumption of 0.01 *M* cerium(IV) sulphate was 0.06 ml too high. Titrations based on 0.5 ml of catalyst mixture and 0.05 ml of diphenylamine solution were accurate, and there was no need for indicator corrections.

Interferences. Hydrochloric acid or chloride ion did not interfere in titrations of antimony(III) in 0.5 *M* sulphuric acid medium when diphenylamine served as indicator. When the chloride concentration was 1.5 *M*, reduction of the oxidized indicator was very slow, so that waits of 1—2 min between titrant additions were necessary. Phosphoric acid did not interfere up to 0.2 *M*. Copper sulphate and manganese(II) sulphate did not interfere up to 0.5 meq.

Titrations of mixtures of arsenic(III) and antimony(III)

Both arsenic(III) and antimony(III) were accurately accounted for in the titration of mixtures in 0.5 *M* sulphuric acid medium, with cerium(IV) sulphate when the iodate—iodide catalyst mixture was used with diphenylamine, diphenylbenzidine or barium diphenylamine sulphonate as indicator.

Sequential titration of iron(II) and antimony(III)

Iron(II) and antimony(III) (*ca.* 0.05 *N*) could be titrated consecutively in 0.5—1 *M* sulphuric acid medium, if 2—3 ml of syrupy phosphoric acid was added per 50 ml of the titration mixture. After the iron(II) end-point, 1 ml of catalyst mixture was added and the titration was completed. The volume of cerium(IV) sulphate between the first and second end-points corresponded to antimony(III). Table II gives some typical results.

Determination of antimony(III) in tartar emetic

Potassium antimonyl tartrate is used in the treatment of schistosomiasis. Antimony(III) in tartar emetic could be readily titrated with cerium(IV) sulphate when diphenylamine, N-phenylanthranilic acid or 2-nitrodiphenylamine was used as the indicator. The absence of chloride ion in this solution appeared to facilitate the use of the last two indicators. With barium diphenylamine sulphonate, the oxidized indicator was reduced only very slowly, waits of 20—25 s between titrant additions being necessary near the end-point. Diphenylamine and N-phenylanthranilic acid were satisfactory in 0.5—2 *M* sulphuric acid medium, whereas a minimum acid concentration of 1 *M* was necessary with 2-nitrodiphenylamine. With the last two indicators a wait of *ca.* 10 s was necessary for full colour development of the oxidized indicator. Results are presented in Table III along with some observations on the stabilitie of the oxidized products.

Titrations of 0.01 *N* solutions of tartar emetic were satisfactory with 0.01 *M* solutions of cerium(IV) sulphate in 0.5 *M* sulphuric acid medium when 0.05 ml of diphenylamine solution or 0.1 ml of N-phenylanthranilic acid solution was used with 0.5 ml of catalyst solution.

DISCUSSION

Cerium(IV) sulphate is a good general oxidizing titrant, but its use for the determination of antimony(III) has not been widely accepted. Hammock *et*

TABLE II

Sequential titration of iron(II) and antimony(III)

Amount of iron(II) (meq)		Amount of antimony(III) (meq)	
Taken	Found	Taken	Found
0.3172	0.3165	0.1227	0.1230
0.1813	0.1804	0.2455	0.2466
0.2267	0.2267	0.2041	0.2041
0.1360	0.1362	0.2864	0.2872

TABLE III

Titration of potassium antimonyl tartrate with cerium(IV) sulphate (1.0 ml of the catalyst mixture and 0.1 ml of indicator solution per 50 ml of titration mixture.)

Indicator	Tartar emetic (meq)		Stability of oxidized indicator
	Taken	Found	
Diphenylamine	0.2230	0.2235	
	0.2676	0.2672	>3 h
	0.3118	0.3120	
	0.3560	0.3574	
N-Phenylanthranilic acid	0.2230	0.2230	
	0.2454	0.2445	10 min
	0.3118	0.3126	
	0.4030	0.4030	
2-Nitrodiphenylamine	0.2330	0.2326	
	0.2454	0.2458	6 min
	0.2900	0.2915	
	0.3792	0.3790	

al. [13] attempted the titration of antimony(III) to an iodine monochloride end-point in the presence of carbon tetrachloride. As the titration was found to be difficult and tedious, even at the optimal concentration of 2.5—3 *M* hydrochloric acid, these authors concluded that iodate and permanganate are preferable to cerium(IV) sulphate for this determination. Rathsburg [4] used the irreversible indicators methylene blue, methyl orange, methyl red and congo red. Furman [5] considered methyl red to be less satisfactory than methyl orange, because of its greater ease of oxidation by cerium(IV). The precautions necessary with methyl orange have been discussed fully by Swift [8]. These indicators have the further disadvantage that iron(II) interferes in the titration of antimony(III). Moreover, arsenic(III) interferes to some extent in the titration of antimony(III) even under the conditions prescribed by Pribil [14] with methyl orange as indicator. Even in the electrometric titration of antimony(III), arsenic(III) interferes unless the concentrations of hydrochloric acid and iodine monochloride catalyst are carefully controlled [4,5,9,14]; and the potential jump is very low [5] (*ca.* 50 mV).

The use of the reversible indicators described here therefore appears to be advantageous. Diphenylamine was observed to be perfectly reversible in this titration and its oxidized product was very stable. Diphenylamine has the further advantage that it works well even in 0.5 *M* sulphuric acid medium, whereas the irreversible indicators require a high concentration of hydrochloric acid. The stabilities of the oxidation product of diphenylamine in the titrations of iron(II), arsenic(III) and antimony(III) under similar conditions are shown in Table IV.

Diphenylamine conveys the further advantage that a sequential titration

TABLE IV

Times of visual stability of the oxidation product of diphenylamine

Titration	Conditions	Time of stability
Iron(II)	1 *N* H_2SO_4 + H_3PO_4	>3 h
Arsenic(III)	1 *N* H_2SO_4 + iodine catalyst	>45 min
Antimony(III)	1 *N* H_2SO_4 + iodine catalyst + 0.3—0.8 *N* HCl	>3 h

of iron(II) and antimony(III) in a single solution is viable. The establishment of diphenylamine as a convenient reversible indicator in the titration of arsenic (III) [11] and antimony(III) gives cerium(IV) sulphate its due placement among oxidizing titrants.

SUMMARY

Diphenylamine, barium diphenylamine sulphonate, N-phenylanthranilic acid and 2-nitrodiphenylamine have been investigated as reversible indicators for the titration of antimony(III) with cerium(IV) sulphate in 0.5—2 *M* sulphuric acid medium. Diphenylamine is the most satisfactory in titrations of antimony(III) in chloride-free solutions, *e.g.* of potassium antimonyl tartrate. Even low chloride concentrations affect the indicator action of N-phenylanthranilic acid or 2-nitrodiphenylamine, but diphenylamine is satisfactory in 1 *M* hydrochloric acid media. Iodine catalyst is necessary to accelerate the reduction of the oxidized indicator by antimony(III). The indicator colour change is vivid and the colour of the oxidized indicator is stable. Titrations of antimony(III) in mixtures with iron(II) and arsenic(III) are also considered.

REFERENCES

1 R. Fiala, Osterr. Chem. Ztg., 50 (1949) 242.
2 L.A. Wooten and C.L. Luke, Ind. Eng. Chem., Anal. Ed., 13 (1941) 771.
3 I.M. Kolthoff and R. Belcher, Volumetric Analysis, Vol. III, Interscience, New York, 1957, p.73.
4 H. Rathsburg, Ber. Bunsenges. Phys. Chem., 61 (1928) 663.
5 N.H. Furman, J. Amer. Chem. Soc., 54 (1932) 4335.
6 A. Petzold, Z. Anal. Chem., 150 (1956) 111.
7 H.H. Willard and P. Young, J. Amer. Chem. Soc., 50 (1928) 1376.
8 E.H. Swift, Introduction to Quantitative Analysis, Prentice-Hall, New York, 1950, p.169 ff.
9 H.H. Willard and P. Young, J. Amer. Chem. Soc., 55 (1933) 3268.
10 R. Pribil, Chem. Listy, 39 (1945) 19.
11 Muralikrishna Gandikota and G. Gopala Rao, Anal. Chim. Acta, 65 (1973) 231.
12 A.I. Vogel, Textbook of Quantitative Inorganic Analysis, The English Language Book Society and Longman, London, 1973, p.386.
13 E.W. Hammock, R.A. Brown and E.H. Swift, Anal. Chem., 20 (1948) 1048.
14 R. Pribil, Chem. Listy, 37 (1943) 205.

Analytica Chimica Acta, 79 (1975) 279—284

Short Communication

A MICROCOULOMETRIC METHOD FOR THE DETERMINATION OF NANOGRAM AMOUNTS OF SULPHUR IN ORGANIC COMPOUNDS

G. de GROOT* and P.A. GREVE

Laboratory of Toxicology, National Institute of Public Health, Sterrebos 1, Utrecht (The Netherlands)

and R.A.A. MAES

Laboratory of Toxicology, State University, Vondellaan 14, Utrecht (The Netherlands)

(Received 10th February 1975)

The determination of sulphur in organic compounds is often time-consuming and complicated. The micro-analytical method of Schöniger [1] is simple and precise, the sulphur being determined as sulphate after destruction of the sample in an oxygen flask; many modified procedures of end-point indication have been reported [2—5], and for the determination of traces of sulphur spectrophotometric titrations have been used, but generally, these methods are insufficiently sensitive for trace analysis [6—10].

Coulometric procedures in combination with electrochemical end-point indication are fast, sensitive and more selective [11—20]. Continuous destruction of the sample in a quartz tube is used in most of these methods; either a reductive or an oxidative method can be used.

The drawbacks of the reductive method are that: (a) halogens and nitrogen are reduced to compounds which interfere in the determination of hydrogen sulphide, and although this problem can be solved [20], the determination then becomes too complicated for routine analyses; (b) because of the high reduction temperature (*ca.* 1150 °C), the lifetime of the quartz tube is limited; and (c) it is difficult to find a catalyst which combines a high reducing activity with a low adsorbing capacity for the reduced products.

The oxidative procedure is therefore generally preferred. In this method, any nitrogen oxides formed during the oxidation interfere in the iodimetric determination of sulphur dioxide; Wallace *et al.* [20] solved this problem simply by adding sodium azide to the electrolyte in the titration cell. Another problem is that the conversion of sulphur to sulphur dioxide is non-stoichiometric, sulphur trioxide being formed also. Mixtures of SO_2 and SO_3 exist in an equilibrium which can be described by:

*Present address: Laboratory of Toxicology, State University, Vondellaan 14, Utrecht (The Netherlands).

$$K_p = \frac{p_{SO_2^2} \cdot p_{O_2}}{p_{SO_3^2}} \quad (1)$$

where p denotes the partial pressures of the respective gases. K_p depends [6] on the absolute temperature (T) according to:

$$\log K_p = 6.38 \log T - 9480/T - 0.0049\ T - 5.41 \quad (2)$$

The value of K_p increases from 0.7 at 800 °C through 2.1 at 900 °C to 6.0 at 1000 °C, so that high temperatures are preferred for the oxidation. In addition to the temperature and the partial oxygen pressure, the design of the combustion tube affects the percentage of sulphur converted to SO_2. The tube must be constructed so that the emerging gases are cooled to room temperature as fast as possible in order to "freeze" the equilibrium. Accordingly, both the combustion and the outlet zone temperatures are 950 °C; the emerging gases then cool in the short distance between the tube outlet and the titration cell.

Experimental

Instrumentation. A block diagram of the instrument is shown in Fig.1. The coulometer used is based on the principles described by Krijgsman *et al.* [21, 22] modified to meet the particular demands of the sulphur determination. The electronic diagram is shown in Fig.2. This coulometer was preferred because of its simplicity, low cost and reliability compared to commercially available instruments of the same sensitivity and versatility. The amplification

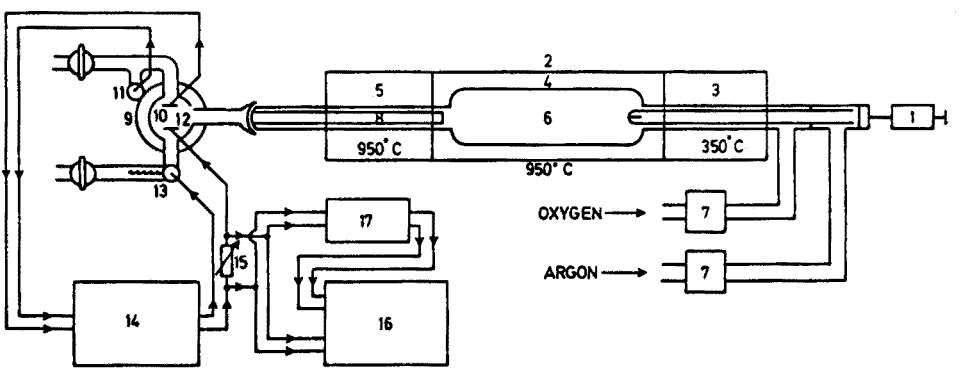

Fig.1. Block diagram of the instrument. 1, Injection syringe, S.G.E. 10A-RN-GP. 2, Furnace, Dohrmann S-300. 3, Inlet zone. 4, Destruction zone. 5, Outlet zone. 6, Combustion tube, Dohrmann P/N 523729. 7, Molecular sieve 5 A. 8, Quartz outlet tube. 9, Titration cell, Dohrmann T-300-P. 10, Indicator electrode, Pt (7 × 7 mm). 11, Reference electrode, Pt wire in saturated I_3^- solution. 12, Generator anode, Pt (7 × 7 mm). 13, Generator cathode, Pt wire. 14, Coulometer. 15, Range-ohm potentiometer. 16, Recorder, Varian A-25 double trace recorder. 17, Integrator, Becker 763. 18, Pressure valve.

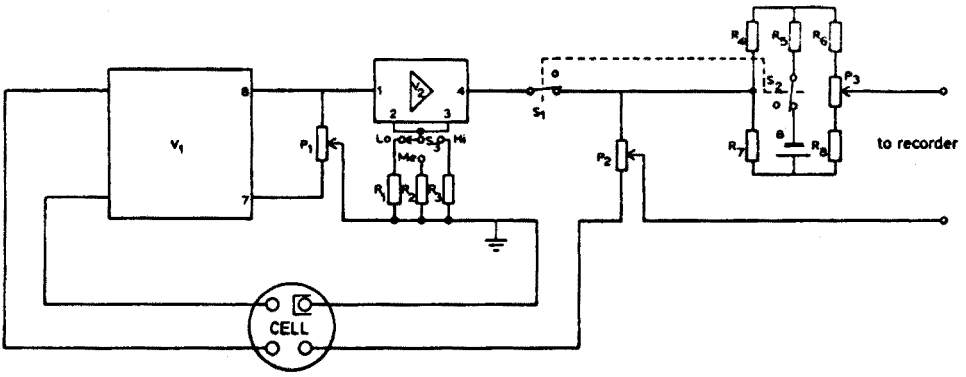

Fig.2. Electronic diagram of the coulometer. V_1, Knick "Messzusatz" type 47. V_2, Knick d.c. amplifier type Hv. S_1, "Function"-switch. S_2, "Function"-switch. S_3, "Gain"-switch. P_1, Potentiometer 10 Ω lin, "Gain set". P_2, "Ten turns" potentiometer 1000 Ω lin, "range-ohms". P_3, "Ten turns" potentiometer 100 Ω lin, "Recorder-zero". R_1, Resistor 1000 Ω, 1/2 W. R_2, Resistor 100 Ω, 1/2 W. R_3, Resistor 10 Ω, 1/2 W. R_4, Resistor 100 Ω, 1/2 W. R_5, Resistor 27 kΩ, 1/2 W. R_6, Resistor 100 Ω, 1/2 W. R_7, Resistor 100 Ω, 1/2 W. R_8, Resistor 100 Ω, 1/2 W. B, Mallory Duracel mercury battery, 1.4 V.

factor can be altered by setting the "Gain" switch as follows: "Lo", 0—0.75 μA output current per mV input signal; "Me", 0—7,5 μA output current per mV input signal; "Hi", 0—75 μA output current per mV input signal. Within each gain set, the amplification can be linearly varied with the "Gain-set" potentiometer.

Reagents. Reference solutions were prepared for the following sulphur compounds: dichlofluanid and parathion (Bayer); tetrasul, tetrasulfoxide and tetradifon (Philips-Duphar); malathion (American Cyanamid Company); promazine.HCl (Wyeth); chlorpromazine.HCl, promethazine.HCl and levomepromazine (Specia); perphenazine (Schering). The solvent is discussed below.

A stock solution of the generator electrolyte was prepared by dissolving 0.2 g of NaI, 20 g of NaBr, 5 g of glacial acetic acid and 6 g of NaN_3 in twice-distilled water and diluting to 1 l. Daily, 5 ml of this solution was diluted with 45 ml of twice-distilled water for actual use.

Procedure. The sample solution (5 μl) is injected with a 10-μl syringe into the inlet zone of the combustion tube. The vapors formed are carried with argon into the combustion zone where the material is burned after addition of oxygen. The products are then swept into the titration cell through the inlet capillary. The titration cell contains the indicator and the generator electrode systems, and is filled with the generator electrolyte containing definite concentrations of triiodide and iodide representing a "bias potential". The SO_2 is oxidized according to the overall reaction:

$$2\,H_2O + SO_2 + I_3^- \rightleftharpoons SO_4^{2-} + 4\,H^+ + 3\,I^-$$

The triiodide concentration is detected by the platinum indicator electrode, the reference platinum electrode being placed in a saturated triiodide solution

in the conventional manner. When the indicator system detects a potential different from the preset bias potential, the generator system operates until the potential is restored to the initial value. The total current that passes through the generator system is integrated, so that the amount of sulphur present in the sample can be calculated.

The optimal working conditions are: oxygen flow, 125 ml min^{-1}; argon flow, 175 ml min^{-1}; inlet zone temperature, 350 °C; combustion zone temperature, 950 °C; outlet zone temperature, 950 °C; range-ohms, 500 Ω. The injection rate must not exceed 0.2 $\mu l\ s^{-1}$, otherwise incomplete combustion will occur.

Special care must be taken in choosing the solvent; it must be sufficiently polar to dissolve the sulphur compounds, and its boiling point should be high enough to avoid selective evaporation of the solvent in the injection needle. A 5:2·5:2·5 (v/v) mixture of hexadecane, acetone and petroleum ether proved satisfactory.

Results and discussion

In the generator electrolyte, iodide and triiodide are kept low, to minimize evaporation of iodine and to ensure maximal sensitivity; bromide serves as a redox buffer in order to obtain a quantitative yield of triiodide, and as a charge carrier in order to maintain a low cell impedance. The triiodide concentration is a function of the bias potential; a potential of 65 mV was found to be optimal. Deviations from this value resulted either in excessive evaporation of iodine or in a slow reaction rate. The stirring rate must be as fast as possible without damaging the titration cell components.

The amplification factor must be adjusted according to the following considerations. If it is too low, there is tailing of the titration curve, but if it is too high, there is overshooting; both effects cause extended titration times. In practice an amplification factor varying between 0.35 (samples with high sulphur content) and 0.60 $\mu A\ mV^{-1}$ (samples with low sulphur content) was found suitable. Under these conditions an analysis can be completed in 3—6 min.

The sulphur content of a sample can be calculated by the following equation

$$S\ (ng\ \mu l^{-1}) = \frac{M\,Q\,10^{11}}{n\,F\,A\,R}$$

where A is the volume injected (μl), M is the molecular weight of sulphur, R is the recovery (%), and n, Q and F have their usual meanings.

The recovery and the linearity of the instrumental response for different sulphur types were determined for prepared standards in the 5—100 p.p.m. range. The results in Table I show that the recoveries averaged 76.0 % and were independent of the type of sulphur linkage. Table II indicates that the percentage recoveries vary with the amount of sulphur, being 78.8 % for 5 ng S μl^{-1}, 76.5 % for 20 ng S μl^{-1} and 74.0 % for 100 ng S μl^{-1}. If a calibra-

TABLE I

The recovery for prepared standards of different sulphur compounds

Sample	S present (ng μl^{-1})		Recovery (%)	No. of detns.	s_r (%)
	Calcd.	Found			
Dichlofluanid	20.0	15.6	77.7	6	1.5
Tetrasul	19.9	15.2	76.5	7	2
Tetrasulfoxide	19.5	14.9	76.3	7	1.5
Tetradifon	20.1	15.4	76.4	8	1.5
Malathion	21.9	16.0	73.1	6	2
Parathion	29.3	23.1	79.0	6	2.5
Promazine.HCl	20.6	15.5	75.2	7	1.5
Chlorpromazine.HCl	18.6	13.9	74.7	5	0.5
Promethazine.HCl	23.5	17.7	75.3	8	1
Levomepromazine	19.8	14.9	75.3	7	1.5
Perphenazine	21.3	16.4	77.0	6	1.5

TABLE II

Variation of recovery with concentration of sample

Sample	S present (ng μl^{-1})		Recovery (%)	No. of detns.	s_r (%)
	Calcd.	Found			
Tetrasul	4.97	3.86	77.7	5	3
Tetrasul	19.9	15.2	76.5	7	2
Tetrasul	92.7	67.5	72.8	11	1.5
Tetradifon	5.02	4.00	79.9	5	5.5
Tetradifon	20.1	15.4	76.4	8	1.5
Tetradifon	87.6	65.9	75.2	9	1

tion curve is prepared, the method can be used to determine 10—500 ng of sulphur in organic compounds. The procedure can be used for the determination of sulphur compounds in surface waters [23].

REFERENCES

1 W. Schöniger, Mikrochim. Acta (Wien), (1956) 869.
2 H. Wagner, Mikrochim. Acta (Wien), (1957) 19.
3 M. Boëtius, G. Gutbier and H. Reith, Mikrochim. Acta (Wien), (1958) 321.
4 L. Gildenberg, Microchem. J., 3 (1959) 169.
5 H. Malissa and L. Machherndl, Mikrochim. Acta (Wien), (1962) 1089.
6 J. Dokládalová, E. Korbl and M. Vecera, Collect. Czech. Chem. Commun., 29 (1964) 1962.

7 J. Dokládalová, Mikrochim. Acta (Wien), (1965) 344.
8 L.L. Farley and R.A. Winkler, Anal. Chem., 40 (1968) 962.
9 J.L. Lambert and D.J. Manzo, Anal. Chim. Acta, 48 (1969) 185.
10 J.B. Davis and F. Lindstrom, Anal. Chem., 44 (1972) 524.
11 D.M. Coulson, L.A. Cavanagh, J.E. de Vries and B. Walter, J. Agr. Food Chem., 8 (1960) 399.
12 E.M. Fredericks and G.A. Harlow, Anal. Chem., 36 (1964) 263.
13 R.L. Martin and J.A. Grant, Anal. Chem., 37 (1965) 644, 649.
14 D.F. Adams, R.K. Koppe and W.N. Tuttle, J. Amer. Pharm. Ass., 15 (1965) 31.
15 D.F. Adams, G.A. Jensen, J.P. Steadman, R.K. Koppe and T.J. Robertson, Anal. Chem., 38 (1966) 1094.
16 I. Cadersky, Z. Anal. Chem., 232 (1967) 103.
17 M.V. Drushel and A.L. Scommers, Anal. Chem., 39 (1967) 1819.
18 D.F. Adams and R.K. Koppe, J. Amer. Pharm. Ass., 17 (1967) 161.
19 M.V. Drushel, Anal. Chem., 41 (1969) 569.
20 L.D. Wallace, D.W. Kohlenberger, R.J. Joyce, R.T. Moore, M.E. Riddle and J.A. McNult Anal. Chem., 42 (1970) 378.
21 W. Krijgsman, W.P. van Bennekom and B. Griepink, Mikrochim. Acta (Wien), (1972) 42.
22 W. Krijgsman, G. de Groot, W.P. van Bennekom and B. Griepink, Mikrochim. Acta (Wien), (1972) 364.
23 R. Wegman, P. Greve and G. de Groot, Sci. Total Environ., in press.

Analytica Chimica Acta, 79 (1975) 285—291

Short Communication

SPECTRAL LINE INTERFERENCE IN THE ATOMIC ABSORPTION SPECTROMETRY OF LANTHANIDES

W. OOGHE and F. VERBEEK
Laboratory of Analytical Chemistry, University of Ghent, J. Plateaustraat 22, B-9000 Ghent (Belgium)
(Received 3rd March 1975)

When the standard addition technique is applied in a.a.s., no allowance need be made for changes in the population of atoms in the ground state caused by the matrix (chemical, ionization and matrix interferences), and only possible spectral interferences have to be investigated [1]. Molecular absorption occurs mainly in the far ultraviolet region, where there are no analytical lanthanide emission lines, hence this investigation can be limited to positive errors originating from overlap of the emission profile of the selected emission line with the absorption profile of a matrix element. Very few cases of this type of interference have been reported [2,3]. Two principal factors govern the degree to which two spectral lines may overlap: the distance between the centers of the emission line and the interfering absorption line, and the profiles of both lines [2]. Spectral line tables [4—6] are used to establish which lines exist in the immediate vicinity of an analytical emission line, and so may overlap.

Experimental

Instrumentation and reagents were the same as described previously [1].

Investigation of synthetic matrices. A synthetic matrix solution was prepared containing potassium and all the possibly interfering elements in concentrations varying from 1 to 10 g l^{-1}, but not the element being determined. This solution was vaporized in the flame under the optimal working conditions for the lanthanide investigated [1]. If no change in absorbance was observed in comparison with a blank solution containing only potassium, spectral line interference could be excluded. If, however, some of the light emitted was absorbed, the investigated lanthanide was present as an impurity in the synthetic matrix, or an interfering element was present in the cathode material of the emission source, or there was spectral line interference. To establish the real cause, the lanthanide investigated was added in increasing amounts to the synthetic matrix. The absorbances were measured and the intersection with the concentration axis was determined. This procedure was repeated at another

slit position and at a less sensitive emission line. Here two different cases could be distinguished:
(1) if independently of the working conditions, the concentration axis was intersected at approximately the same, mostly low concentration value, then this indicated the presence of the investigated lanthanide in the chemicals used for the synthetic matrix;
(2) if different intersection values were obtained, spectral line interference or the presence of an interfering element in the cathode material was involved; in this case, a supplementary investigation was required.

When the synthetic matrix solution was aspirated, there was usually no change of absorbance in comparison with a blank. For a few lanthanides such as dysprosium and erbium a low absorption, and for neodymium a relatively large absorption was found. Table I summarizes the spectral lines near the analytical lines of these three elements and the compositions of the synthetic

TABLE I

Data on the investigation of spectral line interference

	Nd	Dy	Er
Most sensitive absorption line (nm)	492.453	421.172	400.797
Possibly interfering lines (nm)	Pr, 492.459	Se, 421.183 Gd, 421.202	Fe, 400.727 Nd, 400.743 Se, 400.790 Se, 400.830 Pr, 400.871
Composition of synthetic matrix (μg ml^{-1})	Pr, 1000	SeO_2, 4500 Gd_2O_3, 4500	Fe, 1800 Nd_2O_3, 1800 SeO_2, 1800 Pr_6O_{11}, 1800

matrices. The standard addition technique was applied and the intersection values obtained are presented in Table II. Clearly, the intersection values for dysprosium and erbium are independent of the working conditions. Because it has been shown experimentally that SeO_2 and $FeCl_3$ do not contain dysprosium or erbium, this indicates the presence of 44 p.p.m. dysprosium in Gd_2O_3 (0.2 μg Dy ml^{-1} for 4500 μg Gd_2O_3 ml^{-1}) and of 22 p.p.m. erbium in the combined Pr_6O_{11}—Nd_2O_3 matrix (0.08 μg Er ml^{-1} for 3600 μg Pr_6O_{11} + Nd_2O_3 ml^{-1}). However, the presence of neodymium in the Pr_6O_{11} matrix cannot be accepted as an explanation because the intersection values depend on the working conditions (Table II). Moreover, amounts of 1.31 % and 0.97 % of neodymium in praseodymium (13.10 and 9.75 μg Nd ml^{-1} for 1000 μg Pr ml^{-1}) do not correspond with the purity data of the product used (Trona > 99. % purity). The different intersection values obtained at different wavelengths

TABLE II

Absorbance and intersection values obtained for the synthetic matrices given in Table I

Nd added	wavelength (nm)	492.453	492.453	463.42	
(μg ml^{-1})	band width (nm)	0.136	0.470	0.136	
0	absorbance	0.0184	0.0106	0.0009	
25		0.0535	0.0369	0.0250	
50		0.0891	0.0635	0.0482	
75		0.1235	0.0904	0.0721	
	Intersection (μg ml^{-1})	13.10	9.75	0.90[a]	
Dy added	wavelength (nm)	421.172	421.172	404.60	
(μg ml^{-1})	band width (nm)	0.068	0.235	0.068	
0	absorbance	0.0013	0.0011	0.0009	
4		0.0289	0.0261	0.0218	
8		0.0560	0.0508	0.0424	
12		0.0835	0.0752	0.0630	
	Intersection (μg ml^{-1})	0.2	0.2	0.2	
Er added	wavelength (nm)	400.797	400.797	400.797	415.11
(μg ml^{-1})	band width (nm)	0.235	0.068	2.35	0.235
0	absorbance	0.0006	0.0009	0.0006	0.0004
4		0.0424	0.0469	0.0320	0.0246
8		0.0830	0.0923	0.0622	0.0482
12		0.1229	0.1367	0.0894	0.0718
	Intersection (μg ml^{-1})	0.08	0.08	0.08	0.08

[a] The same intersection was obtained for the 494.48-nm Nd line at this bandwidth.

and band widths may be due to spectral interference or the presence of praseodymium in the neodymium lamp. The intersection value of 0.90 μg ml^{-1} obtained by measurements at the 463.42-nm line was confirmed by measurements at the 494.48-nm Nd line.

To check if the observed matrix absorbance was due to the presence of praseodymium in the neodymium lamp or to spectral line interference, a supplementary investigation was necessary. Because the phenomenon described was observed only for the 492.453-nm Nd line, the proposed investigation was applied to this lanthanide.

Investigation of the lamp spectrum of neodymium. When the cathode of the neodymium lamp is contaminated by praseodymium, the most sensitive praseodymium lines, *e.g.* the 492.459-nm line, will be emitted. This line could not be separated from the 492.453-nm neodymium line by the monochromator used, so that erroneous results were obtained when praseodymium was present in the matrix. A neodymium cathode contaminated by praseodymium will emit in the 490—496-nm region a spectrum consisting of the following lines: 490.18 nm Nd, 491.34 nm Nd, 491.40 nm Pr, 492.453 nm Nd

(most sensitive absorption line), 492.459 nm Pr, 493, 97 nm Pr, 494.48 nm Nd, 495.14 nm Pr (most sensitive absorption line), and 495.48 nm Nd. A detailed spectrum of the neodymium lamp was recorded at the lowest possible scanning speed (Fig.1); the 491.40-nm and the 493.97-nm praseodymium lines are absent. Because the 495.14-nm Pr line is the most sensitive emission line, the value 495.14 nm can be interpolated between the 494.48-nm and 495.48-nm Nd lines. Figure 1 shows that no line of this wavelength was emitted by the neodymium lamp, hence the presence of praseodymium in the neodymium cathode material can be ruled out. The only explanation remaining for the observed phenomenon must be spectral interference.

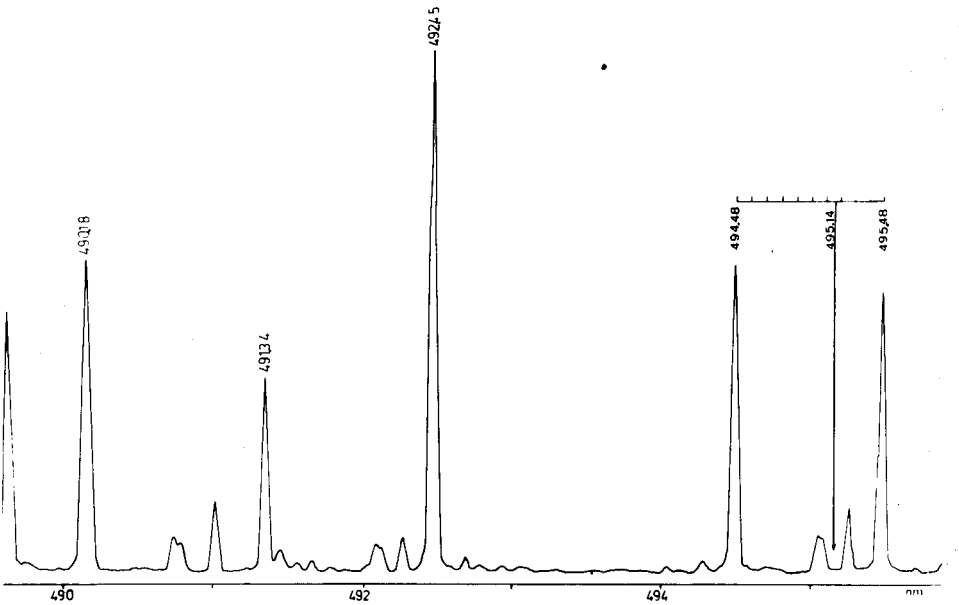

Fig.1. Spectrum of the neodymium lamp between 490 and 496 nm (scanning speed 0.4 nm min^{-1}) and interpolation of the value 495.14 nm.

Addition of the interfering praseodymium to neodymium. Praseodymium was added in increasing concentrations to a 40 μg Nd ml^{-1} solution buffered with potassium ions to prevent ionization interference. The absorbance was determined as a function of the praseodymium concentration, first at the disturbed 492.453-nm Nd line under the optimal working conditions — for neodymium as well as for praseodymium — and then at the undisturbed 463.42-nm neodymium line (Fig.2). With the optimal working conditions for neodymium, two straight lines of very different slopes were obtained. At 463.42 nm, the observed increase in absorbance was insignificant and can be explained by traces of neodymium in Pr_6O_{11}. At 492.453 nm, the increase in absorbance was very pronounced; this indicates that both neodymium and

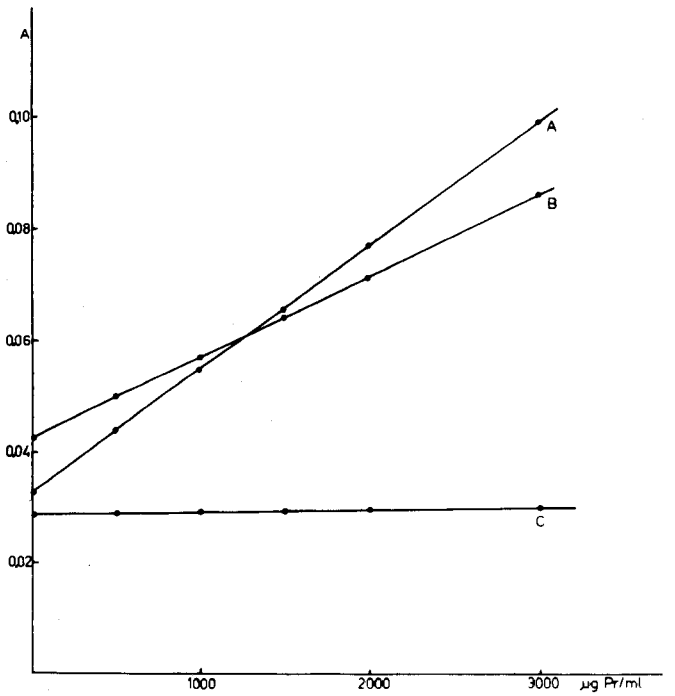

Fig.2. Addition of increasing concentrations of praseodymium to a 40 µg Nd ml^{-1} solution buffered with potassium ions. A, 492.453-nm Nd line; optimal conditions for praseodymium. B, 492.453-nm Nd line; optimal conditions for neodymium. C, 463.42-nm Nd line; optimal conditions for neodymium.

praseodymium absorb light from the neodymium lamp, the latter absorption being proportional to the amount of praseodymium added. Here, spectral interference is the only acceptable explanation, because there is no interference at the 463.42-nm line under the same working conditions. When the parameters were optimized for praseodymium, a still greater increase in the absorbance as a function of the concentration was obtained at the 492.453-nm line. In the absence of neodymium, it is thus possible to determine relatively large amounts of praseodymium with a neodymium lamp.

Reversibility of spectral interference. Further investigation showed that the observed spectral interference was reversible. In the same way as the 492.459-nm Pr absorption line absorbs light from the 492.453-nm Nd emission line of the neodymium lamp, the 492.453-nm Nd absorption line can absorb light from the 492.459-nm Pr emission line of the praseodymium lamp. For praseodymium determinations, this is less important because the 492.459-nm Pr line is not the most sensitive absorption line.

The absorbance values obtained by addition of an increasing concentration

of neodymium to a 200 μg Pr ml^{-1} solution buffered with potassium ions are shown in Fig.3 at the 492.459-nm and the 495.14-nm line of the praseodymium lamp. From the measurements at the 495.14-nm Pr line, it may be concluded that neodymium has no interfering effect on praseodymium; the slight increase in absorbance can be attributed to traces of praseodymium in Nd_2O_3. At the less sensitive 492.459-nm Pr line, there is a pronounced linear increase in absorbance for increasing amounts of neodymium. Because the wavelength setting is the only changed parameter, the absorbance increase must be due to spectral line interference caused by overlap of the 492.453-nm Nd absorban line and the 492.459-nm Pr emission line.

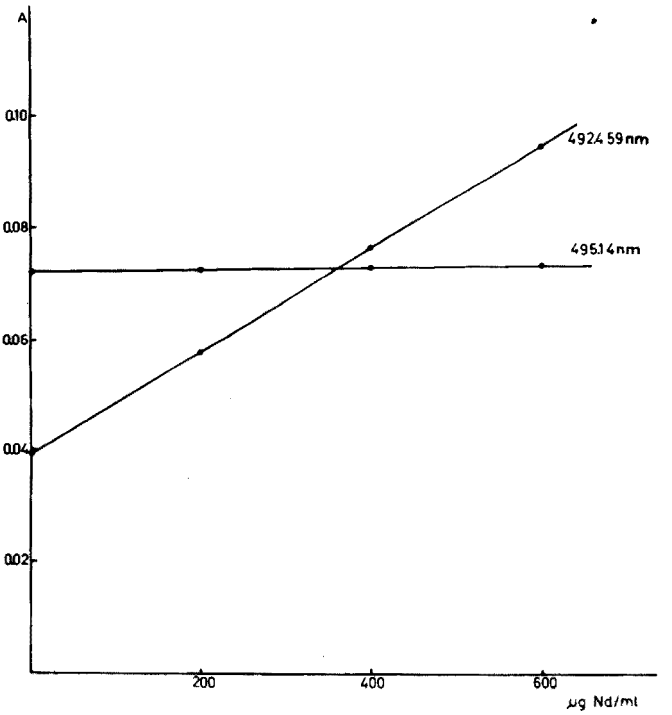

Fig.3. Addition of increasing concentrations of neodymium to a 200 μg ml^{-1} praseodymium solution buffered with potassium ions.

Conclusion

This investigation has shown that of all the analytical lanthanide spectral lines examined, only the 492.453-nm neodymium line is unsuitable for neodymium determinations in the presence of praseodymium. Because praseodymium and neodymium are adjacent elements in the periodic system and are both light lanthanides, they usually occur together in minerals and ores. Thus

neodymium determinations must be carried out either at the 492.453-nm line after separation of praseodymium from the matrix — a laborious and time-consuming procedure — or at the less sensitive 463-42-nm line where no spectral line interference occurs.

REFERENCES

1 W. Ooghe and F. Verbeek, Anal. Chim. Acta, 73 (1974) 87.
2 V.A. Fassel, J.O. Rasmuson and T.G. Cowley, Spectrochim. Acta, Part B, 23 (1968) 579.
3 G.D. Christian and F.J. Feldman, Atomic Absorption Spectroscopy, Wiley-Interscience, New York, 1970.
4 H. Kayser, Tabelle der Hauptlinien der Linienspektren aller Elemente, Springer, Berlin, 1939.
5 J. Kuba, L. Kucera, F. Plzak, M. Dvorak and J. Mraz, Coincidence Tables for Atomic Spectroscopy, Elsevier, Amsterdam, 1965.
6 A.N. Saidel, W.K. Prokofjew and S.M. Raiski, Spektraltabellen, Verlag Technik, Berlin, 1961.

Analytica Chimica Acta, 79 (1975) 292—295

Short Communication

MOLECULAR EMISSION CAVITY ANALYSIS — A NEW FLAME ANALYTICAL TECHNIQUE
PART VI. THE SIMULTANEOUS DETERMINATION OF SULPHATE AND SULPHITE OR THIOSULPHATE IONS

R. BELCHER, S.L. BOGDANSKI, D.J. KNOWLES* and A. TOWNSHEND
Chemistry Department, The University, P.O. Box 363, Birmingham, B15 2TT (England)
(Received 30th April 1975)

The determination of sulphur anions in admixture generally requires a separate procedure for each anion, with a consequent proliferation of reagents and equipment and an appreciable time required to provide the complete analysis. Such analyses are essential, however, in air and water analysis, where sulphate, sulphite and sulphide ions have to be determined. Sulphite is widely used in drink and foodstuffs as an anti-oxidant and bactericide, and its rapid determination in such products, as well as that of its oxidation product, sulphate, is essential. There are numerous other examples where mixtures of sulphur anions have to be analysed.

In a previous paper [1] it was shown that molecular emission cavity analysis (MECA) gave a very rapid, sensitive means of determining individual sulphur anions. The sample solution (3—5 μl) was injected into the MECA cavity; the latter was placed in a hydrogen—nitrogen—air flame, and the blue S_2 emission stimulated within the cavity measured at 384 nm. The time which elapsed between introducing the cavity into the flame and achieving maximal emission intensity (t_m) was characteristic of the anion, and varied from 1.4 s for sulphide to 8 s for sulphate and peroxodisulphate. It was also briefly indicated that mixtures of sulphite and sulphate gave completely resolved responses thus offering the possibility of determining the two anions simultaneously.

The present communication describes the determination of sulphate and sulphite, and of sulphate and thiosulphate ions in admixture, based on their resolved MECA responses.

Experimental

The instrumentation, experimental technique and conditions were as described previously [1].

Analytical reagent-grade ammonium sulphate, sodium sulphite, sodium thiosulphate and disodium EDTA were used. Stock sulphite solution (*ca.* 400 p.p.m. S) were stabilized (for about a week) with 2 ml of 0.05 *M* EDTA solution per 250 ml. Whenever such a solution gave a sulphate response exceeding 1 % of the sulphite response, a fresh solution was prepared.

*On leave from the Preston Institute of Technology, Melbourne, Victoria, Australia.

Determination of sulphate and sulphite in admixture. The test solution should be made 0.1 *M* in phosphoric acid, to remove cationic interferences [1], and should then contain 3—100 p.p.m. of sulphur as sulphite, and 10—300 p.p.m. of sulphur as sulphate. Inject 3 μl of the solution into a cold, silica-lined cavity, and rotate the cavity into the flame. Record the change in emission intensity with time, until the slower, sulphate peak is complete. Rotate the cavity out of the flame, and cool to room temperature (or replace by a cold cavity) before injecting the next sample. Measure the areas under the sulphite and sulphate peaks, and obtain the respective concentrations from calibration plots obtained from measurements made on individual standards under the same conditions.

Determination of sulphate and thiosulphate in admixture. The test solution should be made 0.01 *M* in ammonium dihydrogenphosphate—diammonium hydrogenphosphate buffer solution, pH 7, to remove cationic interferences, without causing the disproportionation of thiosulphate which would occur if phosphoric acid were added [1]. It should then contain 3—100 p.p.m. of sulphur as thiosulphate and 10—300 p.p.m. of sulphur as sulphate. The determination is completed as described above.

Results and discussion

Mixtures of sulphite (3—300 p.p.m. S) and sulphate (10—540 p.p.m. S) all gave completely resolved peaks for sulphite (t_m = 2.4 s) and sulphate (t_m = 8 s). A typical response is shown in Fig.1. The area of each peak was independent of the concentration of the other component of the mixture in all instances (Table I). However, because of the non-linearity of the calibration graphs at high sulphur concentrations [1], optimal ranges for the determinations of sulphite and sulphate are 3—100 p.p.m. and 10—300 p.p.m., respec-

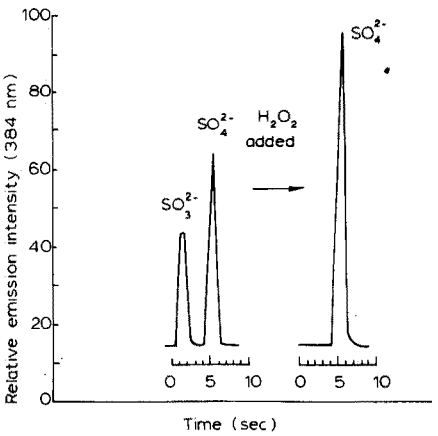

Fig.1. MECA response from a mixture containing: 36 p.p.m. S as Na_2SO_3, and 99 p.p.m. S as $(NH_4)_2SO_4$ in 0.1 *M* H_3PO_4 solution.

TABLE I

Reproducibility of sulphate and sulphite responses in the presence of one another

SO_3^{2-} injected[a] (μg S)	SO_4^{2-} injected[b] (μg S)
0.06 ± 0.01	0.06 ± 0.01
0.18 ± 0.02	0.12 ± 0.01
0.30 ± 0.02	0.18 ± 0.03
	0.30 ± 0.05

[a] Standard deviation of 12 measurements, in presence of 60—302 ng S as sulphate.
[b] Standard deviation of 16 measurements, in presence of 60—426 ng S as sulphite.

TABLE II

Recovery of sulphite plus sulphate after treatment with hydrogen peroxide

μg S	taken[a]	0.35	0.52	0.69
μg S	found[b]	0.37 ± 0.01	0.50 ± 0.01	0.67 ± 0.02

[a] Ratio of sulphur in SO_3^{2-} to that in SO_4^{2-} = 1.3.
[b] Mean of 4 results.

tively. The reproducibilities were similar to those observed for single component solutions. The calibration graphs were therefore unaffected by the presence of the second component, the log emission intensity—log amount of sulphur plots being linear, with slopes of 1.95 for sulphite and 1.5 for sulphate, which are very similar to those found for single-component solutions [1].

As additional proof that the peaks measured were indeed sulphite and sulphate, hydrogen peroxide was added to some sulphite—sulphate mixtures, to oxidize the sulphite ions to sulphate ions. In each instance, the first peak was completely absent, and the sulphate peak had correspondingly increased so that the total amount of sulphate found corresponded to the sum of the initial sulphite and sulphate concentrations. The results are given in Table II, and a typical peak after hydrogen peroxide treatment is included in Fig.1. Such treatment also gives a rapid means of determining total sulphur in sulphite—sulphate mixtures.

Thiosulphate has a similar t_m value (3.0 s) to sulphite. It was found that its MECA peak could be resolved from that of sulphate, in the same way as the sulphate and sulphite peaks could be resolved. Once again, the areas and reproducibilities of each peak were independent of the concentration of the other component in all instances (Table III). The calibration graphs were therefore unaffected by the presence of the second component, and the slopes of the log—log plots were 1.9 and 1.6 for thiosulphate and sulphate,

TABLE III

Reproducibility of sulphate and thiosulphate responses in the presence of one another

$S_2O_3^{2-}$ injected[a] (μg S)	SO_4^{2-} injected[a] (μg S)
0.10 ± 0.01	0.20 ± 0.02
0.20 ± 0.01	0.40 ± 0.04
0.39 ± 0.02	0.80 ± 0.04
0.59 ± 0.05	1.21 ± 0.05

[a] Standard deviation of 15 measurements, in the presence of the range of amounts of the second component shown.

respectively, in agreement with previous measurements on single components [1].

The above results show that mixtures of sulphate and sulphite or thiosulphate can be determined rapidly and sensitively by MECA. It is likely that other binary mixtures of sulphur anions with t_m values separated by more than 3 s (*e.g.* SCN^- and $S_2O_8^{2-}$, S^{2-} and SO_4^{2-}) could also be resolved and determined in the same manner. The use of larger cavities and cooler flame conditions should give greater sensitivities and longer t_m values, and allow resolution of anions with closer t_m values, and of ternary mixtures of sulphur anions. Work on these aspects is in progress, and will be reported later.

D.J.K. thanks the Council of the Preston Institute of Technology for the generous leave provisions afforded him. The authors thank Anacon Inc. for the gift of a MECA spectrophotometer and recorder.

REFERENCES

1 R. Belcher, S.L. Bogdanski, D.J. Knowles and A. Townshend, Anal. Chim. Acta, 77 (1975) 53. (Part V).

Analytica Chimica Acta, 79 (1975) 296—301

Short Communication

AN X-RAY DIFFRACTION STUDY OF THE THERMAL DECOMPOSITIOI OF METAL TETRAMETHYLENEDITHIOCARBAMATES

S. GOMIŠČEK, L. GOLIČ and Z. LENGAR

Department of Chemistry and Chemical Institute "Boris Kidrič", University of Ljubljana (Yugoslavia)

(Received 10th April 1975)

Metal tetramethylenedithiocarbamates (MeTMDTC) are of considerable interest in analytical chemistry, for their properties make them suitable for the separation and preconcentration of various elements [1—5]. In atomic absorption spectrometry, metals are often determined after they have been extracted as MeTMDTC; the organic solutions are either directly sprayed into the flame, or atomized in a graphite-tube furnace [6—10]. The basic processes in a graphite-tube furnace are evaporation of the organic solvent, decomposition of the MeTMDTC and atomization of the decomposition products [11, 12]. A study of the thermal decomposition of MeTMDTC is therefore important in understanding various phenomena in non-flame atomic absorption spectrometry; the data are also of interest for applications of dithiocarbamate chelates in mass spectrometry and gas chromatography.

In this communication are reported the results of a study of the decomposition of MeTMDTC at varying temperatures in inert and oxidizing atmospheres. The compounds formed were identified mainly by the x-ray diffraction method.

EXPERIMENTAL

Apparatus. The MeTMDTC were decomposed in an electric resistance tube furnace. The temperature regulation was accurate to ± 10 °C at the higher temperatures and ± 5 °C at the lower temperatures. Argon and oxygen were introduced into the furnace as required. The x-ray diffraction diagrams were obtained with a Guinier de Wolff (Nonius) powder camera, with Cu Kα rays.

Reagents. The MeTMDTC were prepared by precipitation of metal ions from aqueous solution at pH 2—4 with an aqueous 0.5 % (w/v) NaTMDTC solution. The insoluble metal chelates were filtered, washed and dried at temperatures below 80 °C.

All the reagents were of A.R. quality, except the NaTMDTC which was synthesized by the method of Gleu and Schwab [13].

Procedure. A few mg of MeTMDTC was placed in a silica boat, which was inserted into the tube furnace. Argon or oxygen was passed through the tube at a rate of 30 l min^{-1}. The MeTMDTC was heated for 1 h at 80, 150, 250, 300, 400 or 600 °C. The substance was then powdered, the powder diagram was taken and finally the material was analyzed by the x-ray diffraction method.

The metal content of the decomposition products was determined by complexime tric titration; carbon and sulphur were determined conductometrically, after combustion in oxygen, with the Wösthoff Carmhograph and Sulmhograph apparatus. In some samples, oxygen was also determined by the vacuum extraction method in a graphite capsule at 1850 °C.

RESULTS AND DISCUSSION

In this investigation, the TMDTC chelates of cadmium(II), cobalt(III), iron(III), mercury(II), nickel(II), lead(II), and zinc(II) were studied.

The photographs of the decomposition products obtained by the electron scanning microscope (Figs.1 and 2) show that the structure is either finely crystalline or not visibly crystalline. In some samples, globules and big crystals of definite shape were observed in the basic substance. The crystals were not identified, but the globules were probably carbon, or even graphite, originating from the decomposition of the MeTMDTC.

The x-ray diffraction analyses showed that the precipitated MeTMDTC and their decomposition products are usually crystalline substances, which can be identified from the diagrams obtained. Only the diagrams for cobalt were not very distinct. Table I shows the results of the x-ray diffraction analyses for the decomposition products at all temperatures investigated. The results obtained indicate that, in the presence of oxygen, the MeTMDTC are decomposed to metal oxides, sulphides, and oxysulphur compounds even at 200—250 °C, whereas in argon undecomposed carbamates were often found at these temperatures. The MeTMDTC are decomposed to metal sulphides in argon atmospheres at higher temperatures.

Microanalysis of the decomposition products of the TMDTC chelates of Cd, Cu, Ni, Pb and Zn in argon, confirmed the results of the x-ray diffraction method. The decomposition products in argon are metal sulphides; carbon is also found in the residue. Table II shows the results of these analyses; in the decomposition of the MeTMDTC chelates, the compounds formed are mostly CdS, Cu_2S, NiS, PbS (600 °C) and ZnS.

The results of the microanalysis of the decomposition products in oxygen and the theoretical compositions of certain compounds are given in Table III. Evaluation of these results is more complicated than in the case of argon, for the number of the possible compounds is higher. A full description would require further work.

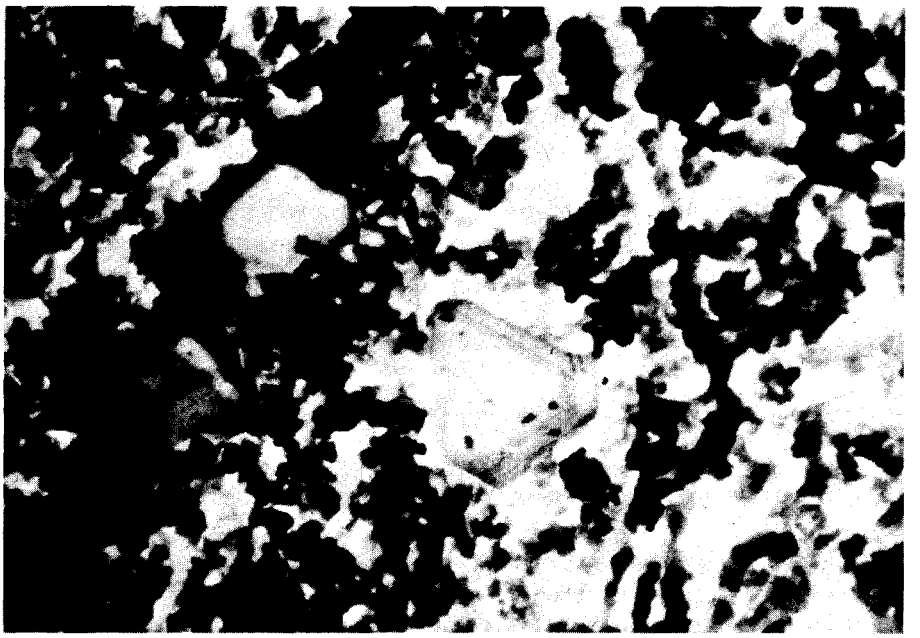

Fig.1. Decomposition products of CuTMDTC at 1000 °C in argon. Secondary electron image; ISI-MINI-SEM apparatus; magnification, × 5000.

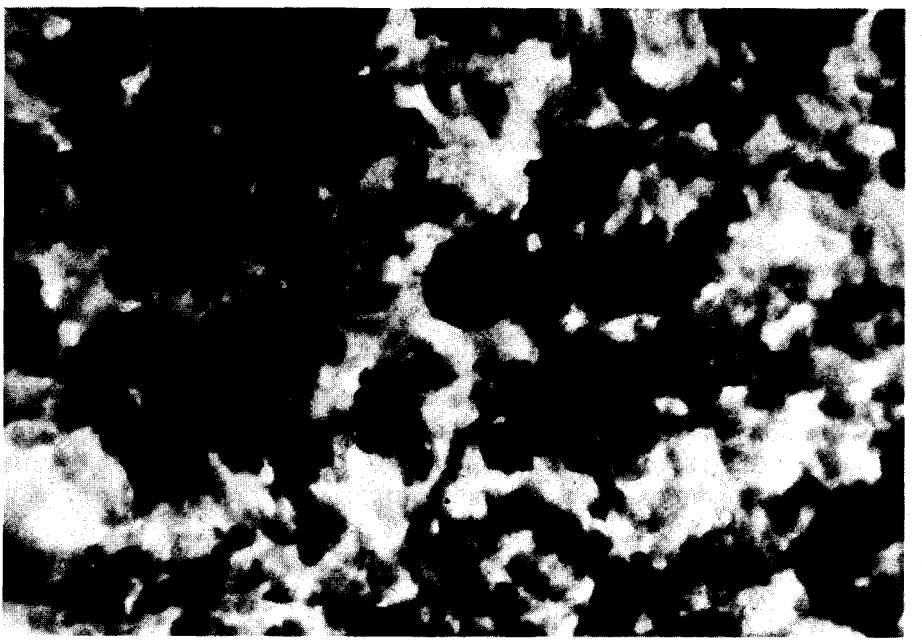

Fig. 2. Decomposition products of CdTMDTC at 600 °C in argon. Secondary electron image; ISI-MINI-SEM apparatus; magnification, × 15000.

TABLE I

Products of decomposition of some MeTMDTC in argon and oxygen

Carbamate	Temp. (°C)	Oxygen	Argon
Cd	80	Carbamate	Carbamate
	150	Carbamate	Carbamate
	250	CdS, CdO	Carbamate
	300	CdS, CdO	CdS, unknown compound
	400	CdS, CdO, unknown compound	CdS
	600	CdS, CdO, unknown compound	CdS
Co	80	—	—
	150	Carbamate	Carbamate
	250	—	Carbamate
	300	CoO, CoS_{1-y} [a]	—
	400	CoO	Co_4S_3
	600	Co_3O_4	CoS_{1-y} [a]
Cu	80	Carbamate	Carbamate
	150	Cu_2S, Cu_2O	Unknown compound
	250	Cu_2S	Cu_2S, CuS, unknown compound
	300	Cu_2S, CuO, CuS, Cu_2O	Cu_2S, CuS
	400	Cu_2S, CuO, CuS	Cu_2S, CuS
	600	Cu_2S, CuO, CuS	Cu_2S, CuS
Fe	80	Carbamate	Carbamate
	150	Unknown compound	Unknown compound
	250	Fe_2O_3	Unknown compound
	300	Fe_2O_3	FeS
	400	Fe_2O_3	FeS
	600	Fe_2O_3	FeS
Hg	80	Carbamate	Carbamate
	150	Carbamate	Carbamate
	250	α-HgS, β-HgS	α-HgS, β-HgS
	300	α-HgS, β-HgS	α-HgS, β-HgS
	400	α-HgS, β-HgS	α-HgS, β-HgS
Ni	80	Carbamate	Carbamate
	150	Carbamate	Carbamate, NiS, Ni_7S_6
	250	Carbamate	Carbamate, NiS, Ni_7S_6
	300	NiS, Ni_7S_6, NiO	Carbamate, NiS, Ni_7S_6, NiS_2
	400	NiS, Ni_7S_6, NiO	NiS, Ni_7S_6, Ni_3S_2
	600	NiO, $NiSO_4$	NiS, Ni_7S_6, Ni_3S_2
Pb	80	Carbamate	Carbamate
	150	Carbamate	Carbamate
	250	Pb_3O_4, PbS, PbO	Carbamate
	300	Pb_3O_4, PbS, PbO	PbS
	400	Pb_3O_4, PbS, PbO	PbS
	600	Pb_3O_4, PbS, PbO Pb_3SO_8, $Pb_3O_2SO_4$	PbS
Zn	80	Carbamate	Carbamate
	150	Carbamate	Carbamate
	250	Carbamate, unknown compound	Carbamate
	300	— [b]	ZnS
	400	ZnS	ZnS
	600	ZnO	ZnS

[a] $y = 0.11—0.2$

[b] Very diffuse lines of ZnS.

TABLE II

Microanalysis of the decomposition products of some MeTMDTC in argon

(The results for Me and S have been corrected for the carbon present. The numbers given in brackets are the theoretical values for the metal(II) sulphides.

Element	Temp. (°C)	Me (%)	S (%)	C (%)
Cd	300	78.3	21.2	8.7
	600	77.7 (77.8)	22.3 (22.2)	9.2
Cu	300	75.5	24.6	13.0
	600	78.3 (79.8)	21.7 (20.2)	16.1
Ni	300	57.1	41.3	18.9
	600	63.6 (64.7)	36.4 (35.3)	11.8
Pb	300	77.7	8.7	0
	600	85.6 (86.6)	14.0 (13.4)	5.5
Zn	300	63.9	36.3	15.9
	600	64.8 (67.1)	35.3 (32.9)	11.9

TABLE III

Microanalysis of the decomposition products of some MeTMDTC in oxygen

(The results have been corrected for the carbon present.)

Found					Theoretical			
Temp. (°C)	Me(%)	S (%)	O (%)	C (%)	Me(%)	S (%)	O (%)	
Cadmium—TMDTC								
300	89.6	3.2	—	2.3	77.8	22.2		for CdS
600	78.5	6.7	—	2.2	87.5		12.5	for CdO
Copper—TMDTC								
300	72.2	9.2	—	6.7	66.4	33.6		for CuS
600	70.2	12.8[a]	10.9	6.2	79.8	20.2		for Cu_2S
		4.2[a]			79.9		20.1	for CuO
					88.8		11.2	for Cu_2O
Nickel—TMDTC								
300	75.3	22.0	—	1.7	64.7	35.3		for NiS
600	72.2	13.2[a]	6.3	2.9	68.8	31.2		for Ni_7S_6
		19.1[a]			78.6		21.4	for NiO
					30.8	20.6	48.6	for $NiSO_4$
Lead—TMDTC								
300	73.9	13.3	—	6.8	86.6	13.4		for PbS
600	83.7	10.7	—	3.5	90.7		9.3	for Pb_3O_4
					92.8		7.2	for PbO
					86.6	2.6	10.8	for Pb_3SO_8
					82.8	4.2	13.0	for $Pb_3O_2SO_4$
Zinc—TMDTC								
300	58.0	29.0	—	18.2	67.1	32.9		for ZnS
600	79.3	0.99	20.8	3.5	80.3		19.7	for ZnO

[a] Parallel determinations.

Conclusion

The x-ray diffraction analyses showed that the MeTMDTC are thermally decomposed to the crystalline substances. The products in argon are metal sulphides and carbon. The possible products of combustion in oxygen are numerous, the most frequently found being oxides, with some sulphides and oxysulphate compounds.

Our thanks are due to Professor H. Malissa, Technical University of Vienna, who provided help with the microanalysis and microscopy. This work was supported by grant 1-104-73 of the Boris Kidrič Foundation, Ljubljana.

REFERENCES

1 F. Wever, W. Koch and H. Malissa, Über die Anwendung disubstituierter Ditiokarbamate in der analytischen Chemie, Westdeutscher Verlag, Köln, 1955.
2 A. Hulanicki, Talanta, 14 (1967) 1371.
3 O.G. Koch and G.A. Koch-Dedic, Handbuch des Spurenanalyse, Springer Verlag, Berlin, 1964.
4 G.D. Thorn and R.A. Ludwig, The Dithiocarbamates and Related Compounds, Elsevier, Amsterdam, 1962.
5 S. Gomišček and H. Malissa, Rudarsko-metalurški zbornik, 1 (1959) 17.
6 J.E. Allan, Spectrochim. Acta, 17 (1960) 467.
7 T.R. Gilbert and A.M. Clay, Anal. Chim. Acta, 67 (1973) 289.
8 S. Gomišček and M. Špan, Anal. Chim. Acta, 69 (1974) 49.
9 P.E. Paus, At. Absorption Newslett., 10(3) (1971) 69.
10 G.D. Renshaw, G.A. Pounds and E.F. Pearson, At. Absorption Newslett., 12(2) (1973) 55.
11 J. Aggett and T.S. West, Anal. Chim. Acta, 63 (1973) 11.
12 S. Gomišček, Z. Lengar, J. Černetič and V. Hudnik, Anal. Chim. Acta, 73 (1974) 97.
13 K. Gleu and R. Schwab, Angew. Chem., 62 (1950) 320.

Analytica Chimica Acta, 79 (1975) 302—307

Short Communication

ACTIVATION ANALYSIS WITH HELIUM-3 PARTICLES FOR TRACES OF OXYGEN IN COPPER

C. VANDECASTEELE* and J. HOSTE
Institute for Nuclear Sciences, Rijksuniversiteit Gent, Proeftuinstraat 86, B-9000 Gent (Belgium)
(Received 3rd April 1975)

The determination of oxygen in copper through the $O(\alpha, nx)^{18}F$ reactions with 45-MeV helium-4 particles has already been described [1]. The method was applied to a low-oxygen copper standard reference material provisionally certified [2] to contain 1.5 ± 0.5 $\mu g\ g^{-1}$ of oxygen. To check the accuracy of the results obtained previously, it seemed appropriate to apply an independent nuclear method. The accuracy obtainable is a function of the accuracy of the range-energy data used to transform the experimental activation curve for relevant nuclear reactions in the standard material to that in the sample. Moreover, the determination of oxygen can be affected by other light elements mainly fluorine and sodium. Activation analysis with helium-3 particles by $O(^3He,nx)^{18}F$ reactions followed by a chemical separation similar to that described previously [1] was chosen. Sensitivity and precision should be similar to those for helium-4 activation, whereas the interferences from fluorine and sodium will obviously be different, and the two methods are based on different range-energy data. A similar comparison between helium-3 and helium-4 activation analysis for oxygen has been applied successfully to the non-destructive determination of oxygen in silicon [3,4].

Experimental

Samples and standards. The samples were 21-mm diameter, 0.7-mm thick discs obtained from cylindrical copper blocks (Eurisotop) as described previously [1]. A stack of 20 muscovite foils (21-mm diameter, *ca.* 14-μm thick) served as standard.

Irradiation. The samples were irradiated under vacuum for 15—20 min with a 2-μA beam of 25-MeV ^3He particles. In front of samples and standards was placed a 25-μm thick, 21-mm diameter copper disc as flux monitor.

The stack of standard mica foils was irradiated for 10 min at an intensity of 0.2 μA.

Chemical treatment. After irradiation, etch the sample twice for about 3 min

* Aspirant of the N.F.W.O.

each time, in separate 6 *M* nitric acid solutions at room temperature, to remove a surface layer of 25—50 μm. The energy of the particles corresponding to the depth of etching varies from *ca.* 19 to 15 MeV. Determine the thickness removed with a micrometer.

Directly after the chemical etch, dissolve the sample in 20 ml of 14 *M* nitric acid, in a steam-distillation apparatus. Before dissolution, add 300 mg of sodium fluoride as carrier, and 5 ml of zinc nitrate solution (5 mg ml^{-1} in 2 *M* nitric acid) and 5 ml of gallium oxide solution (10 mg ml^{-1} in 2 *M* nitric acid) as holdback carriers. As soon as the sample has dissolved, add 30 ml of 85 % phosphoric acid. Increase the temperature to 125 °C, introduce steam, keeping the temperature constant at 125 °C, and collect a total of 150 ml of distillate. After addition of 5 ml of the gallium oxide solution, adjust the distillate to pH 8 with 14 *M* ammonia. Filter off the gallium hydroxide precipitate. Adjust the pH to 4—5, add 10 ml of lead nitrate solution (250 g l^{-1}) and 5 ml of sodium chloride solution (160 g l^{-1}), to precipitate lead chlorofluoride. Filter the precipitate on a membrane filter and wash with 20 ml of the lead nitrate solution. Wrap the precipitate in an aluminum foil and place it between two 1-mm thick aluminum annihilator discs, in a plastic container.

Measurements. Count the precipitate on a Ge(Li) detector with a relative detection efficiency of 15 %, coupled to a 4000-channel analyser. Count for 50 min, every hour, for about 10 h starting 3—5 h after the end of irradiation. Measure the copper flux monitors at a counting position 80 times lower. Count the standard foils, also placed between 2 aluminum annihilator discs, separately in the same low-efficiency geometry.

Determine the yield of the chemical separation by irradiation in an ^{227}Ac—Be isotopic neutron source, by means of the $^{19}F(n,\alpha)^{16}N$ reaction. Count the γ-rays of 7.11-s ^{16}N above 4.5 MeV, as described previously [1].

Calculations. The annihilation peak in the spectrum was manually integrated and the background, obtained by interpolation between the lower and higher energies, was subtracted. After subtraction of the 511-keV natural background activity (about 1 c.p.m.), the decay curve was analysed by the CLSQ program [5].

The oxygen concentration in the sample was calculated from the oxygen concentration in the muscovite, the net ^{18}F activity of the sample, the total ^{18}F activity in the muscovite standard and the equivalent thicknesses for muscovite and copper as deduced from the experimentally determined activation curve for the $O(^3He,nx)^{18}F$ reactions in muscovite [1]. The area of the 1039-keV ^{66}Ga peak in the spectra of the copper flux monitors served as a measure of the beam intensity.

Results and discussion

When copper is irradiated with 15—19-MeV helium-3 particles, the nuclear reactions are as shown in Table I. Figure 1 shows a γ-ray spectrum of an irra-

TABLE I

Main nuclear reactions of 15—19 MeV helium-3 particles with copper and some of its impurities

Reaction	Isotope formed		
	$T_{1/2}$	γ-Ray energy (keV)	% Annihilation radiation
$^{63}Cu(^3He,\alpha n)^{61}Cu$	3.41 h	67(5 %); 283(13 %); 373(2 %); 656(10 %); 1185(4 %)	120
$^{63}Cu(^3He,2p)^{64}Cu$	12.9 h	1348(0.6 %)	38
$^{65}Cu(^3He,\alpha)^{64}Cu$			
$^{63}Cu(^3He,p2n)^{63}Zn$	38.4 min	670(11 %); 961(8 %)	186
$^{65}Cu(^3He,2n)^{66}Ga$	9.4 h	833(6 %); 1039(39 %); 1919(3 %) 2190(6 %); 2752(25 %); 4295(4 %)	114
$^{75}As(^3He,2n)^{76}Br$	16.1 h	559(63 %); 657(19 %); 750(6 %)	133
$^{74}Se(^3He,p)^{76}Br$		850(7 %); 1210(13 %); 1370(5 %)	
$^{76}Se(^3He,p2n)^{76}Br$		1470(7 %); 1860(11 %); 2100(7 %); 2390(4 %); 2780(5 %); 2970(8 %); 3570(2 %)	
$^{121}Sb(^3He,n)^{123}I$	13.3 h	159(83 %)	

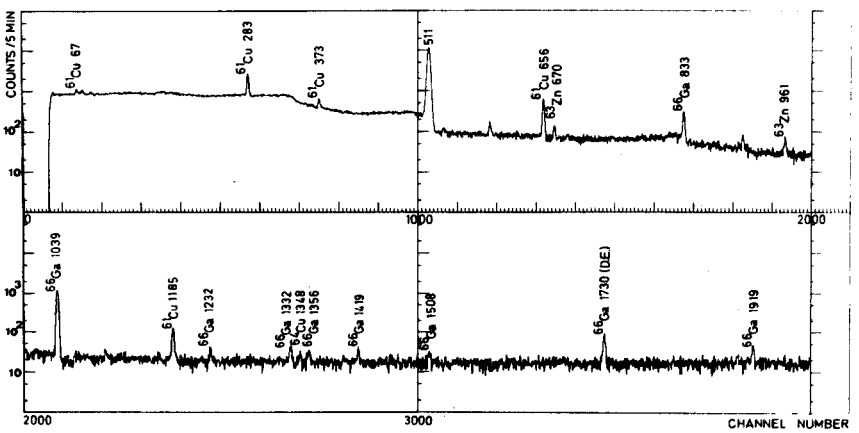

Fig.1. Ge(Li) γ-ray spectrum of a copper sample irradiated for 15 min at 2-μA intensity and counted in a low counting geometry, 200 min after irradiation. Energies are given in keV.

diated copper sample measured; 200 min after irradiation, and for an energy of 17.0 MeV corresponding to the etching depth, the annihilation radiation from the isotopes formed from copper is about $5 \cdot 10^4$ times more intense than that from the ^{18}F formed from 1 $\mu g\ g^{-1}$ of oxygen through the $O(^3He,nx)^{18}F$ reactions. The chemical separation of the ^{18}F thus requires a decontamination factor from matrix radiation of the order of 10^6, if a 5 % interference is ac-

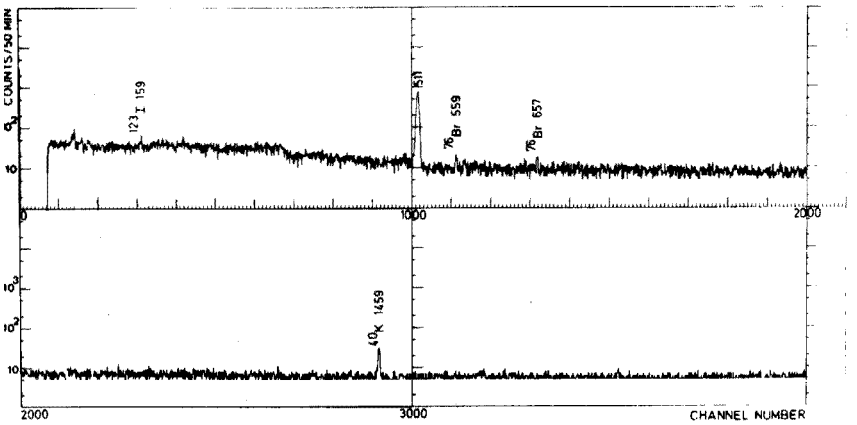

Fig.2. Ge(Li) γ-ray spectrum of a copper sample irradiated for 20 min at 2-μA intensity and counted in the geometry for analysis, 270 min after irradiation. The chemical yield was 69 %. Energies are given in keV.

ceptable, when 1 $\mu g\ g^{-1}$ of oxygen is determined. This is achieved by distillation of fluorosilicic acid followed by precipitation of gallium as the hydroxide and of fluoride as lead chlorofluoride. Figure 2 shows a Ge(Li) γ-ray spectrum of the final lead chlorofluoride precipitate; there are no peaks of isotopes formed from the copper matrix. Besides the annihilation peak, there are only the 559-keV and 657-keV ^{76}Br peaks and the 159-keV ^{123}I peak, which arise from impurities in the copper matrix (Table I). Only ^{76}Br contributes to the annihilation activity, so that analysis of the decay curve can be started with half-lives of 109.8 min and 16.1 h. The contribution of ^{76}Br to the measured peak varies from 1.2 to 2.7 % of the ^{18}F contribution, 4 h after irradiation. A typical decay curve is shown in Fig.3. After iteration, half-lives of 108—114 min (standard deviation *ca.* 2 min) were obtained for the activity attributed to ^{18}F.

After the chemical separation, the intensity of the 1039-keV ^{66}Ga radiation decreased by more than $4 \cdot 10^6$, and that for the 1185-keV ^{61}Cu radiation by more than $3 \cdot 10^5$. The chemical yield averaged 74 %.

The results are summarized in Table II; the relative standard deviation was about 10 %. Neither the average value (t-test) nor the standard deviation (F-

TABLE II

Results for oxygen in low-oxygen copper[a]

Individual results ($\mu g\ g^{-1}$)	Average value ± s
1.06; 1.09; 1.11; 1.19; 0.93	1.08 ± 0.11

[a] Helium-4 activation analysis [1] yielded 1.17 ± 0.13 $\mu g\ g^{-1}$ (10 detns.).

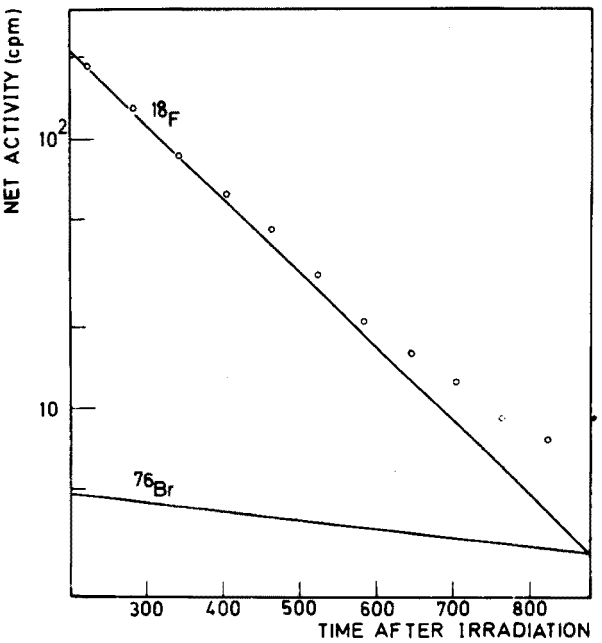

Fig.3. Decay curve for a sample irradiated for 15 min at 2-μA intensity. The chemical yield was 79 %.

TABLE III

Analysis of copper by spark-source mass spectrometry

Element	Concn. ($\mu g\ g^{-1}$)	Element	Concn. ($\mu g\ g^{-1}$)	Element	Concn. ($\mu g\ g^{-1}$)	Element	Con (μg
F	0.030	K	1.3	Fe	11	Sn	6.9
Na	0.8	Ca	0.6	Ni	3.7	Sb	18
Al	0.9	Sc	0.2	As	1.4	Au	1.2
P	0.4	V	0.1	Se	5.3	Pb	50
S	6.1	Cr	0.5	Ag	40	Bi	1.7

test) obtained differed significantly (at the 95 % confidence level) from the data obtained previously [1]. The results also agreed fairly well with those obtained by hydrogen reduction, but the present results are more precise.

Additional information on possible interferences was obtained by spark-source mass spectrometry; Table III gives the results. Since no standard reference coefficients were available for fluorine and sodium in the conditions used, the results are only accurate within a factor of 3; they were obtained by comparing the integrated transmittance of the impurities, measured with an automatic microdensitometer, with that of the matrix element. The rela-

tively high arsenic, selenium and antimony concentrations explain the formation of ^{76}Br and of ^{123}I, which was also noted with helium-4 activation.

When irradiated with helium-3 or helium-4 particles, sodium and fluorine can also yield ^{18}F by the $^{23}Na(^{3}He,2\alpha)^{18}F$ and $^{23}Na(\alpha,2\alpha n)^{18}F$ reactions and by the $^{19}F(^{3}He,\alpha)^{18}F$ and $^{19}F(\alpha,\alpha n)^{18}F$ reactions, respectively; 1 μg of sodium and 1 μg of fluorine represent, respectively, 0.04 and 0.05 μg of oxygen, when irradiated with 15-MeV helium-3 particles [6], but when the energy is 20 MeV, the values are 0.07 and 0.06 μg. With helium-4 particles, the corresponding figures are respectively 0.014 and 2.5 μg at 35 MeV, and 0.043 and 1.7 μg at 40 MeV. If these data are combined with those of Table III, the sodium interference can be calculated as 0.03—0.05 $\mu g\ g^{-1}$ with helium-3, and 0.01—0.03 $\mu g\ g^{-1}$ with helium-4 particles. The interference of fluorine can be estimated as about 0.002 $\mu g\ g^{-1}$ with helium-3 and 0.05—0.07 $\mu g\ g^{-1}$ with helium-4. These interferences are all within the standard deviation of one determination.

With helium-3 irradiation for 15 min at 2-μA intensity, the ^{18}F activity is about 150 c.p.m. for 1 $\mu g\ g^{-1}$ of oxygen 4 h after irradiation. If both the natural background and the ^{76}Br contribution to the measured peak are taken into account, the limit of determination (corresponding to 10 % standard deviation on the ^{18}F activity determined from the first 50 min count) is about 30 ng g^{-1}; this assumes that the selenium and arsenic concentrations are similar to those in the samples analysed here. This limit can of course be lowered by longer irradiation.

Grateful acknowledgment is made to R. Kieffer for valuable technical assistance, to F. Adams (Universitaire Instelling, Antwerpen) for the mass spectrometric data, to the "Comité de gestion du cyclotron", Université Catholique de Louvain, for the use of the cyclotron, and to the NFWO and IIKW for financial support.

REFERENCES

1 C. Vandecasteele, F. Adams and J. Hoste, Anal. Chim. Acta, 76 (1975) 27.
2 G. Kraft, J. Hoste and C. Engelmann, The Certification of Oxygen in Oxygen-free Copper, ITE-Report No 79, Eurisotop Office, Brussels, 1974.
3 E. Schweikert and H. Rook, Anal. Chem., 42 (1970) 1525.
4 C. Vandecasteele, F. Adams and J. Hoste, Anal. Chim. Acta, 71 (1974) 67.
5 J. Cumming in G. O'Kelley (Ed.), Applications of Computers to Nuclear and Radiochemistry, National Academy of Sciences—National Research Council, Nucl. Sci. Ser. Rep. NAS-NS 3107, p. 25.
6 C. Engelmann, J. Radioanal. Chem., 7 (1971) 281.

Analytica Chimica Acta, 79 (1975) 308—312

Short Communication

INJECTION SOLVENT-INDUCED ANOMALIES IN REVERSE-PHASE HIGH-SPEED LIQUID CHROMATOGRAPHY

CHENG-YI WU and JAMES J. WITTICK

Merck Chemical Division, Merck & Co., Inc., Rahway, N.J. 07065 (U.S.A.)

(Received 11th February 1975)

Reverse-phase high-speed liquid chromatography is finding favor in industrial analysis because of the hydrolytic stability of the permanently bonded phase packing materials used; their advantages have been discussed elsewhere [1—3]. However, care must be taken to avoid erroneous interpretation of chromatographic anomalies which can result from the nature of the injected solvent used. The presence of such chromatographic anomalies can mislead the analyst into believing that the sample is decomposing or that the column is not behaving properly. Two examples involving vitamin D_2 and vitamin B_{12} are presented to illustrate the importance of recognizing induced solvent effects in this type of chromatography.

Experimental

A DuPont Model 830 Liquid Chromatograph equipped with a standard u.v. detector (254 nm) was used. The packing material was C_{18}/Corasil (Waters Associates, Milford, Mass.). For vitamin D_2 work, a mobile phase of aqueous 85 % (v/v) methanol and a column 50 cm x 2.1 mm,i.d., were used. For vitamin B_{12} work, the mobile phase was aqueous 12 % (v/v) CH_3CN and three coupled columns, 50 cm x 2.1 mm i.d., were used. Ergocalciferol (vitamin D_2) (USP Reference Standards, 4630 Montgomery Ave., Bethesda, Md. 20014) and cyanocobalamin (vitamin B_{12}; Merck Chemical Division) were used as samples. Spectral-grade methanol and acetonitrile (Matheson, Coleman and Bell, East Rutherford, N.J.) were used. Injections were done manually with syringes (10-μl syringe; Precision Sampling Corporation, Baton Rouge, La.) or with a 100-μl sampling valve (Chromatronix, Berkeley, Calif.). All experiments were performed at ambient temperature.

Results and discussion

In reverse-phase liquid chromatography, either for qualitative or for quantitative work, the selection of a solvent for sample dissolution can be critical. This was discovered when methods for the assay of vitamin D_2 and vitamin B_{12} were under development. Although only one type of reverse-phase

material is discussed in this paper, other reverse-phase packing materials can be expected to behave similarly.

Figure 1A presents the chromatogram for a 5-μl injection of vitamin D_2 (2.05 μg) in 100 % methanol with 85 % methanol/H_2O as the mobile phase. The chromatogram appears to indicate that the vitamin D_2 has decomposed to a certain extent, but chemical reaction between vitamin D_2 and methanol is unlikely. To substantiate this, 1 ml of the vitamin D_2/methanol solution was dried with a stream of nitrogen and the dried residue was then reconstituted with 1 ml of aqueous 85 % methanol (the mobile phase), this methanolic vitamin D_2 solution was then chromatographed (see Fig.1B). The peak eluted at approximately 8 min is almost twice its original height and the tailing has disappeared. An equivalent amount of vitamin D_2 dissolved directly in aqueous 85 % methanol also gave a single peak with no tailing at the same retention time, and with the same intensity as in Fig.1B. Clearly, the tailing is not due to component decomposition, as might be suggested. Acetonitrile, ethanol, and isooctane were also used as solvents for vitamin D_2. The 100 % acetonitrile and 100 % ethanol solutions gave the same type of anomalous chromatogram as that shown for 100 % methanol in Fig.1A. The vitamin D_2/isooctane solution, on the other hand, does not produce a tailing chromatogram (See Fig.1C).

Another example of this induced solvent effect can be seen in the chromato-

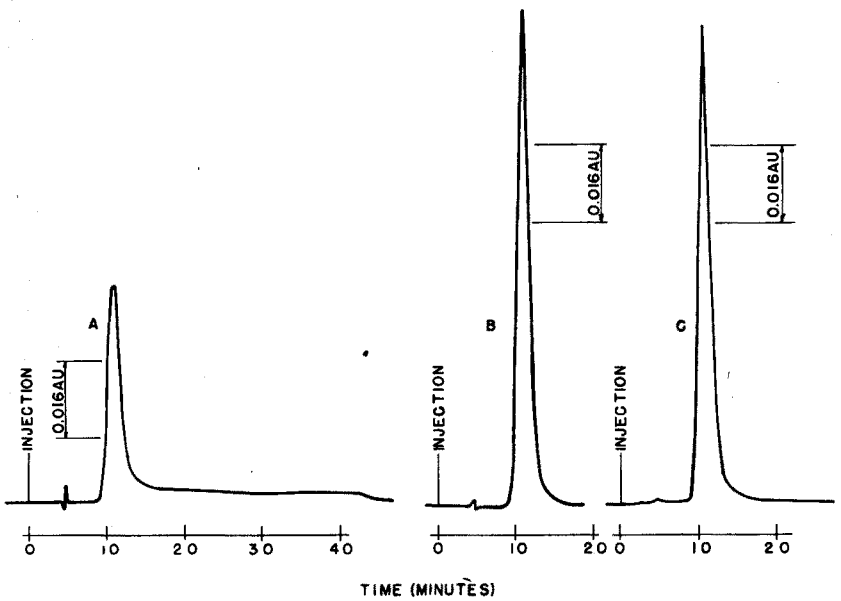

Fig.1. Induced solvent effect on the chromatography of vitamin D_2. Column: 50 cm x 2.1 mm,i.d., C_{18}/Corasil. Mobile phase: CH_3OH/H_2O. Pressure; 250 p.s.i.g.; flow rate: 0.6 ml min^{-1}. Sample concentration: (A) 4.10 mg of ergocalciferol USP reference standard per 10 ml of CH_3OH (solution D); (B) 1 ml of solution D dried with N_2 stream and the residue reconstituted with 1 ml CH_3OH/H_2O; (C) 1 ml of solution D dried with N_2 stream and the residue reconstituted with 1 ml of isooctane. Sample size: 5 μl.

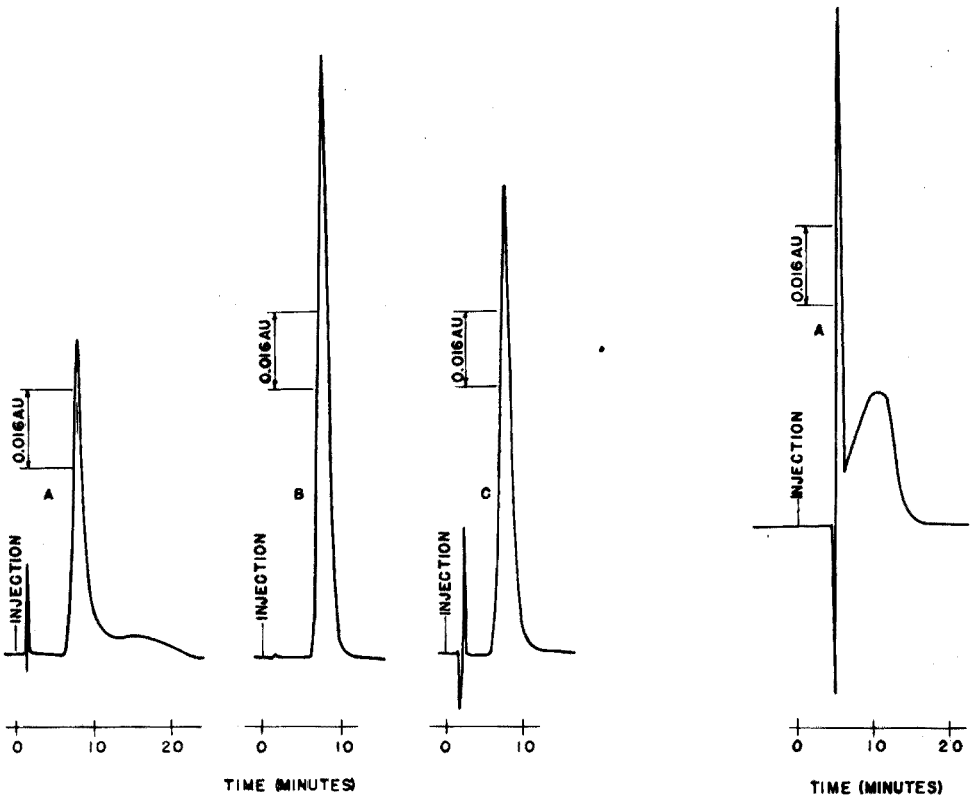

Fig.2. Induced solvent effect on the chromatography of vitamin B_{12}. Column: 3 x 50 cm x 2.1 mm,i.d., C_{18}/Corasil. Mobile phase: CH_3CN/H_2O. Pressure: 700 p.s.i.g.; flow rate: 0.7 ml min^{-1}. Sample concentration: (A) 10.9 mg of anhydrous vitamin B_{12} dissolved in 10 ml of CH_3OH (solution B); (B) 1 ml of solution B dried with N_2 stream and the residue reconstituted with 1 ml 12 % CH_3CN; (C) 1 ml of solution dried with N_2 stream and the residue reconstituted with 1 ml of water. Sample size: 10 μl.

Fig.3. Induced massive solvent effect on the chromatography of vitamin B_{12}. Conditions same as those in Fig.2 except that the sample concentration is 1.09 mg of anhydrous vitamin B_{12} in 10 ml of methanol and sample size is 100 μl.

graphy of cyanocobalamin (vitamin B_{12}). Vitamin B_{12}, which is soluble in alcohols of low molecular weight, was dissolved in methanol; 10-μl (10.9 μg of vitamin B_{12}) was chromatographed, with aqueous 12 % acetonitrile as the mobile phase. A tailing chromatogram was obtained (Fig.2A), but when 1 ml of the same methanol solution was dried with a stream of nitrogen and the residue was reconstituted with 1 ml of the 12 % acetonitrile mobile phase, a symmetrical peak of approximately double the peak height was obtained (Fig.2B). A similar experiment was performed with water to reconstitute the vitamin B_{12} residue; when this aqueous solution was chromatographed, a non-distorted peak was obtained (Fig.2C).

In connection with the vitamin B_{12} experiment, the same amount of vitamin B_{12} (10.9 μg) but in a larger volume (100 μl) was injected into the column using the same mobile phase. The change in column properties, as a result of introducing the larger quantity of methanol, was greatly increased as demonstrated in Fig.3; the chromatogram became totally unrecognizable.

For vitamin D_2, an increase in the methanol percentage in the mobile phase leads to a decrease in the retention time. If 100 % methanol is used as the mobile phase, the vitamin D_2 is eluted at the solvent front. Similarly, for vitamin B_{12}, increased acetonitrile percentage in the mobile phase leads to a shorter retention time. Vitamin B_{12} is not soluble in acetonitrile, but if 100 % methanol is used as the mobile phase, the vitamin B_{12} is also eluted at the solvent front. In both cases, the organic solvent apparently displaces the solute molecules from the packing surface. Therefore, if methanol is used to dissolve the sample and this sample is injected, a shorter retention time should result because the number of displacing molecules, *i.e.*, methanol, has been increased in the vicinity of the solute band on the column. In reality, however, the introduction of the methanol into the column appears to enhance partial adsorption on to the surface of the packing rather than to accelerate displacement.

This contradiction suggests that there may be more than one retention mechanism involved in this type of chromatography. As originally postulated by Kirkland [4], later supported by Novotny *et al.* [5], the separations afforded by the permanently bonded type of packing material probably do not involve any liquid—liquid partition. Rather, the separation mechanism may be attributed to some type of adsorption chromatography at the monomolecular layer of the organic modifier in conjunction with any remaining silanol groups. Our observation seems to substantiate this view. However, the combined adsorption mechanisms may become separable under certain disturbed conditions, such as injecting methanol to a methanol/water system. The injected methanol molecules seem to displace some of the water molecules from the hydrated, inactivated sites (*i.e.*, the hydrated residual silanol groups) and to create new active sites which are relatively small in number compared with the number of normal active sites (i.e. the organic modifier groups). Therefore, only a small fraction of the injected solute molecules will be retained on the new active sites. The adsorption of the solute on the new active sites is sufficiently strong to result in a slow mass transfer; the solute is then gradually desorbed, giving a tailing peak.

The injection of vitamin D_2/isooctane solution does not cause tailing, simply because isooctane does not effectively displace water molecules from the hydrated inactivated sites. Similarly, for vitamin B_{12}, the injection of the 100 % aqueous vitamin B_{12} solution should not generate new active sites and tailing should not occur, as is actually observed (Fig.2C). Increasing the volume of methanol injected in the vitamin B_{12} case should generate new active sites and the tailing should increase. The large, broad peak following the solvent front in Fig.3 shows such a tendency. However, the tailing does not last as long as the small volume injection previously described. This is because there is a high

concentration of methanol in the vicinity of the solute band; the methanol molecules compete effectively with the solute molecules for the new active sites, and prolonged tailing does not result.

Predictably, any polar organic solvents miscible with water can effectively displace the water molecules from the hydrated inactivated sites and generate new active sites, which will retain solute.

Although vitamin B_{12} is water-soluble and vitamin D_2 is fat-soluble, both vitamins are retained on the C_{18}/Corasil column. If a true liquid—liquid partition plays a predominant role in retaining solutes, the vitamin B_{12} should not be retained on this column at all; this also demonstrates that some type of adsorption mechanism is involved.

Conclusions

The most reliable solvent for dissolving sample and standard for liquid chromatography is the mobile phase in use. In this way, the surface properties of the packing material will not be altered as a result of sample introduction. If some other organic solvent must be used to dissolve the sample, care should be taken to recognize that some organic solvents will temporarily but drastically change the surface properties of the packing material and cause anomalous chromatograms.

REFERENCES

1 W.A. Aue and C.R. Hastings, J. Chromatogr., 42 (1969) 319.
2 J.J. Kirkland and J.J. De Stefano, J. Chromatogr. Sci., 8 (1970) 309.
3 J.J. Kirkland in J.J. Kirkland (Ed.), Modern Practice of Liquid Chromatography, Wiley-Interscience, New York, 1971, pp.192—195.
4 J.J. Kirkland, J. Chromatogr. Sci., 9 (1971) 206.
5 M. Novotny, S.L. Bektesh, K.B. Denson, K. Grohmann and W. Parr, Anal. Chem., 45 (1973) 971.

Analytica Chimica Acta, 79 (1975) 313—317

Short Communication

SEPARATION AND SPECTROPHOTOMETRIC DETERMINATION OF DI(4-OCTYLPHENYL) AND MONO(4-OCTYLPHENYL)PHOSPHORIC ACIDS IN MIXTURES

K. BHATTACHARYYA and T.K.S. MURTHY
Chemical Engineering Division, Bhabha Atomic Research Centre, Trombay, Bombay 400 085 (India)
(Received 1st January 1975)

A mixture of di(4-octylphenyl)phosphoric acid (DOPPA) and mono(4-octylphenyl)phosphoric acid (MOPPA) has been recommended [1,2] for the recovery of uranium from commercial wet-process phosphoric acid by liquid—liquid extraction. The extractants lost in the aqueous raffinate can be monitored, when they are employed separately, by a spectrophotometric method based on the formation of an ion-association complex with rhodamine-B in 1,2-dichloroethane [3]. This method (the 'single-phase method') cannot, however, be employed for the individual determination of the two extractants present together. Though both DOPPA and MOPPA can be determined by the extraction-spectrophotometric method recommended earlier for DEPHA [4], under slightly modified conditions, this method is also not applicable for analysis of mixtures. A simple method for the separation of MOPPA from DOPPA coupled with the extraction-spectrophotometric method so that the individual components can be determined in mixtures is described in this communication.

For the determination of DOPPA and MOPPA in the aqueous raffinates, the following three steps were envisaged: their combined extraction from the sample, separation of the two esters, and individual spectrophotometric determination. Earlier results [3] showed that many solvents, including 1,2-dichloroethane, effectively extracted DOPPA from 6 *M* phosphoric acid, but MOPPA could be quantitatively extracted only with chloroform; chloroform was therefore preferred for the combined extraction. However, since chloroform was not a suitable medium for colour development, it was evaporated and the residue taken up in 1,2-dichloroethane before the two esters were separated. Several methods for the separation of mono-alkyl and aryl phosphoric acids from the corresponding diesters have been reported [5—8]; in the present context the method based on the greater solubility of the sodium salt of the monoester in aqueous solution was found to be simplest. DOPPA in the 1,2-dichloroethane layer and MOPPA in the aqueous layer could then be determined by the extraction-spectrophotometric method with rhodamine-B.

Experimental

Reagents. Use a 0.1% rhodamine B solution prepared from purified reagent [4] Prepare standard solutions containing 10 μg ml^{-1} of DOPPA and MOPPA in 1,2-dichloroethane from purified [3] compounds. For the phosphate buffer, adjust the pH of 0.1 *M* phosphoric acid to 4 or 3, as needed with sodium hydroxide. Use reagent-grade solvents after washing with 5 % Na_2CO_3 and water.

A Beckman Model B spectrophotometer with 10-mm glass cells was used.

Recommended procedure. For the preliminary separation, pipette an aliquot of the well mixed sample solution (commercial phosphoric acid) containing not more than 200 μg of MOPPA into a separating funnel, dilute to 10 ml with 6 *M* phosphoric acid and extract with three 10-ml portions of chloroform. Evaporate the combined extracts on a water bath, take up the residue in 10.0—25.0 ml of 1,2-dichloroethane and transfer to another separating funnel. Add 20.0—50.0 ml of 1 % (w/v) sodium carbonate solution and extract for 5 min. Allow the layers to clear and collect them separately.

For the determination of DOPPA in the organic layer transfer an aliquot of the extract, containing 5—25 μg of DOPPA, along with enough fresh solvent to make the total volume 10.0 ml, to a separating funnel. Add 9 ml of phosphate buffer (pH 4) and 1.0 ml of rhodamine B solution, and mix for 2 min. After 20 min, collect the coloured organic layer and measure its absorbanc at 565 nm against 1,2-dichloroethane as blank. Determine the amount of DOPI from a calibration graph prepared with known aliquots of standard DOPPA and a blank (with no DOPPA) treated by the same procedure.

For the determination of MOPPA in the carbonate layer, acidify an aliquot of the solution containing 10—25 μg of MOPPA to pH 3 with phosphoric acid. Add 5 ml of phosphate buffer (pH 3) and 1.0 ml of rhodamine B solution, and dilute to about 10 ml. Extract with 10.0 ml of 1,2-dichloroethane. After the phases have cleared, remove the organic layer and measure its absorbance at 565 nm against 1,2-dichloroethane as blank. Prepare a calibration graph from known aliquots of MOPPA in 1 % sodium carbonate by the same procedure.

Results

The repeated extraction with chloroform for the separation of MOPPA from commercial phosphoric acid [3] served equally well for recovery of DOPPA and was adopted without modification.

The method used for the separation of MOPPA from DOPPA is based on the greater solubility of the sodium salt of MOPPA in water compared to Na-DOPPA. Sodium hydroxide and carbonate solutions of different concentration and different aqueous/organic phase ratios were tested. Initially, 10.0 ml of 1,2-dichloroethane containing 100—400 μg of DOPPA was extracte

TABLE I

Washing of DOPPA from dichloroethane with sodium carbonate (Vol. of 1,2-dichloroethane = 10.0 ml; DOPPA present = 400 μg)

Concn. of Na_2CO_3 (% w/v)	Vol. of Na_2CO_3 soln. (ml)	Time for clean phase sepn. (min)	DOPPA left in org. phase (μg)	Retention (%)
1	5	120	388	97
2	5	40	395	99
5	5	40	400	100
1	10	60	400	100
2	10	50	405	101
5	10	40	395	99
1	20	10	391	98
2	20	10	408	102
5	20	10	404	101

with 5.0, 10.0 and 20.0 ml of 1,2 and 5 % (w/v) sodium hydroxide solution; however, even after 60 min of standing the two phases did not clear, and when the slightly hazy organic layers were analyzed for DOPPA, it was found that the loss of DOPPA to the aqueous phase increased with increasing concentration and volume of sodium hydroxide. The phase separation became poorer, the lower the alkali concentration. The results were better with sodium carbonate (Table I); since 20.0 ml of carbonate solution led to rapid phase separation with quantitative recovery of DOPPA, this condition was chosen for further work.

The efficiency of the method for separation of MOPPA was checked by adding different amounts of MOPPA to 25.0-μg aliquots of DOPPA in 1,2-dichloroethane, carrying out the above carbonate extraction, and determining DOPPA spectrophotometrically. Up to 100 μg of MOPPA caused no significant error.

For the determination of DOPPA in dichloroethane, after the carbonate wash, the extraction-spectrophotometric method recommended for DEHPA [4] proved satisfactory. However, in this case 1.0 ml of 0.1 % rhodamine B was sufficient instead of the 0.2 % reagent required previously. Maximal absorbance occurred at 565 nm for the DOPPA—rhodamine B complex, the molar absorptivity being 100,000.

MOPPA in the carbonate solution could also be determined by extraction of its ion-association rhodamine B complex with 1,2-dichloroethane. The optimal pH for colour development was 3. At lower pH values, blank absorbances increased significantly, whereas at higher pH values, the sample absorbances decreased considerably. The pH should be adjusted carefully within ±0.05 units. A 1.0 ml volume of 0.1 % rhodamine B solution gave maximal colour formation with a reasonably low blank. Under these conditions, the absorbance of the

TABLE II

Separation and determination of DOPPA and MOPPA from 6 *M* phosphoric acid

DCE layer				Sodium carbonate layer			
Aliquot taken (ml)	DOPPA expected (μg)	DOPPA found (μg)	Recovery (%)	Aliquot taken (ml)	MOPPA expected (μg)	MOPPA found (μg)	Recovery (%)
2.5	10.0	9.7	97	6.0	12.0	12.3	103
2.0	16.0	15.7	98	8.0	10.0	9.5	95
1.0	16.0	16.2	101	4.0	8.0	7.9	99
1.0	24.0	23.5	98	4.0	8.0	8.2	102
0.5	20.0	19.2	96	5.0	5.0	5.1	102

extract followed Beer's Law up to about 4 p.p.m. of MOPPA and the calculated molar absorptivity was 77,00.

Various mixtures of DOPPA and MOPPA in 1,2-dichloroethane were prepared containing DOPPA in the range 5—100 p.p.m. and MOPPA in the range 1—10 p.p.m. Six mixtures analysed by the recommended procedure, gave recoveries in the range 97—102 %.

Application of the method for determination of DOPPA and MOPPA in phosphoric acid. To 10-ml aliquots of 6 *M* phosphoric acid, known amounts (0.1—0.5 ml) of ethanolic solutions of DOPPA and MOPPA were added; the mixtures were analyzed by the recommended procedure (with 25.0 ml of 1,2-dichloroethane to dissolve the DOPPA—MOPPA residue, and 50.0 ml of 1 % Na_2CO_3 to extract the MOPPA). The results are summarized in Table II.

During a pilot plant study of solvent extraction for recovering uranium from commercial phosphoric acid with DOPPA + MOPPA (0.1 *M* each) in kerosene, several raffinate samples were analyzed; the combined (soluble and suspended) loss of DOPPA was found to be in the range 25—30 p.p.m. whereas that of MOPPA was 40—45 p.p.m.

Discussion

The proposed extraction-spectrophotometric method for the separation and determination of traces of DOPPA and MOPPA in commercial phosphoric acid involves extraction into chloroform followed by dissolution in 1,2-dichloroethane and back-extraction of the monoester with sodium carbonate. For the determination of DOPPA in the dichloroethane phase, the "extraction-spectrophotometric method" was used, as this avoids the conversion of the sodium salt of DOPPA to the acid which was shown to be necessary for the "single-phase method". For the determination of MOPPA in the aqueous phase

the 'extraction-spectrophotometric method' has a definite advantage, as the single-phase method requires reextraction of the acid into chloroform, evaporation of this solvent and dissolution of the residue in 1,2-dichloroethane. For DOPPA, both methods give about the same sensitivity, but for MOPPA, the extraction method is less sensitive (ϵ = 77,000 against 100,000); the lower molar absorptivity was not caused by incomplete extraction, but probably by the existence of a polymeric form [9] in the organic layer.

Though this method was specifically worked out for the analysis of raffinates for DOPPA and MOPPA, it could equally well be employed for analysing the organic solvent itself for these two constituents after dilution with dichloroethane.

REFERENCES

1 T.K.S. Murthy, V.N. Pai and R.A. Nagle, Proceedings of a Symposium on The Recovery of Uranium, Sao Paulo, 17—20 August, 1970, I.A.E.A., Vienna, 1971, 346.
2 Oak Ridge National Laboratory, Semi Annual Progress Report Feb. 1974, ORNL-TM-4370, 1974, 368.
3 K. Bhattacharyya and T.K.S. Murthy, Anal. Chim. Acta, 76 (1975) 91.
4 K. Bhattacharyya and T.K.S. Murthy, Anal. Chim. Acta, 71 (1974) 107.
5 D.F. Peppard, G.W. Mason, J.L. Maier and W.J. Driscoll, J. Inorg. Nucl. Chem., 4 (1957) 335.
6 D.F. Peppard, J.R. Ferraro and G.W. Mason, J. Inorg. Nucl. Chem., 7 (1958) 232.
7 E. Cerrai and F. Gadda, Nature (London), 183 (1959) 1528.
8 C. Cesarano and C. Lepscky, J. Inorg. Nucl. Chem., 14 (1960) 276.
9 Y. Marcus and A.S. Kertes, Ion Exchange and Solvent Extraction of Metal Complexes, Wiley—Interscience, New York, 1969, p.531.

Analytica Chimica Acta, 79 (1975) 318—321

Short Communication

DYE-SENSITIZED CONTINUOUS PHOTOCHEMICAL ANALYSIS OF THE INDOLE-RELATED COMPOUNDS, 5-HYDROXYINDOLEACETIC ACID, 5-HYDROXYTRYPTAMINE AND TRYPTOPHAN

V.R. WHITE and J.M. FITZGERALD
Department of Chemistry, University of Houston, Houston, Texas 77004 (U.S.A.)
(Received 21st March 1975)

The important experimental parameters which must be considered for dye-sensitized continuous photochemical analysis (d.c.p.a.) have recently been reported [1]. In this technique, a sample is injected into a flowing stream of dye and the whole is exposed to an intense, visible light source; the photochemically produced excited-state dye triplet undergoes a photoredox reaction with the substrate yielding the leuco form of the dye and substrate oxidation products. Digital spectrophotometric measurement of the change in dye concentration (ΔAbs) is a linear function of substrate concentration injected, if proper reaction conditions are used. Of the photoredox reactions reported to date, nitrogen-containing compounds show the most promise for d.c.p.a. [2—4]. Screening studies of the photoredox reactions of catechol amines [5] and many simple organic amines [6] have been reported. In general, tertiary amines and aromatic heterocyclic nitrogen compounds are the most reactive and yield stable photooxidation products [2,3].

This paper reports operating conditions and analytical data for the indole-related compounds 5-hydroxyindoleacetic acid, 5-hydroxytryptamine, tryptophan, and indole itself. The first two substances are of clinical significance [7].

Experimental

Reagents. All the chemicals used were of reagent grade. Methylene blue, rose bengal and tryptophan (Eastman Organic Chemical Co.) were used, and other samples were obtained from Sigma Chemical Co. or J.T. Baker Chemical Co. Solutions of all compounds except 5-hydroxytryptamine were stable at pH 11 for at least 4 h. 5-Hydroxytryptamine decomposed rapidly in alkaline solution; therefore this substrate was prepared and injected at natural pH into a basic dye-carrier stream. In order to minimize any other substrate decomposition effects, all solutions were freshly prepared and serially diluted just before analysis. Dye solutions were prepared as previously

described [1]. Distilled (*not* deionized) water was used for preparation of all solutions [1].

Apparatus and procedures. The instrumentation, apparatus and general procedures have been described previously [1,6]. Only changes in the procedure will be presented here. All analyses were run at 1000-W power applied to the reactor lamp.

Preliminary investigations of the photobleaching of all compounds with methylene blue as the sensitizer showed that the pH for maximum photobleaching was more basic than 10.5. For reasons [1] related to the pK_a of methylene blue, this dye was deemed unsuitable as the sensitizer for indoles. Rose bengal exhibited maximum photobleaching for all four compounds between pH 10.5 and 11, and is quite stable in this pH range [1]; it was therefore used as the sensitizer. Previous studies [2,4] of the photooxidation of tryptophan with both methylene blue and rose bengal were carried out under oxygen-saturated conditions and followed by manometric methods. However, the best photobleaching is obtained with nitrogen-saturated solutions [1]; this practice was continued for this study.

Results and discussion

Table 1 summarizes the conditions used and results obtained for the four indole-related substrates. The majority of the photobleaching reactivity resides in the parent compound, indole; substituent groups increase photobleaching no more than 50 % of that due to the indole ring system alone. Since virtually no structural or pH selectivity for the substrates was found, mixtures were not investigated. A separation procedure for 5-hydroxyindoleacetic acid and 5-hydroxytryptamine has been published [8]; however, the d.c.p.a. limits of detection with rose bengal are slightly higher than normal levels in human urine [7]. Other dyes and/or detectors need to be investigated before clinical application of d.c.p.a. to indole metabolites become possible.

In previous temperature studies of d.c.p.a. substrates [1], caffeine yielded a plot of photoreactivity vs. reactor temperature which was concave downwards. All four substrates here yielded similar curves. In place of graphical presentation, a numerical index is used to report the temperature dependence of substrates in Table 1. The ΔAbs at the temperature where maximum photobleaching occurs is normalized to the ΔAbs observed at 30 °C (minimum available with present apparatus) for the same substrate concentration injected. This normalized index permits comparison of temperature sensitivity between compounds. Indole exhibits the largest temperature dependence of the four compounds studied (Table 1); maximal photobleaching occurs when the photochemical reactor is thermostated at 50 °C. The data in Table 1 also indicate that substituent groups effectively lower the photoredox activation energy; in the extreme case, 5-hydroxytryptamine thermally decomposes at pH 10.5 and should be run at the lowest possible reactor temperature. One

TABLE 1

Experimental conditions and statistical data for indole-related compounds

Compound	Conc. range (mM)	Flow rate (ml min^{-1})[a]	Normalized temperature dependence[b]	Sensitivity[c] (m*Abs* mM^{-1})
5-Hydroxyindole-acetic acid	0.05—1	190	1.65 (44 °C)	318 (4) 305 (2)
Tryptophan	0.01—1	90	1.15 (40 °C)	264 (4) 264 (2)
5-Hydroxy-tryptamine	0.1—1	90	Decomp.[d]	225 (2)
Indole	0.1—1	70	2.39 (50 °C)	194 (1)

[a]Dye sensitizer flow rate for maximal photobleaching.
[b]The ratio of change in absorbance (ΔAbs) at the temperature of maximal photoredox efficiency to change in absorbance at 30 °C (minimum available temperature) for same substrate concentration. Temperature for maximum photobleaching shown in parenthesis. See text for further details.
[c]The slope of the calibration line in units of Δm*Abs*/mM injected. The standard error of the estimate, in m*Abs*, is shown in parentheses. Data for same compound represent day-to-day reproducibility.
[d]Serotonin is thermally unstable at pH 10.5; reactor temperature should be held as low as possible.

generalization can be made: compounds with large temperature dependences, such as indole, require good temperature control if precise statistical data are to be obtained. Thus, the temperature dependence of dye-sensitized photoredox reactions must be investigated in order to determine both the temperature for maximal photobleaching and the degree of curvature of the reactivity profile.

Careful perusal of the flow rate and temperature dependence (Table 1) shows that each of the four compounds presents a distinct kinetic case. First, tryptophan exhibits the usual flow rate behavior [1]; the temperature dependence is small, which is reflected in the excellent day-to-day reproducibility. Secondly, indole shows the largest temperature dependence; even at the highest temperature available with current apparatus (50 °C) the flow rate required for maximum photobleaching by indole, and thus the kinetics of the photoredox reaction, are the slowest of all compounds studied here. Thirdly, 5-hydroxyindoleacetic acid exhibits a moderate temperature dependence, and also requires rapid flow rates. Both of these facts affect the reproducibility (Table 1); the high flow rate required is due to a rapid postphotochemical back-reaction, similar to that observed earlier with caffeine. In the current apparatus design, there is a delay of about 4 s between the time that the sample "plug" exits from the photochemical reactor and the time it enters the detector at a flow rate of 190 ml min^{-1}. At 70 ml min^{-1}, the delay time increases to about 10 s. Therefore, high flow rates are required to sweep the 5-hydroxyindoleacetic

acid—leucodye photoproducts to the spectrophotometer fast enough to offset effects of the rapid back-reaction. Finally, 5-hydroxytryptamine is thermally unstable at pH 10.5 and kinetic competition between photoredox and thermal pathways of oxidation results; this thermal behavior is similar to that previously observed with epinephrine. Despite this variety of kinetic behavior, good analytical data were obtained for all substrates; this is reflected in standard errors of estimate of about 1 % (Table 1).

Financial support from Grant E-384, Robert A. Welch Foundation is gratefully acknowledged.

REFERENCES

1 V.R. White and J.M. Fitzgerald, Anal. Chem., 47 (1975) 903.
2 L. Weil, Arch. Biochem. Biophys., 110 (1965) 57.
3 R.F. Bartholomew and R.S. Davidson, J. Chem. Soc. C, (1971) 2347.
4 G. Jori, G. Galiazzo, A. Marzotto and E. Scoffone, Biochim. Biophys. Acta, 154 (1968) 1.
5 V.R. White and J.M. Fitzgerald, Abstracts 1973 Pittsburgh Conference on Analytical Chemistry and Applied Spectroscopy, p. 194.
6 V.R. White, Ph.D. Dissertation, University of Houston, 1974.
7 N.A. Tietz (Ed.), Clinical Chemistry, Saunders, Philadelphia, 1970, pp. 580—85, 945.
8 C.A. Fisher and M.H. Aprison, Anal. Biochem., 46 (1972) 67.

Analytica Chimica Acta, 79 (1975) 322—325

Short Communication

THE SPECTROPHOTOMETRIC DETERMINATION OF IRON(III) WITH SODIUM 2-BROMO-4,5-DIHYDROXYAZOBENZENE-4'-SULFONATE IN THE PRESENCE OF CETYLPYRIDINIUM CHLORIDE

YOSHINOBU WAKAMATSU
Department of Industrial Chemistry, Hachinohe Technical College, Hachinohe 031 (Japan)
MAKOTO OTOMO
Department of Synthetic Chemistry, Nagoya Institute of Technology, Showa-ku, Nagoya 466 (Japan)
(Received 14th January 1975)

Sodium 2-bromo-4,5-dihydroxyazobenzene-4'-sulfonate (abbreviated as BDAS) was first prepared by Basargin *et al.* [1] as a colorimetric reagent for metals such as aluminum, gallium and indium.

During studies on the sensitizing effects of cationic surfactants on the reaction of this reagent with various metal ions, including iron(III), copper(II) [2], and zirconium [2], it was found that the addition of cetylpyridinium chloride (CPC) to the iron(III)—BDAS complex produced a large bathochromic shift in the wavelength of maximum absorption, and a marked increase in the molar absorptivity. The present communication describes the spectrophotometric determination of trace amounts of iron(III) by means of this ternary complex, which is of comparable or greater sensitivity than recent methods based on xylenol orange [3], indoferron and 1,3-diphenylguanidine [4], substituted triazines [5—7], pyrocatechol violet [8], and nitrosophenols and rhodamine B [9].

Experimental

Reagents. The reagent was synthesized by coupling of 4-bromopyrocatechol with sodium sulfanilate [1] (found: 34.4 % C, 2.3 % H, 6.31 % N). The acid dissociation constants of the reagent were determined spectrophotometrically in the presence of an excess of CPC and found to be $pK_1 = 6.24 \pm 0.07$ and $pK_2 = 11.02 \pm 0.11$ at 25 °C and $\mu = 0.1$. These values are considerably lower than those obtained [1] without CPC ($pK_1 = 6.72 \pm 0.05$ and $pK_2 = 11.9 \pm 0.1$

A standard iron(III) solution was prepared from iron(III) ammonium sulfate, standardized by EDTA titration, and diluted as required.

The CPC solution was prepared in aqueous 20 % (v/v) methanol.

All the other chemicals used were of analytical grade.

Apparatus. A Hitachi model 124 spectrophotometer with 10-mm quartz cells and a Toa Dempa model HM-5A pH meter were used.

Procedure. Transfer an aliquot of iron(III) solution to a 25-ml volumetric flask. Add 2 ml of 10^{-3} *M* BDAS, 2 ml of 10^{-2} *M* CPC and 10 ml of buffer solution adjusted to pH 5.5—6.5 with hexamethylenetetramine (0.25 *M*) and hydrochloric acid. Dilute to the mark with water. After 30 min, measure the absorbance at 565 nm against a reagent blank.

Results and discussion

The absorption spectra of the reagent solution (BDAS and CPC) and of the ternary complex with iron(III) at pH 5.9 are shown in Fig.1. Included for comparison is the spectrum of the binary iron(III) complex at the same pH value. The ternary complex shows a pronounced absorption at 565 nm whereas the binary system gives a broad absorption with a maximum at about 490 nm.

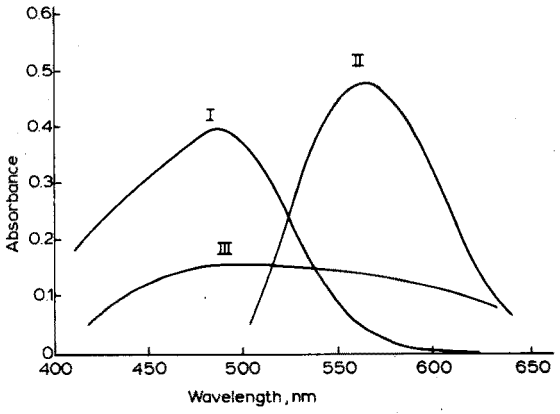

Fig.1. Absorption spectra. pH 5.9. (I) [BDAS] = $2.0 \cdot 10^{-5}$ *M*; [CPC] = $8.0 \cdot 10^{-4}$ *M*; reference, water. (II) [Fe] = 11.2 μg; [BDAS] = $8.0 \cdot 10^{-5}$ *M*; [CPC] = $8.0 \cdot 10^{-4}$ *M*; reference, reagent blank. (III) [Fe] = 11.2 μg; [BDAS] = $8.0 \cdot 10^{-5}$ *M*; reference, reagent blank.

Effect of variables. The absorbance of the solution containing iron(III), BDAS and CPC was examined as a function of pH. The optimal pH for complex formation occurred over the pH range 5.5—8.3; on both sides of this range, the absorbance decreased gradually with change of pH.

The effect of CPC concentration on the complex formation was investigated for solutions containing 11.2 μg of iron(III) ($8.0 \cdot 10^{-6}$ *M*), the pH value being kept constant at 5.9. Maximum color formation was found when the CPC concentration exceeded $5.5 \cdot 10^{-4}$ *M*; both the iron(III) complex and the reagent were precipitated when the CPC concentration was less than about $5 \cdot 10^{-5}$ *M*. In the light of this observation and the known requirement for

the presence of micelles for complex formation [10—12], it is postulated that the uncharged iron(III)—BDAS—CPC and BDAS—CPC species are present as finely dispersed particles protected within the CPC micelles in solution. This suggestion is supported by the observed partial extraction of the ternary complex into chloroform.

The effect of varying BDAS concentration on the color formation was also studied; constant absorbance was obtained when the BDAS concentration exceeded $4.0 \cdot 10^{-5}$ *M*.

Maximum absorbance of the solution containing the ternary iron(III) complex was obtained within 3 min and then remained unchanged over at least 2 h.

Calibration curve. With the above optimal conditions, a linear calibration curve was obtained over the concentration range 0—17 μg of iron ($1.2 \cdot 10^{-5}$ *M*). The apparent molar absorptivity was calculated to be $6.1 \cdot 10^4$ l mole^{-1} cm^{-1} at 565 nm.

Nature of complex. The iron:BDAS ratio in the ternary complex formed at pH 5.8 or 7.8 was determined by the continuous variation method to be 1:3, indicating the formation of the $[Fe(BDAS)_3]$ $(C_5H_5NC_{16}H_{33})_6$; no other complexes were observed. In the binary iron(III)—BDAS system, this ratio was found to be 1:2 at pH 5.7 and 1:3 at pH 7.9. Color development for the binary 1:3 complex (molar absorptivity, $4.5 \cdot 10^4$ l mole^{-1} cm^{-1} at 550 nm) was instantaneous but this was followed by a gradual decrease in absorbance.

The formation of the ternary 1:3 iron(III) complex at pH 5.8 is thought to be connected with the observed low p*K* values for BDAS in the presence of CPC. Since chelate formation between BDAS and metal ions should occur through replacement of the hydrogen atoms of the two hydroxyl groups in the ligand, the decreased p*K* values of BDAS would favor the formation of higher complexes at lower pH values.

Interferences. The extent of interference by a number of foreign ions in the determination of 11.2 μg ($8.0 \cdot 10^{-6}$ *M*) of iron(III) was studied. The following ions caused no interference: a 1000-fold molar amount of the alkali metals, fluoride, chloride, nitrate, sulfate, thiosulfate, and carbonate; a 100-fold amount of magnesium, calcium, zinc, cadmium, nickel, tartrate, and phosphate. The following ions did not interfere when an appropriate masking agent was used: an equimolar amount of copper(II) masked with $8 \cdot 10^{-3}$ *M* thiosulfate; an equimolar amount of zirconium, a 4-fold molar amount of molybdenum(VI) and a 10-fold amount of lead masked with $4 \cdot 10^{-3}$ *M* tartrate; a 10-fold amount of aluminum and thorium masked with $2 \cdot 10^{-2}$ *M* fluoride. However, gallium, indium, titanium, uranium(VI), oxalate, and EDTA interfered severely and must be absent.

We are grateful to the Ministry of Education (Japan) for financial support to one of us (Y. W.).

REFERENCES

1 N.N. Basargin, M.K. Akhmedli and A.A. Kafarova, Zh. Anal. Khim., 25 (1970) 1497.
2 Y. Wakamatsu and M. Otomo, unpublished.
3 M. Otomo, Bunseki Kagaku, 14 (1965) 677.
4 Y. Wakamatsu and M. Otomo, Bunseki Kagaku, 19 (1970) 537.
5 A.A. Schilt, Talanta, 13 (1966) 895.
6 C.D. Chriswell and A.A. Schilt, Anal. Chem., 46 (1974) 992.
7 E. Kiss, Anal. Chim. Acta, 72 (1974) 127.
8 T. Ishito and S. Ichinohe, Bunseki Kagaku, 21 (1972) 1207.
9 S. Motomizu, Anal. Chim. Acta, 56 (1971) 415.
10 V. Svoboda and V. Chromy, Talanta, 12 (1965) 431, 437.
11 J.E. Chester, R.M. Dagnall and T.S. West, Talanta, 17 (1970) 13.
12 H. Kohara, N. Ishibashi and T. Masuzaki, Bunseki Kagaku, 19 (1970) 467.

Analytica Chimica Acta, 79 (1975) 326—329

Short Communication

THE DETERMINATION OF SMALL AMOUNTS OF COPPER AS ITS CARMINIC ACID COMPLEX BY REFLECTANCE SPECTROMETRY

R. REISFELD, S. LEVI, E. GREENBERG and W.J. LEVENE*
Department of Inorganic & Analytical Chemistry, The Hebrew University of Jerusalem (Israel)
(Received 12th February 1975)

The determination of copper at low concentrations is of importance in various situations. The present communication describes the application of reflectometry to the determination of microgram amounts of copper by the method which has recently proved useful for the determination of mercury(II) and lead(II) [1,2]. The reaction takes place on a filter paper at pH 6—7; a well defined homogeneous spot is formed, and the diffuse reflectance of the spot is measured at 600 nm. Copper(II) reacts with carminic acid to form a purple complex with a 1:2 copper(II)—ligand ratio [3].

Experimental

The experimental technique has been described in detail previously [1,2]. The chemicals used were all of reagent grade. The filter paper was Whatman 120. The stock solutions were aqueous 0.5% (w/v) carminic acid and 300 p.p.m. copper(II) solution in triple-distilled water. The carminic acid reagent was suitably diluted for the concentration range of copper determined: for 1—10 p.p.m., 10—45 p.p.m. and 20—260 p.p.m. of copper, 0.125 %, 0.250 % and 0.500 % carminic acid solutions, respectively, were prepared. These dilutions were necessary because the strongly-colored reagent obscured the color of the complex when excessive amounts were present. Reagent-impregnated filter paper could be prepared a few days in advance and stored away from direct light. Calibration curves must be prepared simultaneously with each set of measurements.

In the measurement of interfering ions, solutions containing 50 p.p.m. copper(II) and 10 p.p.m. interfering ion were prepared. When necessary, additional concentrations of interfering ion were also tested.

* Present address: Electro-Optical Industry, Ltd., Rehovot, Israel.

Results

The reflectance spectra of carminic acid and of its complex with copper(II) at different concentrations (Fig.1) show that 600 nm is the optimal wavelength for measuring changes of the reflectance with concentration.

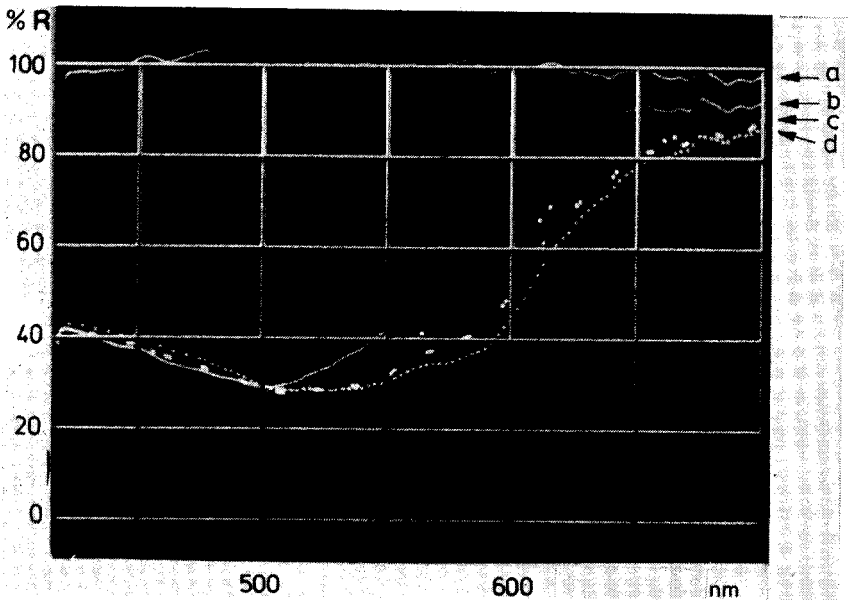

Fig.1. Reflectance spectra of test spots on filter paper. (a) Carminic acid reagent (0.5 % w/v) alone. (b) Reagent + 40 p.p.m. Cu^{2+}. (c) Reagent + 80 p.p.m. Cu^{2+}. (d) Reagent + 120 p.p.m. Cu^{2+}.

It was observed that the Kubelka—Munk function depended on the concentration of the reagent, which was itself red and could interfere with the reflectance measurement. In order to obtain linear calibration graphs over the 1—200 p.p.m. range of copper(II) concentration, three series of measurements with three different dilutions of the reagent were necessary. Linear graphs were obtained in the ranges, 1—10 p.p.m., 10—45 p.p.m. and 50—200 p.p.m., the function $10^{-3}\ (1 - R)^2/2R$ being in the approximate ranges 12—40, 20—120, and 70—390, respectively. The standard deviations of the points from linearity in each range were 0.00071, 0.00187 and 0.00508, and the correlation coefficients were 0.9984, 0.9980 and 0.9984, respectively.

Interfering substances

In order to test for the interference of foreign cations, carminic acid spot tests were performed on solutions containing 50 p.p.m. copper and 10 p.p.m.

of the interfering ion. The following ions did not show any significant change in the reflectance spectrum of the reagent itself or of the copper(II) complex: Ag^{+}, Hg^{2+}, Pb^{2+}, Cd^{2+}, Ba^{2+}, Sr^{2+}, Sn^{2+}, Ca^{2+}, Mg^{2+}, Na^{+} and K^{+}. Tin(II) and calcium(II) were also checked at higher concentrations, but no significant interference was found.

Carminic acid is a reagent for the determination of lead(II), but at concentrations less than half that of the copper(II), lead(II) does not interfere. At these concentrations only nickel(II), iron(II) and iron(III) were found to interfere with the test. The results are summarized in Table I.

TABLE I

Study of possible interferences
(Results are given as % reflectance, each being the average of two tests.)

Foreign ion (X)	Reagent alone (a)	Reagent + 50 p.p.m. Cu (b)	Reagent + 10 p.p.m. X (c)	Reagent + 50 p.p.m. Cu + 10 p.p.m. X (d)	Interference at 0 p.p.m. Cu (a)—(c)	Interferen at 50 p.p. Cu (b)—(d)
Ag^{+}	83.3	62.3	83.0	62.7	0.3	—0.4
Hg^{2+}	82.7	61.3	82.3	61.0	0.4	0.3
Pb^{2+}	83.5	62.3	83.0	62.3	0.5	0.0
Cd^{2+}	82.7	61.3	83.0	61.3	—0.3	0.0
Sn^{2+}	83.5	62.5	82.5	62.3	1.0	0.2
Ni^{2+}	83.5	62.5	82.5	62.7	1.0	—0.2
Fe^{2+}	83.7	62.0	72.5	60.3	11.2	1.7
Fe^{3+}	83.7	62.0	70.8	62.0	12.9	0.0
Ba^{2+}	83.3	62.3	83.3	62.5	0.0	—0.2
Sr^{2+}	83.5	62.5	83.5	62.3	0.0	0.2
Ca^{2+}	83.5	62.3	82.3	62.5	1.2	—0.2
Mg^{2+}	83.3	62.3	83.0	62.0	0.3	0.3
Na^{+}	83.5	62.3	83.0	62.7	0.5	—0.4
K^{+}	83.3	62.3	82.8	61.8	0.5	0.5

Conclusion

Copper can be determined as its carminic acid complex by reflectance spectrometry in the concentration range 1—200 p.p.m. The lower range of determination extending down to 1 p.p.m. is of interest. Linear and highly reproducible calibration graphs are obtained in each of three concentration ranges. Fourteen possible interfering ions were tested; only Fe^{2+}, Fe^{3+} and Ni^{2+} were found to interfere.

This work was supported by the Israel National Council of Research and Development.

REFERENCES

1 R. Reisfeld, E. Greenberg and W.J. Levene, Anal. Chim. Acta, 75 (1975) 253.
2 R. Reisfeld, S. Levi, E. Greenberg and W.J. Levene, Anal. Chim. Acta, 76 (1975) 477.
3 T.C. Jain, J. Indian Chem. Soc., 37 (1960) 727.

Analytica Chimica Acta, 79 (1975) 330—331

Short Communication

ANALYSIS OF PHOSPHOR COATINGS BY LUMINESCENCE THERMAL DEGRADATION

SIMON LARACH and JERRY GERBER
RCA Laboratories, Princeton, N.J. 08540 (U.S.A.)
(Received 17th March 1975)

Phosphor particles are often coated with thin layers of inorganic materials in order to improve various screening factors. As part of a general study on the effect of coatings on the cathodoluminescence of phosphors, the effect of high-density cathode-ray excitation has been investigated [1]. Such studies indicated that there is a luminescence degradation, which is thermal in nature, as a function of time. By plotting this luminescence thermal degradation as a function of coating concentration, obtained by independent analytical means, a method of quantitative analysis was evolved, valid for a particular coating on a particular host phosphor.

Experimental

Green-emitting ZnCdS:Cu:Al and blue-emitting ZnS:Ag were coated [2] with thin layers of various inorganic compounds by conventional techniques. These were then tested in a demountable cathode-ray apparatus [3]. The focussed electron beam was scanned into a small raster, about 2 mm on a side. Power input to the sample was controlled by adjusting the beam current, at a constant 10-kV potential. Currents of 0.1—0.5 μA typically gave a detectable luminescence thermal degradation signal on uncoated samples.

Luminescence degradation was observed with a monochromator and an RCA 7265 (S20 surface) multiplier phototube. Broad slits were used to obtain a 20-nm band-pass centered about the peak of the emission spectrum. Photomultiplier output was plotted against "beam-on" time on an X—Y recorder.

Sample preparation was found to be of importance. The phosphor particles should be in poor thermal contact with each other and with any other surfaces. It was found best to "dust" the phosphor loosely into a depression (1-mm deep) in a multi-sample stainless-steel disk which was placed into the demountable apparatus.

Results and discussion

The technique calls for exciting a "blank" (uncoated) phosphor, and a

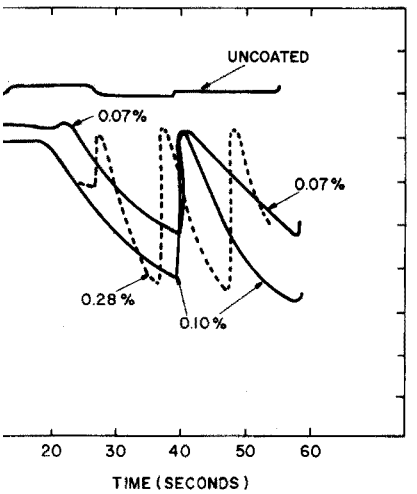

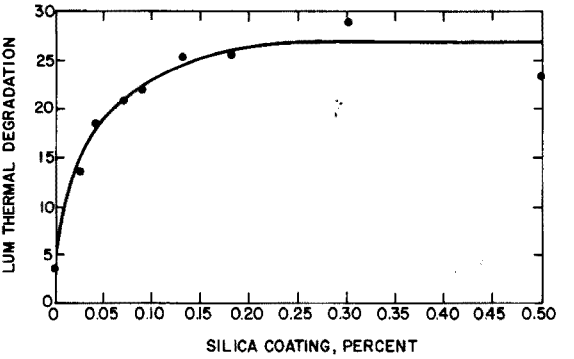

. Peak cathodoluminescence emission intensity as a function of time of excitation for
al coating concentrations. The near-vertical rises occurred where the sample was
ed to a new beam-landing position.

Luminescence thermal degradation as a function of concentration for silica-coated
hors.

ed phosphor, with a high-density cathode-ray beam, and recording the
sion intensity as a function of "beam-on" time. Figure 1 is a plot of the
der traces for a silica-coated, blue-emitting phosphor, operated at 8 kV,
μA, in a focussed spot of 0.25 mm^2, and detecting the emitted photons
9 nm. It can be seen that the rate of decrease of emission intensity,
$(dt$. is proportional to the concentration of the coating. By plotting
$dt)_t$ as a function of coating concentration, a standard curve can be
ed for any coating on any phosphor, which can then be used to analyze
les quantitatively. Figure 2 illustrates such a curve for silica-coatings on
-emitting phosphor particles.
r such "dusted" samples, the degradation reproducibility was ±5 % as
rent portions of the sample were positioned under the raster, this being
dication of sample uniformity.
e proposed method of analysis has detected coatings as low as 0.026 %,
detection limit of 50—100 p.p.m. is indicated for silica coatings.

e assistance of S.A. Trond, of RCA Lancaster, Pa., is gratefully acknowl-
l, for his interest and supply of coated phosphors.

RENCES

erber and S. Larach, to be published.
arach and A.E. Hardy, Proc. IEEE, 61 (1973) 915.
, for example, S. Larach, Anal. Chim. Acta, 41 (1968) 189.

Analytica Chimica Acta, 79 (1975) 332—334

Short Communication

ELECTROGENERATION OF NITROSODISULFONATE ION IN BASIC SOLUTIONS AND COULOMETRIC TITRATION OF CERIUM(III)

M. COSPITO
CAMEN, S. Piero a Grado, Pisa (Italy)
G. RASPI
Istituto di Chimica Generale, Universitá di Siena, Siena (Italy)
(Received 21st March 1975)

In a previous note [1], potassium nitrosodisulfonate was proposed as an oxidant for the titration of some inorganic cations. The reagent, if stored at 0 °C, is sufficiently stable in basic solutions, especially when it is prepared in concentrated borate buffer solution, but for accurate work it requires a frequent standardization.

In the present communication, electrogenerated nitrosodisulfonate ion is suggested as a coulometric titrant; the conditions for quantitative current efficiency in the electrogeneration of the reagent from basic solutions of hydroxylaminedisulfonate are described. The coulometric titration of micro amounts of cerium(III) is discussed as an application of the method, in view of the relevance of cerium(III) determinations in basic solutions.

Experimental

Instrumentation. A Metrohm E211 coulometer was used as a constant-current source. The generating anode was a 1.5-cm^2 platinum foil. The cathode was a 1-cm^2 platinum foil isolated from the anolyte in a tube closed with a fine sintered frit and containing a 1 % (w/w) potassium hydroxide solution. Pretreatment of the electrodes consisted of soaking in a (1 + 1) nitric acid solution. Stirring was done magnetically. The end-point detection system consisted of a platinum wire and a saturated calomel electrode across which a constant voltage (+20 mV) was impressed. The current between the indicating electrodes was measured with a galvanometer possessing a sensitivity of 0.001 $\mu A\ mm^{-1}$.

The current—potential curves used for measuring the current efficiency were obtained at 25 ± 0.1 °C by means of an AMEL Multifunction Assembly, model 463.

Reagents. Potassium hydroxylaminedisulfonate was prepared by the method of Rollefson and Oldershaw [2]. The generating solution was usually obtained

by dissolving 1.35 g of salt in 100 ml of buffer solution. Cerium(III) standard solutions were prepared as usual. All chemicals were reagent grade.

Current efficiency for electrogeneration of nitrosodisulfonate ion. Employ the cell and anode used for coulometric titrations. Place 25.0 ml of supporting electrolyte in the anode compartment equipped with working, auxiliary and a saturated calomel electrode and deaerate the solution with purified nitrogen. Stir efficiently with a magnetic stirrer. Record the current—potential curve by the usual polarographic technique, scanning from 0.0 to +1.2 V at 0.1 V min^{-1}. Add 0.35 g of potassium hydroxylaminedisulfonate and record under identical conditions.

Coulometric titration of cerium(III). Place 25—30 ml of 1.5 *M* potassium carbonate—0.5 *M* potassium hydrogencarbonate buffer solution in the anode compartment of the titration cell provided with generator anode, platinum indicator and saturated calomel electrodes. Deaerate by bubbling purified nitrogen, with stirring of the solution. Impress a constant voltage of +20 mV to the platinum wire *vs.* saturated calomel electrode. Pretitrate the electrolyte by generating nitrosodisulfonate ion, stopping the generation when the indicator current decays below 0.001 μA. Reset the timer, add the sample [0.05—1.5 mg of cerium(III)] and titrate by generating nitrosodisulfonate ion to the same indicator current (below 0.001 μA), with continuous deaeration and stirring. The electrolysis current used was 1 mA in the determination of 0.05—0.5 mg of cerium(III) and 3 mA for higher concentrations. Several titrations can be performed in the same generating solution by adding successive samples of cerium.

Results and discussion

The current efficiencies for electrogeneration of nitrosodisulfonate ion were estimated from the current—potential curves obtained as described previously by Lingane [3]. The current efficiencies obtained for buffer solutions of potassium carbonate—potassium hydrogencarbonate (pH 9.5—11.2) and of boric acid—sodium borate (pH 9.0—9.8) alone or with added 0.1 *M* sodium citrate or sodium tartrate, were found to be essentially quantitative (99—100 %) when the current densities were in the range 0.2—3 mA cm^{-2} and the concentration of hydroxylaminedisulfonate ion was 0.05 *M*, which is near its maximal solubility at 25 °C. Lower current efficiencies were obtained with lower concentrations.

Comparison of the current—potential curves with the potentials of the nitrosodisulfonate—hydroxylaminedisulfonate couple obtained in the same buffer solutions with a platinized platinum electrode indicated that the oxidation of hydroxylaminedisulfonate ion proceeded nearly reversibly.

The choice of 1.5 *M* potassium carbonate—0.5 *M* potassium hydrogencarbonate buffer solution as the supporting electrolyte for the coulometric

titration of cerium(III) represents a suitable compromise among various requirements. This solution was useful in ensuring complete solubilization of cerium(III) and cerium(IV) salts at relatively high concentrations; moreover, it showed an appreciable buffer capacity at a pH of *ca.* 10.5, which is a very good pH value for the stability of solutions of hydroxylaminedisulfonate ion and for quantitative electrogeneration of nitrosodisulfonate ion. The amperometric indicating system used was first devised by Cooke *et al.* [4]; the voltage of +20 mV *vs.* SCE is approximately the point of maximal slope of the S-shaped curve obtained by plotting the potential of the solution as a function of titration time, but any value between −20 and +60 mV *vs.* SCE gave correct results. Because of the rapid reaction rate between cerium(III) and electrogenerated nitrosodisulfonate ion, the attainment of equilibrium near the equivalence point showed no appreciable delay.

Table I gives the results of coulometric titrations of cerium(III) and the precision of the method.

TABLE I

Coulometric titration of cerium(III)

Cerium(III)		No. of detns.	Relative error (%)	s ($\cdot 10^{-3}$)	s_r (%)
Added (mg)	Found (mg)				
1.3075	1.3104	6	+0.2	5.3	0.4
0.9246	0.9223	8	−0.2	3.7	0.4
0.6164	0.6160	8	−0.1	1.5	0.2
0.3082	0.3093	8	+0.4	1.5	0.5
0.1541	0.1548	10	+0.5	1.2	0.8
0.0616	0.0624	10	+1.3	1.4	2.2

We are grateful to the Consiglio Nazionale delle Ricerche of Italy for financial support (contract no. CT74.00731.03) to one of us (G.R.).

REFERENCES

1 M. Cospito and G. Raspi, Anal. Chim. Acta, 74 (1975) 452.
2 G.K. Rollefson and C.E. Oldershaw, J. Amer. Chem. Soc., 54 (1932) 977.
3 J.J. Lingane, Electroanalytical Chemistry, Interscience, New York, 2nd edn., 1958, p.488.
4 W.D. Cooke, C.N. Reilley and N.H. Furman, Anal. Chem., 23 (1951) 1662.

Analytica Chimica Acta, 79 (1975) 335—340

Short Communication

THE DISSOCIATION CONSTANTS OF 2,2′-BIPYRIDINE AND ITS IRON(II) COMPLEX IN WATER—METHANOL MIXTURES

D.K. HAZRA and S.C. LAHIRI
Department of Chemistry, Kalyani University, Kalyani, Nadia, West Bengal (India)
(Received 17th May 1974)

Comparatively little is known about the effect of solvents on the dissociation constants of metal complexes. Pal and Lahiri [1], studied the equilibrium constants of iron(III) salicylate and sulphosalicylate complexes in different solvent mixtures, but, owing to the lack of fundamental data on dissociation constants of phenolic groups, the effect of solvents could not be predicted.

In the present study, the dissociation constants of 2,2′-bipyridine and its iron(II) complex in different methanol—water mixtures were examined. The equilibria involved were:

$$\text{bipyH}^+ \rightleftharpoons \text{bipy} + \text{H}^+ \quad (1)$$

$$\text{Febipy}_3^{2+} + 3\,\text{H}^+ \rightleftharpoons \text{Fe}^{2+} + 3\,\text{bipyH}^+ \quad (2)$$

$$\text{Febipy}_3^{2+} \rightleftharpoons \text{Fe}^{2+} + 3\,\text{bipy} \quad (3)$$

Experimental

Reagents. All chemicals used were of reagent grade (E. Merck). Twice-distilled water was used throughout. Methanol was distilled and the middle fraction was utilized within 48 h. Any traces of water in the organic solvents were neglected.

Iron(II) ammonium sulphate solution was prepared by dissolving a weighed amount in a known quantity of perchloric acid of the required concentration. The solution was standardized by titration with standard potassium dichromate solution in the usual way, and used within several hours.

2,2′-Bipyridine was dissolved in methanol, or in water containing more than one equivalent of perchloric acid.

Determination of pK values. 2,2′-Bipyridine absorbs strongly in the u.v. region; the wavelengths of maximal absorbance change with pH, but, for the ionic and molecular forms (301 nm and 281 nm, respectively), remained unchanged even with 90% (v/v) methanol. For the spectrophotometric determination of the pK values of the ligand, absorbances were measured in excess of 0.1 *M* perchloric acid or 0.1 *M* sodium hydroxide and at intermediate pH

values, at wavelengths of 280, 290, and 300 nm, against blank solutions of the same composition except for the ligand.

In the determination of pK values in aqueous methanol, the accuracy of the results depends on the accuracy of the pH measurement. Therefore, dissociation constants were also determined by pH titration: solutions of the ligand in the range $5 \cdot 10^{-3}$—$1 \cdot 10^{-2}$ *M* were acidified to different extents (30—70%) with known quantities of perchloric acid and the meter readings were taken.

The absorption maximum of the tris(2,2'-bipyridine)iron(II) complex occurs at 524 nm in aqueous solution but changes to 522 or 520 nm if much methanol is present. The maximum wavelength is independent of pH, but the absorptivity is maximal at about pH 5. It was assumed that under the experimental conditions used $Febipy^{2+}$ and $Febipy_2^{2+}$ were not formed, as suggested by Kolthoff *et al.* [2] for ferroin, and that $Febipy_3^{2+}$ alone was formed in water or aqueous methanol. The absorptivities of the tris(2,2'-bipyridine)iron(II) complex were determined from absorbance measurements of solutions containing 6—20-fold excesses of the ligand with different amounts of iron(II), at 520, 522, 524 or 530 nm. The concentration of the complex was taken as equal to that of iron(II), because different excesses of ligand did not affect absorbances, provided that at least a six-fold concentration of ligand was present. The molar absorptivities are given in Table I.

For the determination of the stability constants in water and aqueous methanol the absorbances of solutions containing 8—$20 \cdot 10^{-5}$ *M* iron(II) and 8—$20 \cdot 10^{-5}$ *M* 2,2'-bipyridine were measured at 520 nm, 522 nm (524 nm) and 530 nm. The pH values of the solvents, which were measured and corrected as described previously [3,4], ranged from 2.80 to 3.65. The concentrations of the complex, calculated from the absorbances and the absorptivities of the complex at each wavelength, were found to be the same (within ± 0.2%), and the average value was used in the calculation of the constant for reaction (2).

The weight percentages of the methanol were calculated from the known volumes of the two solvents by volumes and their densities [5] at 25 °C. Dielectric constants were calculated from the data given by Bates and Robinson [10].

A Beckman DU spectrophotometer and a Cambridge bench-type battery-operated pH meter were used.

Results

Dissociation constants of 2,2'-bipyridine. The thermodynamic dissociation constant K_T for equilibrium (1) at the low ionic strengths used can be calculated, in the conventional manner, from:

$$pK_T = [B] + \log U_H + \log \frac{C_{AH^+}}{C_A} \tag{4}$$

$$= [B] + \log U_H + \log \frac{d_M - d}{d - d_i} \tag{5}$$

TABLE I

Dissociation and stability constants in aqueous methanolic solvents at 25 °C

Wt % methanol	pK_T (reaction 1)		ϵ (nm)			pK_a[a] based on		pK^b based on	
	pH-metric	Spectrophotometric	520	522	530	exptl. [H^+]	calcd. [H^+]	exptl. [H^+]	calcd. [H^+]
0		4.47 (±0.02)				4.12 (±0.02)	4.36	17.53	17.77
8	4.40 (±0.02)	4.42 (±0.02)	8450	8510	8400	4.39 (±0.04)	4.67	17.59	17.87
16.4	4.25 (±0.02)	4.30 (±0.03)	8515	8575	8480	4.97 (±0.04)	5.14	17.72	17.89
25.2	4.15 (±0.03)	4.22 (±0.03)	8580	8620	8500	5.08 (±0.05)	5.33	17.54	17.78
34.4	4.01 (±0.05)	4.08 (±0.05)	8685	8740	8590	4.90 (±0.05)	5.25	16.94	17.22
44.1	3.83 (±0.05)	3.90 (±0.05)	8730	8785	8610	5.10 (±0.06)	5.36	16.59	16.85
54.2	3.60 (±0.06)	3.77 (±0.08)	8320	8385	8000	5.12 (±0.06)	5.37	15.92	16.17
64.7	3.32 (±0.06)	3.60 (±0.08)	8500	8550	8110	5.43 (±0.08)	5.56	15.39	15.52
75.9	3.15 (±0.10)		8550	8620	8165	5.50 (±0.08)	5.59	14.94	15.04
87.6	3.04 (±0.12)		8600	8660	8230	5.88 (±0.10)	5.94	15.01	15.06

[a] Reaction (2).
[b] Reaction (3).

where B is the pH meter reading in mixed solvents, log U_H the correction factor in mixed solvents, A represents 2,2′-bipyridine, and d_M, d_i and d are the absorbances of the ligand in the molecular and ionic forms and at intermediate pH values. For the potentiometric determination, log C_{AH^+}/C_A was determined from the fraction neutralized. The glass electrode was calibrated in the aqueous methanol solvents as described previously, and log U_H values were determined before each set of measurements [3,4].

The results are given in Table I.

Dissociation constants of tris(2,2′-bipyridine)iron(II) complex. Under the experimental conditions used, 2,2′-bipyridine is present mainly as bipyH$^+$. In the calculation of the dissociation constant, K_a, for reaction (2), the ionic strength of the mixtures was kept low (*ca.* 10^{-3} *M*), so that it could reasonably be assumed that the activity coefficients for Fe^{2+} and $Febipy_3^{2+}$, and for bipyH$^+$ and H^+, were the same. The concentration of bipyH$^+$ was calculated from $\{[bipy]_{Total} - 3[Febipy_3^{2+}] - [bipy]\}$, where [bipy] ($=C_A$) was calculated where necessary from eqn.(4) with the appropriate pK values from Table I. The concentration of free iron(II) was calculated from $\{[Fe^{2+}]_{Total} - [Fedipy_3^{2+}$

The hydrogen ion concentrations of solutions of the complex were difficult to determine; appropriate corrections of the pH meter readings were essential. Despite corrections, comparison of the calculated and the measured [H^+] values showed considerable deviations, which, of course, increased with increasing content of methanol and increasing [H^+]. Obviously, a slight error in the [H^+] value will have a profound effect on the equilibrium constant of reaction (2).

The equilibrium constants obtained with the theoretically calculated [H^+] and the corrected measured [H^+] values are given in Table I. The correction factors were determined before each set of measurements to ensure maximum accuracy. The equilibrium constant, $K = [Fe^{2+}][dipy]^3/[Fedipy_3^{2+}]$, for reaction (3) was given by $K_a \times K_T^3$; the values found are also given in Table I.

Discussion

The literature pK values for 2,2′-bipyridinium ion in water [7] vary from 4.25 to 4.51; different ionic strengths were used in obtaining these values. The value obtained here at low ionic strength (*ca.* 10^{-3} *M*) — 4.47 ± 0.02 — is in good agreement with the values 4.48 and 4.47 (potentiometry) or 4.51 (spectrophotometry) reported for ionic strength 0.1 by Irving and Mellor [8], and with the values of Nakamoto [9] (4.45) and Anderegg [10] (4.49).

The pK values of 2,2′-bipyridine in methanol—water mixtures were found to be a linear function of the mole-fraction of methanol present. It is known that the dielectric constant in the region 30—80 is a better correlating factor [3]; a plot of pK against $1/D$ was linear up to D = 45. In all these cases, deviations occurred when the methanol content exceeded 60 wt %, probably because of inaccurate [H^+] measurements; errors can occur from high liquid-

junction potentials, low electrode sensitivity, and possibly solute—solvent interactions. The pK values in water obtained from different extrapolations were found to be 4.54, 4.48 and 4.47, which is the same (within experimental error) as the spectrophotometric result (4.47).

The K_a value for reaction (2) in water was $7.56 \cdot 10^{-5}$ at 25 °C; this can be regarded as the thermodynamic value as the ionic strength was low. The corresponding K_a value [11] for the tris-(1,10-phenanthroline)iron(II) complex at low ionic strength is $4.50 \cdot 10^{-6}$ at 25 °C. Different extrapolations of plots of K_a values against the methanol concentration were not satisfactory. Linear relationships were found over a small range but deviations were high at 25.2 wt % of methanol; a slight error (±0.04) in the measurement of $[H^+]$ produced an error in the K_a values of about ± 50%. The pK_a values based on experimentally and theoretically determined H^+ ion concentrations shown in Table I indicate the extent of possible errors.

With regard to the dissociation reaction (3), the pK value of 17.53 at low ionic strength reported here (Table I) is in good agreement with the value of 17.50 (at 0.1 M) obtained by Irving and Mellor [8] by a distribution method; other reported values [11] are 17.58 (μ = 0.33), 17.41 (μ = 0.01), 17.07 (μ = 0.25), and 17.45 (μ = 0.1) [10]. The corresponding tris (1,10-phenanthroline)-iron(II) dissociation reaction has a pK value of 20.55 at zero ionic strength.

Reactions (1)—(3) are "isoelectric" in character, hence changes in the dielectric constant of the solvent should not have significant effects. The solvent effect is probably largely due to solute—solvent interaction, as suggested previously [12,13]. The changes in pK values with increasing methanol content, may be partly due to the greater solubility of 2,2′-bipyridine in methanol, and to differences in solvation of H^+, bipyH^+, Fe(dipy)$_3^{2+}$, and iron(II). However, the effects of solvents on these ions are not clear.

Studies on the dissociation constants of reactions of the type $AH^+ \rightleftharpoons A + H^+$ show a minimum in the pK values at 70 wt % methanol [12]. No such minimum was observed in the present work. For reaction (2), the pK_a value increased as the methanol concentration increased, but deviations occurred in 25 and 34 wt % methanol. For reaction (3), the pK value decreased as the methanol content increased. The correction factors for $[H^+]$ were maximal at about 65 wt % methanol. The changes in molar absorptivities with increasing methanol content are of interest, but are not readily correlated with the other data obtained.

The authors are grateful to Prof. S. Aditya, Department of Applied Chemistry, for laboratory facilities.

REFERENCES

1 S.K. Pal and S.C. Lahiri, Z. Physik. Chem. (Leipzig), 246 (1971) 89; 252 (1973) 177; 255 (1974) 910.
2 I.M. Kolthoff, D.L. Leussing and J.S. Lee, J. Amer. Chem. Soc., 72 (1950) 2173.

3 L.G. Van Uitert and C.C. Haas, J. Amer. Chem. Soc., 75 (1953) 451.
4 S.C. Lahiri and S. Aditya, J. Ind. Chem. Soc., 51 (1974) 319.
5 International Critical Tables, Vol. III, McGraw Hill, New York, 1928, pp.115—117.
6 R.G. Bates and R.A. Robinson, in B.E. Conway and R.G. Barradas (Eds.), Chemical Physics of Ionic Solutions, J. Wiley, New York, 1966, Ch. 12.
7 L.G. Sillen and A.E. Martell, Stability constants of Metal—Ion complexes, Special Publication No. 17., The Chemical Society, London, 1964, pp.616—618.
8 H. Irving and D.H. Mellor, J. Chem. Soc., 1962, 5222.
9 N. Nakamoto, J. Phys. Chem., 64 (1960) 1420.
10 G. Anderegg, Helv. Chim. Acta, 46 (1963) 2397.
11 S.C. Lahiri and S. Aditya, Z. Physik. Chem. (N.F.), 41 (1964) 173.
12 R.G. Bates, J. Electroanal. Chem., 29 (1971) 1.
13 A.S. Quist and W.L. Marshall, J. Phys. Chem., 72 (1968) 684, 1536.

Analytica Chimica Acta, 79 (1975) 341—342

ANNOUNCEMENTS

Tenth International Symposium on Advances in Chromatography

The Tenth International Symposium on Advances in Chromatography will be held November 3—6, 1975, at the Sheraton—München Hotel, in München, German Federal Republic. The 61 papers to be presented at the Symposium represent contributions from 15 countries and deal with various aspects of the theory, applications and instrumentation of chromatography; among others, 18 papers deal with the biomedical—clinical applications of the technique and seven papers discussing basic new developments are grouped together in a session on New Horizons. The M.S. Tswett Chromatography Medals will be presented at the opening session to a selected group of scientists who have contributed significantly to the advancement of chromatography.

A special feature of the meeting will be an exhibition of the latest instrumentation and books. Informal discussion groups will also be held.

The International Symposia on Advances in Chromatography started in 1963. Previous Symposia have been organized in Houston, New York, Miami Beach, Las Vegas and Toronto. This is the first symposium organized in Europe.

Registration should be made in advance. Programs, registration forms for the meeting and hotel reservation cards can be obtained from

Prof.Dr. E. Bayer	or	Prof.Dr. A. Zlatkis
Chemisches Institut		Chemistry Department
der Universität		University of Houston
Auf der Morgenstelle		Cullen Boulevard
Tübingen		Houston, Texas 77004
German Federal Republic		U.S.A.

Fifth International Conference on Modern Trends in Activation Analysis, München, Federal Republic of Germany, September 13—17, 1976.

The next International Conference on Modern Trends in Activation Analysis will be held in Munich, from 13th to 17th September 1976. This Conference, organized in cooperation with the Gesellschaft Deutscher Chemiker, continues the series of Modern Trends Conferences organized at College Station, Texas (1961, 1965), Washington (1968), and Paris (1972). The international response to the previous meetings has been extremely favorable and encouraging. It is therefore clear that Modern Trends '76 again promises to be one of the leading scientific meetings in the analytical field. The international and multidisciplinary character of the Conference will be able to provide a working forum for all those interested in the many facets of activation analysis.

The Conference will consist of a series of invited papers as well as the pre-

sentation of appropriate contributed papers. All major aspects of activation analysis will be discussed, particular emphasis being placed on the application of the method in a wide variety of scientific and technical fields, and papers falling under this broad category from prospective delegates are welcome.

Scope of the Conference

A. Fundamental contributions
   Recent progress in technical development.
B. Applied contributions
   1. Biological and biomedical applications. 2. Environmental and ecological applications. 3. Industrial applications. 4. Applications in geo- and cosmosciences. 5. Applications in archaeology, art and forensic sciences.
C. Inter-disciplinary contributions
   1. Accuracy and precision. 2. Sampling and homogeneity control. 3. Standard materials. 4. Comparisons with other analytical methods.

All correspondence concerning the Conference should be directed to:

Prof.Dr. F. Lux
Institut für Radiochemie der
Technischen Universität München
D-8046 Garching
F.R. Germany

Prize "Biochemical Analysis"

A prize of DM 10000 — donated by Boehringer, Mannheim — is awarded every two years at the "Biochemical Analytik" conference in Munich, Germany, for outstanding work in the field of biochemical instrumentation and analysis. The award will be made during the 1976 conference (9—13th April). One or several papers concerning one theme, either published or accepted for publication between October 1st 1973, and September 30th 1975, may be sent in triplicate before November 15th 1975 to:

Prof.Dr.Dr. Ivar Trautschold, Secretary of the prize "Biochemical Analysis", Medizinische Hochschule Hannover, D-3000 Hannover-Kleefeld, Karl-Wiechert-Allee 9, Germany.

ANALYTICA CHIMICA ACTA, VOL. 79 (1975)

AUTHOR INDEX

ANALYTICA CHIMICA ACTA, VOL. 79 (1975)

SUBJECT INDEX

(Continued from page 3 of cover)

(Continued from page 4 of cover)

Short Communications

Printed in The Netherlands

CONTENTS

(Continued on inside page of cover)